(NASA-CR-180314) SHORT FATIGUE CRACK BEHAVIOR IN NOTCHED 2024-T3 ALUMINUM SPECIMENS Final Report (Johns Hopkins Univ.) 346 p Avail: NTIS HC A15/MF A01 CSCL 20K G3/39

N87-26364

Unclas
0063708

ABSTRACT

Single-edge, semi-circular notched specimens of Al 2024-T3, 2.3 mm thick, were cyclicly loaded at R-ratios of 0.5, 0.0, -1.0, and -2.0, as part of an AGARD-sponsored, round-robin test program. The notch roots were periodically inspected using a replica technique which duplicates the bore surface. The replicas were examined under an optical microscope to determine the initiation of very short cracks and to monitor the growth of short cracks ranging in length from a few tens of microns to the specimen thickness.

In addition to short crack growth measurement, the crack opening displacement (COD) was measured for surface cracks as short as 0.035 mm and for through-thickness cracks using the Interferometric Strain/Displacement Gage (ISDG), a laser-based optical technique. Two very small indentations were placed across the short crack and illuminated with a laser. This formed interference fringe patterns which could be monitored to measure the relative displacement between the two indentations. The resulting load-COD data were then analyzed to determine the closure load.

Cracks initiated mostly at the inclusion particles, and the initiation cycles were in reasonably good agreement with values predicted from the Manson-Coffin relation. The growth rates of short cracks were faster than the long crack growth rates for R-ratios of -1.0 and -2.0. No significant difference

between short and long crack growth rates was observed for R = 0.0. Short cracks had slower growth rates than long cracks for R = 0.5.

The crack compliances show a linear relationship to the surface crack length, without regard to R-ratio or applied stress level. The crack opening stresses measured for short cracks were smaller than those predicted for large cracks, with little difference appearing for positive R-ratios and large differences noted for negative R-ratios.

A considerable improvement in agreement of long and short crack growth rates was achieved for negative R-ratios when the closure effect was considered.

TABLE OF CONTENTS

TABLES

FIGURES

I. INTRODUCTION

Fatigue has been studied in order to predict the exact life of engineering structures and components. The fatigue life can be categorized into three periods: microcrack initiation, propagation of the microcrack to detectable size, and macroscopic propagation. From an engineering point of view, the first two periods are generally classified together as a period of engineering-size crack initiation.

The total fatigue life, in an engineering sense, can be measured by the number of crack initiation cycles and the number of propagation cycles until final failure. The initiation cycles can account for a large portion of the fatigue life of many engineering materials, especially for commercial aluminum alloys, where initiation cycles may constitute up to 90% of the fatigue life [1,2]. This fact alone addresses the importance of studying the behavior of initiation-related small crack problems.

Considerable emphasis has been placed on the study of small crack problems in recent years, not only because small crack behavior determines the fatigue life of many engineering materials but also because the growth rates of small cracks differ from the predictions of conventional linear elastic fracture mechanics (LEFM). In LEFM, crack growth rates depend only upon the value of the stress intensity factor range, ΔK, when the plastic zone is small with respect to all other length

dimensions and provided plane strain conditions are met. But small cracks usually appear on the surface of the specimen; this violates the condition of plane strain. Also, small cracks are not long enough to satisfy the plastic zone condition. The maximum plastic zone, r_{max}, can be estimated using the maximum stress intensity factor, K_{max}, based on Irwin's relation,

$$r_{max} \simeq \frac{1}{2\pi} \left\{ \frac{K_{max}}{\sigma_o} \right\}^2 \qquad (1.1)$$

where σ_o is the flow stress, which is taken as an average value of the yield stress, σ_y , and the ultimate strength, σ_u. Even a crack that is short in the engineering sense can be analyzed based on LEFM if it is long enough with respect to the size of the plastic zone. Small cracks can be categorized in regard to these considerations in the following manner.

> (a) Small cracks which are not long enough for continuum mechanics and LEFM to apply are called microcracks.
> (b) Small cracks which are long enough to use LEFM are called physically short cracks, or simply short cracks here. Typically these cracks are 0.5 - 2 mm long.

A typical value of r_{max} for the specimen used in this study, Al 2024- T3, is approximately 0.05 mm, with K_{max} = 8 MPa and σ_o = 427 MPa.

Many researchers [1,3-12] have observed that small cracks show faster growth rates than those predicted from long crack data. But for some materials in some experiments [13,14], no appreciable difference between the growth rates of small and

long cracks has been observed. Also, the growth behavior of microcracks is influenced by microstructural features such as grain orientation and grain boundaries, limiting the usefulness of a continuum mechanics approach. Several investigators [4,5,15-20] showed that propagation of microcracks was retarded or even halted as a crack front reached a grain boundary.

Many attempts have been made to analyze small crack behavior by modifying the concept of LEFM. Several researchers [21-26] have proposed that the difference in fatigue growth behavior of the long and the short crack is mainly due to the closure effect. When the crack opening stress, S_{op}, is higher than the minimum stress, S_{min}, the effective stress intensity range, ΔK_{eff}, will be

$$\Delta K_{eff} = \frac{Smax - Sop}{Smax - Smin} \Delta K \qquad (1.2)$$

If a smaller opening stress is observed in fatigue growth, the effective crack driving force, ΔK_{eff}, will be larger than the driving force with a larger opening stress, and faster crack growth is expected.

Considering that most cracks emanate from notches in the specimens, the local plasticity due to a notch must be accounted for in an analysis of small crack behavior. Notch plasticity due to applied tensile load will induce a compressive residual stress, σ_{rs}, at the notch root. Then the local effective stress intensity factor range, $\Delta K_{eff,local}$,

will be reduced by the amount of σ_{rs} from ΔK_{eff} when there is no residual compressive stress:

$$\Delta K_{eff,local} \propto \{ \sigma_{max} - \sigma_{rs} - Sop \} \qquad (1.3)$$

where σ_{max} is the local maximum stress. One investigator [17] observed that the growth rates of small cracks are slower when compressive residual stress is present. Other experiments [27,28] showed that the growth rates of small cracks propagating inside of the notch plasticity decrease progressively until they arrest or merge with the long crack curve.

As reviewed above, the anomalous growth behavior of small cracks may result from complications due to several mechanical and metallurgical causes, such as crack closure, local plasticity, and microstructural effects.

To validate the existence of the small crack effect, NASA has sponsored a round-robin test program in which 14 laboratories are participating. In the study recorded here, as part of this round-robin program, the growth rates of small fatigue cracks from a semi-circular notch were measured using the replica method for different R-ratios. The closure behavior of small cracks was observed for various R-ratios and gross stress levels. The closure loads were determined from the load versus crack opening displacement (COD) data, which were obtained using the computer-controlled, laser-based, Interferometric Strain/Displacement Gage (ISDG). In addition,

crack initiation was analyzed and the closure effect on the growth rate was examined.

In this thesis, the definition of "small crack" as it is presented in other works will be reviewed. Various phenomena of small cracks, such as the microstructural effect, differences in the growth behaviors of small and long cracks, the notch plasticity effect, and the closure effect will be discussed as they have been documented in other investigations. Also, the small crack closure measurement techniques described in Section II, Background, will be examined. In Section III, Experimental Procedure, material properties and specimen geometry will be introduced. This section also contains a description of special fixtures which allow accurate specimen alignment and application of the load without any bending effects. A further explanation of the experiment includes details of the loading conditions, measurement procedures used to observe crack growth behavior, and measurement of the crack closure with the ISDG technique.

The results of the crack growth measurements, including an analysis of crack initiation and crack shape as well as a discussion of the changes in short crack growth behavior in the notch relative to changing R-ratios, will be presented in Section IV, Results and Discussion. Results of COD measurement will be given and the crack compliances obtained from the COD-load curve will be discussed as a function of crack length. Since crack closure is known to be an important factor in the

growth behavior of short cracks, the effects of crack length and R-ratio on crack closure will be examined. Finally, the effect of closure on the crack growth rate will be discussed.

In Appendix I, the equation used in calculating the stress intensity factor for short cracks on the notch root and detailed procedures for replicating the surface of the notch root will be described. Measurement of notch displacement using the ISDG and the analysis of notch stress-strain from these measurements will also be presented. The procedure for aligning specimens and fixtures on the test machine will be described, and the check data using a stain-gaged specimen to confirm the alignment will be presented. In addition, representative computer programs are listed which may be used for measuring COD with the ISDG technique, for determining the opening loads, and for calculating and plotting data on the growth rate - stress intensity factor range.

All data resulting from each test, including a listing of test conditions, drawings of crack maps, a plot of the growth rate - stress intensity factor range, and the micrograph of the fracture surface, are attached in Appendix II.

II. BACKGROUND

II-1. Definition of Small Crack

Taylor and Knott [4] defined a crack as "small" when the crack length is less than a certain critical length. In their experiments with a cast nickel-aluminum-bronze material, which had a very coarse microstructure (grain size = 100 microns), cracks larger than 300 μm were observed to have the same propagation characteristics as long cracks. They also observed that the critical crack length for small crack behavior was correlated with the scale of the microstructure.

Lankford [5] hypothesized that the rapid average growth of small cracks might be a consequence of the large size of the crack tip plastic zone relative to that of the crack itself. He examined the relationship between the ratio of the plastic zone size to the crack length in order to deduce the criteria for the microcrack behavior, a faster growth rate than that of the long crack. However, he did not find a clear relationship between this ratio and the microcrack behavior.

Suresh and Ritchie [29] defined short cracks in the following way: either 1) the length of the crack is small compared to relevant microstructural dimensions, 2) the length is small compared to the scale of local plasticity, or 3) the crack is simply physically small. The first category limits the usefulness of continuum mechanics; the second group limits the

use of LEFM in the analysis of their behavior; and the third category represents only the size of the crack length, i.e., typically smaller than 0.5-1 mm.

The short cracks which are divided into these three categories have been shown to propagate more quickly than corresponding long cracks under the same nominal driving force. But Leis and Forte [14] showed that even physically long cracks, i.e., as large as 2.5 mm in the aluminum alloys and 1.25 cm in steel, also exhibit different growth behavior compared to longer-crack trends.

These facts indicate that the cracks are to be called small (or short) when their behavior is shown to be different from the behavior predicted by long crack data (or LEFM analysis). But a definition can not be made simply by using an arbitrary value as the standard. Small crack behavior depends on the material, the geometry of the specimen, and the test environment.

II-2. Initiation and Growth of Small Fatigue Cracks

It has been observed that fatigue cracks initiate at surface inclusion particles or near inclusions in commercial aluminum alloys. Boules and Schijve [30] observed that large inclusions (second-phase particles, size 1-10 microns) were the source of most crack nucleations in the material Al 2024-T3. Also in these experiments, the material was stretched between 4-6% strain to produce cracked inclusions. Then heat treatment was used to remove residual stresses around the cracked inclusions. After cycling this strained material, Boules and Schijve found several microcracks; some of these cracks initiated from the cracked inclusions.

Pearson [1] performed experiments on aluminum alloys to examine the initiation of fatigue cracks on a planar, polished surface and the subsequent growth of very short cracks. He found that cracks initiated at an edge or, most frequently, at a surface inclusion away from an edge ("center" crack). He determined that the edge cracks initiated at very small mechanical imperfections which might remain from the polishing process, and he observed that the center cracks always initiated at a surface inclusion.

Pearson concluded that initiation of a a fatigue crack on a this type of surface made from aluminum alloys DTD 5050 and BS L65 occurs either through tensile cracking at the interface between a surface inclusion and a matrix or by tensile cracking

of the particles themselves. Also, he saw that the crack front of a short center crack was appoximately semi-circular in shape. The mean crack growth rate in the early stages of growth was observed to be much faster than those predicted from long crack data, and the crack propagation curve tended towrds that for the long crack when the crack depth was greater than 0.127 mm.

Swain and Newman [31] experimented on Al 2024-T3 sheets with double edge notches to study the initiation and growth of small cracks (5-500 microns). They noted that cracks initiated either at inclusion clusters or at one or both notches along the bore of the notch rather than at the corner. The inclusion particles were fragmented and formed clusters during the rolling process. The data showed that small cracks grow at stress intensity factor ranges substantially less than the threshold stress intensity factor range obtained from large cracks.

A number of recent studies have demonstrated that small cracks behave differently than large cracks. This appears to be the case when small cracks are analyzed using the concepts of conventional fracture mechanics. Pearson [1], Swain and Newman [31], Leis and Forte [14], de los Rios et al [19], Saxena et al [8], Lankford [5], Taylor and Knott [4], Tanaka [26], and Brent et al [22] showed for various materials that the small crack grows faster than the long crack, based on the parameters of LEFM. The researchers observed that the small crack grows

faster especially below the long crack fatigue threshold stress intensity factor range. But in the experiments of Leis and Forte [14], short cracks grew faster than long cracks in tests above the long crack fatigue threshold values; even crack lengths greater than 2.5 mm in aluminum alloys were observed to grow in a manner similar to that of physically short cracks.

Leis and Forte also noted that there was no apparent anomalous behavior in the initial growth rates of physically short fatigue cracks which initiated from notches. They attributed this similarity in behavior between physically short and long cracks to notch plasticity, which may lead to a constant or decreasing driving force for crack growth until the crack nears the elastic-plastic boundary of the notch field. Other investigators have suggested that anomalous small-crack behavior at notches might be very different from behavior for smooth specimens if notch plasticity was developed.

Leis and Galliher [32] observed crack growth behavior for cracks as small as 25 microns emanating from circular notches in Al 2024-T351 specimens. They found that the corner cracks began with a fast growth rate, then slowed their growth; an increase in the growth rate would follow, approaching the rate of the long crack, when the cracks grew in inelastic regions of the notches. In all cases, the trend shifting from a decreasing to an increasing rate was observed to correlate with the transition of a crack from a corner to a through crack. Leis and Galliher considered this shift as the result of an

inelastic displacement-controlled notch field.

Later, Leis [33] analyzed his previous experiment [32] using two postulates: that inelastic action due to the notch is a major cause of the short crack effect, and that the local value of R is controlled by both the notch field and, to some extent, the crack length. He described crack growth in notches in terms of three categories. The crack tip and its plastic zone are (a)beyond the notch field, (b)beyond the inelastic field but within the elastic field of the notch, or (c)contained within the inelastic field of the notch. To analyze the third group, he applied a pseudoplastic form of the stress intensity factor,

$$\Delta K^P \propto \Delta \varepsilon \tag{2.1}$$

where $\Delta \varepsilon$ is the stable strain range in the material element at the crack length of interest. This relation implies that the crack driving force is under a displacement-controlled field. Leis also formulated the effective pseudoplastic stress intensity factor range:

$$\Delta K^P_{eff} = \frac{Smax - Sop}{Smax - Smin} \Delta K^P \tag{2.2}$$

Results from this analysis agreed reasonably well with experimental data. He concluded that the local notch plasticity and crack closure were a major cause of the so-called short crack effect.

Saxena et al [8] performed experiments on small fatigue crack behavior at notches in an environment consisting of wet hydrogen plus air. They examined the growth of cracks with lengths less than 0.76 mm and observed a dependency of growth rate on cycling frequency in the hydrogen environment. The small cracks grew faster than long cracks at 10 Hz; but at less than 10 Hz, small cracks grew at a rate comparable to that of the long cracks. Also, the trend noted earlier of a shift from decreasing to increasing rates was shown in a plot of growth rate versus ΔK for the small cracks grown faster than long cracks. This trend did not appear to relate to the notch plasticity.

Microstructural effects must be considered when examining the behavior of small cracks. The behavior of microscopically small cracks can be summarized in terms of deceleration or retardation of growth through interactions with microstructural features, such as grain boundaries [4,5,15-20].

Morris et al [17] proposed a model to predict early crack growth in the Al 2219-T851 alloy as a function of both crack length and the location of the surface crack tips relative to the grain boundaries. The researchers observed that the crack growth rate was at a minimum when a crack tip enters into a new grain. In the model, the closure stress, σ_{cc}, was considered as a function of the distance from the tip to the grain boundary:

$$\frac{\sigma cc}{\sigma max} = \frac{\alpha Zo}{2C} \qquad (2.3)$$

where σ_{max} is the maximum applied tensile stress and z_0 is the distance from the crack tip to the next grain boundary. Equation 2.3 shows that the closure stress reaches a maximum when a crack enters into a new grain; the equation agrees with the crack growth behavior in the experiment conducted by Morris' group.

In Larsen's experiment [13], which measured the growth of small fatigue cracks in Ti-6Al-2Sm- Zr-6Mo material, he showed that small cracks propagate faster than long cracks. Also, interestingly, he observed that retardation of the growth rate appeared at several points, not just at one point as other papers have shown.

II-3. Crack Closure and Its Effect on the Growth of Small Fatigue Cracks

Crack closure has been studied as an important factor in the accurate prediction of fatigue crack growth rates. If the opening stress, Sop (or closure stress), is higher than the minimum applied stress in fatigue cycling, S_{min}, then the effective stress range, ΔS_{eff}, is

$$\Delta Seff = Smax - Sop \tag{2.4}$$

The crack growth relationship will be written as follows.

$$\frac{da}{dN} = C (\Delta Keff)^n \tag{2.5}$$

where ΔK_{eff} is proportional to ΔS_{eff}.

Several mechanisms have been suggested for the crack closure. They are (a)plasticity induced closure, (b)oxide induced closure, and (c)roughness induced closure.

Plasticity induced closure, as first proposed by Elber [34], is due to the residual tensile deformation which follows in the wake of a fatigue crack. It is often stated [29,35] that plasticity induced closure is operative in a dominant role under plane stress. The plane stress implies that the plastic zone of the crack is large while the thickness of the specimen is small. Banerjee [36] showed that even in a thin specimen, the stress present at low ratios of stress intensity factor to yield stress need not be plane stress.

Newman [37] proposed a crack closure model based on the plasticity induced mechanism. He modified the Dugdale model to leave plastically deformed material in the wake of the advancing crack tip. He showed that the crack growth law predicted with the proposed closure model agreed quite well with experimental data for long cracks.

Oxide induced closure is generally considered to play a major role only in specific combinations of material and environment. The oxide induced closure mechanism applies particularly in situations where plasticity, the maximum stress intensity factor, and the crack growth rate are very small [35].

It has been suggested [38] that the roughness induced closure mechanism is encountered in situations where the maximum plastic zone is very small (less than the grain size). In such a situation, crack extention occurs through a single slip system which creates zig-zag fracture paths, resulting in significant mode II displacement. This mode II displacement would be important in the development of roughness induced closure. In this sense, roughness induced closure may be more relevant to small fatigue cracks than to long cracks because small cracks exhibit a limited wake of plasticity. McCarver et al [11] and Morris et al [39] have proposed a model which shows the importance of roughness induced closure in small fatigue cracks. The contribution of oxide induced closure of small cracks remains unclear.

Breat et al [22] and Liaw et al [40] suggested that small crack closure is associated with residual stress along the crack due to cyclic loading and fracture surface roughness due to zig-zag fracture paths. James' [23] analysis of short crack closure focused on plasticity induced closure in the wake of the growing crck tip. However, decreasing crack size will cause the closure to decrease without regard to plasticity or roughness, because a smaller crack length means decreasing the wake around the crack tip and the contact area of fracture surfaces.

Several investigators, including Breat et al [22], James et al [10], and Tanaka et al [61], observed a decrease in crack closure as the crack length decreases. But Larsen [13] showed in his fatigue experiment for physically short cracks in a certain material that crack closure did not increase consistently as the crack grew.

Many researchers have attempted to explain the difference in growth behavior of small and long cracks using closure. Morris [16] proposed a microstructural model to fit the empirical closure data, suggesting that the closure stress is a function of the distance of the crack tip from the next grain boundary. Morris et al [17] created the growth rate model to predict growth of microstructurally small fatigue cracks. They showed that the crack growth was at a minimum when the crack entered into the next grain and that the closure stress value was at a maximum in this situation.

Tanaka [61] and Breat [22] measured the growth behavior of small fatigue cracks and compared the results with long crack data. When the growth rates were plotted against the effective stress intensity range, ΔKeff, so that

$$\Delta Keff = Kmax - Kop \tag{2.6}$$

the growth rates of short and long cracks were in agreement.

Liaw [40] re-analyzed data from other experiments and offered an explanation of small crack retardation and the difference in growth rates compared with large cracks. The explanation involved crack closure.

Leis et al [51] reviewed the problem of short fatigue cracks. They stated that short crack problems could be ascribed to a wide range of factors: violation of the limitations of LEFM, incomplete implementation of LEFM, and transients due to initiation. They also determined that phenomenological data do not clearly indicate which factors are of consequence and why. This anomolous behavior of the short crack is attributed to a lack of mechanical and metallurgical similitude. Leis et al concluded that the short crack effect arises primarily because of crack tip plasticity, transients from the initiation process, and incorrect implementation of LEFM. They also emphasized the contribution of local closure to the short crack effect.

II-4. Measurement Techniques for Closure in Small Cracks

The techniques used in measuring the closure behavior of long cracks -- the clip gage, the strain gage, ultrasonics, and the potential difference technique -- generally are not available for short cracks. Special methods must be applied in monitoring small crack closure; these methods must provide sufficient resolution and be easily adaptable to the shapes and geometries of small cracks.

Morris et al [42] measured closure stress on surface micro- cracks with lengths from 70 to 90 microns using scanning electron microscopy (SEM). They measured crack opening displacement with 30,000X magnification at each successive load to take crack compliance data. The crack closure load was determined from the break point in the linear relationship between crack opening and applied stress. James et al [43] used the same method as Morris et al [42] in measuring the closure load for crack lengths from 600 to 1,000 microns.

Zeiken et al [44] measured mean closure loads on a through-edge crack with a length of 500 microns using a back-face strain technique. This technique developed in another experiment [45] determined a closure load from the point where the resulting elastic compliance curves of load versus relative strain deviated from linearity.

Breat et al [22] measured bulk closure load on through-edge cracks with lengths of 300 to 600 microns using a clip gage extensometer. Crack closure was determined from a $P - (\alpha P-\delta)$plot where α was selected in such a way that the linear part of the $P-\delta$ curve above P_{op} was vertical.

Sharpe [41] developed a laser-based interferometric technique; Sharpe and Lee [46] described its use in measuring crack opening displacement. His technique has a very short gage length (a few tens of microns) and high resolution (0.02 micron). The crack compliance data was obtained from the crack opening displacement and closure load was determined by a "reduced data method" which is widely used in closure measurement. Larsen [13] applied a similar technique in measuring the closure load on surface cracks as small as 37 microns.

Williams et al [47] developed a stereo-imaging technique to monitor the crack tip strain field. This technique measures displacement with an accuracy of 0.04 micron at 1,000X magnification. It can be useful in measuring the behavior of small cracks.

All of the preceding techniques have been used to measure short crack closure. However, typical bulk techniques, such as a notch-mouth clip gage or a back-face strain gage (BFS), must be used very carefully when taking surface measurements.

A major problem in the use of compliance methods to determine the crack-opening point involves the exact position of the point at which the compliance is changed, as shown in Figure II-1. James et al [48] indicate that even in long-crack measurements (10-20 mm), when using the BFS (which has about twice the sensitivity of a notch-mouth clip gage) the change in compliance corresponding to the critical 100 microns behind the crack tip is only on the order of 2% for a/w = 0.4. Such a small change is extremely difficult to detect experimentally and the opening point is likely to be underestimated. Better resolution in determining the crack-opening point can be obtained by incorporating an offset elastic displacement circuit into the compliance measurement system. An offset displacement system is defined as

$$\delta' = \delta - a P \tag{2.7}$$

where a is chosen such that δ' is zero once the crack is fully open. With this method, the detectable crack length can be as small as 50 microns.

Techniques involving a SEM or laser-based interferometry are much more useful in measuring the small crack's behavior because they can measure crack opening displacement directly on the crack surface. Then the sensitivity in measuring the displacement is very high and the compliance change can be seen more clearly than is possible by the bulk technique.

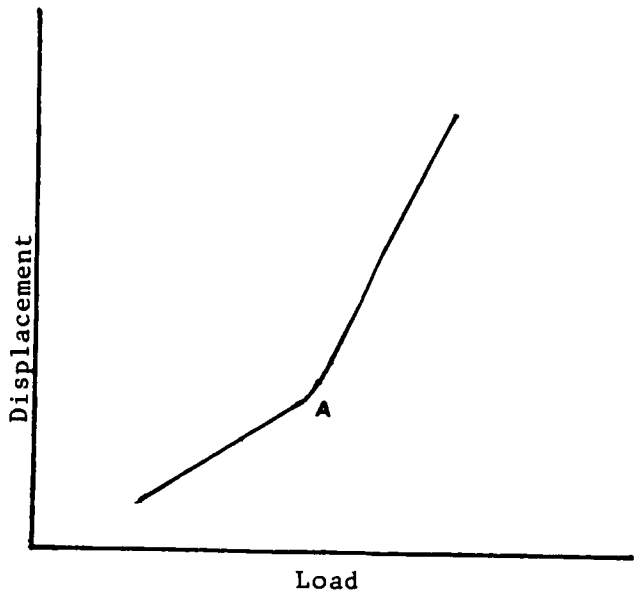

a) Compliance change is shown at point A

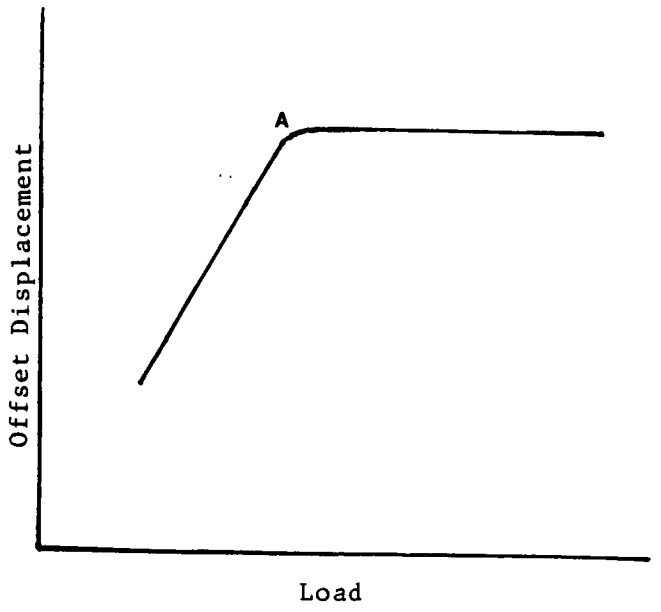

b) Offset displacement curve

Figure II-1. Typical load - displacement curve to determine crack opening point [48]

III. EXPERIMENTAL PROCEDURE

III-1. Materials and Specimens

The material used in this study was Al 2024-T3, an aluminum alloy which is widely used in the structures of airplanes. The stress-strain data of this material were found for monotonic and cyclic cases as follows [49].

$$\begin{aligned} s &= E\,e && \text{for } e \leqq e_1 \\ s &= K\,e^{n_1} && \text{for } e_1 \leqq e \leqq e_2 \\ s &= K\,e^{n_2} && \text{for } e > e_2 \end{aligned} \qquad (3.1)$$

where s is the stress in MPa
E is the elastic modulus in MPa
e is the strain
K_1 and K_2 are the material constants in MPa
n_1 and n_2 are the power hardening coefficients

The following values were found for monotonic and cyclic cases.

	E	K_1	K_2	e_1	e_2	n_1	n_2
Monotonic	73100	1013	431	0.0047	0.006	0.2	0.032
Cyclic	73100	5135	917	0.0049	0.0071	0.499	0.15

The specimens, which had a stress concentration factor of 3.17 (detailed in Appendix I-C), were supplied by NASA Langley Research Center and manufactured at Wright-Patterson Air Force Base. The material had a yield stress of 359 MPa and an

ultimate strength of 496 MPa [31]. The specimens had the single edge-notched geometry shown in Figure III-1. They had been chemically polished to remove the possible residual stress due to machining. They had also been given number labels; the same numbers were used in this study. Further preparation of the notch surface was carried out before the tests. The notch area was cleaned with acetone and etched with Keller's etchant for 25 seconds. Etching removed a very thin layer of material and revealed the grain structure, as shown in Figure III-2.

III-2. SPECIMEN FIXTURES

The loading conditions in this study included tension-tension conditions as well as tension-compression. The specimen fixture had to be carefully designed, and a procedure for aligning the specimen was developed so that the loading could be carried out without any bending or torsional effects.

As shown in Figure III-3, the devices include two base fixtures and two grip sets. The base fixture was constructed with a spherical joint, by which the parallelism of the base fixture to the test machine table (refer to Figure III-3) could be adjusted, and a mechanism which could raise a small block to contact with the specimen end for compressive loading. The base fixtures used in this experiment were made for a previously

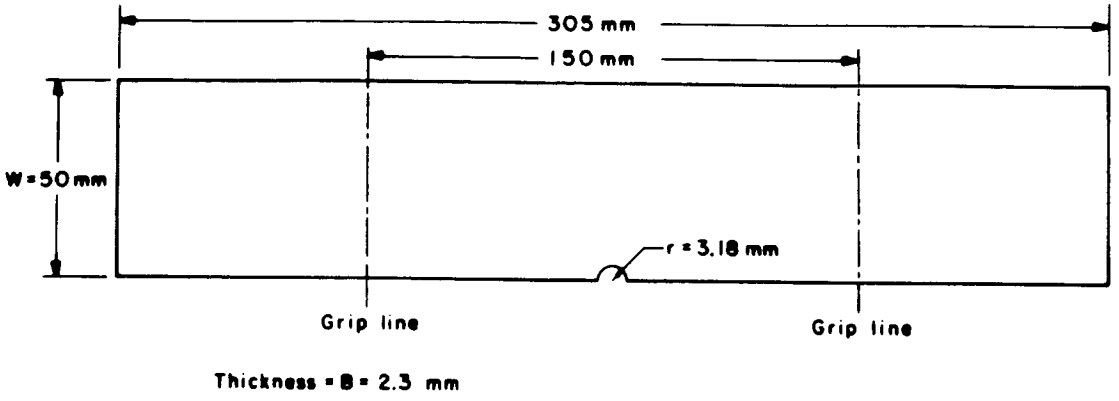

Figure III-1. Dimension of the specimen with a single-edge notch

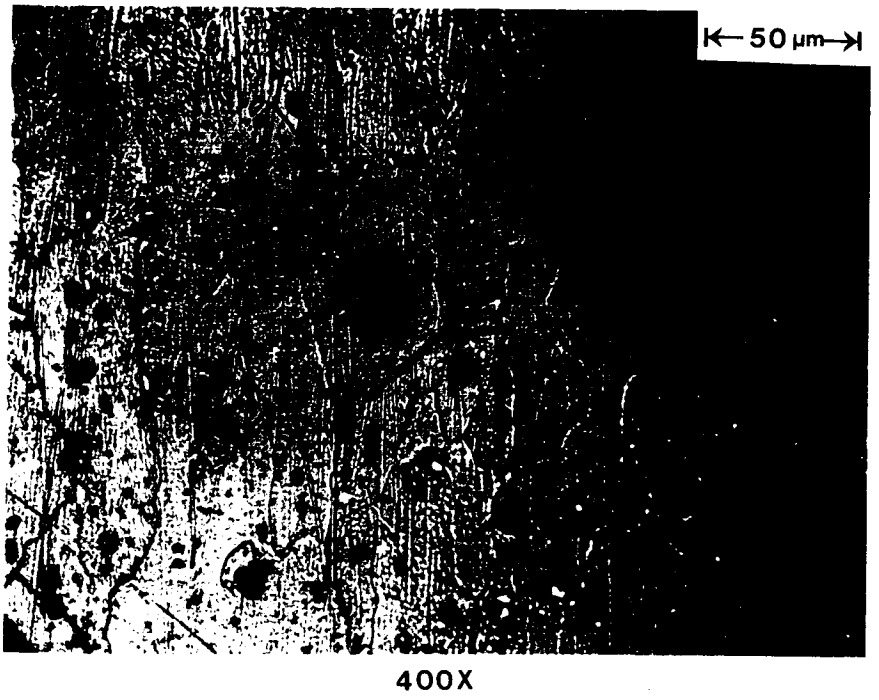

Figure III-2. Micrograph of typical grain structures of AL2024-T3 material

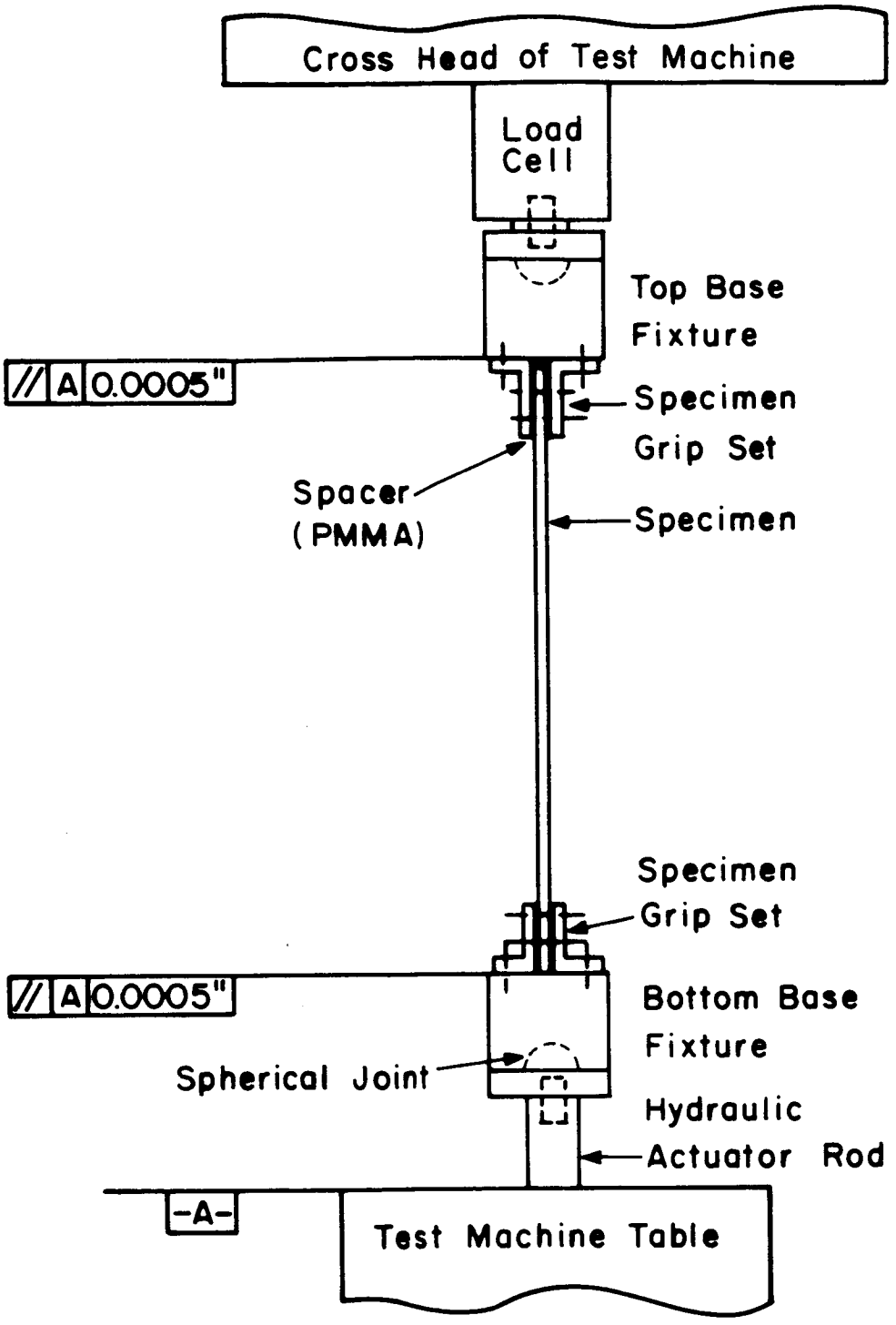

Figure III-3. Specimen fixtures and sketch of set up

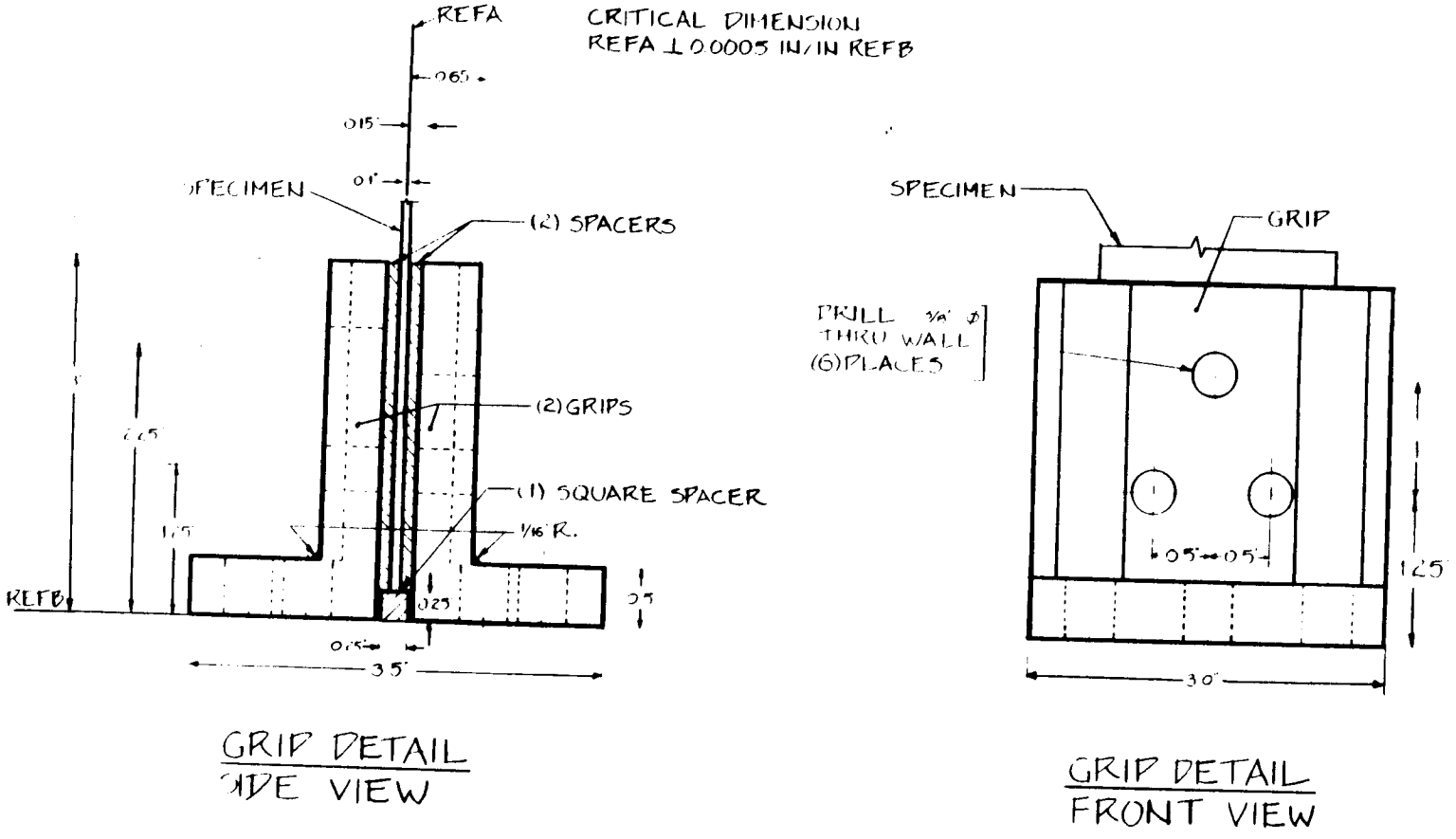

Figure III-4. Design of specimen grip set

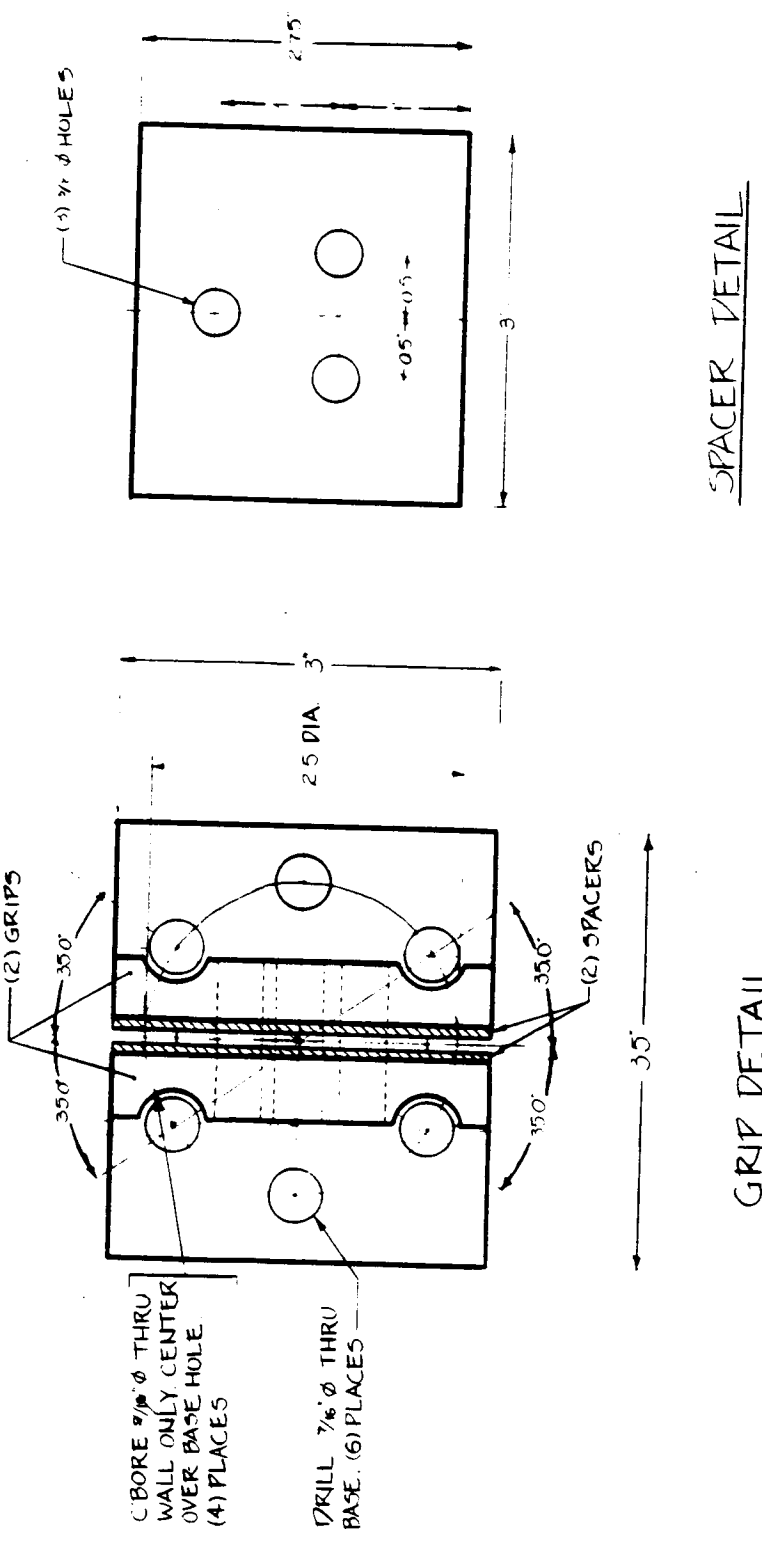

Figure III-4. Design of specimen grip set (continued)

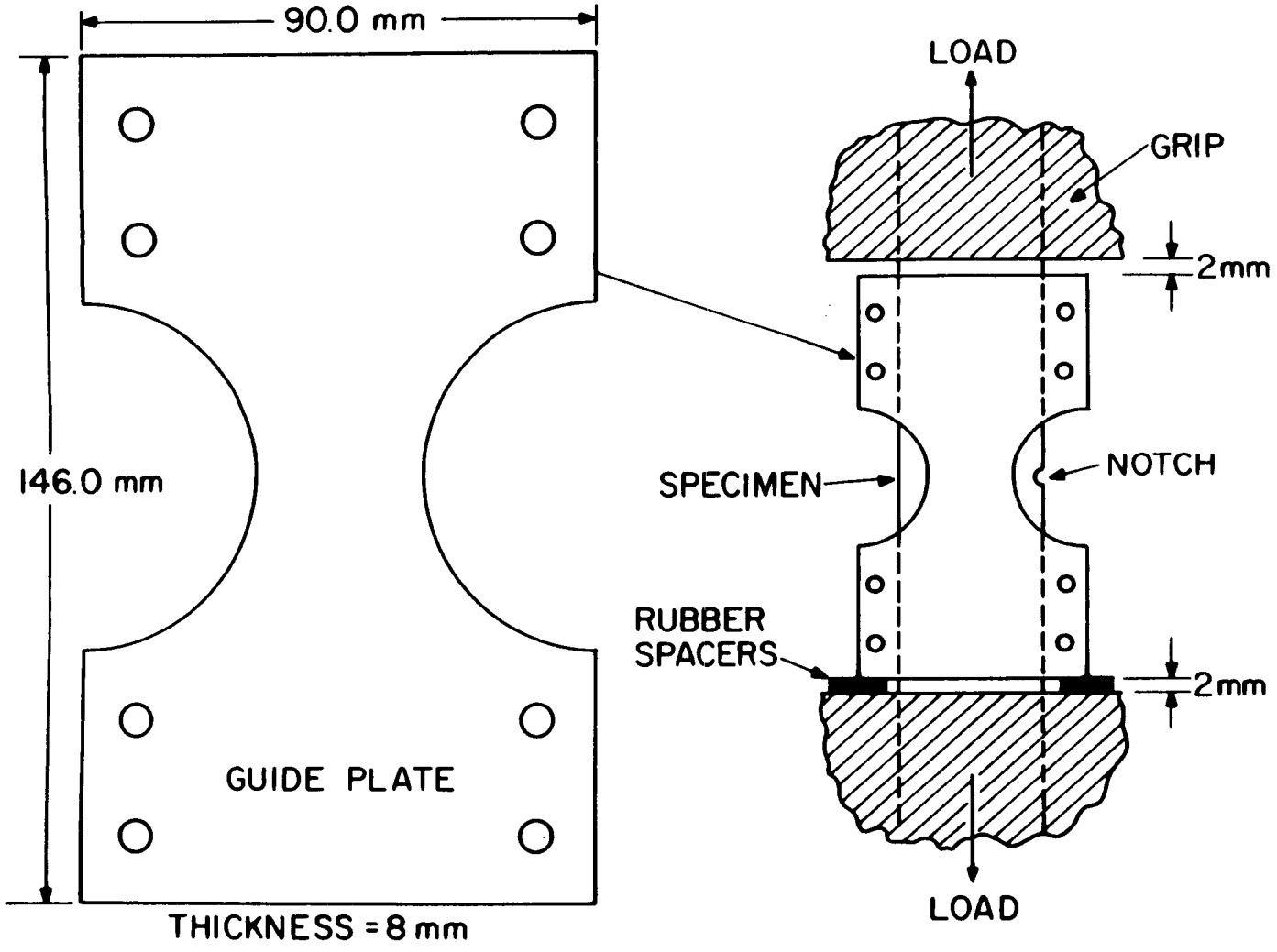

Figure III-5. Guide plate for compressive loads

conducted test. Only the specimen grip sets were made for this study. Figure III-4 shows the shape and dimensions of the grip. Part of the grip set was aligned and fixed to the base fixture. The other part of the grip set could be loosened to insert a specimen. The procedure of aligning fixtures and specimens is described in detail in Appendix I-D.

Three bolts were used at each end of the specimen to hold the specimen in place. The plastic (PMMA) spacers were used to prevent cracking in the gripping area.

For the compressive load tests, anti-buckling guides were made as shown in Figure III-5. To avoid unneccessary effects, the guides were not fastened tightly during the tests.

III-3. TEST SCHEDULE AND LOADING PROCEDURES

Test conditions were specified by NASA as part of an AGARD round-robin test program. The conditions are listed in Table III-1. Loading was to be performed under constant amplitude conditions at four different R-ratios: 0.5, 0.0, -1.0, and -2.0. Three different stress ranges were carried out for each loading, and two specimens were tested for each stress range. For each pair of specimens, one specimen was tested and data on crack length against cycles were recorded until a crack grew all the way across the notch root. The purpose of this

procedure was to obtain information on crack growth. The other specimen in the pair was tested until the crack length was less than 0.5 mm along the bore of the notch in order to examine the small crack characteristics. A total of 24 specimens were scheduled to be tested, all randomly selected for each test condition. Loading was performed using a MTS electro-hydraulic test machine with a capacity of 20 kips. The wave form for fatigue loading was sinusoidal, and the wave frequency was 20 Hz.

The crack lengths were monitored by a replica technique at regular intervals during the cycling; crack opening displacements were measured by ISDG technique at the end of each test. If a test was halted during fatigue cycling, the minimum load was maintained at the same or a higher value than the minimum load in the test to prevent excessive residual stress due to unloading.

For all tests, where the applied stress is less than zero, anti-buckling guides were used. All tests were conducted under laboratory air and room temperature conditions.

TABLE III-1
TEST SCHEDULE

Stress ratio, R	Maximum Gross Stress, Smax(MPa)	Specimen Number	*Estimated Fatigue Life (kilocycles)
0.5	225	A-54-04 A-65-07	50
	205	A-71-05 A-68-22	130
	195	A-71-05 A-59-13	500
0.0	145	A-52-03 A-51-16	50
	120	A-82-16 A-59-30	130
	110	A-57-14 A-80-28	500
-1.0	105	A-55-27 A-67-08	50
	80	A-65-24 A-72-07	150
	70	A-55-08 A-83-23	200
-2.0	75	A-52-21 A-74-20	20
	60	A-75-16 A-84-20	60
	50	A-80-11 A-68-05	250

* Number of cycles required for the longest crack length, through the thickness of the specimen [49]

III-4. CRACK LENGTH MEASUREMENT

The crack growth along the bore of the notches was monitored using the acetate replica method described in Appendix I-B. The replica technique has several advantages in this application, particularly in measuring small cracks:

a) The sheets of replica can be stored permanently so that they can be examined again at a later time to find the smaller cracks.

b) The surface of the bore of the notch can be thoroughly examined, even the area far from the center of the specimen which is very difficult to observed directly with a regular microscope.

The fatigue loading was interrupted periodically to take the replicas. In general, 25-30 replicas were taken during a longer test, which was continued until a crack grew through the specimen. The interval between replicas differed between specimens. It was chosen based on the estimated fatigue life; i.e., every two kilocycles for the life less than 50 kilocycles, every five kilocycles for the life between 50 and 200 kilocycles, and every ten kilocycles for over 200 kilocycles.

The replica was taken at 80% of maximum load because the cracks were expected to be fully open at this point. Each replica was taped on a microslide and observed with an optical microscope at either 200X or 400X magnification.

III-5. CLOSURE MEASUREMENT

Crack opening displacements (COD) were measured using a laser-based interferometric technique. Only a brief discusssion will be included here; for more details, see reference 41.

The Interferometric Strain/Displacement Gage (ISDG) technique is especially useful in the study of small cracks, since it has a very small gage length, from 20 μm to about 100 μm, and can measure the relative displacement with a resolution of approximately 0.02 micron. Two small indentations were placed across a short fatigue crack with a Vicker's microhardness tester, as shown in Figure III-6. When these two indentations are illuminated with a laser, interference fringe patterns are produced. As the indentations move away from each other, the fringe patterns also move, and this motion is easily associated with the relative displacement, Δd:

$$\Delta d = \frac{\Delta m_u + \Delta m_l}{2} \cdot \frac{\lambda}{\sin \alpha_o} \qquad (3.2)$$

where λ is the wave length of the laser and α_o is the angle betweem the incident laser beam and the reflected pattern. Δm_u and Δm_l are the relative fringe motion of the two patterns in the plane containing the axis of measurement. λ is equal to 632.8 nm for the He-Ne laser used in this experiment, while α_o is approximately 42^o. Thus the calibration factor, $\frac{\lambda}{\sin \alpha_o}$

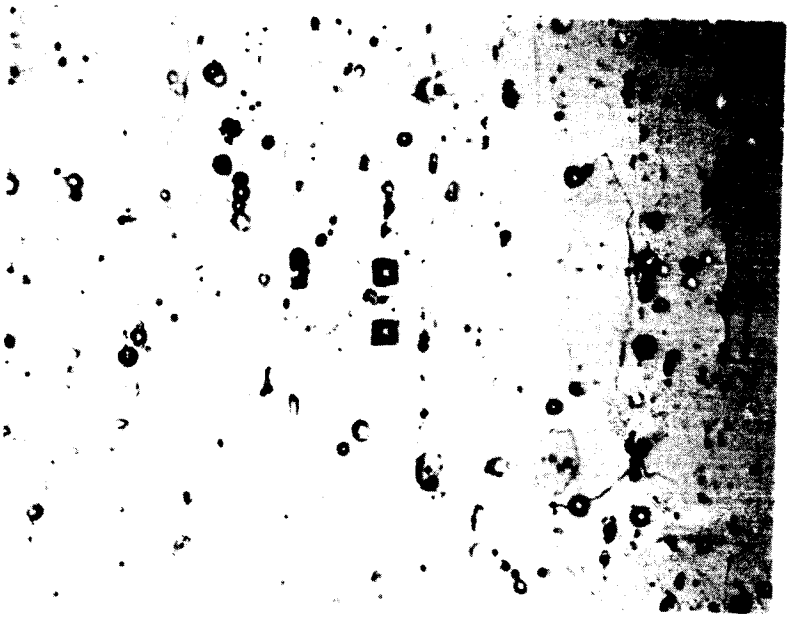

a. Indentations were placed with a spacing of 20 μm across a 35 μm long crack (400x)

b. Indentations were placed with a spacing of 75 μm across a through-thickness (2.3mm) crack. (200x)

Figure III-6. Typical micrograph of indentations across a crack

is about 1 micron. While the ISDG technique has been used for COD measurements on flat specimens, some changes were required to enable COD measurements along the bore of semi-circular notches in a long specimen.

Spurious reflections from the semi-circular region which interrupted the interference fringes were eliminated by spraying the entire notch area, except for the immediate area around the crack, with flat black paint, as shown in Figure III-7. A large rigid body motion due to the greater elongation of a long specimen moved the indentations out of the incident laser beam as the load was applied. The problem was solved by rewriting the loading and data acquisition programs to allow readjustment of the laser beam. The loading and data acquisition programs are listed in Appendix I-E.

Closure loads were automatically determined from COD versus load data by a computer program, which is listed in Appendix I-E. It is recognized that highly accurate values for closure loads are not easily determined. Closure loads can be defined with reasonable accuracy by using a reduced data method [46,48,50].

A typical example of this method is shown in Figure III-8. A least-square line is fitted to the upper linear portion of the COD curve. In the linear portion, it is assumed that the crack is fully opened. The reduced data are obtained by subtracting values of the fitted line from the original data. Then the closure load is defined at the point where the reduced

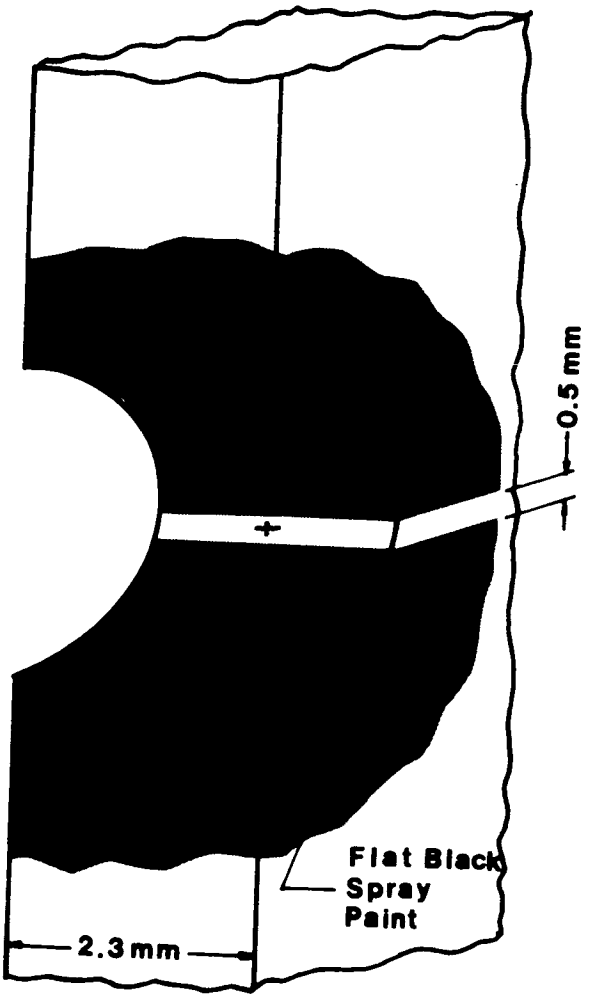

Figure III-7. Black paint spray on the notch root except the crack area to prevent spurious reflection of laser beam

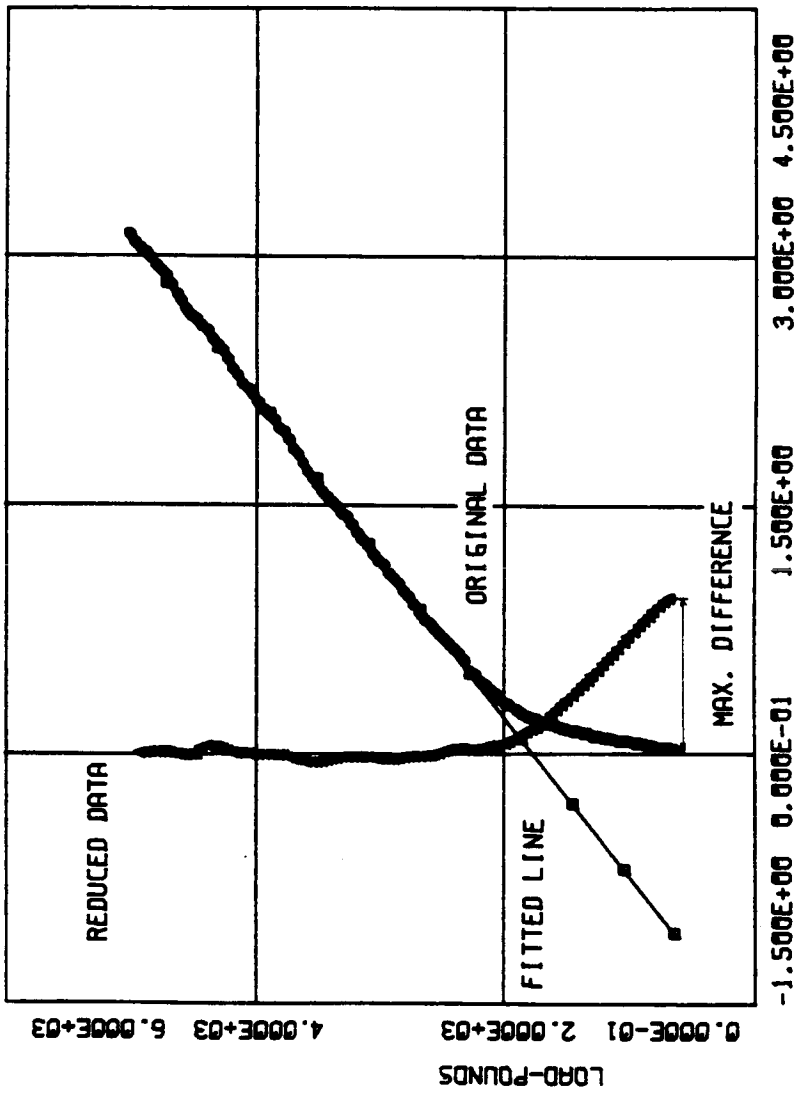

Figure III-8. Reduced data method from a load-COD curve

data become zero. It is too ideal a case to pick the point where the data are exactly equal to zero because the linear portion of the original data is not perfectly linear. It is more reasonable that the closure load be determined at the point where the deviation of the reduced data becomes 10% of the maximum difference. These procedures incorporate a computer program to prevent arbitrary errors which accompany measurements made by eye.

IV. RESULTS AND DISCUSSION

Results of the crack growth tests are summarized in Table IV-1. The column heading "Initiation Cycles" corresponds to the number of cycles completed when the first crack was observed through examination of the replica under an optical microscope. "Location" implies the location of the crack at its point of origin. The following abbreviations were used in this column:

C : Edge of the specimen at the notch root
N : Near the edge of the specimen at the notch root
S : Center of the specimen at the notch root

The cracks labeled "C" were corner cracks, while those labeled "S" were surface cracks. Cracks labeled "N" were originally surface cracks but usually changed to corner cracks as they grew. The heading "Crack Length" implies the total surface length, which corresponds to 2a for a surface crack and a for a corner crack, as defined in Figure IV-6. "L1, L2,..L5" in the "Final Crack Length" column designates several cracks wich appeared in the same specimen simultaneously or sequentially. "Total Test Cycles" means the number of cycles completed at the time when the crack grew through the section. The tested lives are in reasonably good agreement with the estimated fatigue life in Table III-1.

TABLE IV-1
SUMMARY OF TEST RESULTS

R	Maximum Stress (MPa)	Specimen Number	Initiation Cycles (X1000)	Initial Crack Length (mm)	Location	Final Crack Length (mm)	Total Test Cycle (X1000)
0.5	225	A-54-04	26	0.080	N	L1 0.5	
		A-65-07	42	0.033	S	L1 2.3	121
					S	L2.. L1	
					S	L3.. L1	
					S	L4.. L1	
	205	A-71-05	20	0.044	S	L1 2.25	117
					S	L2 0.251	
					S	L3 0.174	
					S	L4 0.114	
					N	L5 0.169	
		A-68-22	35	0.049	N	L1 0.545	
					S	L2 0.18	
	195	A-84-03	690	0.098	C	L1 1.55	760
		A-59-13	130	0.027	S	L1 0.403	
					S	L2..L1	
					S	L3 0.022	
0.0	145	A-52-03	6	0.025	S	L1..L3	
					S	L2 0.131	
					S	L3 2.25	53
					S	L4..L3	
		A-51-16	8	0.022	S	L1 0.038	
					S	L2 0.245	
					N	L3 0.234	
	120	A-82-16	60	0.093	C	L1 2.25	138
		A-59-13	No crack found in 660,000 cycles				
	110	A-57-14	80	0.225	S	L1 2.19	130
		A-80-28	100	0.082	C	L1 0.40	
-1.0	105	A-55-27	4	0.032	S	L1 2.25	20
					C	L2 0.431	
					C	L3 0.22	
					C	L4..L1	
					S	L5 0.164	
		A-67-08	7	0.044	S	L1 0.398	
					S	L2 0.19	
					C	L3 0.19	
					C	L4 0.19	
					C	L5 0.218	

TABLE IV-1 (cont.)
SUMMARY OF TEST RESULTS

R	Maximum Stress (MPa)	Specimen Number	Initiation Cycles (X1000)	Initial Crack Length (mm)	Location	Final Crack Length (mm)	Total Test Cycle (X1000)
-1.0	80	A-65-24	40	0.016	S	L1 2.25	125
					S	L2 0.343	
					S	L3 0.229	
					S	L4 0.055	
					S	L5..L1	
		A-72-07	40	0.050	S	L1 0.050	
	70	A-55-08	120	0.065	S	L1 2.25	290
					S	L2 0.30	
					S	L3 0.20	
					S	L4..L1	
		A-83-23	70	0.044	C	L1 0.382	
					C	L2 0.267	
					S	L3 0.229	
					C	L4 0.20	
					S	L5 0.065	
-2.0	75	A-52-21	2	0.027	S	L1 2.25	20
					S	L2 0.071	
					S	L3 0.518	
					S	L4..L1	
					S	L5..L1	
		A-74-20	4	0.035	S	L1 0.035	
	60	A-75-16	15	0.010	S	L1 1.809	110
					S	L2..L1	
					C	L3..L1	
					S	L4 2.175	
					S	L5..L4	
		A-84-20	15	0.015	S	L1 1.809	
					C	L2..L1	
					S	L3..L1	
					S	L4 2.175	
					S	L5..L4	
	50	A-80-11	715	0.050	S	L1 0.10	
		A-68-05	30	0.093	C	L1 1.515	362
					C	L2..L3	
					C	L3 2.25	
					S	L4 0.436	

Two of the 24 specimens tested in this experiment showed some unexpected behavior. The specimen A-84-03, which was cycled with a maximum stress of 195 MPa (54% of yield stress) at R = 0.5, was broken during cycling at almost 760 kilocycles. A crack was found at 690 kilocycles at the center of the notch root and grew as a surface crack. This crack propagated quickly, growing from 0.561 mm to 1.55 mm in 10 kilocycles at 740 kilocycles.

The broken fracture surface was photographed with an SEM at Kentron International Inc. [60] to examine the fatigue propagation (Figure IV-1). The first micrograph was taken at 1 mm from the notch; the second and third are at 8 mm and 15 mm, respectively. Even the picture at 25 mm shows the striation marks which prove fatigue cracking. The plane strain fracture toughness for Al 2024-T3 is 44 MPa-$m^{\frac{1}{2}}$ [60]. An approximate calculation of the critical crack length based on the plane strain fracture toughness is 13 mm. But the thickness (2.3 mm) of this material is not enough to satisfy the plane strain condition,

$$B \geq 2.5 \frac{(K_{IC})^2}{(\sigma_{ys})^2} \qquad (4.1)$$

where B would be greater than 37 mm for K_{IC} = 44 MPa-$m^{\frac{1}{2}}$ and σ_{ys} = 359 MPa. Therefore, the fracture toughness of this specimen will be larger than K_{IC} and the critical crack length will be

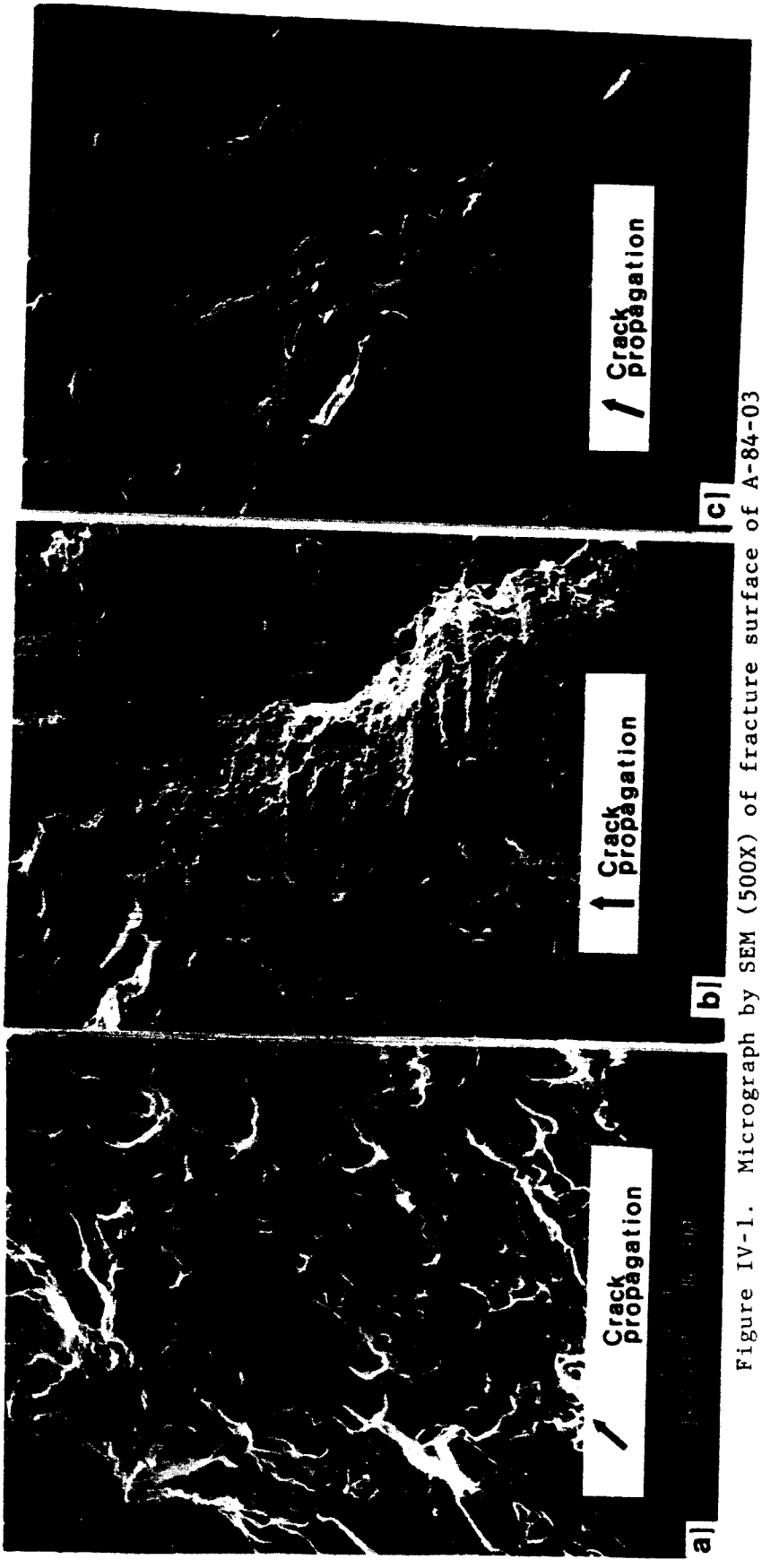

Figure IV-1. Micrograph by SEM (500X) of fracture surface of A-84-03 a), b), c) are taken at 1mm, 8mm, 15mm from the notch respectively.

(courtesy of [60])

longer.

For another specimen, A-59-30, which was cycled with a maximum stress of 120 MPa at R = 0.0, no crack was observed after 660 kilocycles. The estimated fatigue life [49] at this load condition is 130 kilocycles. No explanation could be made for this unexpected behavior.

IV-1. Analysis of Replicas

For each loading condition, two specimens were tested. In one, a crack was allowed to grow through the thickness of the specimen (approximately 2.3 mm) in order to obtain growth data; in the other, a small crack (up to 500 μm) was grown so that short crack behavior might be examined. From five to 70 replicas were taken for each test to monitor the initiation and growth of each crack. These replicas were observed closely under an optical microscope. The length and location of each crack were measured and crude maps were sketched on the magnified scale. Crack maps of all the tests are shown in Appendix II.

A typical example of a crack map, tracing the growth of a crack from first observation through the thickness of the specimen, is shown in Figure IV-2. This is the data from specimen number A-55-08 with a maximum remote stress of 70 MPa at a stress ratio of -1.0. The width of the sketch corresponds

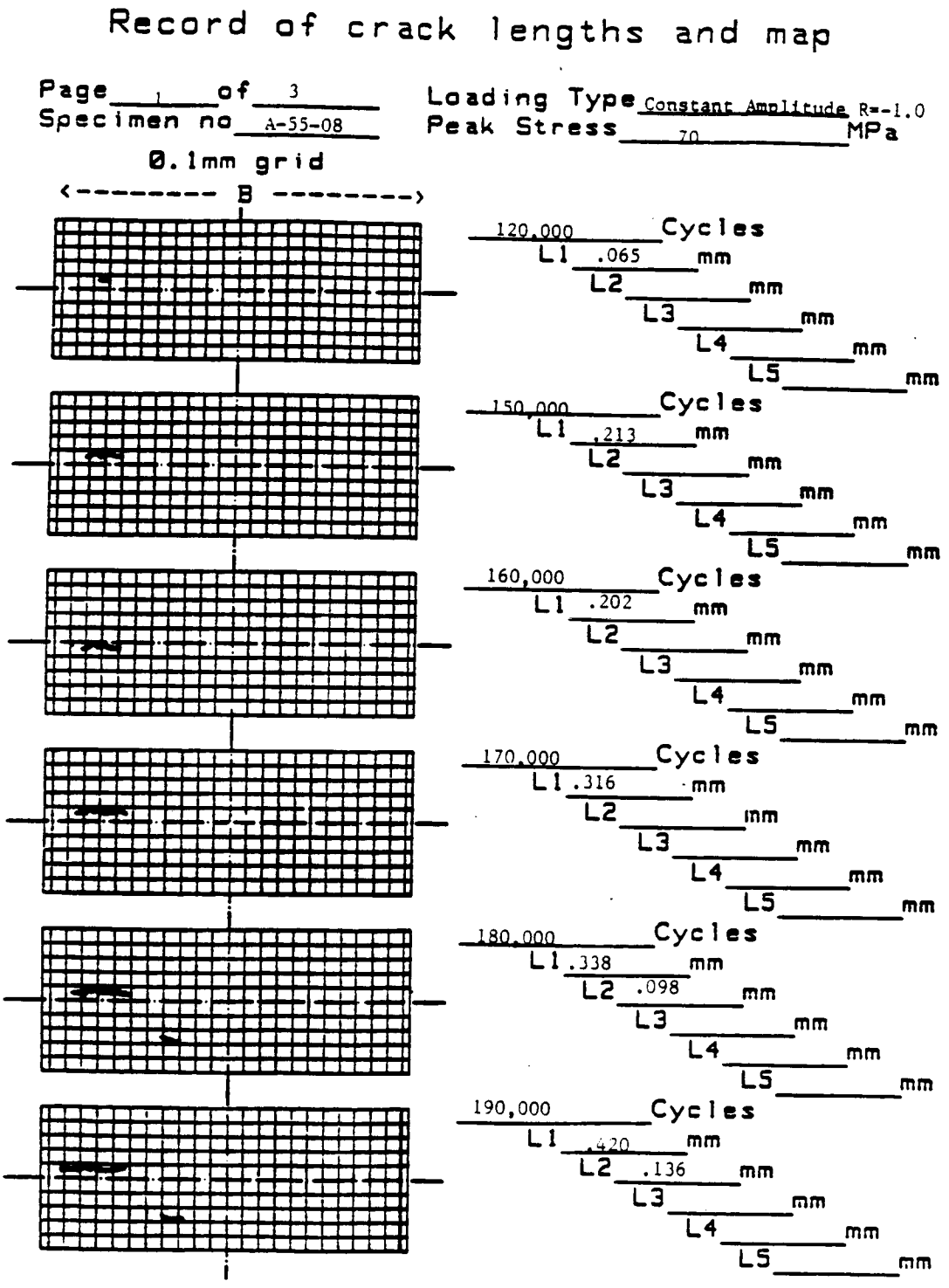

Figure IV-2. Typical example of a crack map

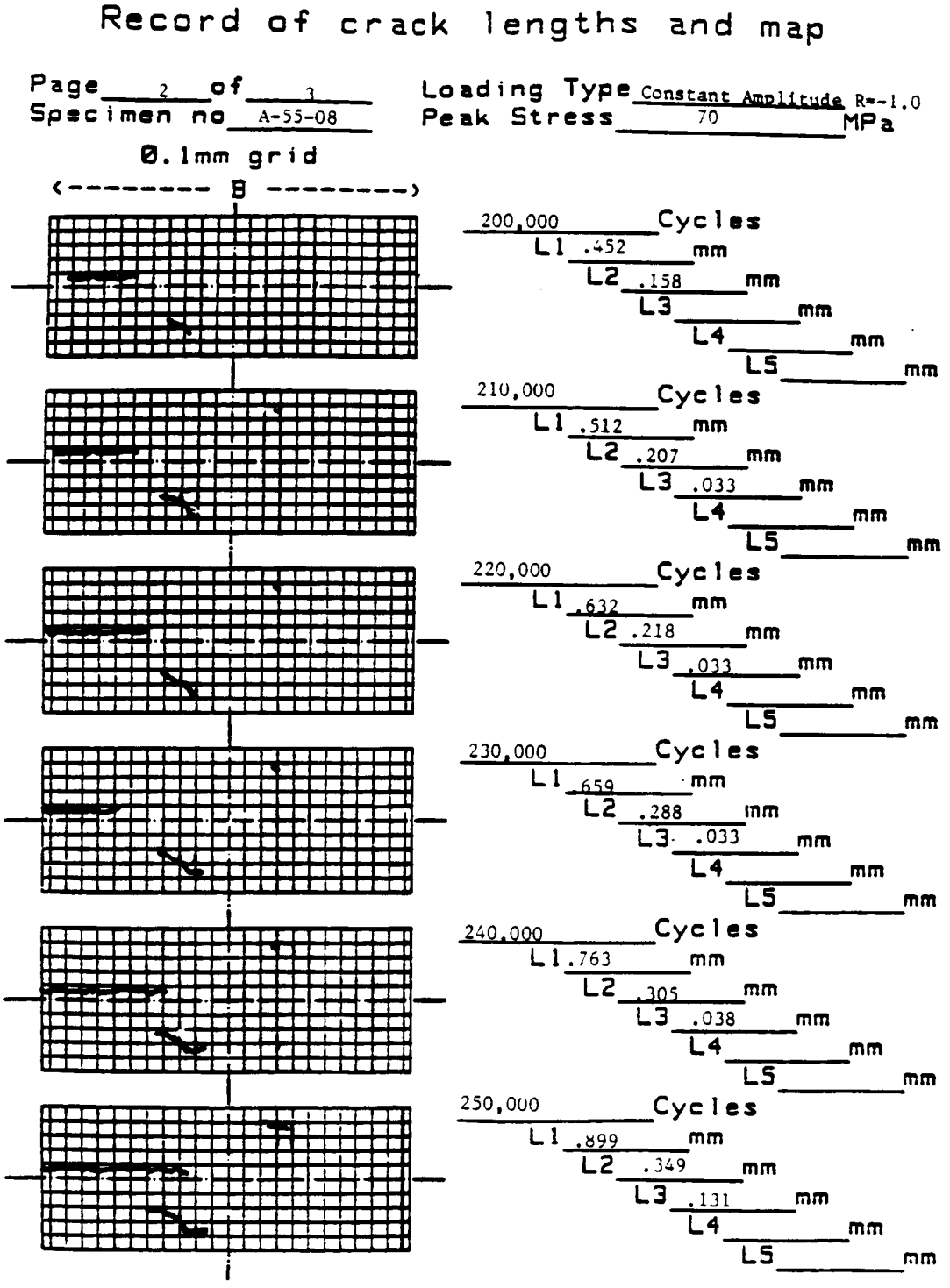

Figure IV-2. Typical example of a crack map (continued)

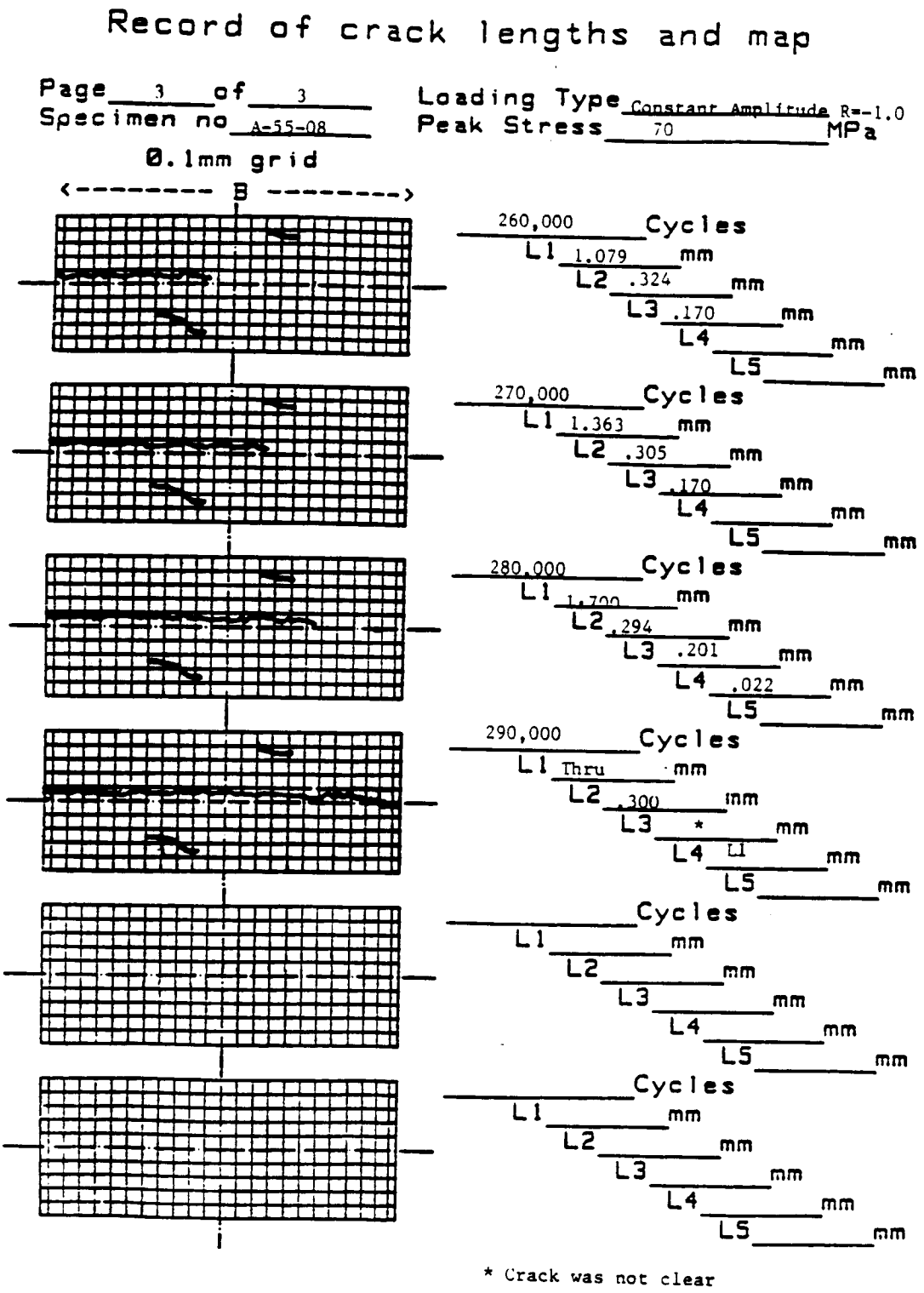

Figure IV-2. Typical example of a crack map (continued)

to the specimen thickness, and all dimensions are at the same scale. The crack originated along the centerline of the notch root near the edge of the specimen after 120,000 cycles. Replicas were taken every 10,000 cycles for this test, so the first visible crack was 65 micrometers long before it was found. The crack grew toward the center and the edge. Another crack initiated near the center of the specimen at 180,000 cycles. A third crack appeared at the upper side of the notch at 210,000 cycles. The first crack grew continuously, but the second and third cracks stagnated after growing for a short time. Information about crack initiation and the crack growth rate behavior can be obtained from the crack maps.

IV-2. Crack Initiation Analysis

It was convenient to examine crack initiation by observing the replicas, even after the tests were finished. The smallest observable crack was approximately 10 μm long, viewed under an optical microscope at 400X magnification. The number of cycles, crack lengths, and locations measured when each crack was first observed are shown in Table IV-1. The number of cycles to crack initiation appeared to be of the same order of magnitude as the loading condition, with the same stress ratio and stress level, except for the case of the smallest stress levels at R = 0.5 and R = -2.0. This result can be regarded as quite consistent, considering that most fatigue test data have shown a tendency to be scattered over a substantially large band. The first observed crack lengths varied from 10 to 100 micrometers, since the replicas were taken at certain fixed intervals, as mentioned before.

In most cases, a single crack nucleated and several other cracks appeared sequentially. In only three specimens out of the 24 tested -- one where S_{max} = 195 MPa and R = 0.5 and two with S_{max} = 105 MPa and R = -1.0 -- were multiple cracks initiated at the same time. Considering the stress, multiple initiation was expected at the highest applied stress level, as in the case where R = -1.0. But this was not true for R = 0.5.

Most of the crack nucleations were observed along the bore of the notch rather than at the corner. The cases where initiation occurred at a corner may be attributed to mechanical defects from the machining procedure.

It was found that most surface cracks which were initiated at the bore of the notch were nucleated at the inclusion particles, as shown in Figure IV-3. This phenomenon was observed in many other experiments [1,3,18,30,31,42,43,52], especially in commercial aluminum alloys [1] and has been called brittle initiation. If the crack is initiated in this brittle manner, the plastic zone may be considered quite small (estimated to 10^{-3} in [52]). But this estimation is limited to the very beginning of crack initiation. Another estimation of plastic deformation at the crack tip [53] is calculated as follows.

$$r_o = 0.002 \left(e_m / S_o / E \right)^2 \qquad (4.2)$$

where r_o is the radius of the plastic zone

e_m is the maximum value of the applied tensile strain

S_o is the yielding stress

E is the elastic modulus

Using this equation, the size of the plastic zone surrounding a crack in Al 2024-T3 was calculated to be 0.05 mm, given that $e_m = 0.0049$ (measured at the root of the notch by ISDG technique, when the corresponding remote stress was 110

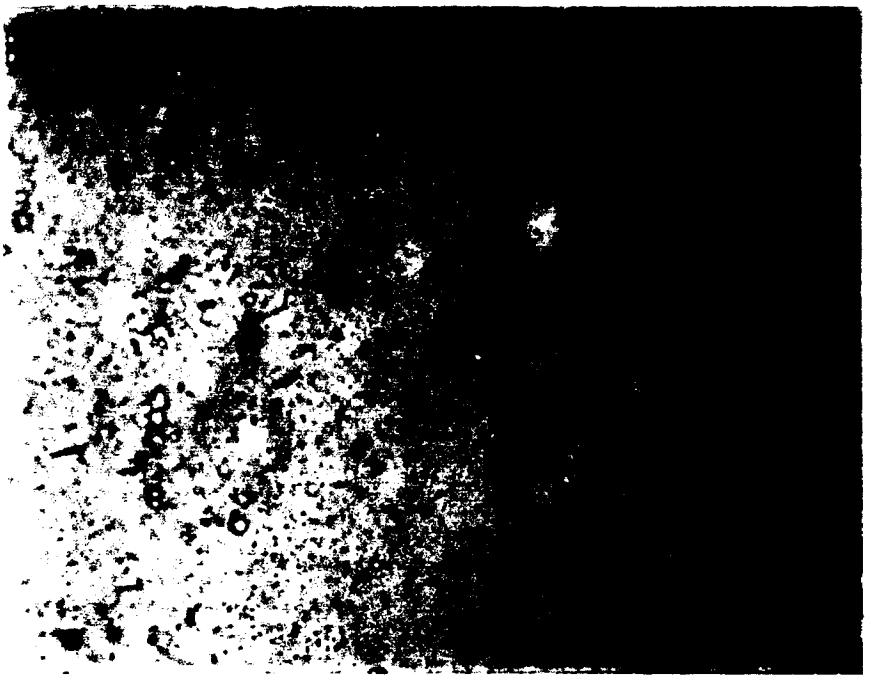

400X

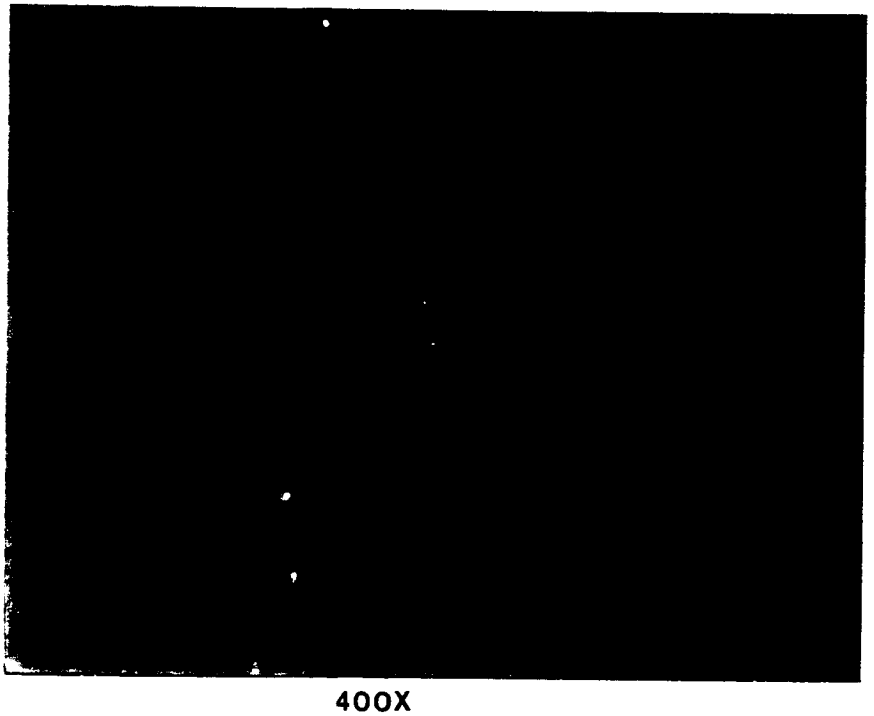

400X

Figure IV-3. Micrograph of the example of crack initiation at inclusions.

MPa), S_o = 359 MPa, and E = 73,100 MPa.

Based on the lower extreme of brittle initiation (former case of above estimation), the criteria of linear elastic mechanics (LEFM) are satisfied at a crack length of about 0.01 mm. For the latter case, a crack length must be longer than 0.5 mm to apply LEFM. But the applied stress must be low enough to avoid general yielding in the notch root for any case.

Crack initiation cycles were calculated from the Manson-Coffin equation and Neuber's rule as follows. The Manson-Coffin relationship is expressed in the form

$$\frac{\Delta\varepsilon}{2} = \frac{\sigma_f - \sigma_m}{E} (2N)^b + \varepsilon_f (2N)^c \qquad (4.3)$$

where E is the elastic modulus
σ_f, ε_f, b, and c are material constants; for Al 2024-T3, these are equal to 1100 MPa, 0.22, 0.124 and 0.59, respectively [59]
σ_m is the mean stress
$\Delta\varepsilon$ is the total strain amplitude

$\Delta\varepsilon$ is obtained by solving two simultaneous equations, Neuber's rule and the stress-strain relationship, using an iteration method:

$$\Delta\varepsilon \, \Delta\sigma = K_t^2 \, \Delta e \, \Delta s \qquad (4.4)$$

and

$$\Delta\varepsilon = \frac{\Delta\sigma}{E} + \left(\frac{\Delta\sigma}{K'}\right)^{\frac{1}{n'}} \qquad (4.5)$$

where $\Delta\varepsilon$ and $\Delta\sigma$ are the notch strain and stress amplitudes
Δe and Δs are the remote strain and stress amplitudes
K_t is the stress concentration factor, equal to 3.17 for the geometry of the specimen used in this experiment
K' and n' are material constants, equal to 655 and 0.065 respectively for Al 2024-T3

As shown in Table IV-2, initiation cycles observed in this experiment are in good agreement with values predicted by the Manson- Coffin equation for the two highest stress levels at each R-ratio, with the best agreement at R = -1.0 and -2.0. Figure IV-4 shows this agreement of tested initiation cycles and calculated values for R = -1.0 in which the mean stresses are zero for all applied stress ranges. The close agreement in short fatigue lives was expected, since the Manson-Coffin relationship was derived for low-cycle fatigue.

TABLE IV-2
TEST RESULTS OF CRACK INITIATION

Stress Ratio, R	Maximum Stress (MPa)	Specimen Number	Tested Initiation Cycles (X1000)	Predicted Initiation Cycles (X1000)	Ratio of Initiation Cycles* To Total Life*
0.5	225	A-54-04	26		0.21
		A-65-07	42	22.5	-
	205	A-71-05	20		0.17
		A-68-22	35	54.3	-
	195	A-84-03	690		0.91
		A-59-13	130	90.2	-
0.0	145	A-52-03	6		0.11
		A-51-16	8	30.5	-
	120	A-82-16	60		0.43
		A-59-30	*	191.8	-
	110	A-57-14	70		0.61
		A-80-28	100	428.2	-
-1.0	105	A-55-27	4		0.2
		A-67-08	7	3.0	-
	80	A-65-24	40		0.32
		A-72-07	40	38.4	-
	70	A-55-08	120		0.41
		A-83-23	70	157.4	-
-2.0	75	A-52-21	2		0.1
		A-74-20	4	2.2	-
	60	A-75-16	15		0.14
		A-84-20	15	16.5	-
	50	A-80-11	715		-
		A-68-05	30	114.3	0.08

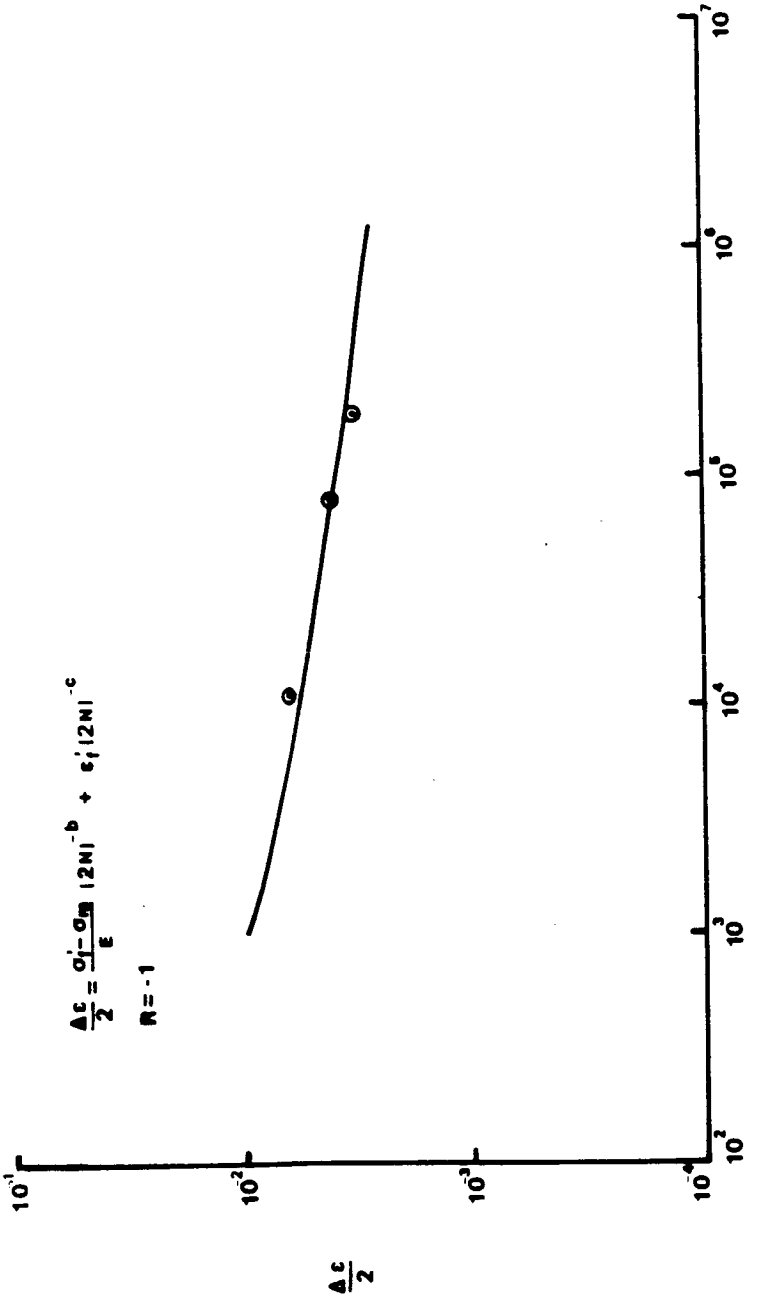

Figure IV-4. Crack initiation life compared with predicted value by Manson-Coffin relationship

In addition, the ratio of initiation cycles to tested total life (the test was stopped when the crack grew through the section) is shown in Table IV-2. The ratio appears with a range of 0.1 to 0.9. For some pure metals in which the crack usually initiated at a slip band (in a ductile manner), the number of cycles required to produce a detectable crack was known to be a small proportion (a few percent) of the total life. In experiments with commercial aluminum alloys, Pearson [1] showed that the number of cycles to the initiation of a crack was equal to 40-60% of failure, a much higher ratio than is found in the pure metals.

The ratios of crack initiation cycles to tested total life are plotted against stress ranges for different R-ratios in Figure IV-5. The data is scattered in a wide band, but a tendency toward increasing crack initiation life with decreasing stress ratio can be observed, except in the cases where ΔS = 102.5 MPa at R = 0.5 and for $\Delta S \doteq$ 150 MPa at R = -2.0.

Also, the range of crack initiation life to tested total life is observed to be 10-40% for R = -1.0 and -2.0, and 20-90% for R = 0.5 and 0.0. This dependence of crack initiation life on R-ratio was shown by Sova et al [2]: approximately 70% of fatigue life at R = 0.5 and 0.0 and 40% of fatigue life at R = -0.5 and -1.0 for the material Al 2024- T3, the same material used in this study.

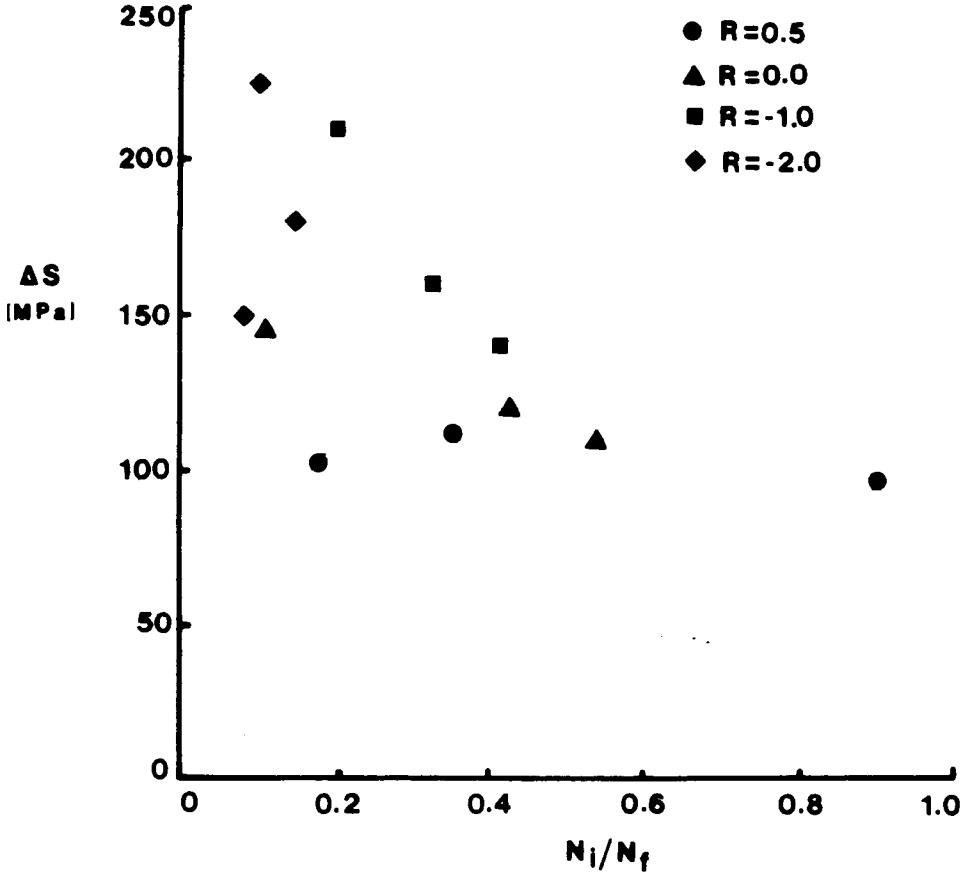

Figure IV-5. Crack initiation life versus fatigue stress range

IV-3. Crack Shape

After testing, the specimens were broken open to examine the shapes of short and through-thickness cracks. The typical short crack, defined as a surface crack less than 0.5 mm long, was observed to be either a semi-elliptical surface crack or a quarter-elliptical corner crack, as shown in Figure IV-6. The dimensions of a semi-elliptical surface crack are given in this figure; 2a is the surface crack length and c is the crack depth. For a quarter-elliptical corner crack, a is the surface crack length and c is the crack depth. The surface crack lengths and crack depths as measured from the broken surface are listed in Table III-3 with the calculation value of the crack depth, c, taken from the following empirical equation [49]:

$$c/a = 0.9 - 0.25 \left(a/t \right)^2 \qquad (4.6)$$

where a is the half-length of the crack for a surface crack and the edge length for a corner crack. The parameter t represents half the specimen thickness for a surface crack and the full specimen thickness for a corner crack, as defined in Appendix I-A, Figure A-1.

The crack depths could not be measured during the tests; yet this value was needed in order to calculate the stress intensity factor without significant error. The calculated crack depth values agree quite well with measured values, as

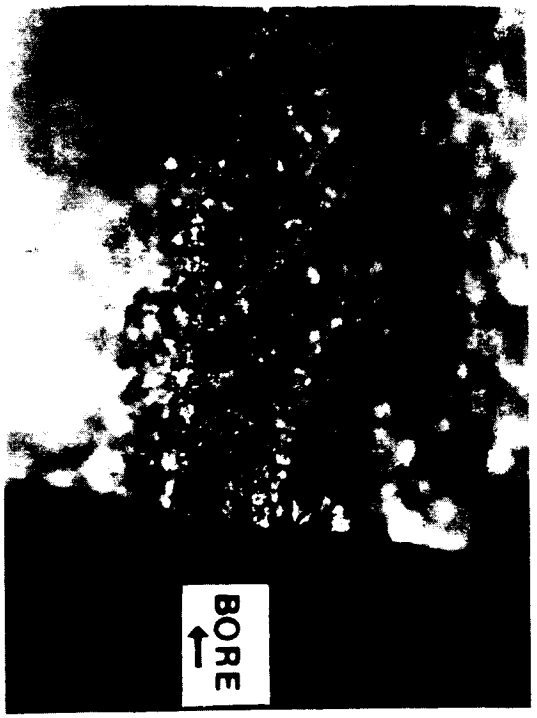

Micrograph of fracture surface
(50X)

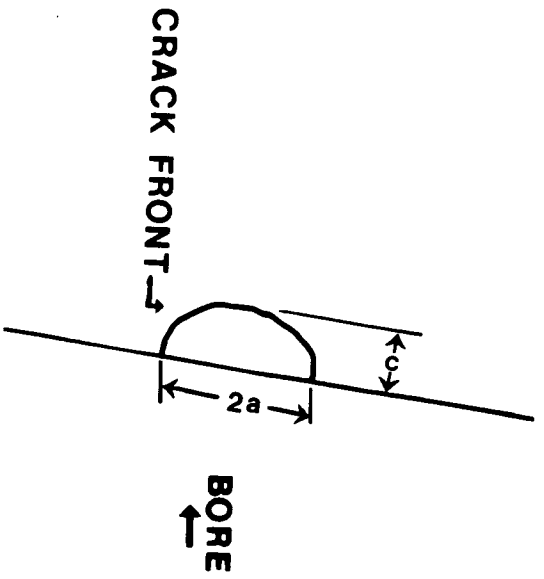

Tracing of crack front

a) Semi-elliptical surface crack

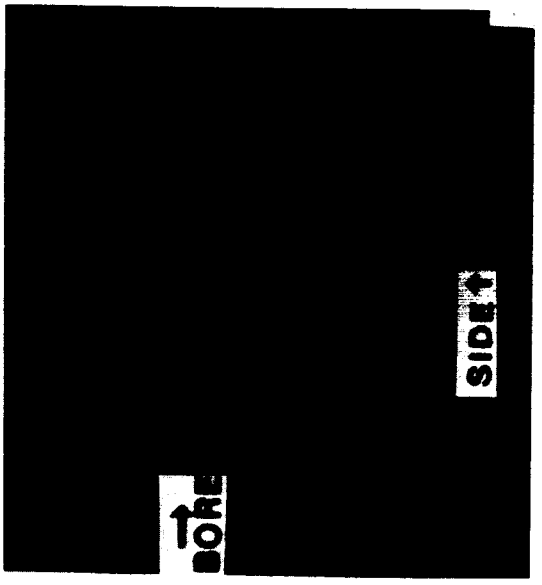

Micrograph of fracture surface
(50X)

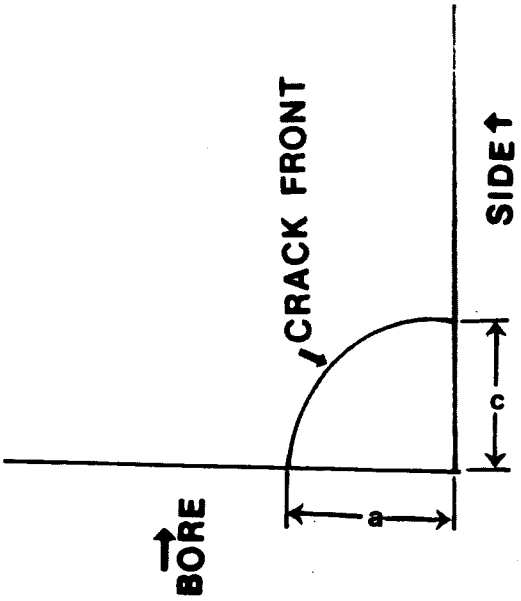

Tracing of crack front

b) Quarter-elliptical corner crack

Figure IV-6. Typical crack shape of short cracks observed in this study.

Table IV-3 shows. This agreement has been proven in other work [31]. Therefore, the crack depths calculated from the above equation may be used to find the stress intensity factor without significant error.

TABLE IV-3
DIMENSIONS OF SMALL CRACKS

Specimen Number	Surface Crack Length (mm)	Crack Shape	Measured Crack Depth (mm)	Calculated Crack Depth (mm)
A-54-04	0.54	C	0.42	0.478
A-68-22	0.545	C	0.48	0.483
A-59-13	0.403	S	0.18	0.180
A-51-56	0.245	S	0.12	0.110
A-80-28	0.414	C	0.38	0.370
A-67-08	0.398	S	0.18	0.173
A-83-23	0.229	C	0.32	0.333
A-84-20	0.174	C	0.16	0.156
A-80-11	0.100	S	0.04	0.045

S : semi-elliptical surface crack
C : quarter-elliptical corner crack

TABLE IV-4
DIMENSIONS OF THROUGH-THICKNESS CRACKS

Specimen Number	Surface Crack Length (mm)	Crack Depth* Measured (mm)
A-65-07	2.3	1.31
A-71-05	2.25	2.27
A-52-03	2.25	1.1
A-82-16	2.25	2.69
A-57-14	2.19	1.65
A-65-24	2.25	1.26
A-55-08	2.25	1.3
A-52-21	2.25	1.35
A-75-16	2.175	0.88
A-68-05	2.25	1.23

The through-thickness cracks which were grown in surface length up to the thickness of the specimen (approximately 2.3 mm) appeared to have a relatively large crack depth, as shown in Figure IV-7. The measured values of the crack depths, which were averaged by three points, are listed in Table IV-4. The expected depth of the semi-elliptical surface crack is 0.73 mm, from Equation 4.6, when the observed length is equal to the thickness of the specimen. All values in Table IV-4 are significantly greater than 0.73 mm. Specimen A-82-16 showed an especially large value of 2.69 mm for the crack depth. The crack in specimen A-82-16 was initiated as a corner crack (see crack map in Appendix II); the depth was expected to be approximately the same as the surface length. But the depth of the quarter-elliptical corner crack with a surface length of 2.3 mm would be 1.5 mm according to Equation 4.6.

The crack growth rate becomes faster as the crack length approaches the thickness of the specimen (to be discussed in the section entitled "Crack Growth Rate"). But the replicas were taken at certain intervals, every 2,000 to 10,000 cycles. Thus in the interval between the last two measurements, a crack may grow to its full length and then continue to grow in the direction of depth. However, such an oversized through-thickness crack must be considered an edge crack rather than a surface crack, and the crack growth data from the last cycling interval must be omitted when observing the growth behavior of the surface crack.

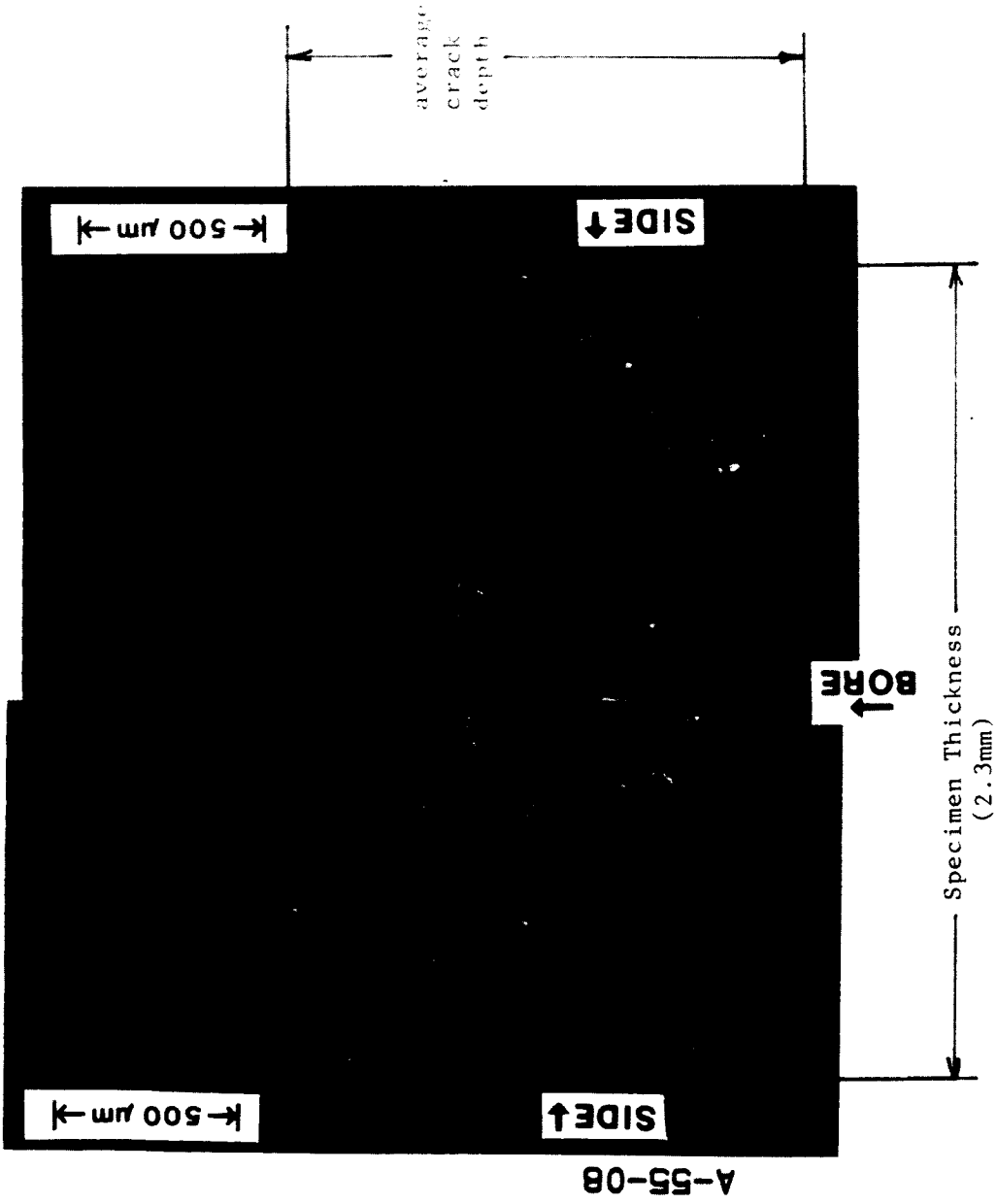

Figure IV-7. Typical photograph of through-thickness crack

IV-4. Crack Growth Rate Results and Discussion

Crack growth was monitored using the replica technique at certain cyclic intervals. The first observable surface crack lengths, those visible under an optical microscope with 400X magnification, tended to be one or two times the grain size of the specimen, or a few tens of microns long. The material's typical grain size was 25 μm in the direction of crack growth.

The stress intensity factor range, ΔK, was calculated from the approximate equation for semi-elliptical surface cracks and quarter-elliptical corner cracks, as described in Appendix I-A. The full load range was used in calculations of ΔK, including compressive loads for negative R-ratios. The crack depth, c, for these calculations was estimated from Equation 4.6.

All crack growth data -- crack length, number of cycles, K, da/dN (growth rate), and the plot of da/dN versus ΔK for each specimen -- are included in Appendix II. Also found in Appendix II are data sheets containing information on test conditions. The ΔK values for R = 0.5 appeared smaller than those for R = -2.0, even with much higher maximum stress levels, because the stress ranges are smaller in the case of R = 0.5 than for R = -2.0.

The crack growth rates were calculated with a simple point-to-point method:

$$\frac{da}{dN} = \frac{a}{N} = \frac{a_{n+1} - a_n}{N_{n+1} - N_n} \quad \text{in mm/cycle} \qquad (4.7)$$

where a_n is the crack length at N_n cycles. The corresponding stress intensity factor range was calculated at an average crack length, a, as

$$a = \frac{a_{n+1} + a_n}{2} \qquad (4.8)$$

A typical set of data including crack lengths, cycles, stress intensity range (ΔK), and growth rate (da/dN) is presented in Table IV-5. The data are for specimen A-65-07, tested with S_{max} = 225 MPa (63% of the yielding stress) and R = 0.5. The first observed crack was a surface crack, 0.033 mm long and located at the center of the bore. ΔK was calculated based on the average crack length; da/dN was calculated by the point-to-point method described earlier in this section.

By examining the da/dN data, it can be determined that the crack grew inconsistently as the number of cycles increased. Crack growth slowed in the neighborhood of 46,000 to 54,000 cycles and also during the period from 60,000 to 64,000 cycles, due to the micro-structure effect mentioned before.

Crack growth data taken at the very end of cycling was not used in the calculation of da/dN. This is because the crack length was measured only on the notch root, while the crack was observed to grow as an edge crack through the thickness at the last cycling. The process was discussed in Section IV-3.

TABLE IV-5
TYPICAL CRACK GROWTH DATA

Specimen Number A-65-07
Tested With Smax = 225 MPa and R = 0.5

Cycles (X 1000)	Crack Length 2a (mm)	K (MPa-M)	da/dN (X10 mm/cycle)
42	0.033		
44	0.038	1.88	1.250
46	0.044	2.02	1.500
54	0.049	2.14	0.312
56	0.065	2.36	4.000
60	0.071	2.57	0.750
64	0.087	2.76	2.000
70	0.114	3.09	2.250
72	0.125	3.35	2.750
74	0.136	3.49	2.750
80	0.158	3.69	1.833
84	0.174	3.90	2.000
86	0.185	4.04	2.750
92	0.213	4.24	2.333
96	0.349	4.96	17.000
98	0.392	5.62	10.750
100	0.425	5.87	8.250
102	0.463	6.09	9.500
104	0.507	6.34	11.000
106	0.518	6.50	2.750
108	0.632	6.85	28.500
110	0.719	7.37	21.750
112	0.801	7.78	20.500
114	0.970	8.33	42.250
118	1.875	10.32	113.125
121	2.300	12.41	

The crack growth rate versus ΔK is plotted for the different R-ratios -- R = 0.5, 0.0, -1.0, and -2.0 -- in Figures IV-8, IV-9, IV-10, and IV-11, respectively. The crack growth ranges are from a few tens of microns (as mentioned above) to through the thickness of the specimen (approximately 2.3 mm). The data points of all four plots show unsteady growth: acceleration in the beginning of crack growth and then deceleration. This pattern repeats itself several times. It is believed that this unsteady growth, which is especially large in the early stages, is due to microstructural effects which have been noted in other investigations [4,5,15-20]. In particular, the repetition of acceleration and deceleration was observed by Larsen [13].

Growth-rate data for long cracks are also plotted in Figures IV-8 through IV-11. These data are from experiments performed several years ago and from more recent tests on the same lot of material [49] used in this study. As the cracks grow, the crack growth rate tends to approach the rate of the long crack and the scatter band tends to narrow. This indicates that the short crack behavior is changing to the behavior of the long crack.

Figure IV-8, for R = 0.5, shows a definite slowing of the growth rate for short cracks relative to the rate for long cracks. As described in Appendix I-C, all the stresses applied in R = 0.5 produce plastic deformation at the notch root due to the stress concentration. The compressive residual stress, σ_{rs},

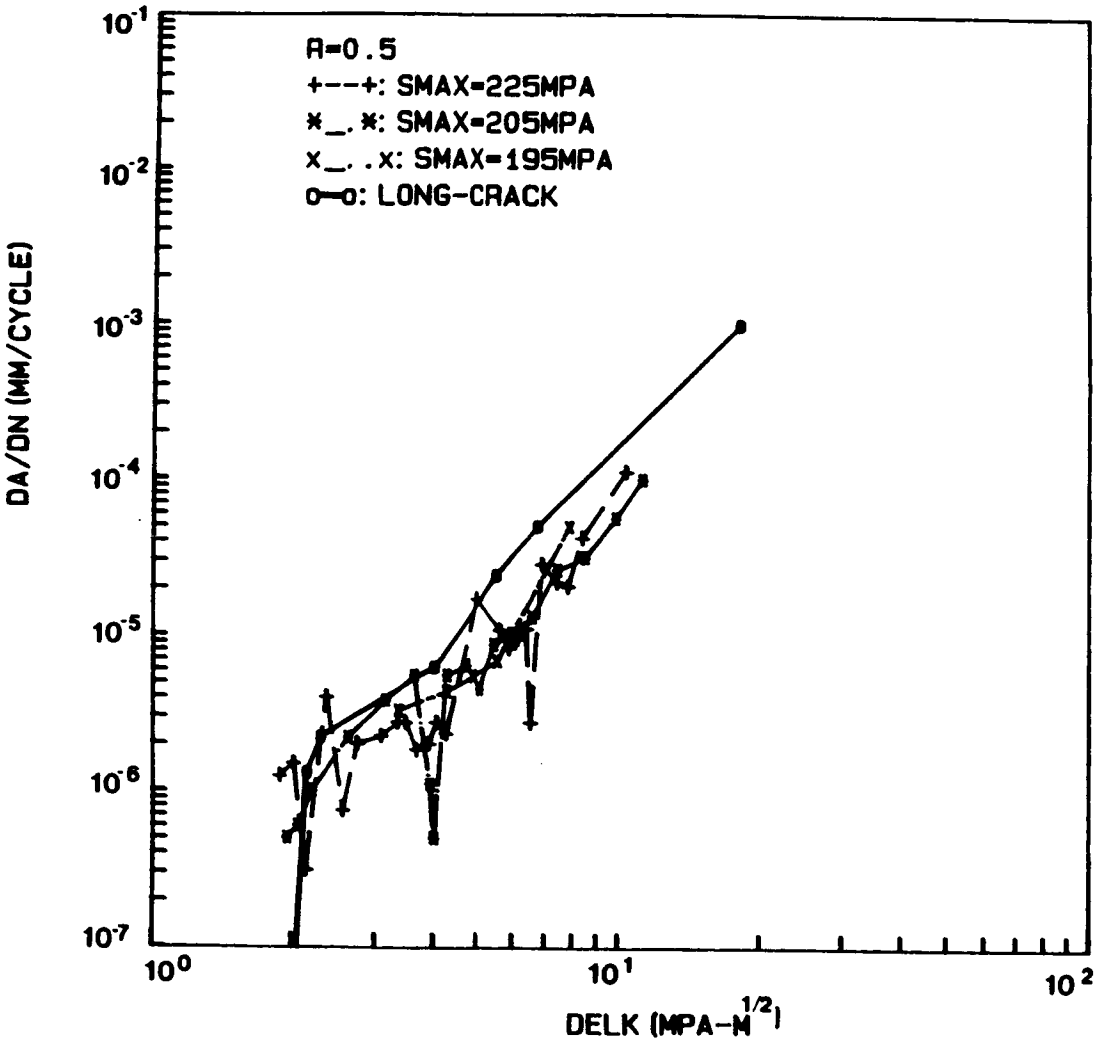

Figure IV-8. da/dN - ΔK plot for R = 0.5

is present in subsequent cycling from $\frac{1}{2}S_{max}$ to S_{max}. This σ_{rs} changes with the local R-ratio:

$$R_{local} = \frac{\sigma_{min} + \sigma_{rs}}{\sigma_{max} + \sigma_{rs}} \qquad (4.9)$$

A change in R-ratio will affect the crack growth rate, since the growth rate is known to be a function of R as well as of ΔK. The residual stress was not measured in this study, but an estimate based on Neuber's relation shows it to be very small, since the specimen is not unloaded after the first cycle. Thus the R-ratio would change little.

In addition to the change in local R-ratio, another explanation may be given. The growth rates of short cracks which propagate on the surface of the notch root under conditions of plasticity may be slower than those of long cracks which grow under plane stress conditions. Growth under plane stress and inside the area of plastic deformation is slow due to residual compressive stress [54]. Zurek et al [28] studied the growth of short cracks when a compressive residual stress existed. They noted a decrease in ΔK with the residual stress, σ_{rs}, which is negative:

$$\Delta K' = (\sigma_{max} + \sigma_{rs} - \sigma_{cc})\ f(a) \qquad (4.10)$$

where σ_{cc} is the closure stress and f(a) is the coefficient dependent upon crack geometry. Zurek's group also observed an improvement in agreement of prediction with experimental data when the residual stress was taken into account.

Data for R = 0.0 is shown in Figure IV-9. Some differences between the short and long crack growth rates can be observed in the lower ΔK range. The loading in this case caused initial plastic deformation at the notch for the two highest stresses, as shown in Appendix I-C, but all three growth rates are similar.

Figure IV-10, for R = -1.0, shows faster growth rates for short cracks than for long cracks. All three loadings for R = -1.0 left the notch root in an elastic condition, so no retardation of the crack growth due to notch plasticity was expected. The stress effect, meaning faster crack growth at higher stresses, may also be clearly observed in this plot.

The same growth behavior is observed in Figure IV-11 for R = -2.0, i.e., a faster growth rate for short cracks and the result of the stress effect. Here the two highest loads produced yielding in compression at the notch root, but no corresponding effect on the growth rate behavior was observed.

The so-called "small crack effect" was seen under the loading conditions of R = -1.0 and -2.0. This faster growth was observed through almost the entire range of ΔK, for crack lengths up to the thickness of the specimen (2.3 mm). Thus it may be said that the small crack effect appeared to a crack length of 2.3 mm. The small crack with this length has been called a "physically short crack" [14,29] or a "mechanically short crack" [26].

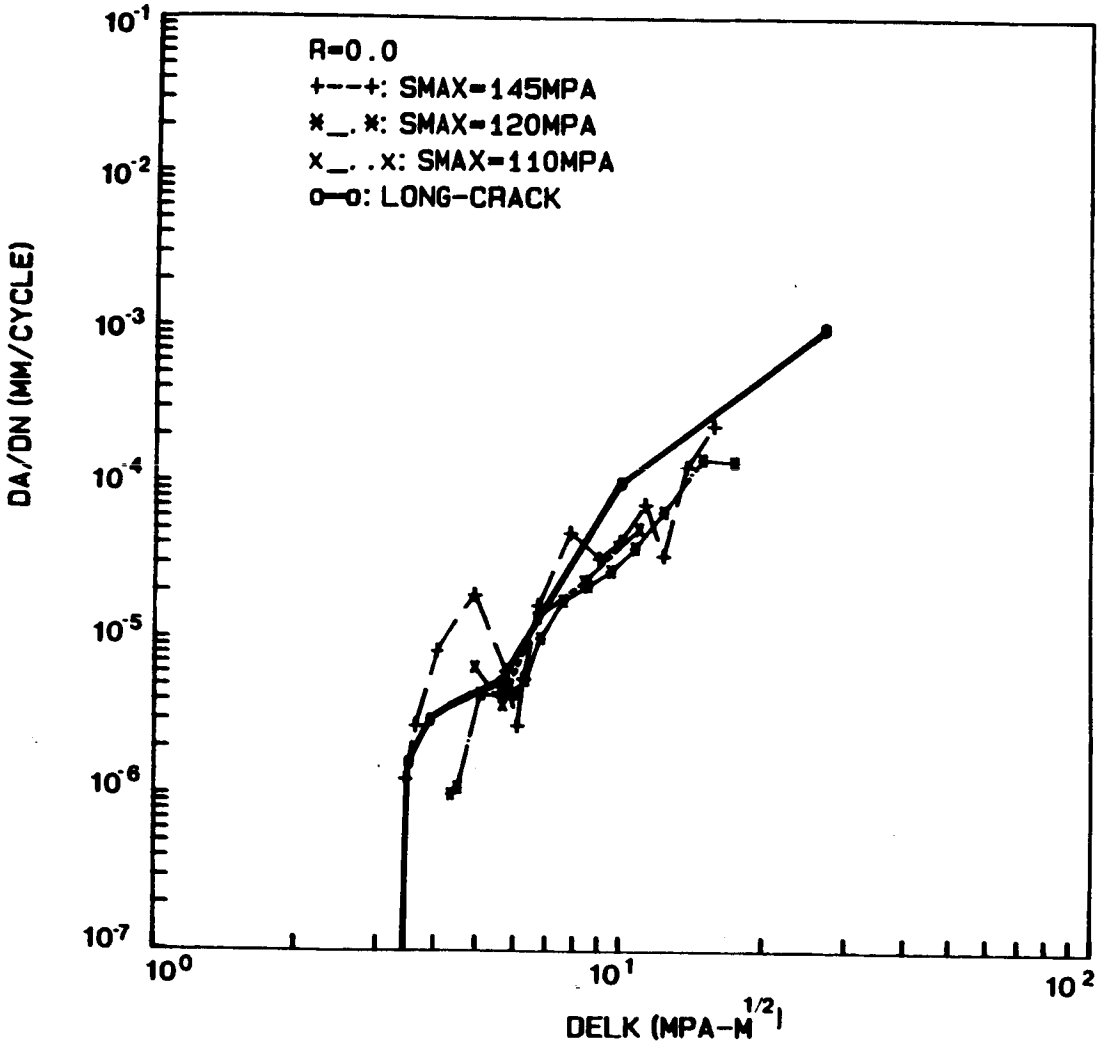

Figure IV-9. da/dN - ΔK plot for R = 0.0

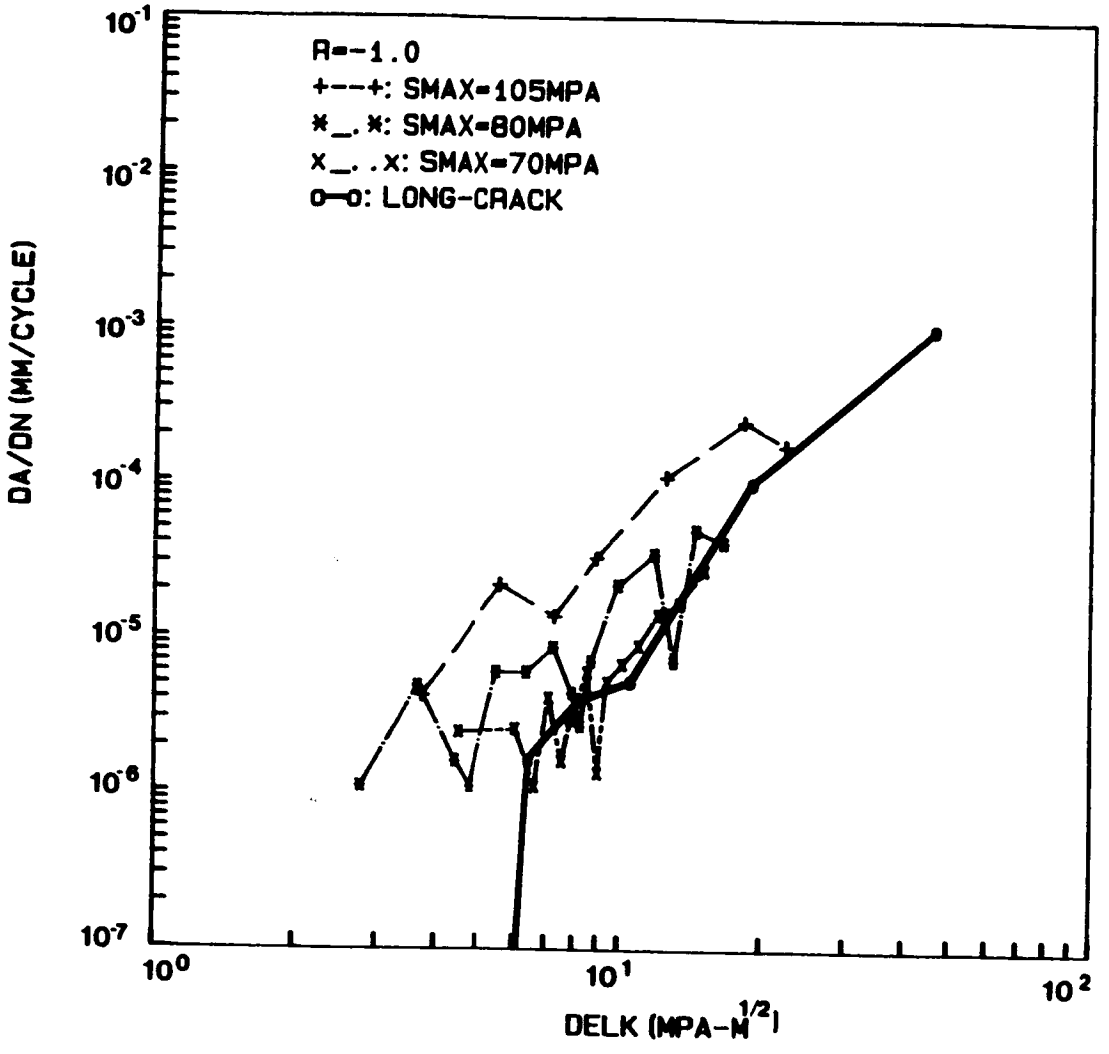

Figure IV-10. da/dN - ΔK plot for R = -1.0

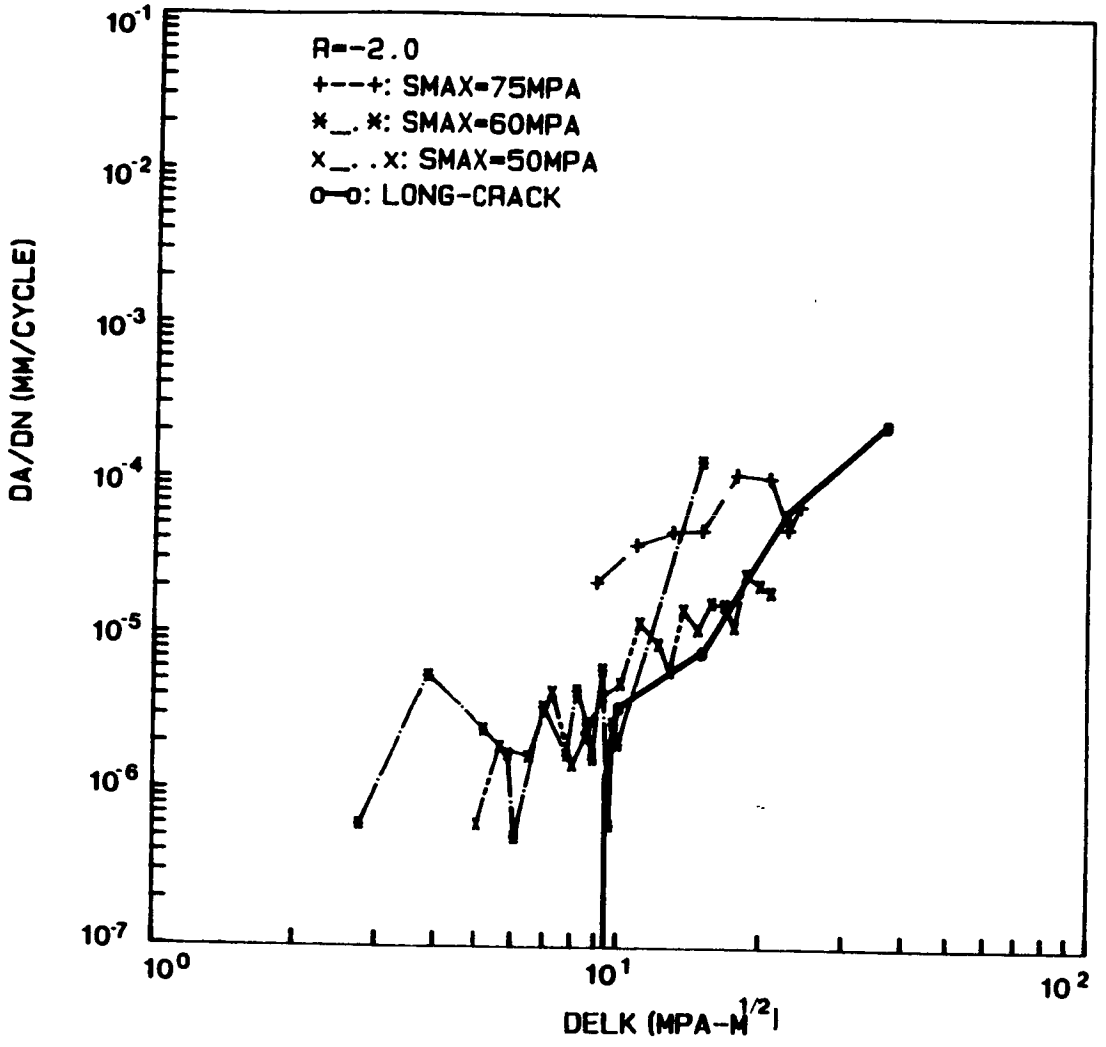

Figure IV-11. da/dN - ΔK plot for R = -2.0

IV-5. Crack Closure Results and Discussion

Crack closure loads (P_{op}) were measured using the ISDG technique for short and through-thickness cracks. The ISDG technique measures the crack opening displacement (COD), and the closure stress is determined by a reduced data method (described in Section III-5) with computerized analysis. A typical procedure is shown in Figure III-8, and all plots used in determining the closure stress are included in Appendix II. In addition to closure stresses, information about the compliance of the cracks was easily obtained from the COD measurement.

The results of measured closure stress, compliance values, and corresponding crack lengths are tabulated in Table IV-6. The smallest crack length for which closure stress was measured was 0.035 mm; most of the short crack lengths were less than 0.5 mm. The closure stresses were usually measured on the center of the crack. Only two cracks (* in Table IV-6) were measured mear the crack tip, but no remarkable difference was found. More measurements would be necessary to determine the effect of position on measurement for small surface cracks.

TABLE IV-6
RESULTS OF CLOSURE LOAD AND COMPLIANCE MEASUREMENTS

R	Maximum Stress (MPa)	Specimen Number	Crack Length 2a (mm)	Crack Length Depth (mm)	Crack Shape	Normalized Closure Load (Pop/Pmax)	Compliance (μm/Nt)
0.5	225	A-54-04	0.54	0.42	C	0.34*	1.59 E-4
		A-65-07	2.3	1.31	T	0.29	14.0 E-4
	205	A-68-22	0.18	-	S	0.32	1.3 E-4
			0.54	0.48	C	0.38*	-
	195	A-59-13	0.403	0.18	S	0.39	2.17 E-4
0.0	145	A-52-03	2.25	1.1	T	0.33	15.0 E-4
		A-51-16	0.245	0.12	S	0.32	1.34 E-4
	120	A-82-16	2.25	2.69	T	0.21	31.2 E-4
	110	A-57-14	2.19	1.65	T	0.30	24.5 E-4
		A-80-28	0.414	0.38	C	0.34	4.21 E-4
-1.0	105	A-55-27	2.25	-	T	0.0	10.8 E-4
		A-67-08	0.19	-	S	0.0	0.9 E-4
	80	A-65-24	2.25	1.26	T	0.12	17.7 E-4
		A-72-02	0.05	0.23	S	0.12	0.46 E-4
	70	A-55-08	2.25	1.3	T	0.0	17.9 E-4
		A-83-23	0.2	0.1	S	0.18	0.91 E-4
-2.0	75	A-52-21	2.25	1.35	T	-0.18	20.1 E-4
		A-74-20	0.035	-	S	0.0	0.15 E-4
	60	A-75-16	2.175	0.88	T	-0.12	10.4 E-4
		A-84-20	0.17	0.16	S	-0.38	1.09 E-4
	50	A-68-05	2.25	1.23	T	-0.13	16.8 E-4
		A-80-11	0.1	0.04	S	0.0	0.53 E-4

S : Semi-elliptical surface crack
C : Quarter-elliptical corner crack
T : Through-thickness crack

* Measured near the tip behind the crack

A. Results of COD Measurement

Typical plots of load versus COD are shown in Figures IV-12, IV-13, IV-14, and IV-15 for R = 0.5, 0.0, -1.0, and -2.0, respectively.

Figure IV-12a shows the load-COD for a crack with a surface length of 0.5 mm and a crack which grew through the thickness of the specimen (2.3 mm). The 0.5-mm crack originated near the edge of the specimen at the notch root and grew into a corner crack. Indentations were placed 50 microns apart near the edge of the crack for the 0.5-mm crack and 100 microns apart for the through-thickness crack. The maximum cyclic load was 5,800 lbs (225 MPa) with a minimum load of 2,900 lbs. The change in the slope of the compliance for the 0.5-mm crack is unclear in Figure IV-12a, since it is plotted on a large scale in order to compare the magnitude with the through-thickness crack data. The usual COD plot for such a short crack length is plotted on a smaller scale, as shown in Figure IV-12b.

The COD of the 0.5-mm crack increased slightly until a substantial load was applied, when it began to increase linearly with the load. The linear increase means that the crack is fully open. This behavior can be seen clearly on an enlarged scale such as the one in Figure IV-12b. The pattern of increase in the COD changes at 2,000 lbs to a linear form which corresponds quite well to the linear-square-fitted line shown in the plot. The transition point is obtained easily from the

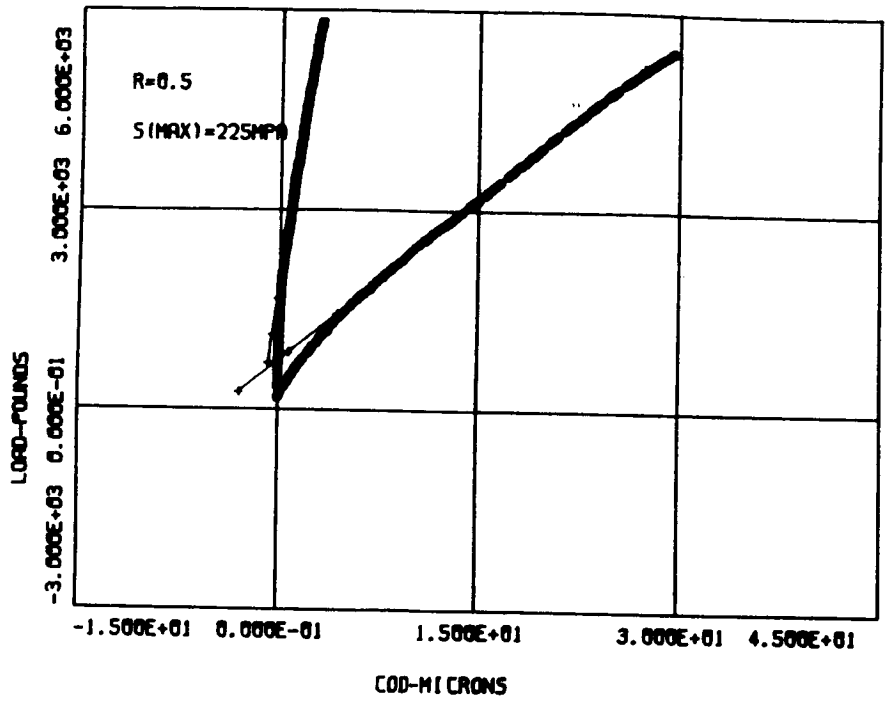

a) in a large scale

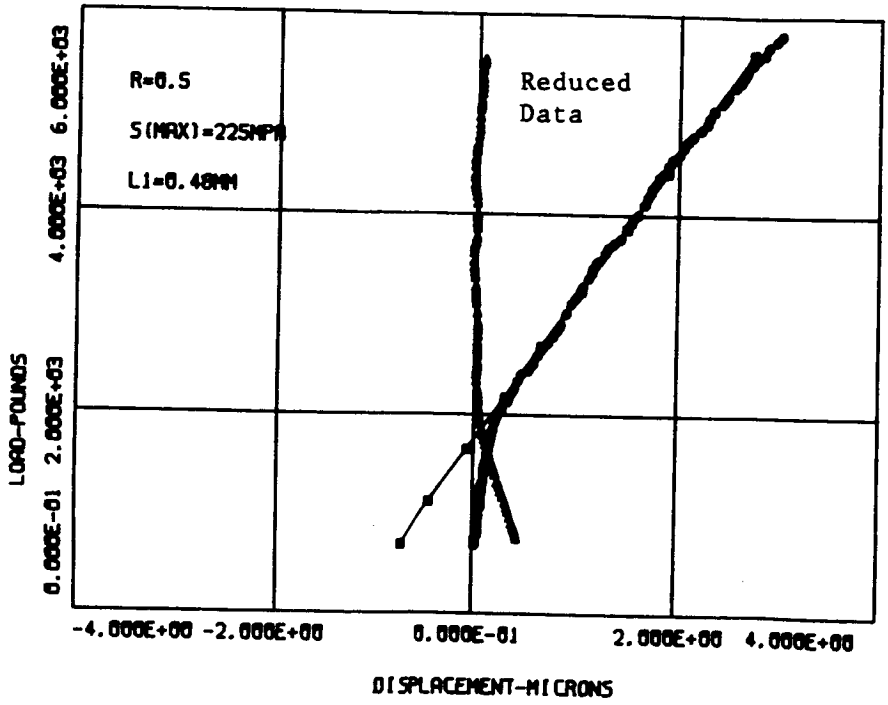

b) in an enlarged scale

Figure IV-12. Typical COD-Load plot for R = 0.5

reduced data. This value is the crack opening load, Pop, which is equal to 1,980 lbs for the data in Figure IV-12b. The compliance value which is obtained from the upper linear portion of the COD curve is equal to 1.59×10^{-4} μm/Nt for the 0.5-mm crack and 14.0×10^{-4} μm/Nt for the through-thickness crack.

Figure IV-13 is for a crack with a surface length (2a) of 0.245 mm and a through-thickness crack. Indentations were placed at the center of the crack in both cases. The maximum cyclic load was 3,750 lbs (145 MPa) with a minumum load of 0 lbs. The maximum COD at the maximum load was 1.44 microns for the 0.245-mm crack and 23.0 microns for the through-thickness crack. The COD curves show behavior similar to the case of Figure IV-12a. The compliance value was 1.24×10^{-4} μm/Nt for the 0.245-mm crack and 15.0×10^{-4} μm/Nt for the through-thickness crack.

Figure IV-14 shows the COD curves for fully reversed loading; the maximum cyclic load was 2,715 lbs (105 MPa) and the minimum was -2,715 lbs. The sharply sloped curve is for a surface crack with a length of 0.19 mm, and the large-COD-valued curve is for a through-thickness crack. It can be seen clearly from these curves that the slope transition point in the COD curve of the through-thickness crack occurs in the compressive load region. This implies that the crack was opened fully in compressive load. This phenomenon will be discussed later.

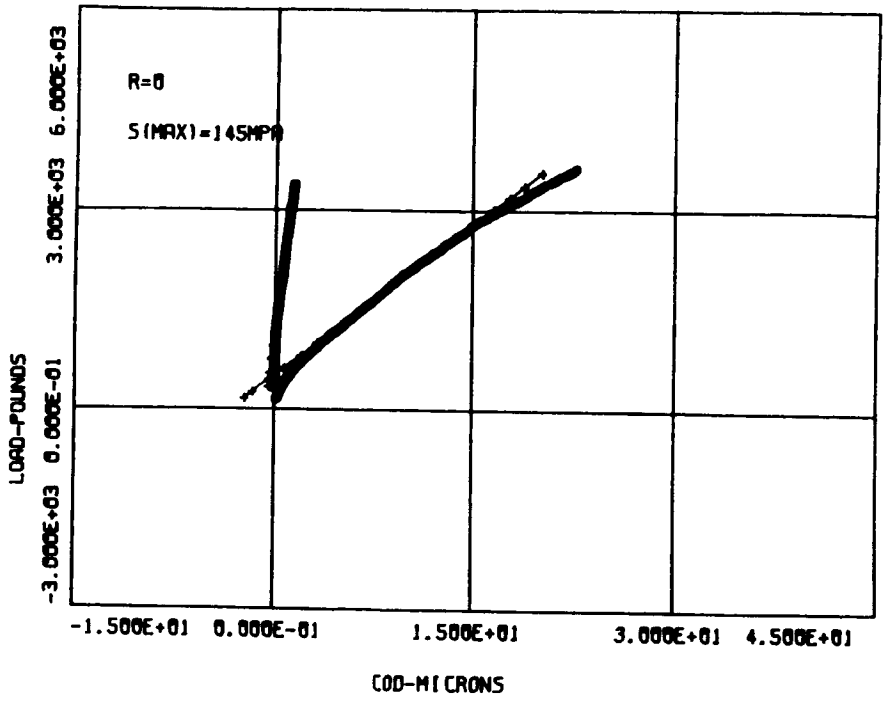

Figure IV-13. Typical COD-Load plot for R = 0.0

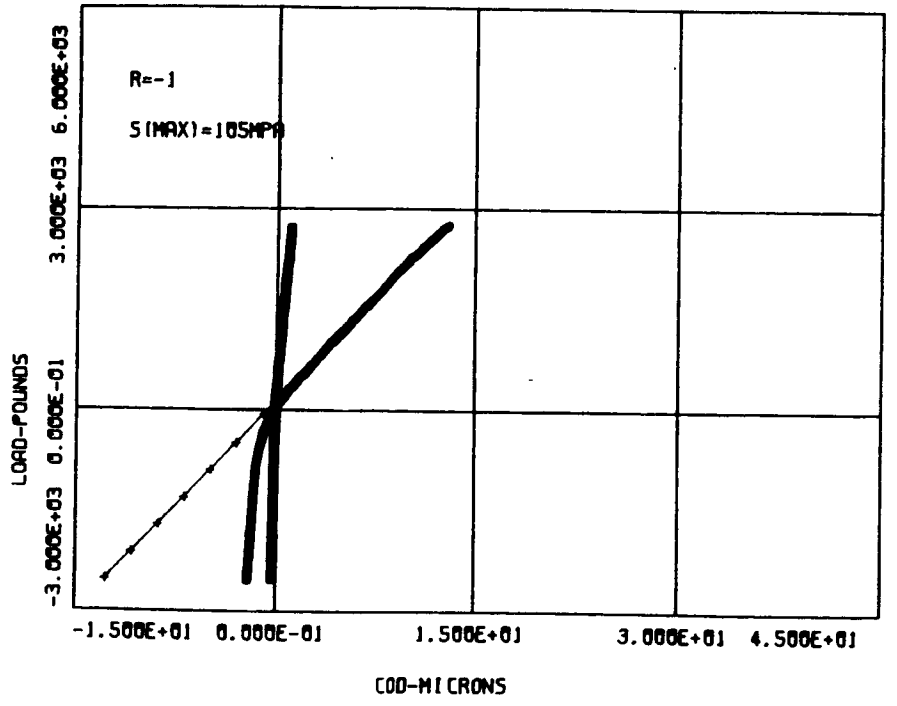

Figure IV-14. Typical COD-Load plot for R = -1.0

Figure IV-15 shows the COD curves for R = -2.0; the maximum cyclic load was 1,550 lbs and the minimum was -3,100 lbs. The steep curve is for a corner crack with a length of 0.16 mm, while the curve with the sharp bend is for a through-thickness crack. The COD curves of the chort cracks in Figures IV-14 and IV-15 are plotted again on an enlarged scale in Figure IV-16.

As shown in this plot, when the cracks are closed in the compressive load region, the bore of the notch behaves as an elastic material until the crack begins to open. The displacement measured from the indentations across the crack in the compressive load region was -0.25 micron for the specimen with the 0.19-mm crack. The indentations were 50 microns apart; so the strain, e, is

$$e(\text{measured}) = -0.25/50 = -0.005$$

The elastic modulus of this material is 73,100 MPa, and the stress concentration factor for the geometry of this specimen is 3.17 [49]. Calculating the strain at the center of the notch for the applied gross stress of -105 MPa gives

$$e(\text{calculated}) = \frac{-105 \text{ Mpa}}{73100 \text{ Mpa}} \times 3.17$$

$$= -0.0046$$

The measured strain agrees well with the strain value calculated from the elastic modulus. This is evidence of elastic behavior in the compressive region.

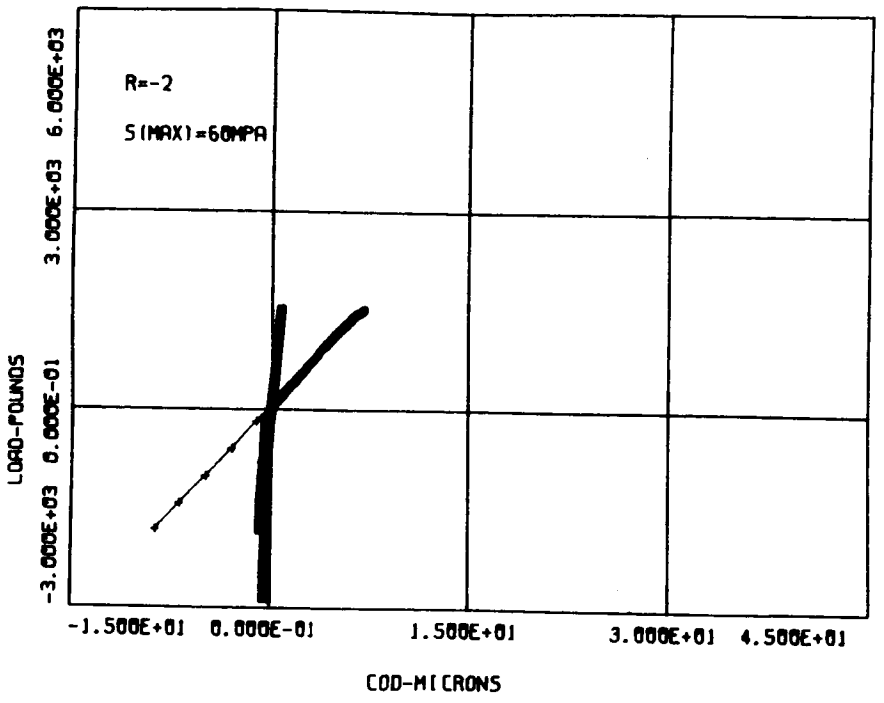

Figure IV-15. Typical COD-Load plot for R = -2.0

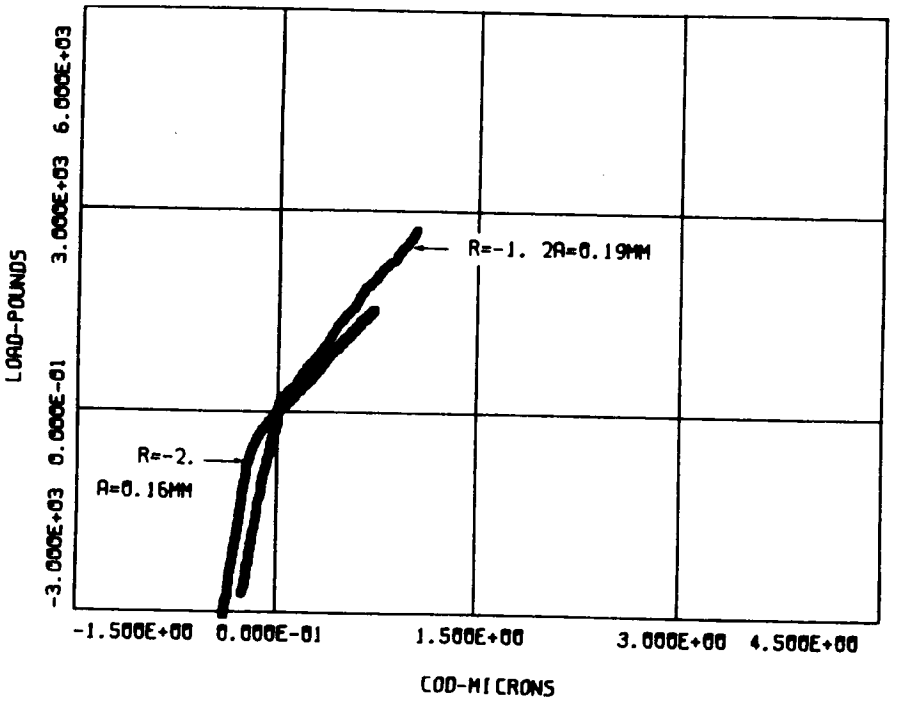

Figure IV-16. COD-Load plot in enlarged scale

B. Comparison of Compliances For Crack Lengths

It was shown in the "Crack Shape" section that surface cracks are semi-elliptical in shape and that corner cracks are quarter- elliptical. The measured crack depths were shown to be a constant ratio, approximately 0.9, to the semi-surface crack length for most cases. Thus the crack lengths can be compared simply with the surface lengths for this case where there is a constant ratio of surface length to depth.

Figure IV-17 is the comparison of compliance values for surface crack lengths of short cracks with the semi-elliptical shape and lengths up to 0.5 mm. Each data point was tested at a different stress level, S_{max}, but no variation in compliance due to S_{max} were noted. Also, no dependence of compliance upon the variation of R was found for these semi-elliptical short cracks. The compliance showed a linearly proportional relationship to the surface crack length, as seen in the plot. Similar results have been reported in other papers [16,43]. Morris [16] found a linear relationship between compliance and crack length and no variation of compliance with the applied stress level for surface microcracks tested at R = -1.0. James and Smith [43] also observed the linear relationship of compliance and crack length for surface microcracks tested at R = 0.1.

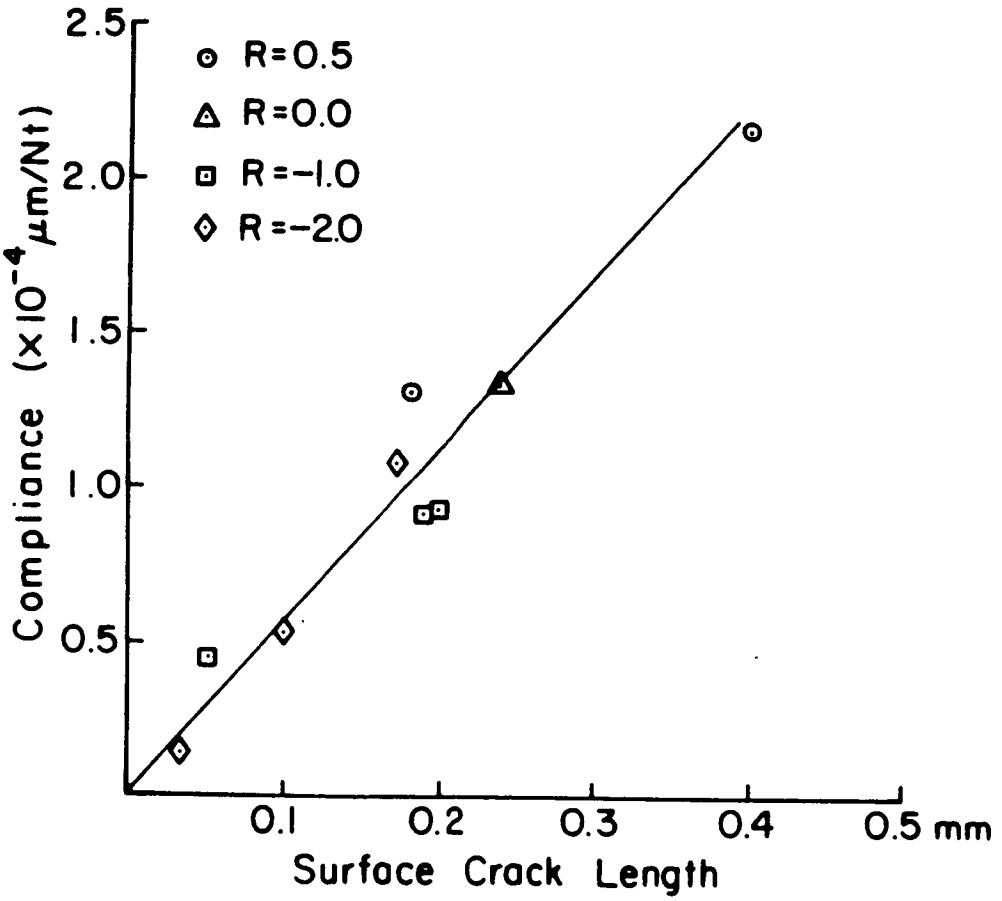

Figure IV-17. Short crack compliances - surface crack length for semi-elliptical surface crack

Figure IV-18 shows a comparison of compliance values for crack lengths of through-thickness cracks. As explained in the "Crack Shape" section, the through-thickness cracks must be considered edge cracks rather than surface or corner cracks because the crack depths were substantially deeper than what was expected from a semi-elliptical surface crack or a quarter-elliptical corner crack. The linear relationship was observed between the compliances and crack lengths of less than 2 mm measured in the depth direction.

This linear relationship of compliance values and crack lengths implies that COD is proportional to crack lengths in a linear fashion, which is the result from LEFM.

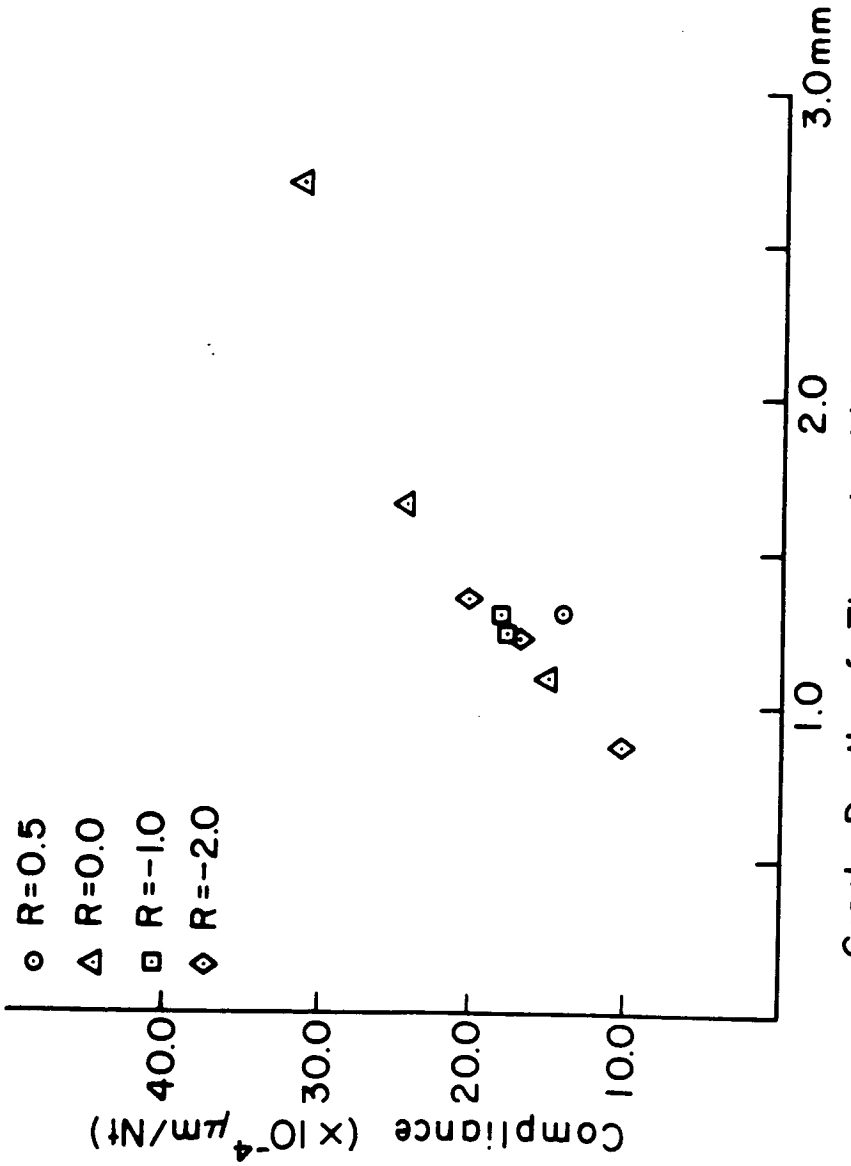

Figure IV-18. Crack compliances - crack length for through-thickness crack

C. Effect of Crack Length on Crack Closure Load

Figure IV-19a shows variations of opening load levels with crack lengths for short surface cracks whose lengths ranged from 0.035 mm to 0.5 mm. The solid lines represent the opening stress ratio predicted for short cracks form Newman's calculated data [62]. Each data point was tested at a different stress level, but Newman's prediction was calcualted for a specific stress level: S_{max}/S_o = 0.25 for R = 0.0; S_{max}/S_o = 0.15 for R = -1.0 and -2.0. S_o is the flow stress, which is taken as an average value of the yield stress (359 MPa) and the ultimate tensile stress (496 MPa for Al 2024-T3).

Measured opening stress ratios for R = 0.5 were below the minimum cyclic stress for such a case. Newman's prediction for R = 0.5 shows the opening stress to be the same as the minimum applied stress. Most of the measured opening ratios are smaller than the levels predicted for R = 0.0, -1.0, and -2.0. Predicted values show rapid increases in the opening stress level while the crack is still very short (less than 0.08 mm), with stabilization for the opening stress for crack lengths greater than 0.1 mm. Measured Data shows scattering in a wide band for lengths less than 0.2 mm. It can be observed from Figure IV-19a as a general trend that the opening stress levels increase as the crack lengths increase, except in the case where R = -2.0.

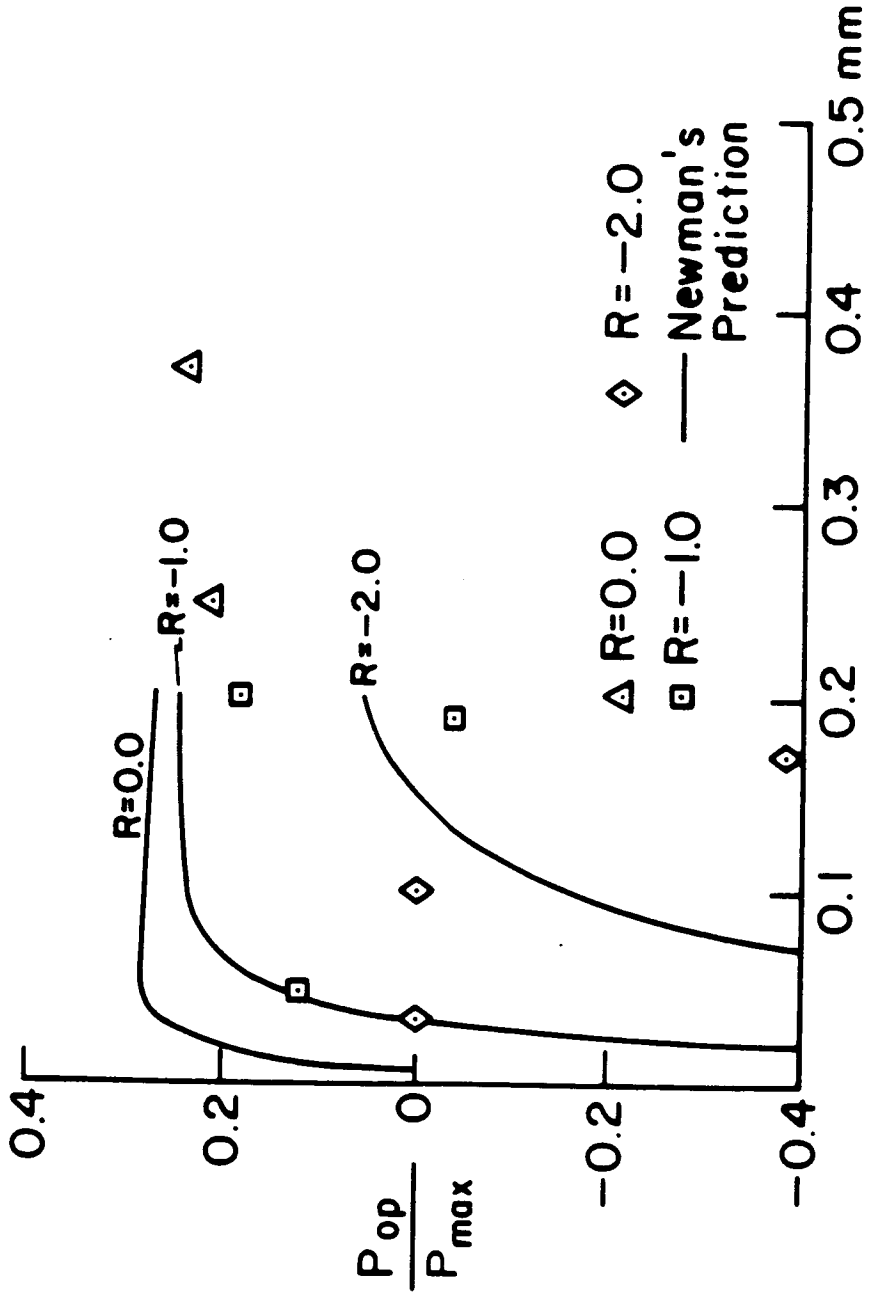

a) for short surface crack

Figure IV-19. Crack opening load ratio - crack length

Figure IV-19b shows the opening load ratio versus crack length measured in the specimen width direction for through-thickness cracks. Also, opening stress ratio values predicted for a long crack from Newman's equation [58] are plotted to compare with measured data. The opening ratios for short, through-thickness cracks tested in this experiment appear smaller in general compared to the values predicted for long cracks. The difference between the opening stress levels is relatively small for positive R-ratios and substantially large for negative R-ratios. No dependence of opening stress levels on crack length was observed for through-thickness cracks.

D. Effect of R-ratios on Crack Closure Levels

The effect of R-ratios on closure levels has been studied by many investigators. Elber [34] observed the relationship between the closure stress, S_{op}, and the R-ratio and proposed the empirical equation for the material Al 2024-T3,

$$\frac{S_{op}}{S_{max}} = 0.5 + 0.1\,R + 0.4\,R^2 \qquad (4.11)$$

where S_{max} is the maximum cyclic stress. Schijve [55] modified the above equation to apply where $R \geq -1$:

$$\frac{S_{op}}{S_{max}} = 0.45 + (0.1+a)R + (0.45-2a)R^2 + aR^3 \qquad (4.12)$$

where a is a constant with values from 0.10 to 0.15. The above formulas were obtained from the long crack data.

Newman [58] used his closure model to propose a general crack opening stress equation for long cracks as a function of constraint, stress ratio, and stress level. The proposed equations are

$$\frac{S_{op}}{S_{max}} = A_o + A_1R + A_2R^2 + A_3R^3 \quad \text{for } R \geq 0 \qquad (4.13)$$

and

$$\frac{S_{op}}{S_{max}} = A_o + A_1R \quad \text{for } -1 \leq R < 0 \qquad (4.14)$$

when $S_{op} \geq S_{min}$.

The coefficients are

$$A_0 = (0.825 - 0.34\alpha + 0.05\alpha^2) \cdot [\cos(\pi \cdot Smax/2\sigma_o)]^{1/2}$$

$$A_1 = (0.415 - 0.071\alpha)(Smax/\sigma_o)$$

$$A_2 = 1 - A_0 - A_1 - A_3$$

$$A_3 = 2A_0 + A_1 - 1$$

where α is a constraint factor, $\alpha = 1$ for plane stress and $\alpha = 3$ for plane strain condition, and σ_o is a flow stress which is taken to be the average between the uniaxial yield stress and the uniaxial ultimate tensile strength of the material. The yield stress is 359 MPa and the ultimate tensile strength is 496 MPa for Al 2024-T3; thus, the flow stress will be 427.5 MPa. The constraint factor was chosen as 1.73. It was used by Newman in correlating the crack-growth rate data for large cracks in a specimen with the same geometry as the ones used in this study.

Normalized opening stress ratios for long cracks were predicted from Schijve's equation and Newman's equation and compared with short crack data measured in this study. The results are compiled in Table IV-7.

The measured opening loads for short cracks at R = 0.5 appeared below the minimum cyclic load, as shown in Table IV-6. It may be reasonable to define the opening load as equivlaent to the minimum cyclic load for such a case. So opening load ratios are changed to be the same as the R-ratio in Table IV-7.

The dependence of opening stress on the maximum applied stress was not clearly observed in the short crack data measured in this study.

Figure IV-20 shows a plot of opening load ratio versus R-ratio for short cracks tested in this study. It can be observed from the plot that opening load levels of short cracks are strongly dependent on R ratio. The opening stress ratio for long cracks, predicted by Schijve and Newman's equations, are also plotted in Figure IV-20.

TABLE IV-7
COMPARISON OF Pop/Pmax FOR SHORT AND LONG CRACKS

R	Smax	Average Pop/Pmax of Short Cracks	Predicted Pop/Pmax of Long Cracks Newman	Schijve
0.5	225	0.5	0.548	
	205	0.5	0.554	0.62
	195	0.5	0.556	
0.0	145	0.32	0.355	
	120	0.21	0.365	0.45
	110	0.32	0.368	
-1.0	105	-0.05	0.298	
	80	0.12	0.322	0.35
	70	0.08	0.331	
-2.0	75	-0.09	0.275	
	60	-0.25	0.300	
	50	-0.06	0.314	

An interesting point is made by Figure IV-20: the differences in opening load ratio levels of small and long cracks are not remarkably large at R = 0.5 and 0.0, but they are substantial for R = -1.0 and -2.0. From Table IV-7,

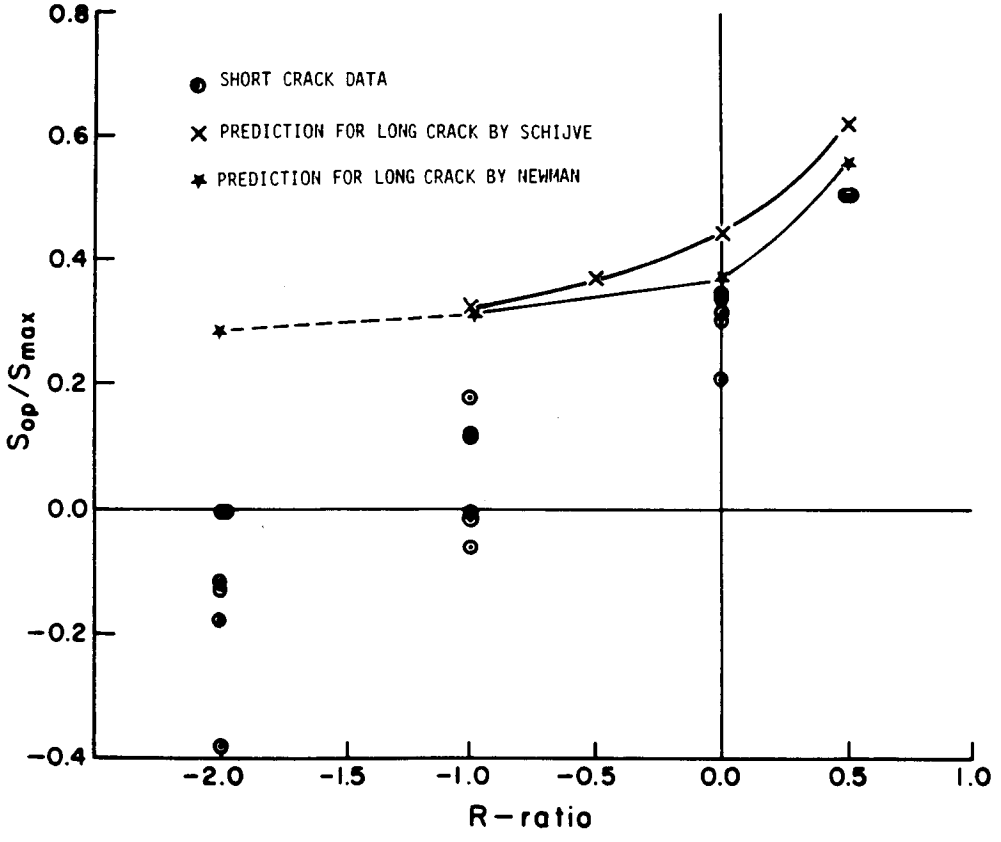

Figure IV-20. Crack opening load - R-ratio for short cracks

normalized opening load levels of short cracks at R = 0.5 and 0.0 are approximately 10% lower than those predicted by Newman for long cracks. But at R = -1.0 and -2.0, the short crack data are more than 100% lower than the data for the long cracks in most cases. This means that the short crack growth rate should be much faster that the long crack growth rate at R = -1.0 and -2.0 and that there should be no appreciable difference in the two rates at R = 0.5 and 0.0.

IV-6. Crack Closure Effect on Crack Growth Rates

Many attempts [16,17,21,22,33,40,61] have been made to relate the difference between short and long crack growth behavior with the concept of crack closure. The effective stress intensity range, ΔK_{eff}, is calculated as follows.

$$\Delta K_{eff} = U \times \Delta K \tag{4.15}$$

where U is the effective stress range ratio with the value

$$U = 1 - \frac{Sop/S_{max}}{1 - R} \tag{4.16}$$

The effective stress range ratios are calculated in Table IV-8 with the values from Table IV-7.

TABLE IV-8
COMPARISON OF EFFECTIVE STRESS RANGE RATIO

R	Smax (MPa)	U For Short Crack	U For Long Crack Newman	U For Long Crack Schijve
0.5	225	1.0	0.90	
	205	1.0	0.89	0.76
	195	1.0	0.89	
0.0	145	0.68	0.64	
	120	0.79	0.63	0.55
	110	0.68	0.63	
-1.0	105	0.53	0.35	
	80	0.44	0.34	0.33
	70	0.46	0.34	
-2.0	75	0.36	0.24	
	60	0.42	0.23	-
	50	0.35	0.23	

For R = 0.5, measured opening stresses for short cracks are below S_{min}, as shown in Table IV-6. Here closure stresses have no influence on crack growth. But closure levels predicted by Schijve and Newman, also shown in Table IV-6, are higher than S_{min}. Thus the growth rate of the long crack data would shift to the left and produce less agreement with short crack data.

Figure IV-21 shows da/dN versus ΔK_{eff} for R = 0.0. The measured opening stresses for short cracks are approximately 10% lower than the long crack values predicted from Newman; there is little change in the agreement between the rates as compared to rates which do not display the closure effect shown in Figure IV-9.

Table IV-7 shows a considerable difference -- more than 100% -- in the opening stress levels of short and long cracks. The average value of U for the short crack at R = -1.0 is 0.48; the average value of U as predicted for the long crack by Newman is 0.34. Therefore, the plot of da/dN versus ΔK_{eff} would shift to the left by a substantial amount in both cases. Figure IV-22 shows the good agreement in growth rates of short and long cracks based on ΔK_{eff}. This implies that the short crack growth rates were approximately 40% faster than the those of the long cracks due to the closure effect for the case of R = -1.0.

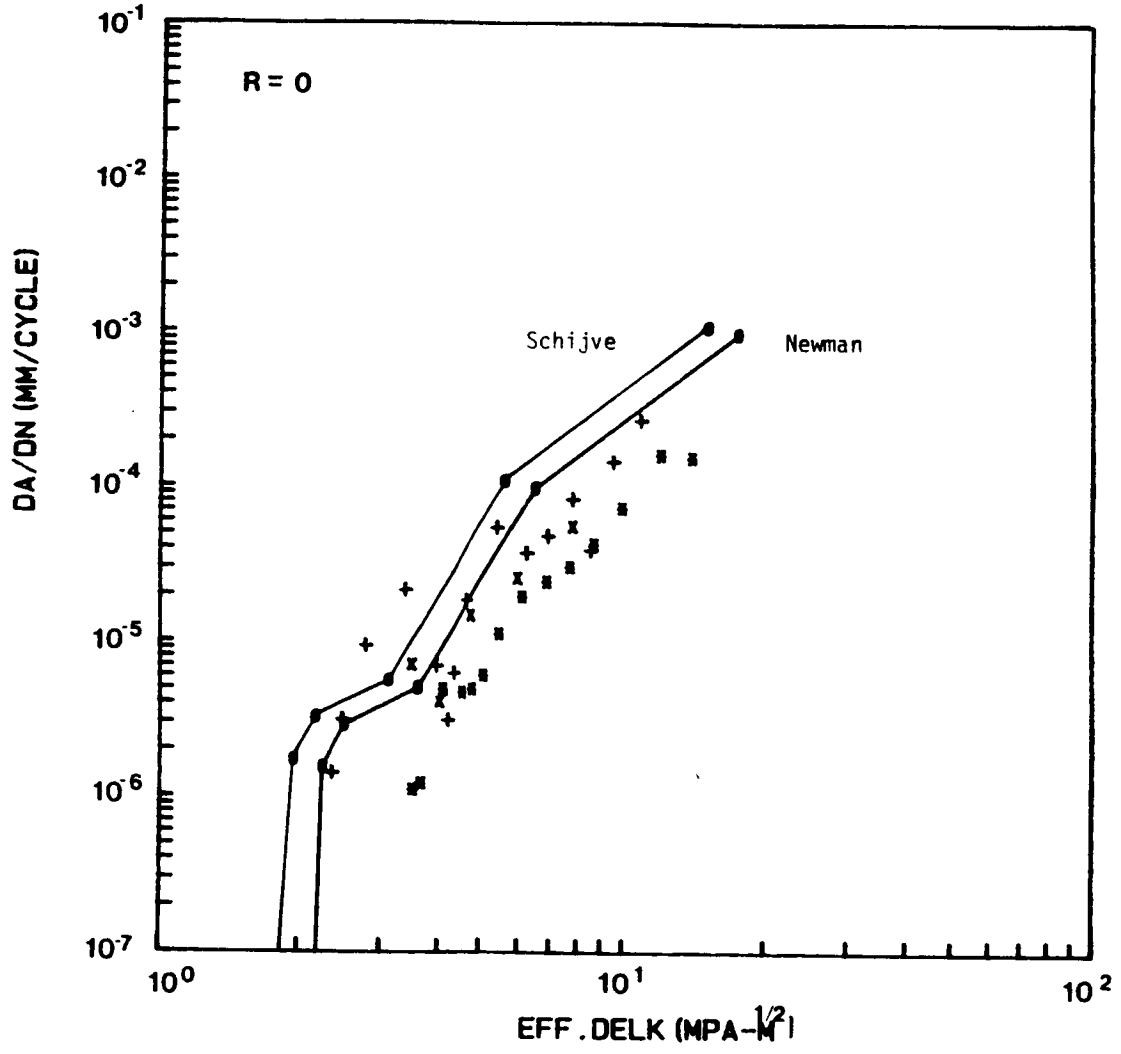

Figure IV-21. da/dN - ΔK_{eff} plot for R = 0.0

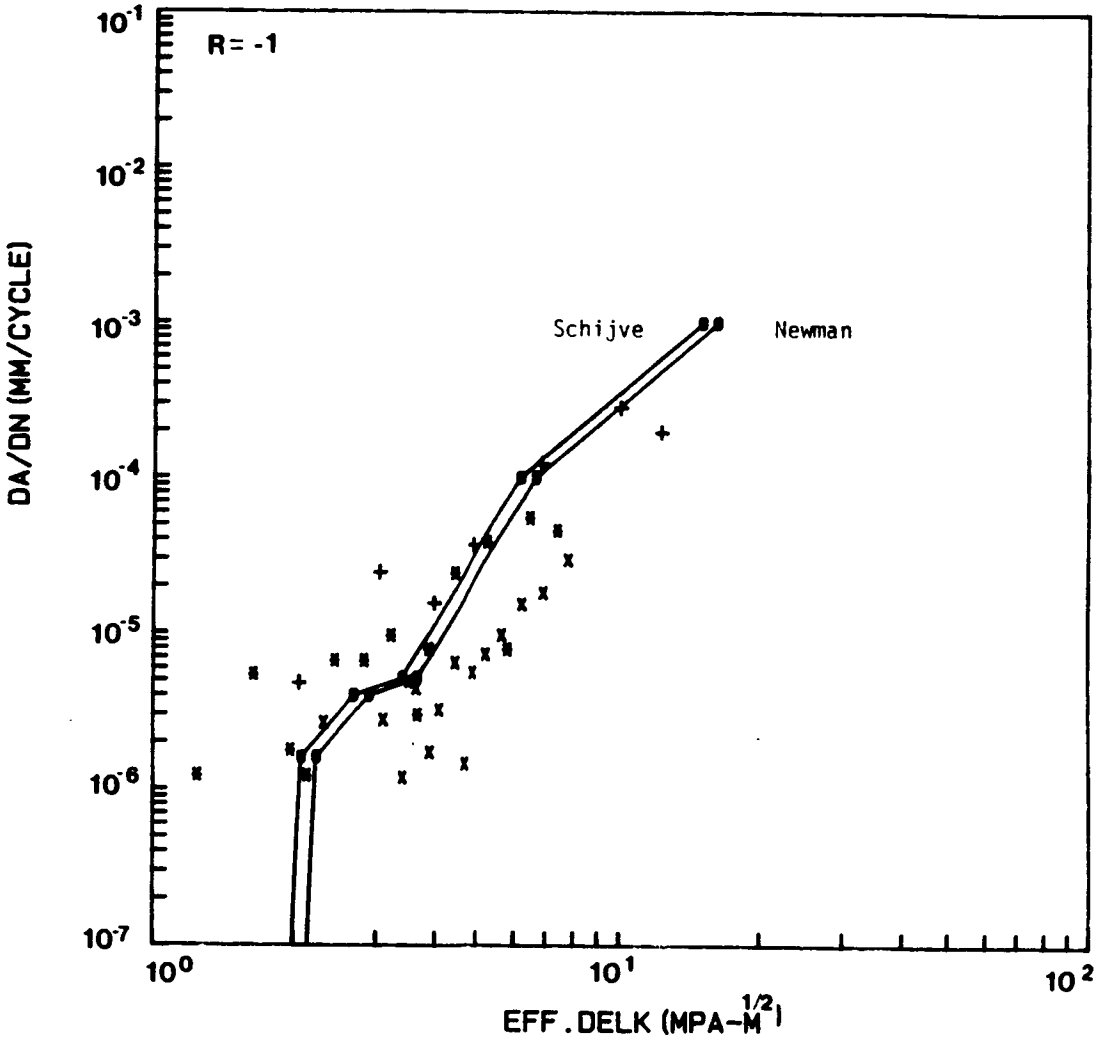

Figure IV-22. da/dN - ΔK_{eff} plot for R = -1.0

For R = -2.0, growth rates for short and long cracks recalculated with closure stresses are in reasonably good agreement, as Figure IV-23 shows. The use of ΔK_{eff} gives considerable improvement in the coalescence of the growth rate data for R = -1.0 and -2.0. But in addition to the closure effect, the complexity of notch plasticity must also be considered when examining the difference in growth rate behavior of short and long cracks for R = 0.5, 0.0, and -2.0.

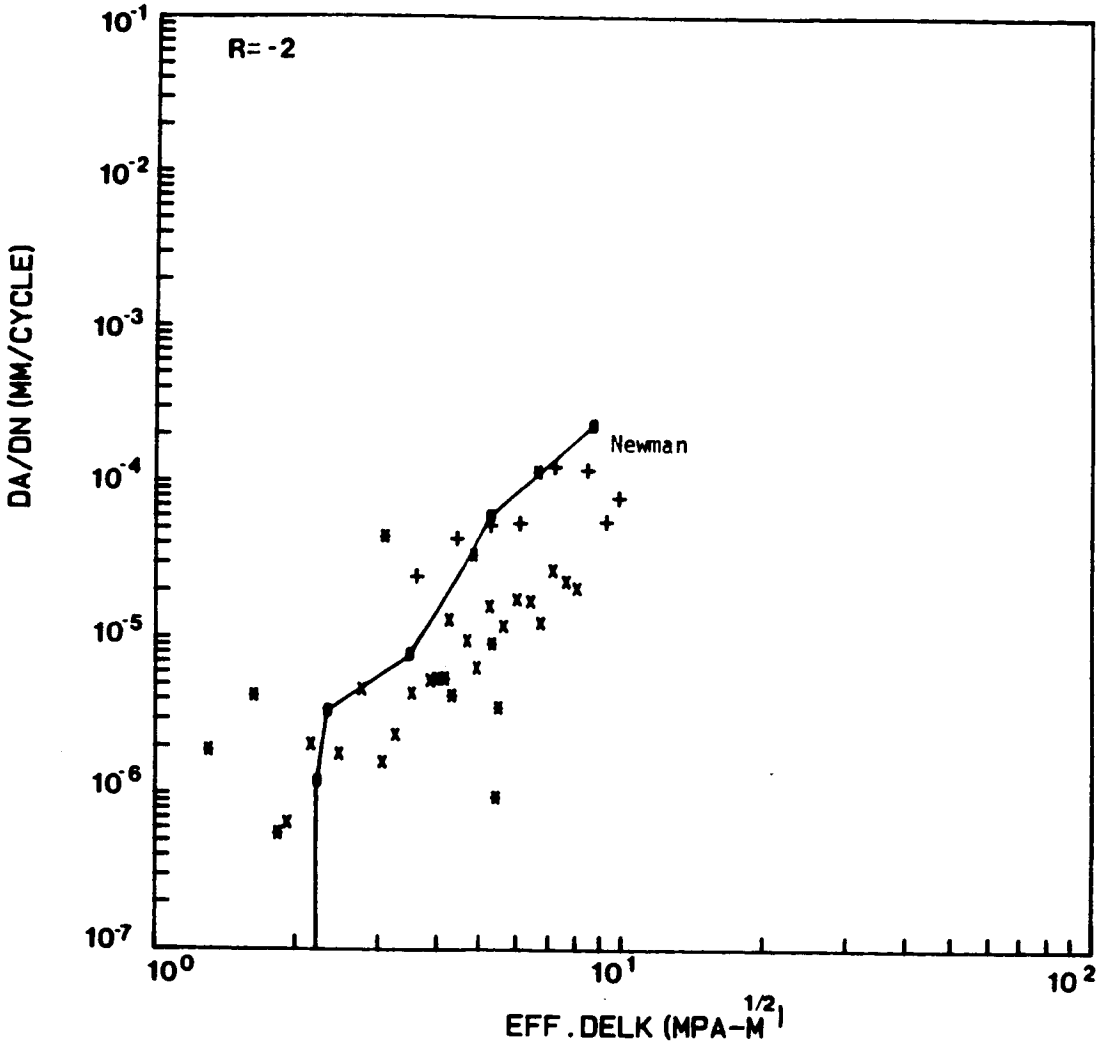

Figure IV-23. da/dN - ΔK_{eff} plot for R = -2.0

V. CONCLUSIONS

Based on the study of short fatigue cracks growth and short crack closure behavior, involoving an experimental study of short surface or corner cracks (0.035 - 0.5 mm) and short through-thickness cracks (0.8 - 2.7 mm, average depth) in notched Al 2024-T3 specimens, the following conclusions may be made.

1. Crack initiation and growth were observed successfully using the replica technique. Most of the cracks originate at the center of the notch root rather than at the corner. Those cracks which originate at a corner initiate at inclusions.

2. The initiation cycles observed in this experiment are in reasonably good agreeement with the values predicted by the Manson- Coffin relationship. The ratios of initiation cycles to tested life vary from 0.1 to 0.9.

3. The shapes of short surface and corner cracks, as determined from examination of the broken test specimens, are usually semi- elliptical and quarter-elliptical, respectively. The aspect ratios are in good agreement with the equation

$$c/a = 0.9 - 0.25\ (a/t)^2$$

4. The growth rates of short cracks in these aluminum specimens differs in general from those of long cracks in the same material. Short cracks grow faster than the long cracks for negative R-ratios and slower than the long cracks for R = 0.5. At R = 0.0, the two kinds of cracks grow at about the same rates. Also, there is a stress effect on the growth rates of the short cracks at negative R ratios.

5. The laser-based Interferometric Strain/Displacement Gage is capable of measuring the crack opening displacement (COD) across very short cracks at the roots of the notches. Since it measures so close to the crack surface, the resulting load-COD curves clearly show the crack closure effect. This technique is also used to measure the strain at a notch root.

6. The crack compliances of short surface cracks, obtained form COD curves, show a linear relationship with the crack length. The compliances of short through-thickness cracks also vary linearly with crack length (in the direction of depth).

7. The crack closure load ratios measured for the short cracks were in general lower than those predicted for longer cracks. There is only a slight difference for positive R-ratios, but the difference is significant for negative R-ratios, where the measured closure ratios for the short cracks were nearly zero or less than zero.

8. An attempt to explain the difference between the growth rates using an effective stress intensity factor range to account for the crack closure was partially successful. This approach improved the correlation between long and short crack growth for R = -1.0 and -2.0, but did little to explain results for positive R-ratios. Micro-structural effects and the plasticity of the notch root add to the complexity of this problem.

VI. REFERENCES

1. Pearson, S.: Initiation of Fatigue Cracks in Commercial Aluminum Alloys and the Subsequent Propagation of Very Short Cracks. Engineering Fracture Mechanics, vol. 7, no. 2, pp. 235-247, 1975.

2. Sova, J. A.; Crews, J.H., Jr.; and Exton, R. J.: Fatigue-Crack Initiation and Growth in Notched 2024-T3 Specimens Monitored by a Video Tape System. NASA TN D-8224, 1976.

3. Hudak, S. J., Jr.: Small Crack Behavior and the Prediction of Fatigue Life. Transactions of ASME, vol. 103, pp. 26-35, 1981.

4. Taylor, D.; and Knott, J. F.: Fatigue Crack Propagation Behavior of Short Cracks: The Effect of Microstructure. Fatigue and Fracture of Engineering Materials and Structures, vol. 4, no. 2, pp. 147-155, 1981.

5. Lankford, J.: The Effect of Environment on the Growth of Small Fatigue Cracks. Fatigue and Fracture of Engineering Materials and Structures, vol. 6, no. 1, pp. 15-31, 1983.

6. Fujimura, S.; Hayashi, T.; and Yamada, T.: Short Crack Growth and Life Prediction in Low-Cycle Fatigue of Smooth Specimens. Engineering Fracture Mechanics, vol. 21, no. 2, pp. 85-101, 1985.

7. El Haddad, M. H.; Smith, K. N.; and Topper, T. H.: Fatigue Crack Propagation of Short Cracks. Transactions of ASME, vol. 101, pp. 42-46, 1979.

8. Saxema, A.; Wilson, W. K.; Roth, L. D.; and Liaw, P. K.: The Behavior of Small Fatigue Cracks at Notches in Corrosive Environments. International Journal of Fracture, vol. 28, pp. 69-82, 1985.

9. Gangloff, R. P.: in "Advances in Crack Length Measurement" (ed. C. J. Beevers), 175; 1983, Warley, West Midlands, Engineering Materials Advisory Services Ltd.

10. James, M. R.; and Morris, W. L.: Effect of Fracture Surface Roughness on Growth of Short Fatigue Cracks. Metallurgical Transactions A, vol. 14A, pp. 153-158, 1983.

11. McCarver, J. F.; and Ritchie, R. O.: Fatigue Crack Propagation Thresholds for Long and Short Cracks in Reni 95 Nickel-based Superalloy. Material Science of Engineering, vol. 55, pp. 63-67, 1982.

12. Tanaka, K.; Hojo, M.; and Nakai, Y.: Fatigue Growth

Initiation and Early Propagation in 3% Silicon Iron. ASTM STP 811, pp. 207-232, 1983.

13. Larsen, J. M.: Advanced Experimental Methods for Monitoring the Behavior of Small Cracks. Presentation given at AGARD Strutures and Materials Panel Specialists Meeting, San Antonio, TX, April 1985.

14. Forte, T. P.; and Leis, B. N.: Fatigue Growth of Initially Physically Short Cracks in Notched Aluminum and Steel Plates. ASTM STP 743, pp. 100-124, 1981.

15. Morris, W. L.: Noncontinuum Crack Tip Deformation Behavior of Surface Microcracks. Metallurgical Transactions, vol. IIA, pp. 1117-1123, July 1980.

16. Morris, W. L.: Microcrack Closure Phenomena for Al 2219-T851. Metallurgical Transactions A, vol. 10A, pp. 5-11, 1979.

17. Morris, W. L.; James, M. R.; and Buck, O.: Growth Rate Models for Short Surface Cracks in Al 2219-T851. Metallurgical Transactions A, vol. 21A, pp. 57-64, 1981.

18. Kung, C. Y.; and Fine, M. E.: Fatiuge Crack Initiation and Microcrack Growth in 2024-T4 and 2124-T4 Aluminum Alloys. Metallurgical Transactions A, vol. 10A, pp. 603-610, 1979.

19. de los Rios, E. R.; Mohamed, Hussain J.; and Miller, K. J.: A Micro-Mechanics Analysis for Short Fatigue Crack Growth. Fatigue and Fracture of Engineering Materials and Structures, vol, 8, no. 1, pp. 49-163, 1985.

20. Tanaka, K.; Nakai, Y.; and Yamashita, M.: Fatigue Growth Threshold of Small Cracks. International Journal of Fracture, vol. 17, pp. 519-533, 1981.

21. Newman, J. C., Jr.: Behavior of Short Cracks in Airframe Components. AGARD Conference Proceedings No. 328, pp. 6.9-6.26, AGARD, France, 1981.

22. Breat, J. L.; Mudry, F.; and Pineau, A.: Short CRack Propagation and Closure Effects in A508 Steel. Fatigue and Fracture of Engineering Materials and Structures, vol. 6, no. 4, pp. 349-358, 1983.

23. James, M. N.; and Knott, J. F.: An Assessment of Crack Closure and the Extent of the Short Crack Regime in QIN (HY 80) Steel. Fatigue and Fracture of Engineering Materials and Structures, vol. 8, no. 2, pp. 177-191, 1985.

24. McEvily, A. J.; and Minakawa, K.: Crack Closure and the Growth of Short and Long Fatigue Cracks. Scripta Metallurgica, vol. 18, pp. 71-76, 1984.

25. Ritchie, R. O.; and Zaiken, E.: On the Development of Crack Closure and the Threshold Condition for Short and Long Cracks in 7150 Aluminum Alloy. Metallurgical Transactions A, vol. 16, pp. 1467-1477, 1985.

26. Tanaka, K.: Short-Crack Fracture Mechanics in Fatigue Conditions. Current Research on Fatigue Cracks, pp. 79-100, Society of Material Science, Japan, 1985.

27. Hommouda, M. M.; and Miller, K. J.: ASTM STP 668, pp. 703-, 1979.

28. Zurek, A. K.; James, M. R.; and Morris, W. L.: The Effect of Grain Size on Fatigue Growth in Short Cracks. Metallurgical Transactions A, vol. 14A, pp. 1697-1705, 1983.

29. Suresh, S.; and Ritchie, R. O.: Propagation of Short Fatigue Cracks. International Metals Reviews, vol. 29, no. 6, pp. 445-475, 1984.

30. Bowles, C. Q.; and Schijve, J.: The Role of Inclusions in Fatigue Crack Initiation in an Aluminum Alloy. International Journal of Fracture, vol. 9, no.2, pp. 171-179, 1973.

31. Swain, M. H.; and Newman, J. C., Jr.: On the Use of Marker Loads and Replicas for Measuring Growth Rates for Small Cracks. Presented at AGARD Specialists Meeting, Siena, Italy, April 1984.

32. Leis, B. N.; and Galliher, R. D.: Growth of Physically Short Corner Cracks at Circular Notches. ASTM STP 770, pp. 399-421, 1982.

33. Leis, B. N.: Displacement Controlled Fatigue Crack Growth in Inelastic Notch Fields: Implications for Short Cracks. Engineering Fracture Mechanics, vol. 22, no. 2, pp. 279-293, 1985.

34. Elber, W.: The Significance of Fatigue Crack Closure. ASTM STP 486, pp. 230-242, 1971.

35. Banerjee, S.: A Review of Crack Closure. AFWAL-TR-84-4031, 1984.

36. Banerjee, S.: Influence of Specimen Size and Configuration on the Plastic Zone Size, Toughness, and Crack Growth. Engineering Fracture Mechanics, vol. 15, pp. 343-390, 1981.

37. Newman, J. C., Jr.: A Crack-Closure Model for Predicting Fatigue Crack Growth Under Aircraft Spectrum Loading. ASTM STP 748, pp. 52-84, 1981.

38. Ritchie, R. O.; and Suresh, S.: Some Consideration on Fatigue Crack Closure Induced by Fracture Surface Morphology.

Metallurgical Transactions, vol. 13A, pp. 937-940, 1982.

39. Morris, W. L.; James, M. R.; and Buck, O.: A Simple Model of Stress Intensity Range Threshold and Crack Closure Stress. Engineering Fracture Mechanics, vol. 18, no. 4, pp. 871-877, 1983.

40. Liaw, P. K.; and Logson, W. A.: Crack Closure: An Explanation for Small Fatigue Crack Growth Behavior. Engineering Fracture Mechanics, vol. 22, no. 2, pp. 115-121, 1985.

41. Sharpe, W. N., Jr.: Application of the Interferometric Strain/ Displacement Gage. Optical Engineering, vol. 21, no. 3, pp. 483-488, 1982.

42. Morris, W. L.; and Buck, O.: Crack Closure Load Measurement for Microcracks Developed During the Fatigue of Al 2219-T851. Metallurgical Transactions A; vol. 8A, pp. 597-601, 1977.

43. James, M. N.; and Smith, G. C.: Surface Microcrack Closure in Fatigue. International Jounal of Fracture ; vol. 22, pp. R69-R75, 1983.

44. Zeiken, E.; and Ritchie, R. O.: On the Development of Crack Closure and the Threshold Condition for Short and Long Fatigue Cracks in 7150 Aluminum Alloy. Metallurgicl Transactions A, vol. 16A, pp. 1467-1477, 1985.

45. Dutta, V. B.; Suresh, S.; and Ritchie, R. O.: Fatigue Crack Propagation in Dual-Phase Steels: Effects of Ferritic-Martensitic Microstructures on Crack Path Morphology. Metallurgical Transactions A, vol. 15A, pp.1193-1207, 1984.

46. Sharpe, W. N.; and Lee, J. J.: Near Tip Crack Displacement Measurements During High-Temperature Fatigue. ASTM STP 905, pp. 253-264, 1986.

47. Williams, D. R.; Davison, D. L.; and Lankford, J.: Fatigue-Crack-tip Plastic STrains by the Stereoimaging Technique. Experimental Mechanics, pp. 134-139, April 1980.

48. James, M. N.; and Knott, J. F.: Critical Aspects of the Characterization of Crack Tip Closure by Compliance Technique. Material Science and Engineering, vol. 72, pp. L1-L4, 1981

49. Edwards, P. R.; and Newman, J. C., Jr.: AGARD Collaborative Effort on Short Cracks (Introduction to Participants). NASA Langley Research Center, 1984.

50. Lee, J. J.: A Study of Fatigue Threshold and Crack Closure at Elevated Temerature. Master's thesis, The Johns Hopkins University, 1984.

51. Leis, B. N.; Kanninen, M. F.; Hopper, A. T.; Ahmad, J.; and Broek, D.: A Critical Review of the Short Crack Problem in Fatigue. AFWAL-TR-83-4019.

52. Morris, W. L.; Buck, O.; and Marcus, H. L.: Crack Intiation and Early Propagation in Al 2219-T851. Metallurgical Transactions A, vol. 7A, pp. 1161-1165, 1976.

53. Drucker, D. C.; and Rice, J. C.: Plastic Deformation in Brittle and Ductile Fracture. Engineering Fracture Mechanics, vol. 1, pp. 500-602, 1970.

54. Newman, J. C., Jr.: Private communication. January 1986.

55. Schijve, J.: Some Formulas for the Crack Opening Stress Level. Engineering Fracture Mechanics, vol. 14, pp. 481-465, 1981.

56. Suresh, S.: Crack Initiation in Cyclic compression and its Applications. Engineering Fracture Mechanics, vol. 21, no. 3, pp. 453-463, 1985.

57. Sehitoglu, H.: Crack Opening and Closure in Fatigue. Engineering Fracture Mechanics, vol. 21, no. 2, pp. 329-339, 1985.

58. Newman, J. C., Jr.: A Crack Opening Stress Equation for Fatigue Crack Growth. International Journal of Fracture, vol. 24, pp. R131-R135, 1984.

59. Fuchs, H. O.; and Stephens, R. I.: Metal Fatigue in Engineering. Wiley Interscience Publication, 1980.

60. Swain, M. H.: Private communication, July 1985.

61. Tanaka, K.; and Nakai, Y.: Propagation and Nonpropagation of Short Fatigue Cracks at a Sharp Notch. Fatigue of Engineering Materials and Structures, vol. 6, no. 4, pp. 315-327, 1983.

62. Newman, J. C.; Swain, M. H.; and Phillips, E. P.: An Assessment of the Small-crack EFfect for 2024-T3 Aluminum Alloy. Presented at the Second International Workshop on Small Fatigue Cracks, January, 1986.

APPENDIX I

A. Stress Intensity Factor Calculation

The calculation of the stress intensity factor range (K) assumes either that a semi-elliptical surface crack is located at the center of the edge notch or that a quarter-elliptical corner crack is located at an edge, as shown in Figure A-1. For a surface crack found at other locations along the bore of the notch, the calculation is adequate if the crack is small compared to the thickness of the specimen.

To calculate the stress intensity factor at the point where the crack intersects the notch surface, the crack length, a, and the crack depth, c, must be known. When the crack length, a, is measured then the crack depth, c, is calculated from the following equation for either a surface or corner crack:

$$c/a = 0.9 - 0.25\,(a/t)^2$$

where a, c, and t are defined in Figure A-1.

The stress intensity factor range equation [49] for a surface crack located at the center of the edge notch and subjected to remote uniform stress is

$$\Delta K = \Delta S\sqrt{\pi a}/Q \cdot Fsn$$

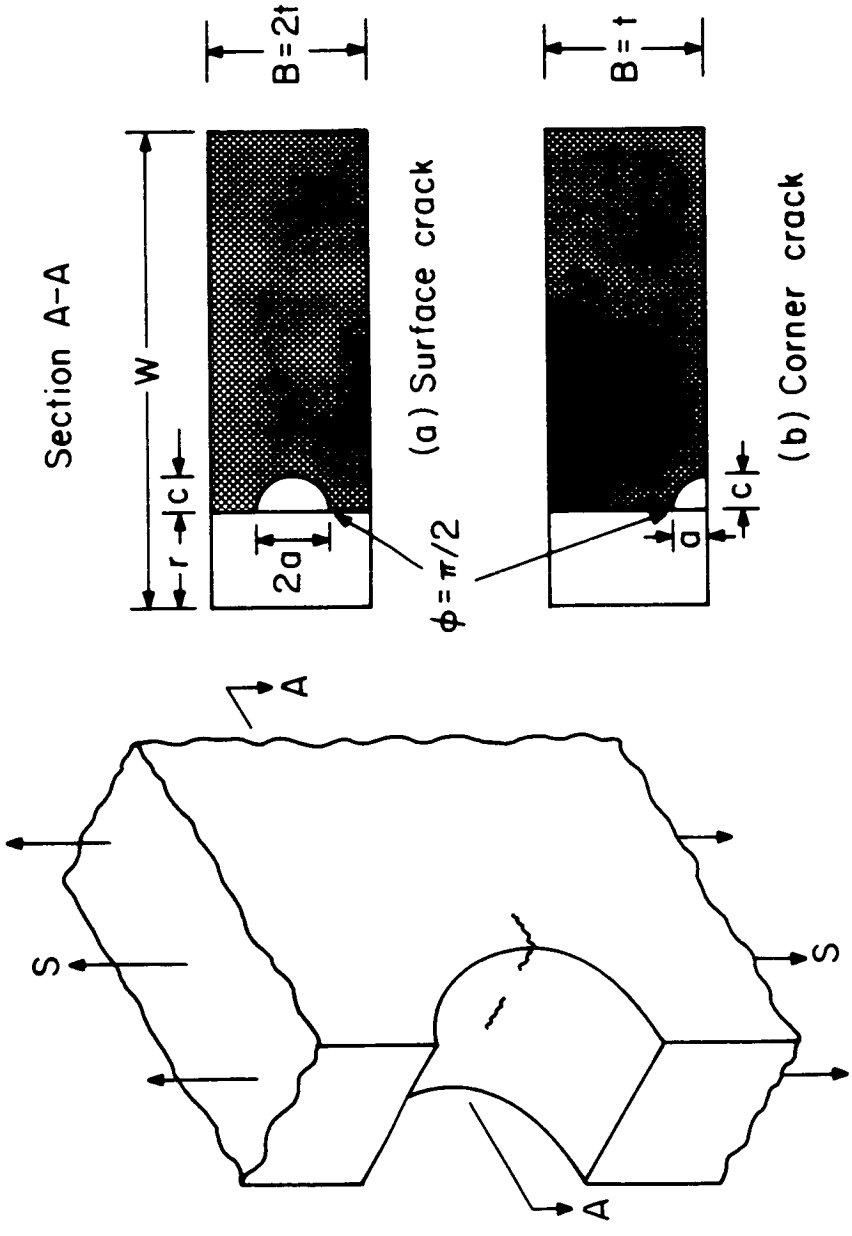

Figure A-1. Definition of dimensions for surface crack and corner crack at a notch in a finite plate

The equation for a quarter-elliptical corner crack is

$$\Delta K = \Delta S\sqrt{\pi a/Q} \cdot Fcn$$

for $0.2 \leqq a/c \leqq 2$ and $a/t < 1$.

These equations are modified from the empirical stress intensity factor equations, which are obtained by fitting to the finite element results for two-symmetric, semi-elliptical surface cracks and for two-symmetric, quarter-elliptical corner cracks at a hole in a finite plate, as shown in Figure A-2.

The stress range, ΔS, is the full range, Smax - Smin, for constant amplitude loading.

The shape factor,Q, is given by

$$Q = 1 + 1.464\ (a/c) \text{ for } a/c \leqq 1$$

$$Q = 1 + 1.464\ (c/a) \text{ for } a/c > 1$$

The functions Fcn and Fsn are found as follows.

$$Fcn = Fsn\ (1.13 - 0.09\ a/c) \text{ for } a/c \leqq 1$$

$$Fcn = Fsn\ (1 + 0.04\ c/a) \text{ for } a/c > 1$$

$$Fsn = [M1 + M2\ (a/t) + M3\ (a/t)\ ]\ g1\ g2\ g3\ g4\ f1\ f2$$

where for $a/c \leq 1$ and $\phi = \pi/2$,

$$M1 = f2 = 1$$

and for $a/c > 1$ and $\phi = \pi/2$.

$$M1 = f2 = (c/a)^{1/2}$$

Other subfunctions of Fsn are

$$M2 = 0.05 \; / \; [0.11 + (a/c)^{1.5}]$$

$$M3 = 0.29 \; / \; [0.29 + (a/c)^{1.5}]$$

$$g1 = 1$$

$$g2 = \frac{1 + 0.358k + 1.425k^2 - 1.578k^3 + 2.156k^4}{1 + 0.08k^2}$$

$$k = \frac{1}{1 + 0.1564\ c/r}$$

$$g3 = 1 + 0.1\ (1 + a/t)^{10}$$

$g4 = 1.14 - 0.1 \; / \; (1 + c/r)^{1/2}$ for $0.2 \leq (a/c) \leq 2$, $(a/t) < 1$, and $\phi = \pi/2$.

The finite-width correction, f1, is

$f1 = (-0.2n + 9.4n - 19.4n + 27.1n)$ where $n = (c+r)/w$.

B. Replica Method

A replica of the notch surface is made after each cyclic interval which is specified in Section II, Experimental Procedure. At each cyclic interval, the specimen is held under a constant applied stress, $S = (0.8)S_{max}$, while the replica is taken. The replica material is acetylcellulose film, with a width of 0.034 mm (Item Number 14640, Ernest F. Fullan, Inc.), which is cut into pieces about 8 mm X 30 mm.

Prior to making each replica, the notch surface is cleaned with acetone. A piece of the replica material is held in place loosely against the notch surface using a metal or glass rod with a diameter slightly smaller than that of the notch. A few drops of acetone, applied with an injector or a swab, are allowed to flow between the film and the notch surface. The film is then touched lightly to the notch surface and left to adhere and dry for at least five minutes. While the replica is in place on the specimen, the surface is checked for flaws such as bubbles or other artifacts using a low-magnification microscope with a relatively long focussing length.

Once dry, the replica is slowly peeled from the specimen. Best results are obtained when the replica is handled with tweezers. One of the top corners of the finished replica film is chipped away to aid in orienting the replica for analysis under the microscope. Each replica is attached with double-sided tape to a microslide, labeled with the number of

cycles run at that point in the experiment, and stored in a box marked with the specimen number. Analysis of the replicas from the last replica to those made early in the life of the specimen permits easy location of the crack.

Occasionally a replica will be twisted or have an unusually large curvature, making crack length measurements less accurate. For this reason, the position of the crack tip from each replica should be marked on a montage of micrographs from a relatively flat replica. A holder can be made from a thin metal plate with a slit at the center; this will keep the replica flat when it is observed under an optical microscope.

C. Stress-strain Analysis of the Notch

The data in Table C-1 concerning elastic normal stress distribution along the center line of the specimen were taken from reference 18. The table gives the location, x, normalized by the hole radius, r, against the stress concentration $\sigma yy/S$, where S is the gross stress.

TABLE C-1
STRESS CONCENTRATION AROUND THE NOTCH

x/r	σyy/S	x/r	σyy/S
1.00	3.170	1.15	2.378
1.01	3.096	1.20	2.206
1.02	3.027	1.30	1.944
1.03	2.962	1.40	1.756
1.04	2.901	1.50	1.618
1.05	2.843	1.60	1.513
1.06	2.787	1.70	1.433
1.07	2.734	1.80	1.370
1.08	2.683	1.90	1.319
1.09	2.634	2.00	1.280
1.10	2.587		

The notch plastic zone was estimated using Irwin's method for each loading condition, based on the elastic normal stress distribution around the notch as shown above. Table C-2 shows the calculated notch plastic zone radius, r*, for a yield stress of 359 MPa.

As shown in Table C-2, since the stress at the notch was above the yielding point for several loading conditions, notch stress-strain was analyzed using Neuber's rule,

$$\varepsilon \cdot \sigma = K_t^2 \cdot e \cdot s$$

and the stress-strain relationship,

$$\varepsilon = \frac{\sigma}{E} + \left(\frac{\sigma}{K}\right)^{\frac{1}{n}}$$

where ε and σ are local strain and stress, e and S are remote strain and stress, K_t is the elastic stress concentration factor, E is the elastic modulus, and K and n are constants in the stress-strain curve.

TABLE C-2
ESTIMATED NOTCH PLASTIC ZONE

R	Smax	Radius of Notch Plastic Zone (mm)
0.5	225	1.59
	205	1.27
	195	1.11
0.0	145	0.41
	120	0.08
	110	-
-1.0	105	-
	80	-
	70	-
-2.0	75	0.47*
	60	0.08*
	50	-

*Yielding in compression for Smin

For the material Al 2024-T3 and the specimens used in this study, the constants are:

E = 73,100 MPa
K = 455 MPa [59]
n = 0.032 [59]

The notch stress and strain with the remote stress are calculated by Neuber's rule, while the notch strain was measured against the remote stress using the ISDG technique.

Two indentations with a spacing of 50 microns were set on the root of the notch and the relative displacement between the indentations was measured as shown in Figure C-1. From the curve of Figure C-1, the measured displacement for the remote stress of 145 MPa, corresponding to 3,749 lbs, is 0.35 m. Thus, the measured notch strain will be

$$\frac{0.35\ \mu m}{50\ \mu m} = 0.0070$$

This measured value is quite close to the value calculated by Neuber's rule (0.0077), within 10%.

Table C-3 shows the notch stress and strain, comparing values calculated from Neuber's rule and measured values.

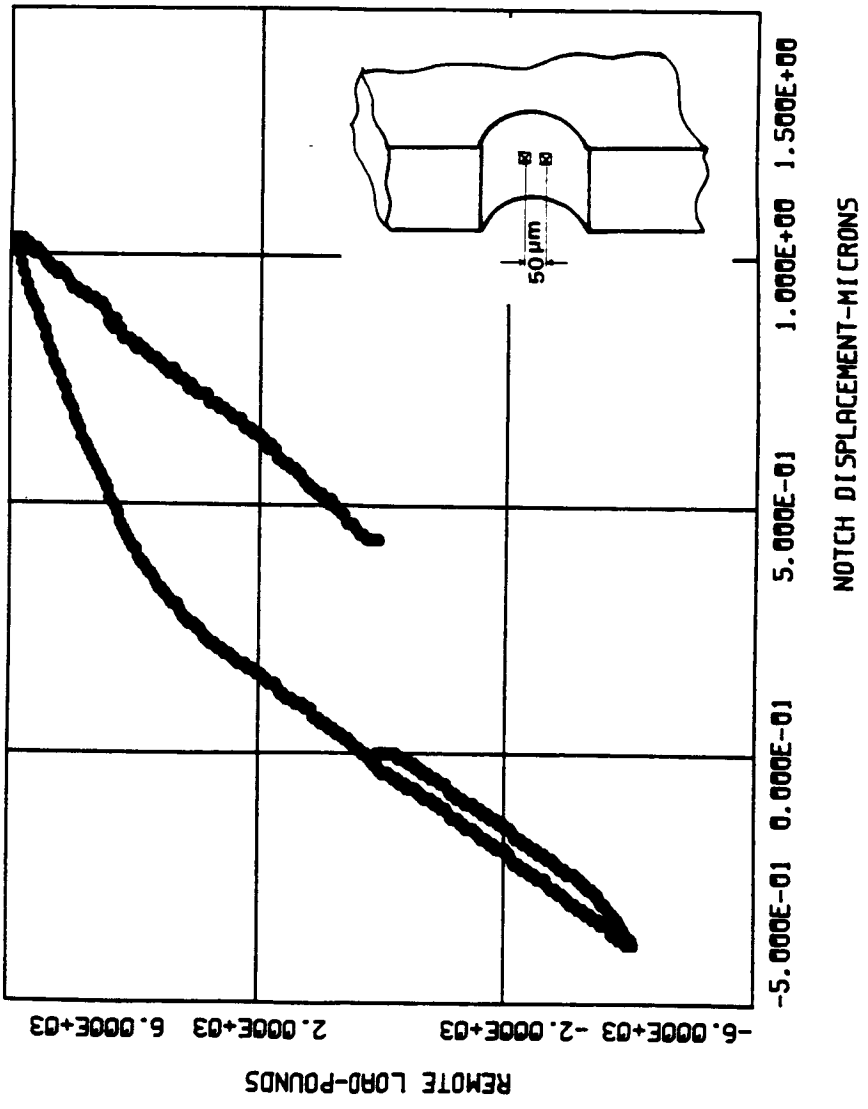

Figure C-1. Displacement measurement at the Notch root using ISDG

D. Alignment of Grips and Checks

As shown in Figure III-3, the fixtures gripping a specimen consist of two parts: the base fixtures, which are attached at the bottom to the hydraulic ram of the test machine and at the top to the load cell, and the specimen grip sets, which are attached to the base fixtures.

The bottom base fixture, which has a spherical joint inside, was aligned to be parallel to the test machine table. This was accomplished by adjusting the spherical joint. The parallelism was achieved through the following steps.

1. A dial gage with a precision of 0.0005 inch was mounted on the test machine table and the probe was positioned vertically on the edge of the bottom base fixture.

2. The hydraulic ram was brought to the bottom of the machine, instead of being allowed to float in the hydraulic liquid, and rotated.

3. The dial indicator was monitored while the hydraulic ram was rotating. Dial gage variations could not exceed 0.0005 inch.

4. If the variations were greater than 0.0005 inch, the appropriate adjusting bolts in the base fixture were tightened.

5. Procedures 3 and 4 were repeated until the bottom base fixture was parallel to the table.

The top base fixture has the same structure as the bottom base fixture. It was also aligned parallel to the table in a procedure similar to the bottom base fixtue alignment described above. In this second procedure, however, the dial gage was

mounted on the bottom base fixture and the probe was positioned vertically on the edge of the top base fixture.

After the base fixtures were aligned, the specimen grips were attached to the base fixtures and aligned using a strain-gaged specimen. Five strain gages (Micro-Measurement; CEA-13-062UW-120) were placed as shown in Figure D-1 on each side of a specimen which had the same dimensions as the study specimens but did not have a notch.

The alignment procedure for the specimen grips was as follows.

1. Specimen grips were finger-tightened at the top (or the bottom) base fixture. The strain-gaged specimen was put in place, the other specimen grip was tightened by hand, and the specimen was loosely fastened.

2. Another specimen grip was placed at the other side of the specimen and aligned parallel to the specimen as accurately as possible; then that pair of grips was tightened by hand and the specimen loosely fastened.

3. Approximately 300 lbs of tension load was applied; then the specimen was tightly fastened.

4. The test machine was unloaded and one set of specimen grips (top or bottom) was fastened tightly.

5. The other set of specimen grips was loosened from the base fixture and adjusted while reading the strain from the strain indicator. Before any readings were taken, the strain was set to zero while the specimen was in a free condition.

After the specimen grips were aligned, one grip from each of the two pairs (same side top and bottom) was never loosened until it had to be aligned again; this was the "reference grip." To check for misalignment, strain gage readings were

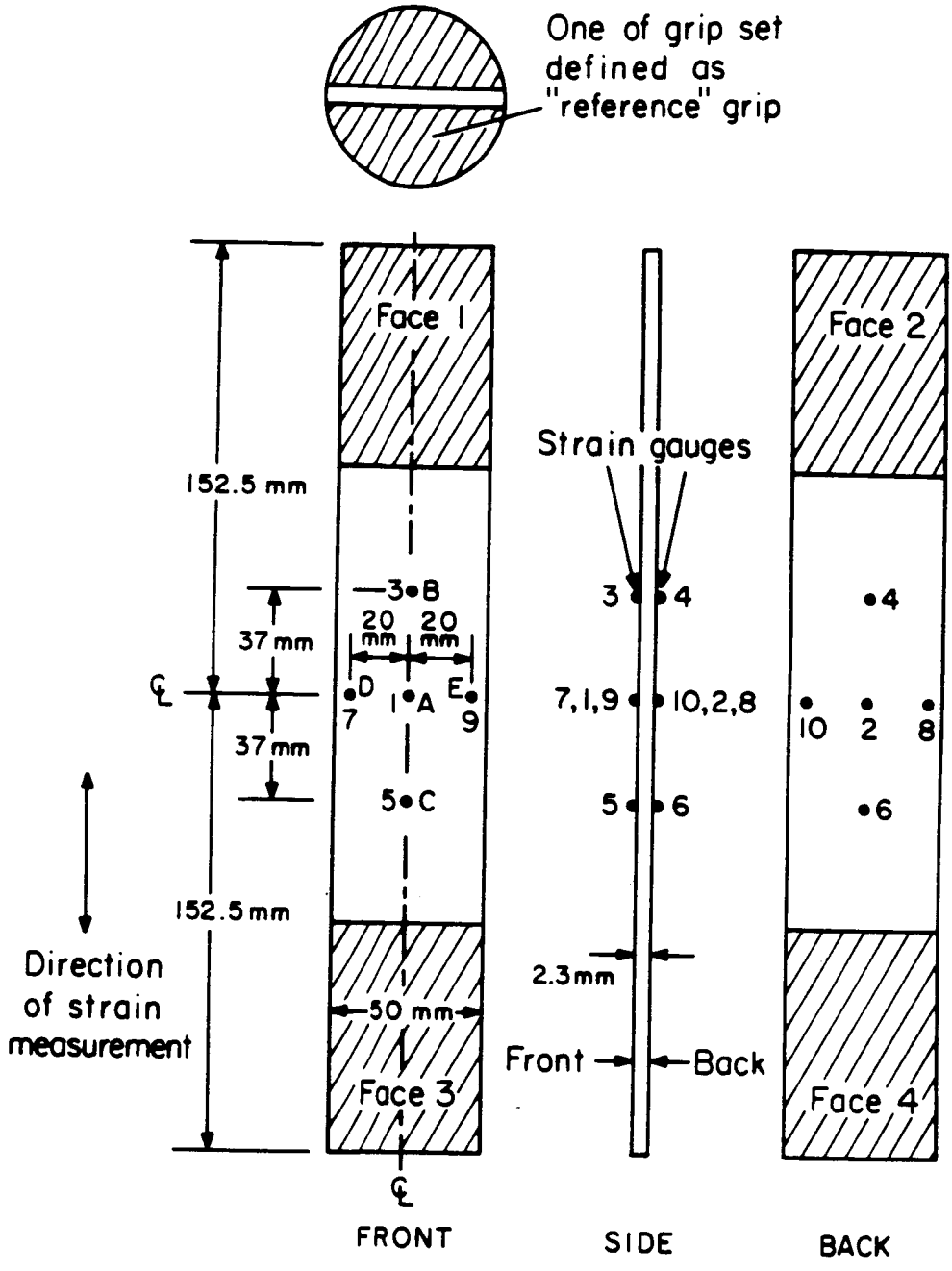

Figure D-1. Strain-gaged specimen to check alignment

taken at zero load and at 10 KN (= 2,240 lbs) load in the manner described below.

1. The strain-gaged specimen was placed so that the front face (face 1 in Figure D-1) was in contact with the reference grip (the standard position). The grips were tightened, and strains on all gages were read at zero load. This strain reading was labeled e_{nSo} at gage number n, standard position, zero load.

2. A tensile load of 10 KN was applied and the strains were measured (strain = e_{nSo}).

3. The specimen was unloaded and removed, then replaced so that face 4 (see Figure D-1) was in contact with the reference grip (reverse position). Grips were tightened, and strains were read on all gages (strain = e_{nR10}).

Strain measurements from the above procedure are shown in Table D-1. The bending strains are given by the difference between e_{nS} and e_{nR}, such as $e_{1So} - e_{1Ro}$. The final bending strain values are the average of those obtained from opposite gages, such as 1 and 2. The resulting bending strains at A, B, and C are plotted in Figure D-2.

The criteria of misalignment for lateral bending, e_L, and rotational bending, e_R, are [49]:

$$e_L \leqq 20 \text{ microstrain}$$
$$e_R \leqq 10 \text{ microstrain}$$

The measured values of e_L and e_R at zero load are

$$e_L = 12 \text{ microstrain}$$
$$e_R = 12 \text{ microstrain}$$

while at a load of 10 KN,

$$e_L = 13 \text{ microstrain}$$
$$e_R = 3 \text{ microstrain}$$

which nearly satisfies the bending criteria.

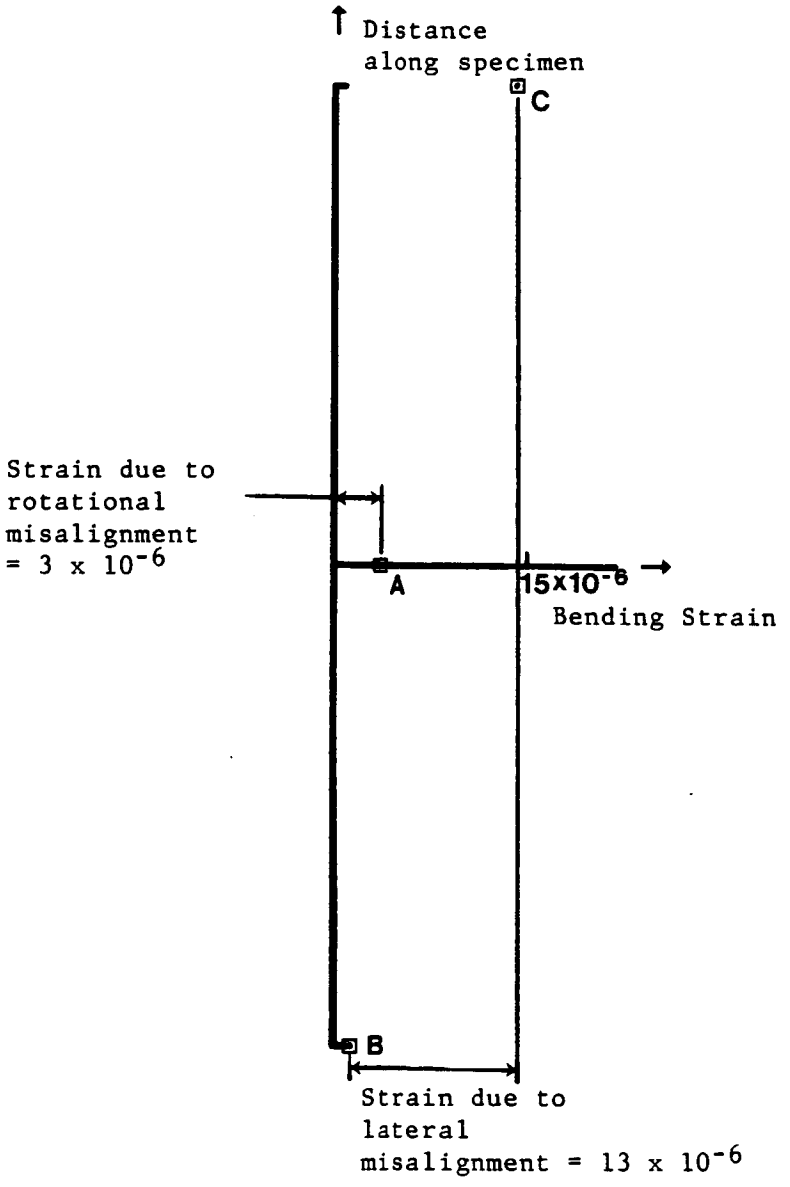

Figure D-2. Plot of bending strain measurement

TABLE D-1
STRAIN MEASUREMENT FOR ALIGNMENT CHECK

Position	Gage	Strain (X 10E-6) SX	RX	Bending Strain	Average	S1X	R1X	Bending Strain	Average
A	1	-17	-30	13		1152	1149	3	
	2	13	24	11	12	1181	1184	3	3
B	3	-19	-29	10		1144	1145	-1	
	4	14	21	7	8.5	1190	1193	3	1
C	5	-10	-31	21		1162	1149	13	
	6	7	27	20	20.5	1183	1198	15	14
D	7	-19	-25	6		1188	1186	2	
	8	15	30	15	10.5	1186	1187	1	1.5
E	9	-18	-38	20		1143	1141	2	
	10	16	21	5	12.5	1187	1188	1	1.5

The criterion for torsional misalignment, which is the difference in the bending strain at points D and E, is less than 15 microstrain [49]. The measured value of the difference between points D and E is 2 microstrain at zero load and 0 microstrain at a load of 10 KN.

The criterion for the tensile strain range is defined as follows.

$$0.95 \leq \frac{e_{TD}}{e_{TE}} \leq 1.05$$

where

$$e_{TD} = (e_{7S10} + e_{8S10} + e_{7R10} + e_{8R10} - e_{7S0} - e_{8S0} - e_{7R0} - e_{8R0})$$

$$e_{TE} = (e_{9S10} + e_{10S10} + e_{9R10} + e_{10R10} - e_{9S0} - e_{10S0} - e_{9R0} - e_{10R0})$$

The measured value of the tensile range is

$$\frac{e_{TD}}{e_{TE}} = 1.01$$

which satisfies the criterion well.

E. Test and data program list

```
C ***************** NACOM6.FOR ****************************************
C
C        This is the REVISED version of NACOMP to measure
C        COMPLIANCE for R<0. of small crack.
C                                        June 85, J.J.LEE

         DIMENSION RAM(1200)
         DIMENSION IRAM(1200),LB(600),IDSP(600),XRAM(1200),LD(600)
         BYTE ICHAR
         INTEGER*4 INN,INNI,IN1,NC
         INTEGER IFLNM(10),ISP(10)
         INTEGER CH1,CH2,CH1N,CH2N

         TYPE*,'USING 20,000 LB L/C ? -- Y=1'
         ACCEPT*,IGA

         IF(IGA.NE.1)GO TO 650

 3       CONTINUE

         WRITE(7,*)'SPECIMEN NO. ?'
         READ(5,5)ISP
         TYPE*,'No. of cycle  ? '
         READ(5,*)IP
         WRITE(7,*)'FILE NAME FOR COMPLIANCE?'
         READ(5,5)IFLNM
 5       FORMAT(10A2)

         OPEN(UNIT=1,NAME=IFLNM,ACCESS='DIRECT',
     *   INITIALSIZE=10,RECORDSIZE=604)
         WRITE(7,8)'COMPLIANCE FILE=',IFLNM
 8       FORMAT(20A,10A2)

         WRITE(6,10)  IFLNM
 10      FORMAT(/,T6,'*******************************************'
     *          /T6,'*',1X,'COMPLIANCE MEASUREMENT',16X,'*'
     *          /T6,'*******************************************'
     *          /T11,'COMPLIANCE FILE =',10A2/)

         WRITE(6,12) ISP

         WRITE(6,11) IP
 11      FORMAT(10X,'MEASURED CYCLE = ',I6,1X,'CYCLES')
 12      FORMAT(10X,'SPECIMEN NO. = ',5A2)

         CALL AOUT(0,0,1)
         CALL AOUT(0,1,1)
         CALL AOUT(0,2,1)

         WRITE(7,*)'** HOOK UP MTS MACHINE **'
         CALL ISLEEP(0,0,4,0)

C --- input the information and print ---

         TYPE*,'MAX. LOAD ?'
         ACCEPT*,PMAX
         TYPE*,'MIN. LOAD ( =INITIAL LOAD) ?'
         ACCEPT*,PMIN
         TYPE*,'NO. OF STEPS IN LOADING(same no. in unloading)?'
         TYPE*,'    ---100,200,300,..to 600---- '
         ACCEPT*,NOS
```

```
      WRITE(6,15) NOS
15    FORMAT(10X,'NO. OF STEPS IN LOADING(same no. in unloading)='
     1       ,I5)

      TYPE*,'REFLECTED ANGLE AO ? (REAL) and BASE LENGTH DO ?(REAL)'
      ACCEPT*,AO,DO
      TYPE*,'DEALY IN EACH INCREMENT ? ( ITICK)'
      ACCEPT*,ITICK

      FS=1.

      IF(PMIN.GT.0.) GO TO 20

      TYPE*,'** LOADING IN COMPRESSION **'
      TYPE*,'----- IS IT O.K. ?   Y=1 -----'
      ACCEPT*, KO
      IF(KO.NE.1) GO TO 650
      WRITE(7,*)'** SET THE INITIAL LOAD (PMAX) **',PMAX
      RL=-(PMAX-PMIN)
      GO TO 25

20    TYPE*,'** SET THE INITIAL LOAD ** ',PMIN
      CALL ISLEEP(0,0,5,0)
      RL=PMAX-PMIN

25    DO=DO*100.
      WRITE(6,50) PMAX,PMIN,AO,DO/100.
50    FORMAT(//10X,'MAX. LOAD =',F10.3,/10X,'MIN. LOAD =',F10.3
     *   /10X,'REFLECTED ANGLE =',F7.3,/,10X,
     *   'INITIAL DISTANCE OF INDENT.=',F7.3,1X,'MICRONS')

C ----make and store a ramp wave

      DO 110 K=0,NOS
         QK=K*1.
         XRAM(K)=QK/FLOAT(NOS)*RL
110      CONTINUE

      DO 120 K=NOS+1,NOS*2
         QK=K*1.
         XRAM(K)=(FLOAT(NOS*2)-QK)/FLOAT(NOS)*RL
120      CONTINUE

      DO 125 K=0,NOS*2
         IRAM(K)=XRAM(K)*2048./20000.+.5
125      CONTINUE

150   IF(PMAX.GT.19900) GO TO 650

160   CONTINUE

C --- call VIEW and check MLC, MSP---

      NPTS=60
      NAV=10

      CALL VIEW(NAV,MLC1,MSP1,MLC2,MSP2)


      WRITE(7,*)'CONTINUE? Y=1,N=2'
```

```
        ACCEPT*,ILT

        CH1=MLC1*8-1024
        CH2=MLC2*8-1024
        CALL AOUT(CH1,0,1)
        CALL AOUT(CH2,1,1)

        IF(ILT.EQ.1)GO TO 360

 200    CONTINUE

        TYPE*,'RUN JUNK ? Y=1,N=2'
        ACCEPT*,ILC

        IF(ILC.EQ.2) GO TO 650

C ---run JUNK ---

        CALL JUNK

C ---check MSP, MLC ---

 350    CONTINUE

        CALL VIEW(NAV,MLC1,MSP1,MLC2,MSP2)

        CH1=MLC1*8-1024
        CH2=MLC2*8-1024
        CALL AOUT(CH1,0,1)
        CALL AOUT(CH2,1,1)

        TYPE*,'O.K ? Y=1, N=2'
        ACCEPT*,ILC

        IF(ILC.NE.1) GO TO 200

360     CH1=MLC1*8-1024
        CH2=MLC2*8-1024
        CALL AOUT(CH1,0,1)
        CALL AOUT(CH2,1,1)

        WRITE(6,30) MLC1,MSP1,MLC2,MSP2
        TYPE*, '*** NOW START LOADING ***'
        CALL ISLEEP(0,0,1,0)
 30     FORMAT(//,10X,'MLC1 =',3X,I5,10X,'MSP1=',3X,I5,/,10X,'MLC2=',
     *          3X,I5,10X,'MSP2=',3X,I5,//5X,'***  Maximum Values '
     *         ,1X,'***'/)

C ---initialize the data of SND ---

        SO=(MSP1+MSP2)*4
        AO=AO*3.1416/180.
        CC=0.6328/(2*SO*SIN(AO))
        CH1N=CH1
        CH2N=CH2
        NDSPO=0
        NQ=1
        NDSP=0
        CALL SND(NPTS,MSP1,MSP2,CH1N,CH2N,CH1,CH2,NAV,CC,NDSP,NDSPO)
        CH1N=CH1
        CH2N=CH2
```

```
      NDSP=0

405     CALL AOUT(0,2,1)

        NS=1
        NQ=0

35      FORMAT(2X,'NS(odd no. is loading)=',I5,1X,'NQ=',I6,2X,I8,1X,
     *          'LB',I9,1X,'MICRN/100')

        DO 410 IK=1,NOS
           NQ=NQ+1
           CALL AOUT(IRAM(IK),2,1)
           CALL ISLEEP(0,0,0,ITICK)
           CALL AIN(LD(NQ),2,1)
           CALL SND(NPTS,MSP1,MSP2,CH1N,CH2N,CH1,CH2,NAV,CC,NDSP,NDSP0)
        LB(NQ)=10*LD(NQ)
        DSP2=NDSP
        DSP3=DSP2/(1-DSP2/D0)
        IDSP(NQ)=DSP3+.5

410        CONTINUE

      WRITE(1'NS)NS,(LB(KR),IDSP(KR),KR=1,NQ)

        WRITE(6,35)NS,NQ,LB(NOS),IDSP(NOS)
        WRITE(7,35)NS,NQ,LB(NOS),IDSP(NOS)

        NS=NS+1
        NQ=0

        DO 420 IL=NOS+1,NOS*2
           NQ=NQ+1
           CALL AOUT(IRAM(IL),2,1)
           CALL ISLEEP(0,0,0,ITICK)
           CALL AIN(LD(NQ),2,1)
           CALL SND(NPTS,MSP1,MSP2,CH1N,CH2N,CH1,CH2,NAV,CC,NDSP,NDSP0)
        LB(NQ)=10*LD(NQ)
        DSP2=NDSP
        DSP3=DSP2/(1-DSP2/D0)
        IDSP(NQ)=DSP3+.5

420        CONTINUE

      WRITE(1'NS)NS,(LB(KR),IDSP(KR),KR=1,NQ)

      IF(I.GT.NI) GO TO 600


        CALL KEYBRD(ICHAR)
        IF(ICHAR.EQ.'S') GO TO 600


        NS=NS+1



      CALL AOUT(0,2,1)

600   CONTINUE
```

```
 620    CALL AOUT(0,2,1)

        CLOSE(UNIT=1)
        TYPE*,'** WANT TO MEASURE ONCE MORE? Y=1, N=2,3,...'
        READ(5,*)LNS
        IF(LNS.EQ.1)GO TO 3

 650    STOP
        END

C ********SUBROUTINE JUNK ********************
        SUBROUTINE JUNK
        BYTE ICHAR

        DO 300 JK=1,30000
           CALL AOUT(1032,3,1)

           DO 310 IK= 1,257
              IAL=8*IK-1032
              CALL AOUT(IAL,0,1)
              CALL AOUT(IAL,1,1)
 310       CONTINUE
           CALL KEYBRD(ICHAR)
           IF(ICHAR.EQ.'S') GO TO 350
        CALL AOUT(0,3,1)

 300    CONTINUE
 350    RETURN
        END

C ************ subroutine SND ********

        SUBROUTINE SND(NPTS,MSP1,MSP2,CH1N,CH2N,CH1,CH2,NAV,CC,NDSP,NDSPO)
        INTEGER T1,T2,CH1,CH2,CH1N,CH2N
        INTEGER*4 NDSP,NDSPO,NDS
        DIMENSION T1(60),T2(60),IV1(60),IV2(60)
        ISH=0
258     DO 260 J=1,NPTS
        J1=J
        T1(J)=CH1-8*((NPTS/2)-J1)
        T2(J)=CH2-8*((NPTS/2)-J1)
260     CONTINUE
        DO 270 J=1,NPTS
        CALL AOUT(T1(J),0,1)
        CALL AOUT(T2(J),1,1)
        CALL AIN(IV1(J),0,1)
        CALL AIN(IV2(J),1,1)
270     CONTINUE
        JS=NPTS/2
        CALL AOUT(T1(JS),0,1)
        CALL AOUT(T2(JS),1,1)
        IMPT1=0
        IMPT2=0
        DO 280 KJ=1,NAV
        IMPT1=IV1(KJ)+IMPT1
        IMPT2=IV2(KJ)+IMPT2
280     CONTINUE
        IV3=IMPT1
        IV4=IMPT2
        CH1=T1(1)
```

```
          CH2=T2(1)
          N9=NPTS-NAV-1
          DO 300 KK=2,N9
          KT=KK+NAV-1
          IV3=IV3+IV1(KT)-IV1(KT-NAV)
          IV4=IV4+IV2(KT)-IV2(KT-NAV)
          IF(IV3.GE.IMPT1)GO TO 290
          IMPT1=IV3
          CH1=T1(KK)
 290      IF(IV4.GE.IMPT2)GO TO 300
          IMPT2=IV4
          CH2=T2(KK)
 300      CONTINUE
 304      IF(ISH)305,308,306
 305      CH1N=CH1
          NDSPO=NDSP-CC*100.*(CH2-CH2N)
          ISH=0
          GO TO 336
 306      CH2N=CH2
          NDSPO=NDSP-CC*100.*(CH1N-CH1)
          ISH=0
          GO TO 336
 308      DSP=((CH1N-CH1)+(CH2-CH2N))*CC*100.
          NDS=DSP+.5
 310      NDSP=NDSPO+NDS
 250      IF((CH1N-CH1).LE.(8*MSP1))GO TO 252
          CH1=CH1+8*MSP1
          ISH=-1
          GO TO 258
 252      IF((CH1-CH1N).LE.(8*MSP1))GO TO 254
          CH1=CH1-8*MSP1
          ISH=-1
          GO TO 258
 254      IF((CH2-CH2N).LE.(8*MSP2))GO TO 256
          CH2=CH2-8*MSP2
          ISH=+1
          GO TO 258
 256      IF((CH2N-CH2).LE.(8*MSP2))GO TO 336
          CH2=CH2+8*MSP2
          ISH=1
          GO TO 258
 336      RETURN
          END

C ****** Subroutine VIEW ********

          SUBROUTINE VIEW(NAV,MLC1,MSP1,MLC2,MSP2)
          INTEGER T1,T2
          DIMENSION T1(257),T2(257),IV1(257),IV2(257),AV1(257),AV2(257)
          CALL ISLEEP(0,0,1,0)
          DO 360 J=1,257
          T1(J)=8*J-1032
          T2(J)=8*J-1032
 360      CONTINUE
          DO 370 I=1,257
          CALL AOUT(T1(I),0,1)
          CALL AOUT(T2(I),1,1)
          CALL AIN(IV1(I),0,1)
          CALL AIN(IV2(I),1,1)
 370      CONTINUE
          IMPT1=0
```

```
      IMPT2=0
      DO 380 KJ=1,NAV
      IMPT1=(IV1(KJ)+IMPT1)
      IMPT2=(IV2(KJ)+IMPT2)
380   CONTINUE
      AV1(1)=IMPT1/10
      AV2(1)=IMPT2/10
      N9=257-NAV-1
      DO 400 KK=2,N9
      KT=KK+NAV-1
      AV1(KK)=AV1(KK-1)+(IV1(KT)-IV1(KT-NAV))/NAV
      AV2(KK)=AV2(KK-1)+(IV2(KT)-IV2(KT-NAV))/NAV
400   CONTINUE
      DO 420 II=168,88,-1
      II2=II+2
      II3=II+6
      II4=II+8
      A1=AV1(II)
      A2=AV1(II2)
      A3=AV1(II3)
      A4=AV1(II4)
      S1=A3-A4
      S2=A1-A2
      IF(S1.GT.0.)GO TO 420
      IF(S2.LT.0.)GO TO 420
      MLC1=II
      GO TO 430
420   CONTINUE
430   M1=MLC1-30
      DO 440 IJ=M1,1,-1
      IJ2=IJ+2
      IJ3=IJ+6
      IJ4=IJ+8
      A1=AV1(IJ)
      A2=AV1(IJ2)
      A3=AV1(IJ3)
      A4=AV1(IJ4)
      S1=A3-A4
      S2=A1-A2
      IF(S1.GT.0.)GO TO 440
      IF(S2.LT.0.)GO TO 440
      MC1=IJ
      GO TO 450
440   CONTINUE
450   MSF1=MLC1-MC1
      DO 470 JJ=88,168
      JJ2=JJ-2
      JJ3=JJ-6
      JJ4=JJ-8
      B1=AV2(JJ)
      B2=AV2(JJ2)
      B3=AV2(JJ3)
      B4=AV2(JJ4)
      S1=B3-B4
      S2=B1-B2
      IF(S1.GT.0.) GO TO 470
      IF(S2.LT.0.) GO TO 470
      MLC2=JJ
      GO TO 480
470   CONTINUE
480   N1=MLC2+30
```

```
      DO 490 JI=N1,250
      JI2=JI-2
      JI3=JI-6
      JI4=JI-8
      B1=AV2(JI)
      B2=AV2(JI2)
      B3=AV2(JI3)
      B4=AV2(JI4)
      S1=B3-B4
      S2=B1-B2
      IF(S1.GT.0.)GO TO 490
      IF(S2.LT.0.)GO TO 490
      MC2=JI
      GO TO 492
490   CONTINUE
492   MSP2=MC2-MLC2
      WRITE(7,*)'MLC1=',MLC1,'MSP1=',MSP1
      WRITE(7,*)'MLC2=',MLC2,'MSP2=',MSP2
      RETURN
      END
```

```
C ***************** NAFIT.FOR ****************************************
C       This is a program to get LEAST SQUARES straight line
C       and get CLOSURE LOAD from smoothing curve by average
C       of data from NACOM*.FOR
C                                JULY 1985  J.J. LEE
C
        DIMENSION X(600),Y(600),XD(600),YL(600),LB(600),IDSP(600)
        INTEGER FLNN(10),ISPCM(10)
        COMMON X,Y,I1,I2,I3

        K2=1
        WRITE(7,*)'** SPECIMEN NO. ? **'
        READ(5,3) ISPCM

        TYPE*,' MIN. & MAX. DISPL ; XMIN=? XMAX=?'
        ACCEPT*,XMIN,XMAX
        TYPE*,' MIN. & MAX. LOAD ; YMIN=? YMAX=?'
        TYPE*,'... WANT metric unit ? ....'
        TYPE*,'       1 LB = 4.448 Nt '
        ACCEPT*,YMIN,YMAX

2       WRITE(7,*)'** FILE NAME? **'
        READ(5,3)FLNN
3       FORMAT(10A2)
        TYPE*,'          NO. OF STEPS ?'
        ACCEPT*, NOS
        TYPE*,'          LOADING (=1) or UNLOADING (=2) '
        ACCEPT*, NS
        TYPE*,'  .... READING INCREMENT ? (every pt =1, every other =2)'
        ACCEPT*, IR

        OPEN(UNIT=1,NAME=FLNN,TYPE='OLD',ACCESS='DIRECT',
     *  INITIALSIZE=20,RECORDSIZE=604)

        WRITE(6,10) FLNN
10      FORMAT(5X,'********************** FILE NAME =',5A2,2X,
     *          '**********************************'//)

        WRITE(6,20) ISPCM
20      FORMAT(10X,'                          SPECIMEN = ',5A2)

        READ(1'NS) NS,(LB(K),IDSP(K), K=1,NOS)

        DO 50 I=1,NOS,IR
           WRITE(7,*) NS,I,LB(I),IDSP(I)
50         CONTINUE

        DO 60 J=1,NOS,IR
           X(J)=FLOAT(IDSP(J))/100.
           Y(J)=FLOAT(LB(J))
C       WRITE(7,*) 'Y=',Y(J),'X= ',X(J)
60         CONTINUE

        SUMX=0.
        SUMX2=0.
        SUMY2=0.
        SUMY=0.
        SUMXY=0.

        WRITE(7,*) '**** Choose LINEAR PORTION ****'
        TYPE*,'.........FROM ? (load in pounds)
```

```
      READ(5,*)PF
      TYPE*,'.........TO ? (load in pounds) '
      READ(5,*)PT

      DO 70 K=1,NOS,IR
         IF(Y(K).GE.PF) GO TO 80
70       CONTINUE
80    M1=K

      DO 90 L=M1,NOS,IR
         IF(Y(L).GE.PT) GO TO 100
90       CONTINUE
100   M2=L

      WRITE(7,*) '.....M1=',M1,'...M2=',M2

      DO 112 I=M1,M2,IR
      SUMX=SUMX+X(I)
      SUMX2=SUMX2+X(I)**2
      SUMY2=SUMY2+Y(I)**2
      SUMY=SUMY+Y(I)
      SUMXY=SUMXY+X(I)*Y(I)
112   CONTINUE

115   M=(M2-M1)/IR+1

118   BX=SUMX/M
      BY=SUMY/M
      ALX=SUMX2-SUMX**2/M
      ALY=SUMY2-SUMY**2/M
      ALXY=SUMXY-SUMX*SUMY/M
      A2=ALXY/ALX
      A1=BY-A2*BX
      R=ALXY/SQRT(ALX*ALY)
      C=1/(A2*4.445)

      WRITE(7,*)'A2=',A2,'R=',R,'C(um/Nt)=',C
      WRITE(6,*)'LINEAR PORTION = ',PF,' TO ',PT,' pounds'
      WRITE(6,*)' A1=',A1,'A2=',A2,' Correlation R=',R,'C(um/Nt)=',C


      WRITE(7,*)'DO YOU WANT PLOT? Y=1,N=2'
      READ(5,*)IP
      IF(IP.NE.1)GO TO 140
C     WRITE(7,*)'DO YOU WANT CALCULATE THE NEXT COMPLIANCE? Y=1,STOP=2'
C     READ(5,*)IST
C     IF(IST.NE.1)GO TO 200
C     GO TO 15

120   CONTINUE

      CALL PLTSET
      CALL PLTSCL(XMIN,XMAX,YMIN,YMAX,1.,1.,9.,7.)

      IF(K2.EQ.1) GO TO 133

      WRITE(7,*) 'MIN & MAX DISPL; XMIN=? XMAX=?'
      READ(5,*)XMIN,XMAX
      WRITE(7,*)'MIN & MAX LOAD; YMIN=? YMAX=?'
      READ(5,*)YMIN,YMAX
```

```
      CALL PLTSET
      CALL PLTSCL(XMIN,XMAX,YMIN,YMAX,1.,1.,9.,7.)

133   WRITE(7,*)'DO LABELLING? Y=1,N=2'
      READ(5,*)LAB
      IF(LAB.NE.1)GO TO 135
      CALL PLTMOV(4.,7.1,1)
      CALL PLTSTR(ISPCM,10,3.,1)
      CALL PLTAXS(5,4)
135   CALL PLTSMV(XMIN,YMIN)
      BYTE CHAC(5)

      TYPE*,'PLOT raw data? Y=1,N=2'
      READ(5,*) NS1
      I1=11
      I2=NOS
      I3=IR
      IF(NS1.NE.1) GO TO 140

      CALL PLOT


140   DO 170 I=1,NOS,IR
          XD(I)=(Y(I)-A1)/A2
          X(I)=XD(I)
170   CONTINUE

      TYPE*,'PLOT fitting line? Y=1,N=2'
      ACCEPT*,INS
      IF(INS.NE.1) GO TO 171


      CALL PLTSET
      CALL PLTSCL(XMIN,XMAX,YMIN,YMAX,1.,1.,9.,7.)
      CALL PLTSMV(XMIN,YMIN)
      I3=20
      CALL PLOT

171   TYPE*,'** CALCULATION for CLOSURE value ? Y=1,N=2'
      ACCEPT*,JNS
      IF(JNS.NE.1) GO TO 193

      IF(NS.NE.2) GO TO 175
      DO 172 J=1,NOS,IR
         XD(J)=FLOAT(IDSP(NOS+1-J))/100.-X(J)
 172  CONTINUE
      GO TO 185

175   DO 180 J=1,NOS,IR
         XD(J)=FLOAT(IDSP(J))/100.-X(J)
180   CONTINUE

185   DO 186 J=11,NOS-5,IR
          SUMXD=XD(J)+XD(J+1)+XD(J+2)+XD(J+3)+XD(J+4)
          XA(J)=SUMXD/5.
          X(J+2)=XA(J)
 186  CONTINUE

      P10=X(13)*.1
      DO 187 K2=31,NOS-20,IR
          IF(ABS(X(K2)).LE.P10) GO TO 188
```

```
 187    CONTINUE
 188    YO=X(K2)*A2+A1
        IF(NS.NE.1) GO TO 189
        WRITE(7,*)'--OPENING LOAD =',Y(K2)
        WRITE(6,*)'-- OPENING LOAD =',Y(K2),'from data --'
        GO TO 190
        WRITE(7,*)'-- CLOSURE LOAD=',Y(K2)
 189    WRITE(6,*)'-- CLOSURE LOAD =',Y(K2),'10% of max. difference -'

 190    CONTINUE
        WRITE(6,191) (I,X(I),Y(I),I=K2-6,K2+6,IR)
 191    FORMAT(/11X,'I',8X,'X(I)',8X,'Y(I)'//(I13,2F13.5))

        TYPE*,'...PLOT for CLOSURE ? ...Y=1  N=2'
        ACCEPT*, NSP
        IF(NSP.NE.1) GO TO 193

        CALL PLTSET
        CALL PLTSCL(XMIN,XMAX,YMIN,YMAX,1.,1.,9.,7.)
        CALL PLTSMV(XMIN,YMIN)
        I3=IR
        I1=13
        I2=NOS-5
        CALL PLOT
        GO TO 193

 193    WRITE(7,*)'Do you want to write characters on X-axis? Y=1,N=2'
        READ(5,*)IX
        IF(IX.NE.1)GO TO 195
        BYTE CHAR(20),CHARY(20),CHARR(20),CHARS(20),CHARC(20)
        CALL PLTSET
        CALL PLTSCL(XMIN,XMAX,YMIN,YMAX,1.,1.,9.,7.)
        CALL PLTMOV(4.,0.2,1)
        WRITE(7,*)'Input 'DISPLACEMENT-MICRONS'(or other)for X-X'
        READ(5,194)CHAR
 194    FORMAT(20A1)
        CALL PLTSTR(CHAR,20,2.,1)
        CALL PLTMOV(-3.5,2.,1)
        WRITE(7,*)'Input at KEYBRD'LOAD-NEWTON'(or other)for Y-Y'
        READ(5,194)CHARY
        CALL PLTSTR(CHARY,20,2.,4)

        CALL PLTMOV(1.,4.,1)
        TYPE*,' Input 'R=..''
        READ(5,194) CHARR
        CALL PLTSTR(CHARR,20,2.,1)

        CALL PLTMOV(0.,-.5,1)
        TYPE*,' Input 'S(MAX)=...''
        READ(5,194) CHARS
        CALL PLTSTR(CHARS,20,2.,1)

        CALL PLTMOV(0.,-.5,1)
        TYPE*,' Input 'CRACK LENGTH=...''
        READ(5,194)CHARC
        CALL PLTSTR(CHARC,20,2.,1)

 195    WRITE(7,*)'Do you plot next ? Y=1;N=2'
        READ(5,*)K1
        IF(K1.NE.1)GO TO 200
```

```
      WRITE(7,*)'Plot with the same truncation & scale? Y=1;N=2'
      READ(5,*)K2
      CLOSE(UNIT=1)
      GO TO 2

200   CLOSE(UNIT=1)
      STOP
      END

C ************** SUBROUTINE PLOT ****************************
      SUBROUTINE PLOT
      DIMENSION X(600),Y(600)
      COMMON X,Y,I1,I2,I3
      BYTE CHAC(5)

      WRITE(7,*)'Pts.with cross input M20,sqr.M22,circle M23,tris1.M24'
      READ(5,131)CHAC
131   FORMAT(5A1)
      WRITE(7,*) '..... I1=',I1,'I2=',I2
140   DO 150 I=I1,I2,I3
      XD=X(I)
      YL=Y(I)
C     WRITE(7,*)'I=',I,' Y=',Y(I),'  X=',X(I)
      CALL PLTSMV(XD,YL)
      CALL PENDN
      CALL SOUT(CHAC,3)
150   CONTINUE
      CALL PENUP
      RETURN
      END
```

```
C ****************** NADADN.FOR*************************************
C
C      THIS IS TO PLOT THE DA/DN vs DELK on LOG-LOG SCALE
C    ON THE NEW PLOTTER(LVP16).
C    THIS IS COMBINED with DADNPL.FOR and NASIF.FOR.
C
C
                                    AUG. 1985  J.J.LEE

        DIMENSION XK(100),YD(100),DADN(100),DELK(100),N(100)
        DIMENSION CL(100),AAVG(100)
        INTEGER FLNM(10),ISPCM(10),OFLNM(10),SYMB(5)
        COMMON A,Smax,Smin,B,R,W,NS1,DELK1

3       TYPE*,'** SPECIMEN NO ? **'
        READ(5,4) ISPCM
4       FORMAT(10A2)

        TYPE*,'*** from OLD FILE ? Y=1, N=2'
        ACCEPT*, NS2
        IF(NS2.NE.1) GO TO 10
        TYPE*,'.... OLD FILE NAME ?...'
        READ(5,4) OFLNM
        TYPE*,'..... NO. OF DATA ?'
        ACCEPT*,NOS
        OPEN(UNIT=1,NAME=OFLNM,TYPE='OLD',ACCESS='DIRECT',
     *       INITIALSIZE=10,RECORDSIZE=604)

        READ(1'NS2)(K,N(K),CL(K),DELK(K),DADN(K),K=0,NOS)
        CLOSE(UNIT=1)
        DO 5 K=1,NOS
           WRITE(7,*) K,'A=',CL(K),'mm','DELK=',DELK(K),'MPa'
5          CONTINUE
        GO TO 35

10      B=2.3E-3
        R=3.18E-3
        W=50.E-3

        TYPE*,'** CARTEGORIZE THE CRACK ***'
        TYPE*,'       SURFACE CRACK=2, CORNER CRACK=1'
        ACCEPT*,NS1

        TYPE*,'Smax=  (MPa)'
        ACCEPT*,SMAX
        TYPE*,'Smin=  (MPa)'
        ACCEPT*, Smin

        WRITE(7,*)'NO. OF DATA ?'
        READ(5,*)NOS

        TYPE*,'... INPUT THE DATA ....'
C       TYPE*,'     <<    for END OF DATA type in 1000 >>'

        DO 20 ID=0,NOS
           WRITE(7,*) 'I=',ID,';CYCLES;CRACK LENGTH(in mm)'
           READ(5,*) N(ID),CL(ID)
20         CONTINUE

C ....DADN is calculated in 1.E6*MM/CYCLE ....
        DO 22 I=1,NOS
```

```
            DADN(I)=(CL(I)-CL(I-1))*1000./((N(I)-N(I-1))*NS1)
 22         CONTINUE
          DADN(0)=0.0

C ..... FOR SURFACE CRACK CL=2*A ,CORNER CRACK CL=A ...
C         DELK is calculated for AVG. a ......

          AAVG(0)=0.0
 25       DO 30 J=1,NOS
             AAVG(J)=(CL(J)+CL(J-1))/(FLOAT(NS1)*2.)
             A=AAVG(J)
             CALL NASIF
             DELK(J)=DELK1
             WRITE(7,*) J,'C.L=',A*1000*NS1,'MM','DELK=',DELK(J)
 30          CONTINUE

          IF(NS2.EQ.1) GO TO 35
          TYPE*,'*** STORE DATA IN A FILE ***'
          WRITE(7,*)'FILENAME?'
          READ(5,4)FLNM

          OPEN(UNIT=1,NAME=FLNM,ACCESS='DIRECT',
      *   INITIALSIZE=10,RECORDSIZE=604)

          NS=1
          WRITE(1'NS) (K,N(K),CL(K),DELK(K),DADN(K),K=0,NOS)
          CLOSE(UNIT=1)
          TYPE*,'..... DATA FILE IS GENERATED ....'

C .... DA/DN=DADN*1.E-6 (MM/CYCLE)....
C..... STORE DA/DN DATA with DADN unit ...

 35       DO 40 I=1,NOS
          YD(I)=DADN(I)*10.**(-6)
          XK(I)=DELK(I)
 40       CONTINUE

          TYPE*,'<<<< WANT TO PRINT THE DATA ?  Y=1,N=2 >>>>'
          ACCEPT*,NS3
          IF(NS3.NE.1) GO TO 49
 45       WRITE(6,46) ISPCM,SMIN/SMAX,SMAX,NOS
 46       FORMAT(///,5X,'** DA/DN DATA **'//,10X,'SPECIMEN'
     1     ,' NO. = ',10A2,/10X,'STRESS RATIO=',F3.1,//10X,'MAX.STRESS=',
     2     F5.1,1X,'MPa',/10X,'NO.OF DATA=',I5//
     2     7X,'CYCLE(X1000)',3X,'CRK L 2a(mm)',1X,'AVG. a(mm)',3X,
     3     'DELK(MPa-M)',3X,'DADN(mm/CYCLE)',/)

          WRITE(7,*) '.... NOS=',NOS

          DO 47 J=0,NOS
             WRITE(6,48) J,N(J),CL(J),AAVG(J),DELK(J),DADN(J)
 47       CONTINUE
 48       FORMAT(/2X,I3,4X,I5,10X,F5.3,7X,F5.2,12X,F5.2,2X,F8.3,1X,
     1           'X1.E-6')
          TYPE*,' <<< WANT TO PLOT ?  Y=1,N=2 ....'
          ACCEPT*, NP
          IF(NP.NE.1) GO TO 165


C ..............
C ........LABELING LOG-LOG SCALE & PLOT.......
```

```
C ...........

49      TYPE*,'   <<< WANT TO PLOT ? Y=1, N=2 >>>'
        ACCEPT*, NP2
        IF(NP2.NE.1) GO TO 165

        WRITE(6,*) 'IN;SP1;IP1250,750,7400,6900;SC0,2000,0,6000'

        TYPE*,'..... WANT TO LABEL(=1) or PLOT THE DATA only(=2)?'
        ACCEPT*,NS5
        IF(NS5.EQ.2) GO TO 125
        TYPE*,'.... NOW LABELING .....'
        TYPE*,'   ?? CHECK A PAPER ON THE PLOTTER ??'
        TYPE*,'      READY ?  Y=1'
        ACCEPT*,  NS4

        WRITE(6,*) 'PU0,0PD2000,0,2000,6000,0,6000,0,0PU'
        WRITE(6,*) 'CP40,-3.;DT ;SI.2,.3;LBDELK(MPA-M '
C       WRITE(6,*) 'LB1/2) ;'
        WRITE(6,*) 'PA0,0;CP-7,12;DI0,1;SI.2,.3;LBDA/DN(MM/CYCLE) '
        WRITE(6,*) 'PA800,6000;CP0,4;DI1,0;SI.3,.4;LB',ISPCM,' '
        WRITE(6,*) 'DI1,0;TL1.5,0'
        IY=0
C       TYPE*,'... II= ?'
C       ACCEPT*,II
        II=6

        DO 60 I=1,II
        EI=I*1.
        YI=1.*10.**(EI-1.)
        IY=ALOG10(YI)*1000
        IF(IY.EQ.3999)  IY=4000
C       WRITE(7,*) 'LOG(YI)=',IY
        WRITE(6,*) 'PA0,',IY,';YT'
        WRITE(6,*) 'CP-4,-.25;LB',IY/1000,' '
        IF(IY.GE.6998) GO TO 70
          DO 55 J=1,8
          Y=YI*((J+1)*1.)
          JY=ALOG10(Y)*1000
C         WRITE(7,*) 'LOG(Y)=',JY
          CALL ISLEEP(0,0,0,20)
          WRITE(6,*) 'PA0,',JY,';YT'
C          WRITE(6,*) 'CP-5,-.25;LB',YY,' '
55        CONTINUE
60      CONTINUE
70      IX=0
        WRITE(6,*) 'DT ;SI;DI1,0'

        DO 100 I=1,3
           FI=1.*I
           XI=10.**(FI-1.)
           LX=ALOG10(XI)*1000
        WRITE(6,*) 'PA',LX,',0;XT'
C       WRITE(6,*) 'CP-5,-.95;LB',LX/1000,' '
C       WRITE(6,*) 'CP0,-1.2;SI.2,.3;LB10 '
           IF(LX.GE.1998) GO TO 120

           DO 80 J=1,8
              XJ=XI*((J+1)*1.)
              LXJ=ALOG10(XJ)*1000
              CALL ISLEEP(0,0,0,20)
```

```
              WRITE(6,*)'PA',LXJ,',0;XT'
 80           CONTINUE
100       CONTINUE
120       CONTINUE

C .... PLOT THE DATA ....

125       TYPE*,'.... WHICH SYMBOL ? (+=1,*=2,x=3,o=4)'
          READ(5,*) NS6
127       FORMAT(2X,'J=',I3,3X,'X=',F7.1,3X,'Y=',F7.1)
          WRITE(6,*)'DT '
          IF(NS6.EQ.2) GO TO 135
          IF(NS6.EQ.3) GO TO 145
          IF(NS6.EQ.4) GO TO 155

          DO 130 J=1,NOS
          X=(ALOG10(XK(J)))*1000.
          Y=(ALOG10(YD(J))+7.)*1000.
          WRITE(7,127) J,X,Y
          WRITE(6,*) 'SM+ ;PA',X,Y,'PD;LT3'
130       CONTINUE
          WRITE(6,*) 'PU'
          GO TO 165

135       DO 140 J=1,NOS
          X=(ALOG10(XK(J)))*1000.
          Y=(ALOG10(YD(J))+7.)*1000.
          WRITE(7,127) J,X,Y
          WRITE(6,*) 'SM* ;PA',X,Y,'PD;LT4'
140       CONTINUE
          WRITE(6,*) 'PU'
          GO TO 165

145       DO 150 J=1,NOS
          X=(ALOG10(XK(J)))*1000.
          Y=(ALOG10(YD(J))+7.)*1000.
          WRITE(7,127)J,X,Y
          WRITE(6,*) 'SMx ;PA',X,Y,'PD;LT6'
150       CONTINUE
          WRITE(6,*) 'PU'
          GO TO 165

155       DO 160 J=1,NOS
          X=(ALOG10(XK(J)))*1000.
          Y=(ALOG10(YD(J))+7.)*1000.
          WRITE(7,127)J,X,Y
          WRITE(6,*) 'SMo ;PA',X,Y,'PD'
160       CONTINUE
          WRITE(6,*) 'PU'

165       TYPE*,'ANOTHER PLOT ? Y=1,N=2,3,..'
          READ(5,*) NS7
          IF(NS7.EQ.1) GO TO 3


333       STOP
          END

C ******** SUBROUTINE NASIF **********
          SUBROUTINE NASIF
```

```
      COMMON A,Smax,Smin,B,R,W,NS1,DELK1

C   This is to calculate S.I.F. for small surface crack
C and corner crack of edge notched specimen from NASA.
C (ref. Instruction to Participants )
C                          June, 1985  ;

      REAL M1,M2,M3
C ...All the unit are in METRIC (L=m , SIF=MPa-m**1/2 , S=MPa)....

      DELS=SMAX-SMIN

      A=A*1.E-3

C ...FOR CORNER CRACK NS1=1 ,SURFACE CRACK NS1=2
C ...        '          T=B    ,      '         T=B/2

      T=B/FLOAT(NS1)
      C=A*(.9-.25*(A/T)**2)

C     TYPE*,'CRACK DEPTH msed  c =  (mm)'
C     ACCEPT*, CD
C     CD=CD*1.E-3
      WRITE(7,*) 'CALCULATED c = ', C, 'm'
C     WRITE(7,*) 'MEASURED   c = ', CD, 'm'

C     TYPE*, 'WHICH VALUE OF c BE USED ? ..Calc.=1, Measd =2'
C     ACCEPT*, NS2
C     IF(NS.EQ.2) C=CD

      TYPE*, '... CHECK  0.2<a/c<2  and a/t<1 ...'
      WRITE(7,*) 'a/c= ',A/C
      WRITE(7,*) 'a/t= ',a/t

      IF(A/C.GT.1.) GO TO 50
      Q=1.+1.464*(A/C)**1.65
      M1=1
      G1=1
      FF=1
      GO TO 60

50    Q=1+1.464*(C/A)**1.65
      M1=(C/A)**.5
      FF=M1
      G1=1

60    M2=.05/(.11+(A/C)**1.5)
      M3=.29/(.23+(A/C)**1.5)
C .... V means Ramda in equ. 10 and U means Gamma in equ. 14 ....
      V=1/(1+.1564*C/R)
      G2=(1+.358*V+1.425*V**2-1.578*V**3+2.156*V**4)/(1+.08*V**2)
      G3=1+.1*(1-A/T)**10
      G4=1.14-.1/(1+C/R)**.5
      U=(C+R)/W
      FW=1-.2*U+9.4*U**2-19.4*U**3+27.1*U**4

      FSN=(M1+M2*(A/T)**2+M3*(A/T)**4)*G1*G2*G3*G4*FF*FW

      IF(NS1.NE.1) GO TO 100

      DELK1=DELS*FSN*SQRT(3.14159*A/Q)
```

```
        GO TO 300

C ....CORNER CRACK .....

100     IF(A/C.GT.1.) GO TO 150
        FCN=FSN*(1.13-.09*A/C)
        GO TO 160

150     FCN=FSN*(1+.04*C/A)

160     DELK1=DELS*FCN*SQRT(3.14159*A/Q)

C180    IF(NS1.NE.1) GO TO 200
C       TYPE*,' .... NOW! CALCULATED ....'
C       TYPE*,'
C       TYPE*,'
C       WRITE(7,*) ' S.I.F RANGE for surface crack = ', DELK,' MPa-m1/2'
C       GO TO 300

C200    WRITE(7,*) ' S.I.F RANGE for corner crack = ',DELK,' MPa-m1/2'

300     RETURN
        END
```

Appendix II.

TEST DATA

SPECIMEN NUMBER: A-54-04

DATE: 5/16/85

PARTICIPANT'S NAME: Joo-Jin Lee

John Cieslowski

TEST TEMPERATURE: 24°C

RELATIVE HUMIDITY: 66 %

WAVEFORM TYPE: Sinusoidal wave, 20 Hz

LOADING SEQUENCE TYPE: Constant amplitude

R-RATIO = 0.5

S max = 225 MPa

S min = 112.5 MPa

FINAL LENGTH OF CRACK: 0.5 mm

COMMENTS:

AGARD Short Crack DATA CHART

Record of crack lengths and map

Page 1 of 4
Specimen no A-54-04

Loading Type Const. Amplitude R=0.5
Peak Stress 225 MPa

0.1mm grid

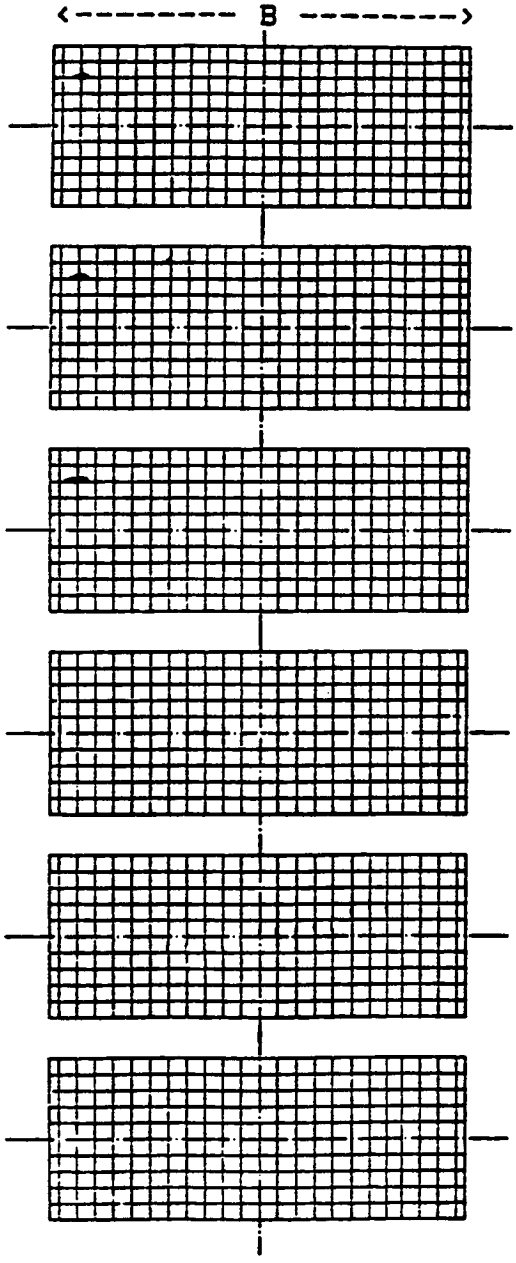

26k Cycles
L1 .080 mm
L2 ____ mm
L3 ____ mm
L4 ____ mm
L5 ____ mm

30k Cycles
L1 .105 mm
L2 ____ mm
L3 ____ mm
L4 ____ mm
L5 ____ mm

34k Cycles
L1 .125 mm
L2 ____ mm
L3 ____ mm
L4 ____ mm
L5 ____ mm

____ Cycles
L1 ____ mm
L2 ____ mm
L3 ____ mm
L4 ____ mm
L5 ____ mm

____ Cycles
L1 ____ mm
L2 ____ mm
L3 ____ mm
L4 ____ mm
L5 ____ mm

____ Cycles
L1 ____ mm
L2 ____ mm
L3 ____ mm
L4 ____ mm
L5 ____ mm

AGARD Short Crack DATA CHART

Record of crack lengths and map

Page 2 of 4 Loading Type Const. Amplitude R=0.5

Specimen no A-54-04 Peak Stress 225 MPa

0.1mm grid

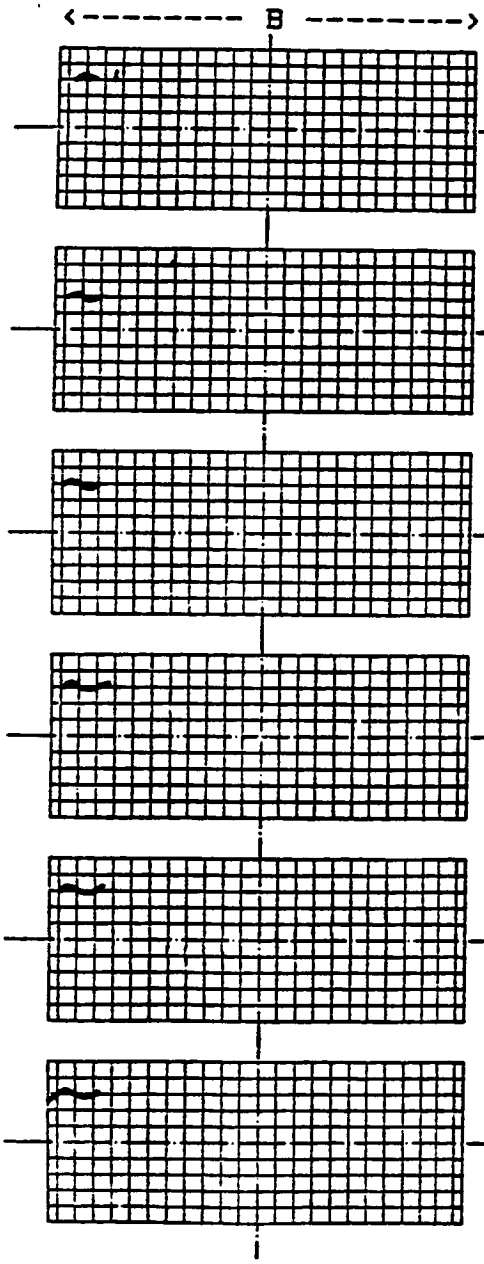

38K Cycles
L1 .135 mm
L2 mm
L3 mm
L4 mm
L5 mm

40K Cycles
L1 .140 mm
L2 mm
L3 mm
L4 mm
L5 mm

42K Cycles
L1 .190 mm
L2 mm
L3 mm
L4 mm
L5 mm

44K Cycles
L1 .210 mm
L2 mm
L3 mm
L4 mm
L5 mm

48K Cycles
L1 .210 mm
L2 mm
L3 mm
L4 mm
L5 mm

50K Cycles
L1 .275 mm
L2 mm
L3 mm
L4 mm
L5 mm

AGARD Short Crack DATA CHART

Record of crack lengths and map

Page 3 of 4 Loading Type R=0.5

Specimen no A-54-04 Peak Stress 225 MPa

0.1mm grid

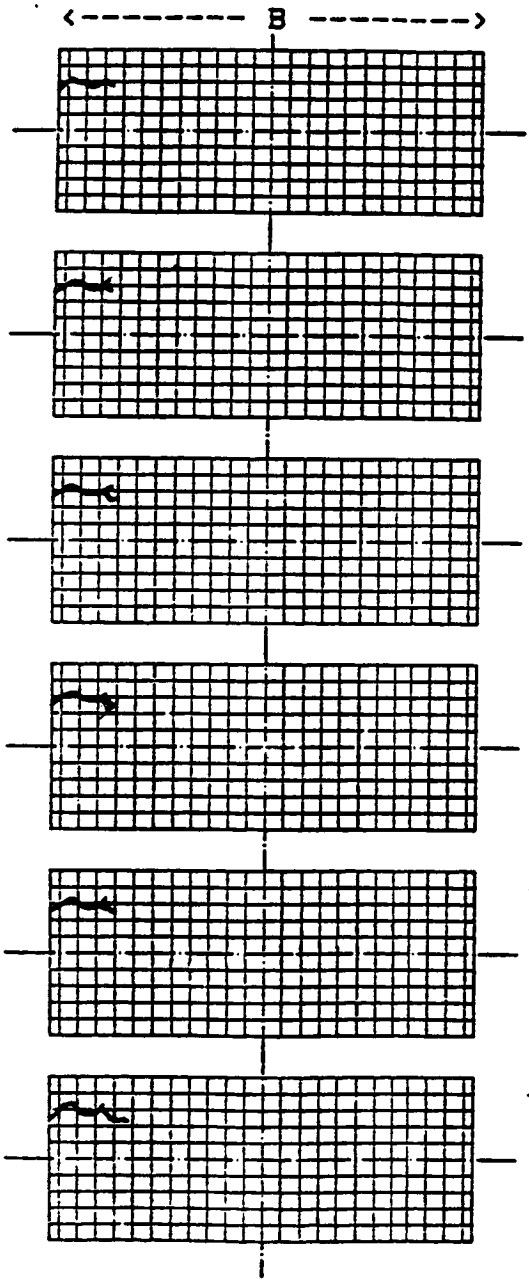

52 K Cycles
L1 .305 mm
L2 mm
L3 mm
L4 mm
L5 mm

54k Cycles
L1 .305 mm
L2 mm
L3 mm
L4 mm
L5 mm

56k Cycles
L1 .330 mm
L2 mm
L3 mm
L4 mm
L5 mm

58k Cycles
L1 .335 mm
L2 mm
L3 mm
L4 mm
L5 mm

60k Cycles
L1 .345 mm
L2 mm
L3 mm
L4 mm
L5 mm

62K Cycles
L1 .410 mm
L2 mm
L3 mm
L4 mm
L5 mm

AGARD Short Crack DATA CHART

Record of crack lengths and map

Page 4 of 4 Loading Type R=0.5

Specimen no A-54-04 Peak Stress 225 MPa

0.1mm grid

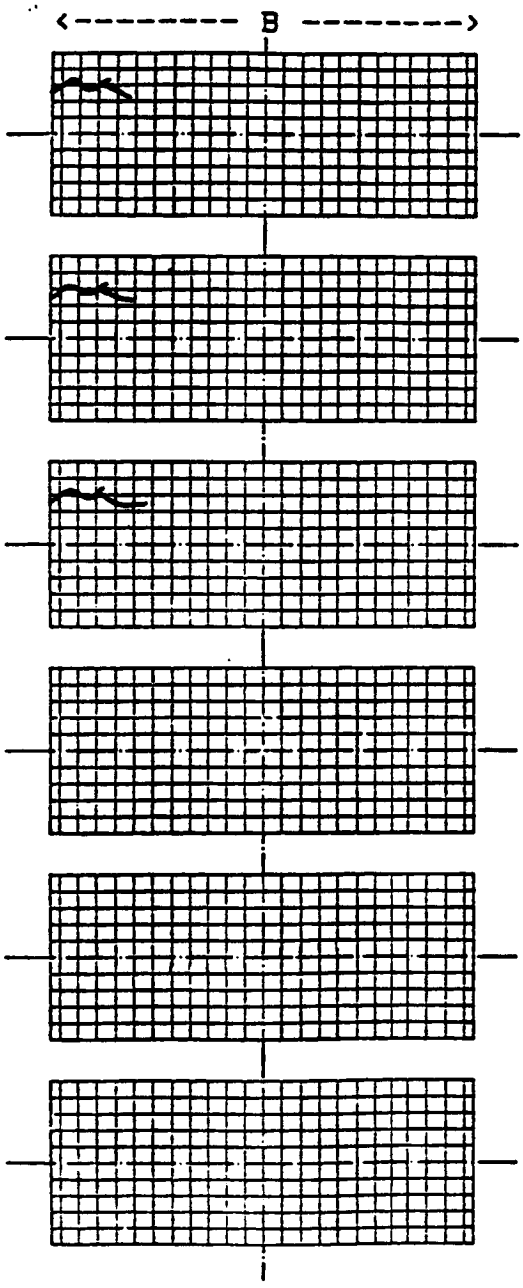

64 k Cycles
L1 .410 mm
L2 ____ mm
L3 ____ mm
L4 ____ mm
L5 ____ mm

66k Cycles
L1 .420 mm
L2 ____ mm
L3 ____ mm
L4 ____ mm
L5 ____ mm

68k Cycles
L1 .500 mm
L2 ____ mm
L3 ____ mm
L4 ____ mm
L5 ____ mm

____ Cycles
L1 ____ mm
L2 ____ mm
L3 ____ mm
L4 ____ mm
L5 ____ mm

____ Cycles
L1 ____ mm
L2 ____ mm
L3 ____ mm
L4 ____ mm
L5 ____ mm

____ Cycles
L1 ____ mm
L2 ____ mm
L3 ____ mm
L4 ____ mm
L5 ____ mm

** DA/DN DATA **

SPECIMEN' NO. = A5404.L1
NO. OF DATA = 18
R= 0.50
SMAX=225.0 MPa
Near Edge → corner crack @ 50k

	CYCLE(X1000)	CRK L. 2a(mm)	AVG. a(mm)	DELK(MPa-M)	DADN(mm/CYCLE)
0	26	0.080	0.000	0.00	0.000 X1.E-6
1	30	0.105	0.093	4.05	6.250 X1.E-6
2	34	0.125	0.115	4.48	5.000 X1.E-6
3	38	0.135	0.130	4.74	2.500 X1.E-6
4	40	0.140	0.137	4.87	2.500 X1.E-6
5	42	0.190	0.165	5.29	25.000 X1.E-6
6	44	0.210	0.200	5.77	10.000 X1.E-6
7	48	0.210	0.210	5.90	0.000 X1.E-6
8	50	0.275	0.242	6.29	32.500 X1.E-6
9	52	0.305	0.290	6.81	15.000 X1.E-6
10	54	0.305	0.305	6.96	0.000 X1.E-6
11	56	0.330	0.317	7.09	12.500 X1.E-6
12	58	0.335	0.332	7.23	2.500 X1.E-6
13	60	0.345	0.340	7.31	5.000 X1.E-6
14	62	0.410	0.377	7.65	32.500 X1.E-6
15	64	0.410	0.410	7.94	0.000 X1.E-6
16	66	0.420	0.415	7.98	5.000 X1.E-6
17	68	0.500	0.460	8.35	40.000 X1.E-6

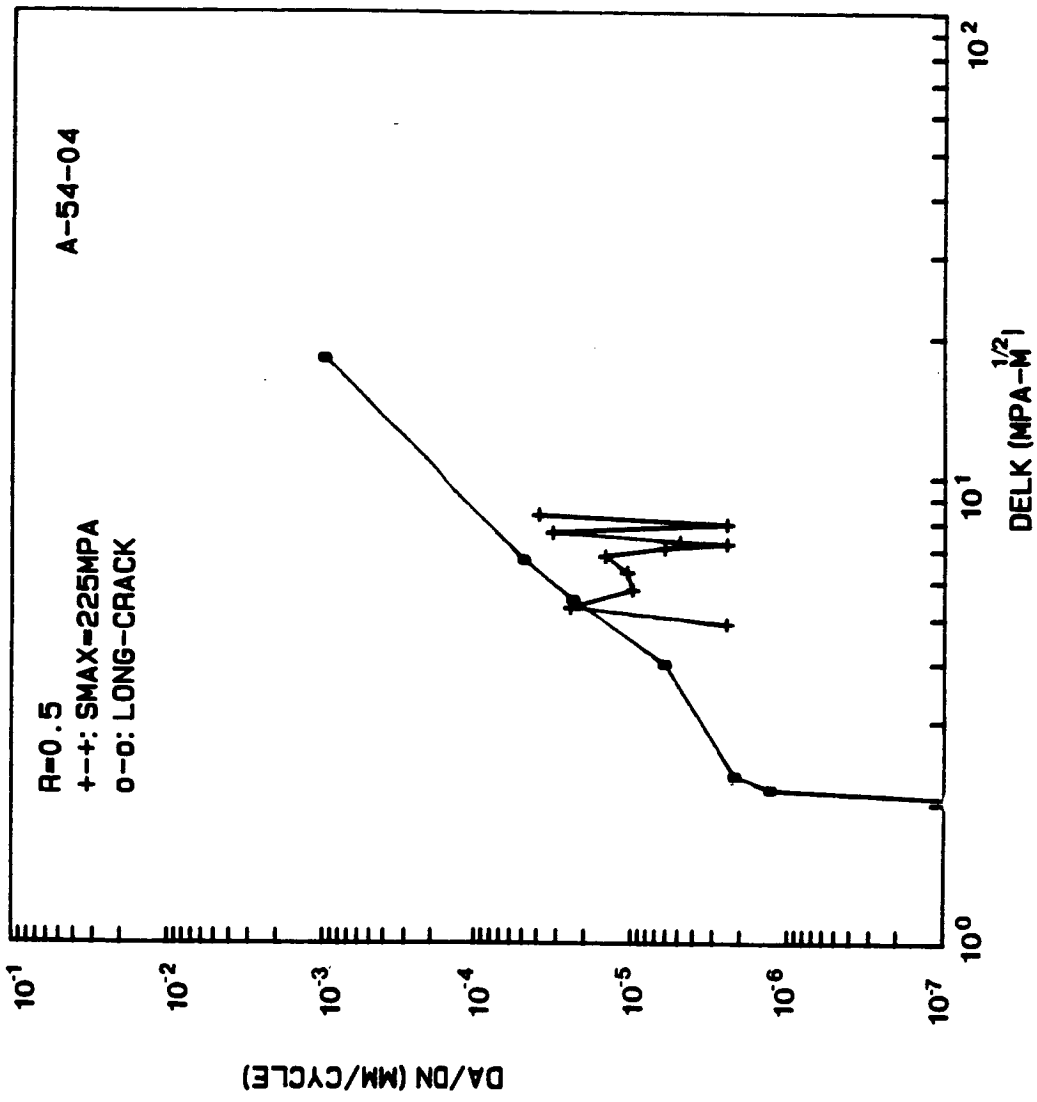
A-54-04
R=0.5
+-+: SMAX=225MPA
o-o: LONG-CRACK
DA/DN (MM/CYCLE)
DELK (MPA-M^1/2)
10^-1
10^-2
10^-3
10^-4
10^-5
10^-6
10^-7
10^0
10^1
10^2

A-54-04

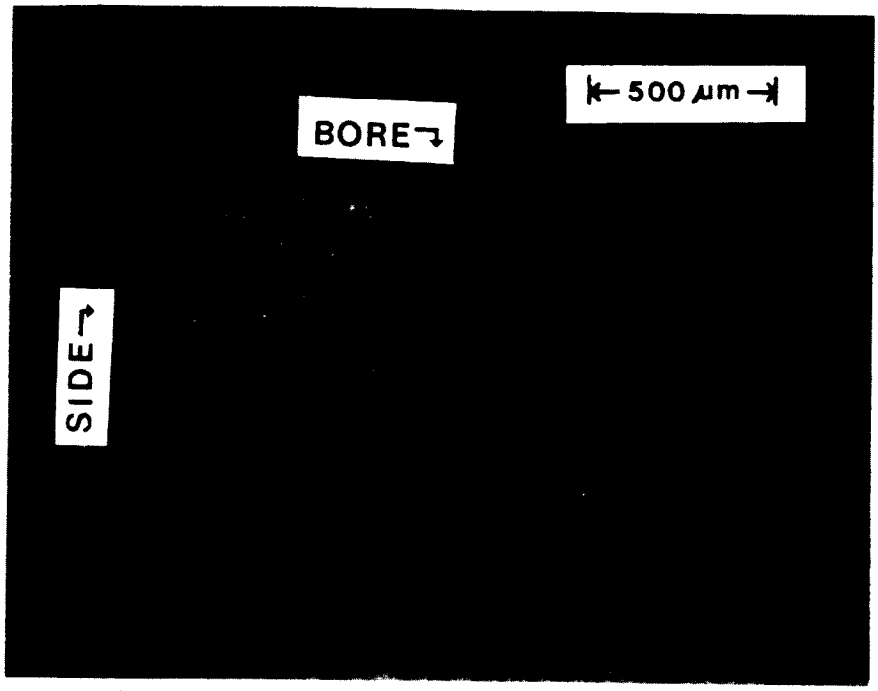

A-54-04

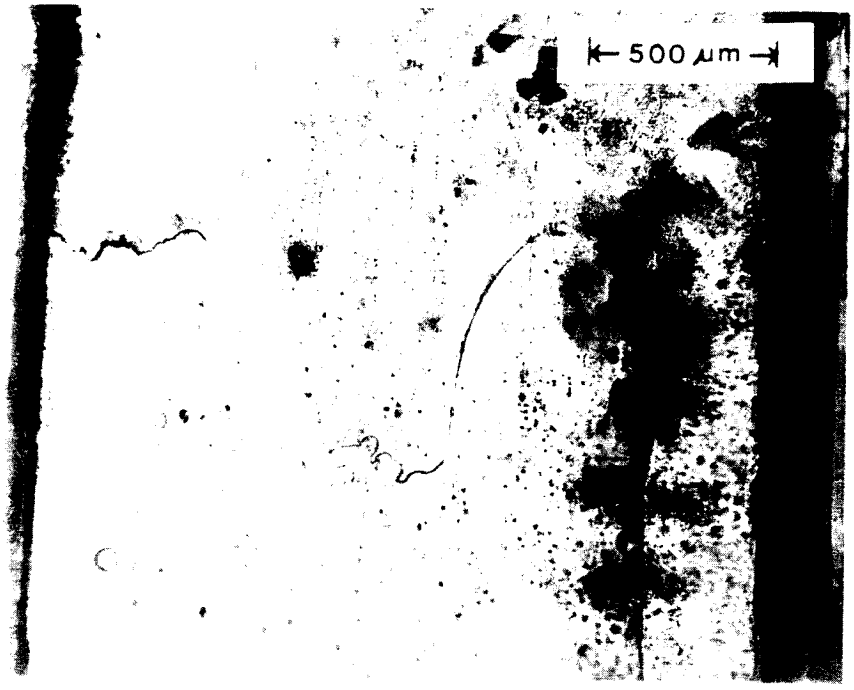

Cycles @ 68K cycles

TEST DATA

SPECIMEN NUMBER: A-65-07

DATE: 5/21/85

PARTICIPANT'S NAME: Joo-Jin Lee

John Cieslowski

TEST TEMPERATURE: 24°C

RELATIVE HUMIDITY: 62%

WAVEFORM TYPE: Sinusoidal wave, 20 Hz

LOADING SEQUENCE TYPE: Constant amplitude

R-RATIO = 0.5

S max = 225 MPa

S min = 112.5 MPa

FINAL LENGTH OF CRACK: 2.3mm (Thru-thickness)

COMMENTS:

Crack was found 0.9mm above the center line.

AGARD Short Crack DATA CHART

Record of crack lengths and map

Page 1 of 8 Loading Type Const. Amplitude R=0.5

Specimen no A-65-07 Peak Stress 225 MPa

0.1mm grid

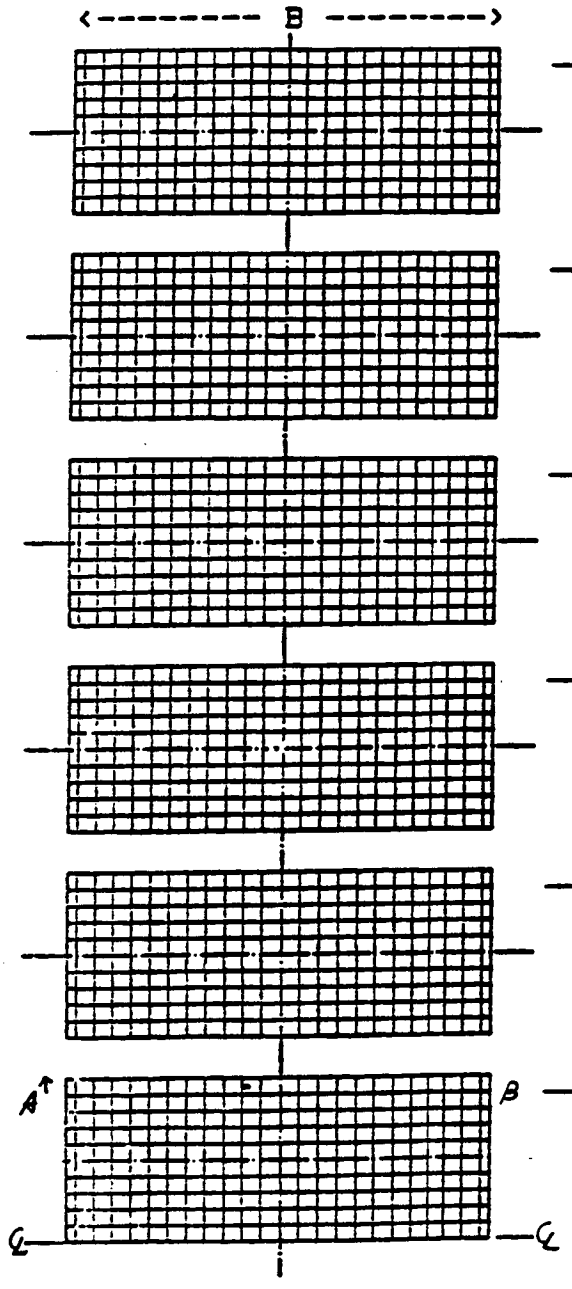

_____ Cycles
L1 _____ mm
L2 _____ mm
L3 _____ mm
L4 _____ mm
L5 _____ mm

_____ Cycles
L1 _____ mm
L2 _____ mm
L3 _____ mm
L4 _____ mm
L5 _____ mm

_____ Cycles
L1 _____ mm
L2 _____ mm
L3 _____ mm
L4 _____ mm
L5 _____ mm

_____ Cycles
L1 _____ mm
L2 _____ mm
L3 _____ mm
L4 _____ mm
L5 _____ mm

_____ Cycles
L1 _____ mm
L2 _____ mm
L3 _____ mm
L4 _____ mm
L5 _____ mm

42k Cycles
L1 .033 mm
L2 _____ mm
L3 _____ mm
L4 _____ mm
L5 _____ mm

AGARD Short Crack DATA CHART

Record of crack lengths and map

Page 2 of 8 - Loading Type R = 0.5

Specimen no A-65-07 Peak Stress 225 MPa

0.1mm grid

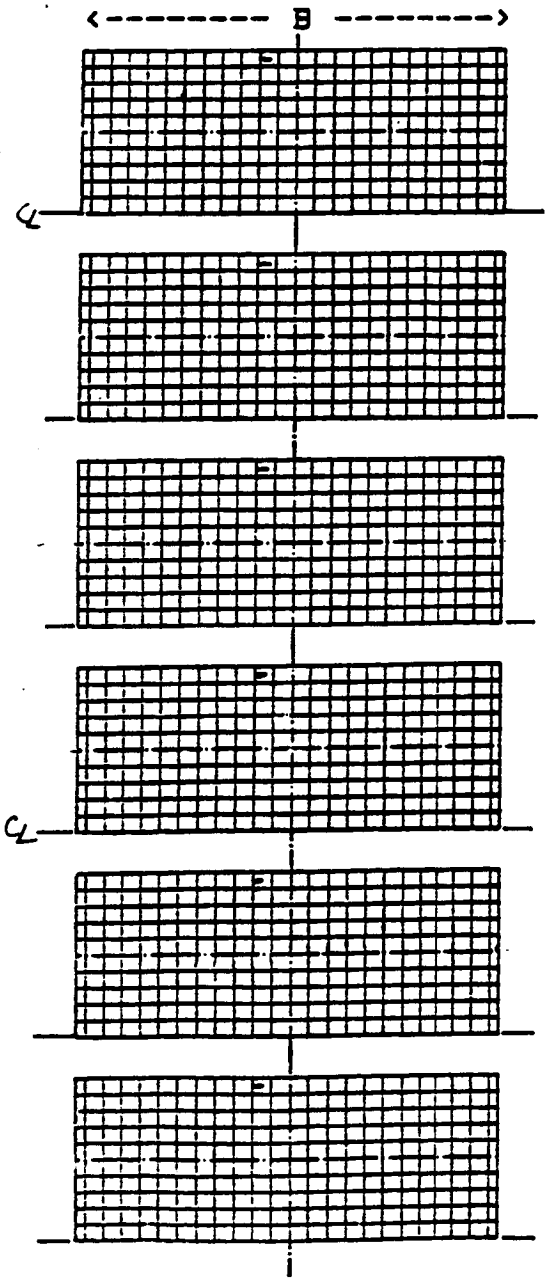

44k Cycles
L1 .038 mm
L2 ____ mm
L3 ____ mm
L4 ____ mm
L5 ____ mm

46k Cycles
L1 .044 mm
L2 ____ mm
L3 ____ mm
L4 ____ mm
L5 ____ mm

48k Cycles
L1 .044 mm
L2 ____ mm
L3 ____ mm
L4 ____ mm
L5 ____ mm

50k Cycles
L1 * mm
L2 ____ mm
L3 ____ mm
L4 ____ mm
L5 ____ mm

52k Cycles
L1 * mm
L2 ____ mm
L3 ____ mm
L4 ____ mm
L5 ____ mm

54k Cycles
L1 .049 mm
L2 ____ mm
L3 ____ mm
L4 ____ mm
L5 ____ mm

* Not clear

AGARD Short Crack DATA CHART

Record of crack lengths and map

Page 3 of 8 Loading Type R=0.5

Specimen no A-65-07 Peak Stress 225 MPa

0.1mm grid

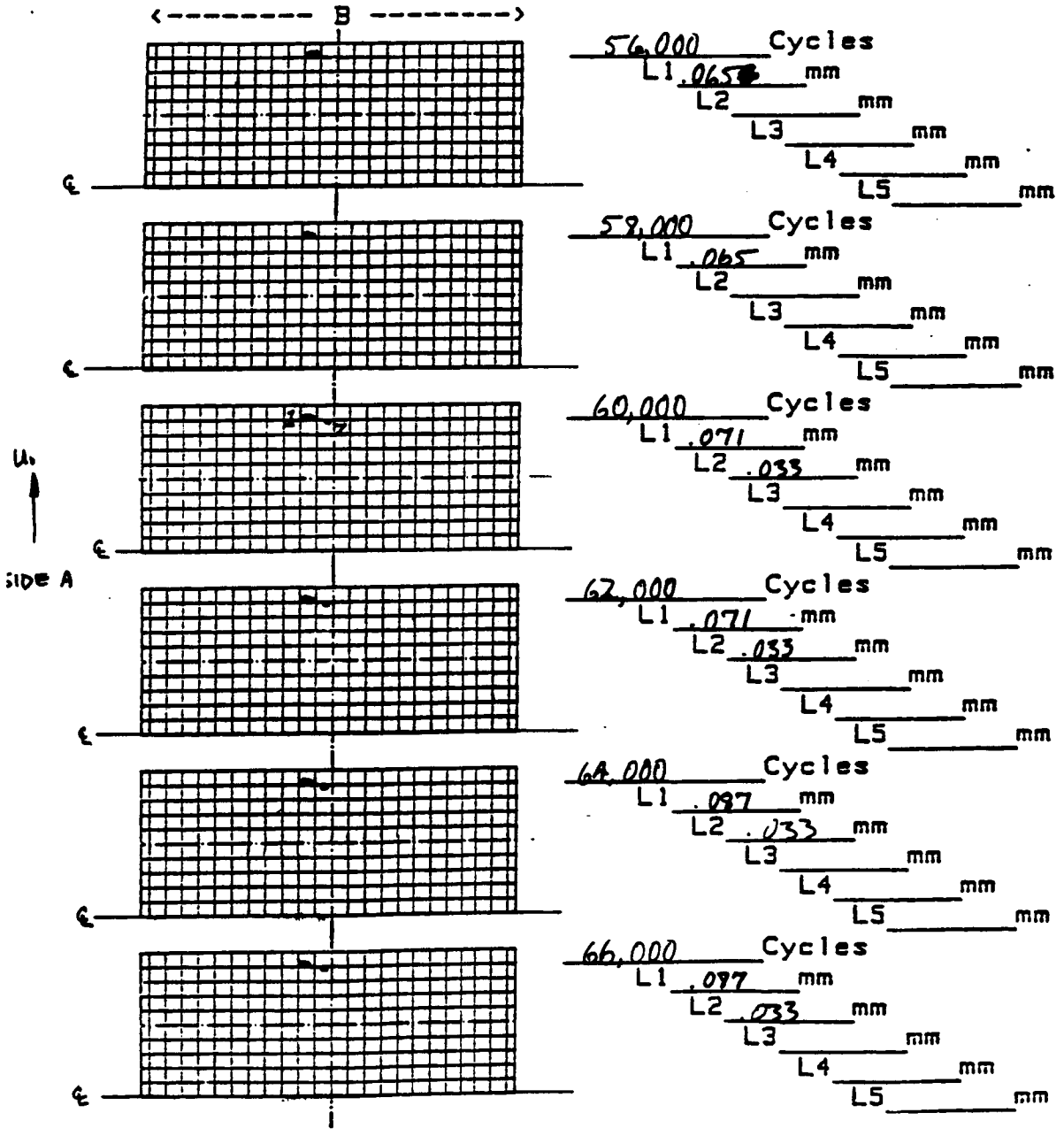

AGARD Short Crack DATA CHART

Record of crack lengths and map

Page 4 of 8 Loading Type R=0.5

Specimen no A-65-07 Peak Stress 225 MPa

0.1mm grid

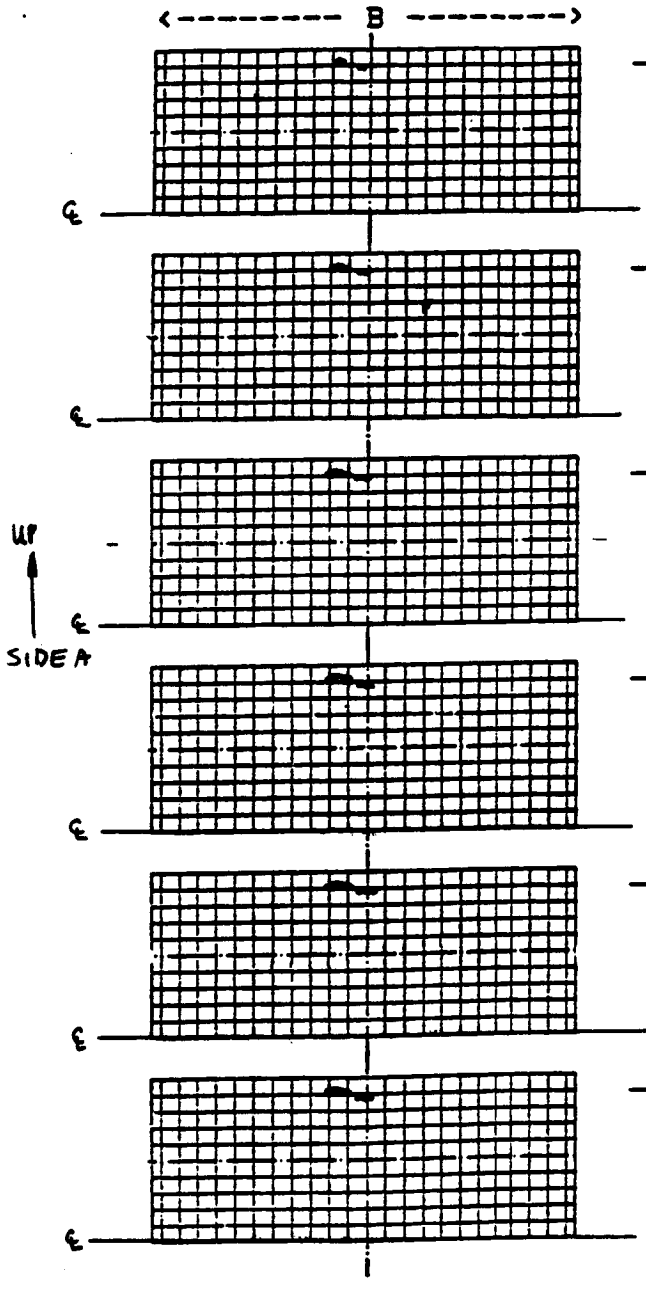

69,000 Cycles
L1 .087 mm
L2 .053 mm
L3 ____ mm
L4 ____ mm
L5 ____ mm

70,000 Cycles
L1 .114 mm
L2 .055 mm
L3 ____ mm
L4 ____ mm
L5 ____ mm

72,000 Cycles
L1 .125 mm
L2 .055 mm
L3 ____ mm
L4 ____ mm
L5 ____ mm

74,000 Cycles
L1 .136 mm
L2 .071 mm
L3 ____ mm
L4 ____ mm
L5 ____ mm

76,000 Cycles
L1 .136 mm
L2 .071 mm
L3 ____ mm
L4 ____ mm
L5 ____ mm

78,000 Cycles
L1 .136 mm
L2 .071 mm
L3 ____ mm
L4 ____ mm
L5 ____ mm

AGARD Short Crack DATA CHART

Record of crack lengths and map

Page 5 of 8 Loading Type R=0.5

Specimen no A-65-07 Peak Stress 225 MPa

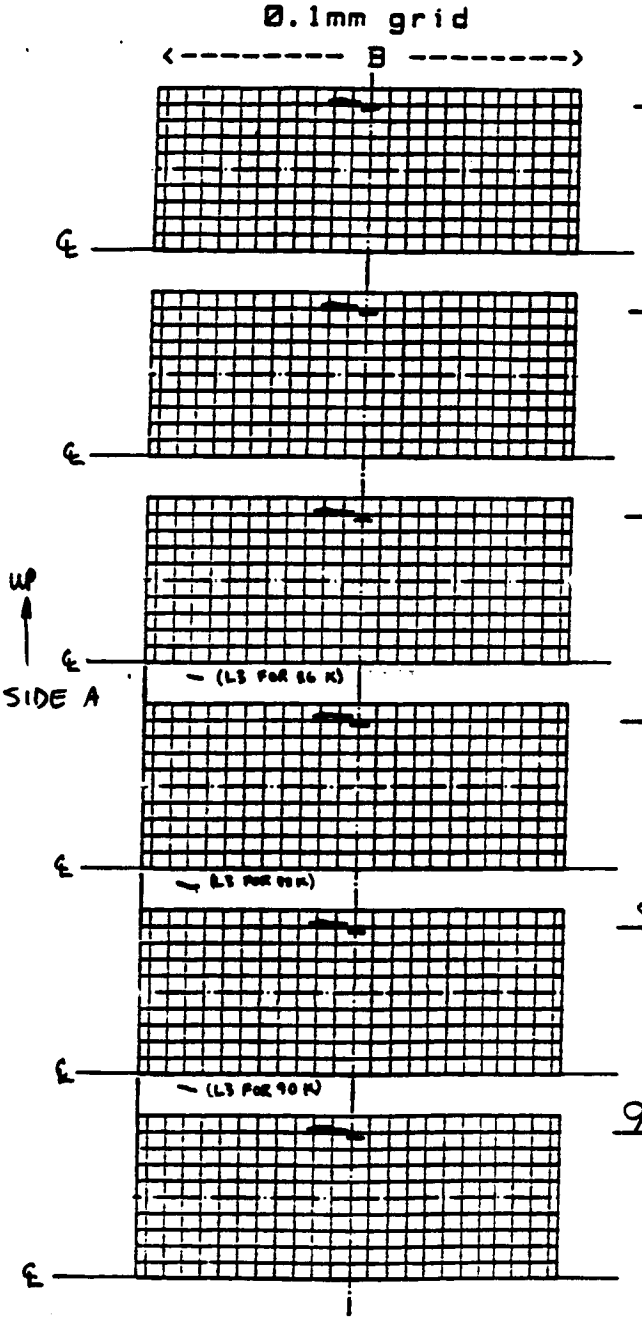

80,000 Cycles
L1 .158 mm
L2 .093 mm
L3 ____ mm
L4 ____ mm
L5 ____ mm

82,000 Cycles
L1 .158 mm
L2 .093 mm
L3 ____ mm
L4 ____ mm
L5 ____ mm

84,000 Cycles
L1 .174 mm
L2 .098 mm
L3 ____ mm
L4 ____ mm
L5 ____ mm

86,000 Cycles
L1 .185 mm
L2 .104 mm
L3 .076 mm
L4 ____ mm
L5 ____ mm

88,000 Cycles
L1 * mm
L2 .104 mm
L3 .076 mm
L4 ____ mm
L5 ____ mm

90,000 Cycles
L1 * mm
L2 .104 mm
L3 .076 mm
L4 ____ mm
L5 ____ mm

* Not clear

AGARD Short Crack DATA CHART

Record of crack lengths and map

Page 6 of 8 Loading Type R=0.5

Specimen no A-65-07 Peak Stress 225 MPa

0.1mm grid

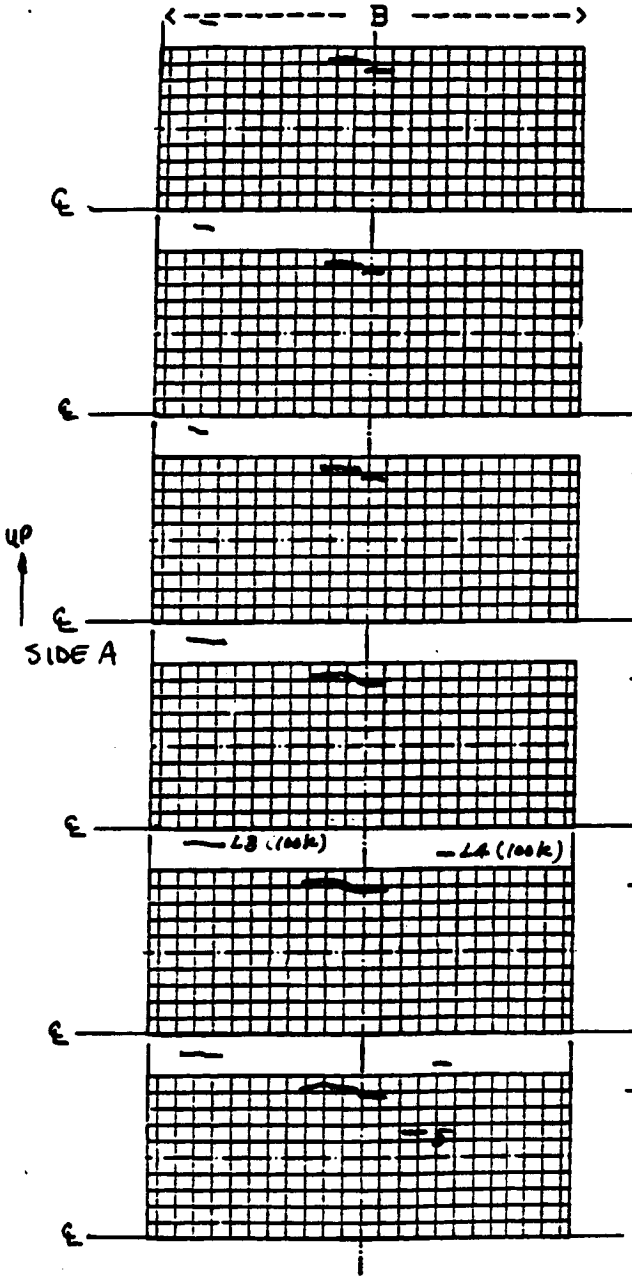

92,000 Cycles
L1 .213 mm
L2 .131 mm
L3 .076 mm
L4 ____ mm
L5 ____ mm

94,000 Cycles
L1 * mm
L2 .131 mm
L3 .076 mm
L4 ____ mm
L5 ____ mm

96,000 Cycles
L1 .349 mm
L2 ~1 mm
L3 .076 mm
L4 ____ mm
L5 ____ mm

98,000 Cycles
L1 .372 mm
L2 ____ mm
L3 .195 mm
L4 ____ mm
L5 ____ mm

100,000 Cycles
L1 .425 mm
L2 ____ mm
L3 .191 mm
L4 .087 mm
L5 ____ mm

102,000 Cycles
L1 .463 mm
L2 ____ mm
L3 .196 mm
L4 .087 mm
L5 .129 mm

* Not clear

AGARD Short Crack DATA CHART

Record of crack lengths and map

Page 7 of 8 Loading Type R=0.5
Specimen no A-65-07 Peak Stress 225 MPa

0.1mm grid

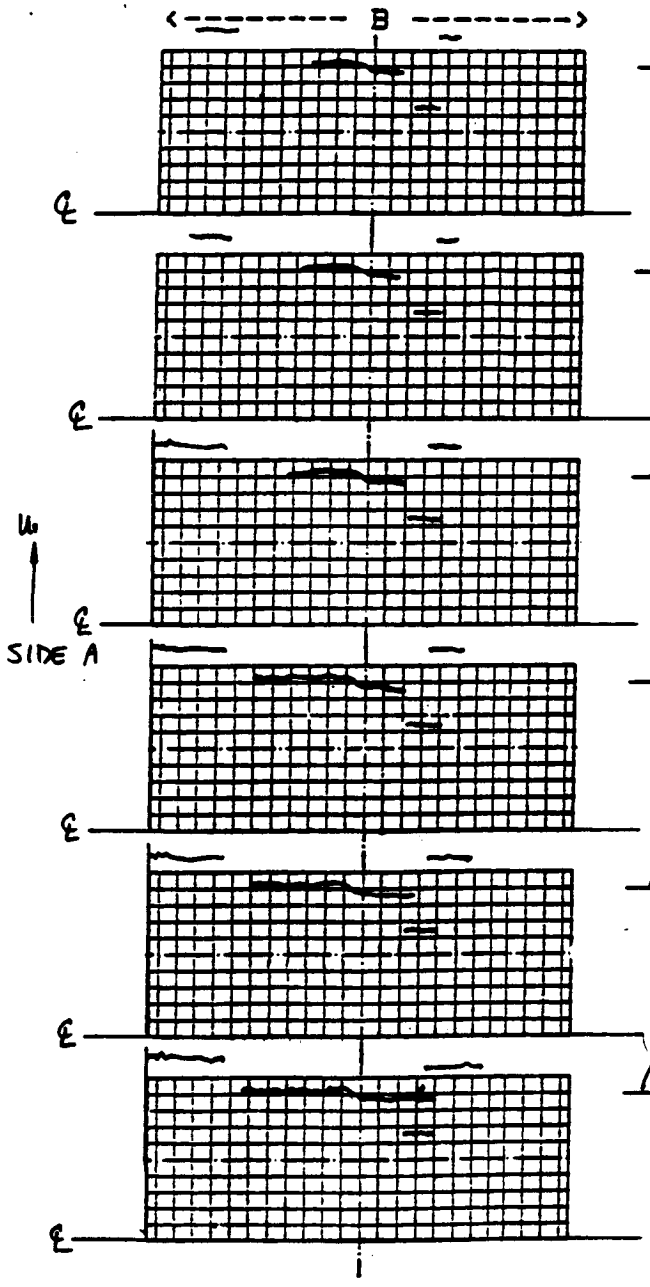

104,000 Cycles
L1 .507 mm
L2 mm
L3 .201 mm
L4 .112 mm
L5 .177 mm

106,000 Cycles
L1 .518 mm
L2 mm
L3 .201 mm
L4 .112 mm
L5 .177 mm

108,000 Cycles
L1 .632 mm
L2 mm
L3 .321 mm
L4 .142 mm
L5 .125 mm

110,000 Cycles
L1 .719 mm
L2 mm
L3 .348 mm
L4 .140 mm
L5 .168 mm

112,000 Cycles
L1 .901 mm
L2 mm
L3 .348 mm
L4 .174 mm
L5 .147 mm

114,000 Cycles
L1 .970 mm
L2 mm
L3 .408 mm
L4 .278 mm
L5 .158 mm

AGARD Short Crack DATA CHART

Record of crack lengths and map

Page 8 of 8 Loading Type R=0.5

Specimen no A-65-07 Peak Stress 225 MPa

0.1mm grid

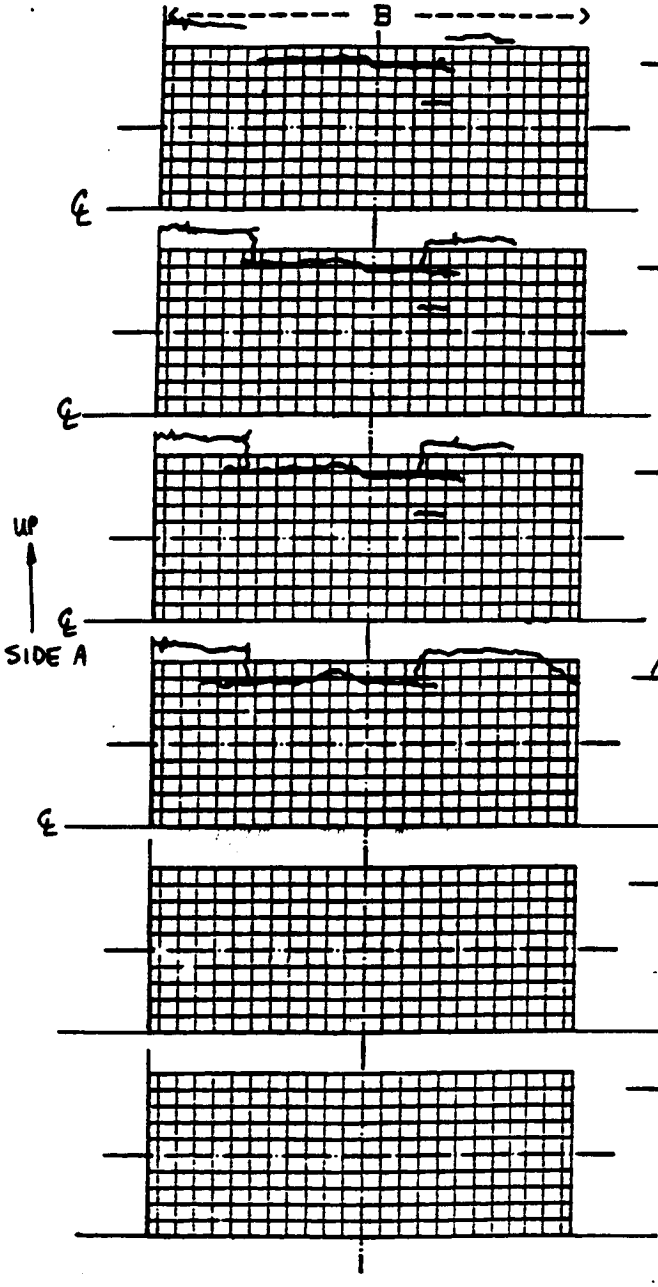

116,000 Cycles
L1 * mm
L2 ____ mm
L3 .408 mm
L4 .278 mm
L5 .158 mm

118,000 Cycles
L1 1.975 mm
L2 ____ mm
L3 ____ mm
L4 ____ mm
L5 .142 mm

119,000 Cycles
L1 1.842 mm
L2 ____ mm
L3 ____ mm
L4 ____ mm
L5 .150 mm

121,000 Cycles
L1 THRU (2,3) - mm
L2 ____ mm
L3 ____ mm
L4 ____ mm
L5 ____ mm

____ Cycles
L1 ____ mm
L2 ____ mm
L3 ____ mm
L4 ____ mm
L5 ____ mm

____ Cycles
L1 ____ mm
L2 ____ mm
L3 ____ mm
L4 ____ mm
L5 ____ mm

* Not clear

** DA/DN DATA **

SPECIMEN' NO. = A-65-07.L1
NO. OF DATA = 26
R= 0.50
SMAX=225.0 MPa
surface crack

	CYCLE(X1000)	CRK L. 2a(mm)	AVG. a(mm)	DELK(MPa-M)	DADN(mm/CYCLE)
0	42	0.033	0.000	0.00	0.000 X1.E-6
1	44	0.038	0.018	1.88	1.250 X1.E-6
2	46	0.044	0.021	2.02	1.500 X1.E-6
3	54	0.049	0.023	2.14	0.312 X1.E-6
4	56	0.065	0.029	2.36	4.000 X1.E-6
5	60	0.071	0.034	2.57	0.750 X1.E-6
6	64	0.087	0.039	2.76	2.000 X1.E-6
7	70	0.114	0.050	3.09	2.250 X1.E-6
8	72	0.125	0.060	3.35	2.750 X1.E-6
9	74	0.136	0.065	3.49	2.750 X1.E-6
10	80	0.158	0.073	3.69	1.833 X1.E-6
11	84	0.174	0.083	3.90	2.000 X1.E-6
12	86	0.185	0.090	4.04	2.750 X1.E-6
13	92	0.213	0.100	4.24	2.333 X1.E-6
14	96	0.349	0.140	4.96	17.000 X1.E-6
15	98	0.392	0.185	5.62	10.750 X1.E-6
16	100	0.425	0.204	5.87	8.250 X1.E-6
17	102	0.463	0.222	6.09	9.500 X1.E-6
18	104	0.507	0.242	6.34	11.000 X1.E-6
19	106	0.518	0.256	6.50	2.750 X1.E-6
20	108	0.632	0.287	6.85	28.500 X1.E-6
21	110	0.719	0.338	7.37	21.750 X1.E-6
22	112	0.801	0.380	7.78	20.500 X1.E-6
23	114	0.970	0.443	8.33	42.250 X1.E-6
24	118	1.875	0.711	10.32	113.125 X1.E-6

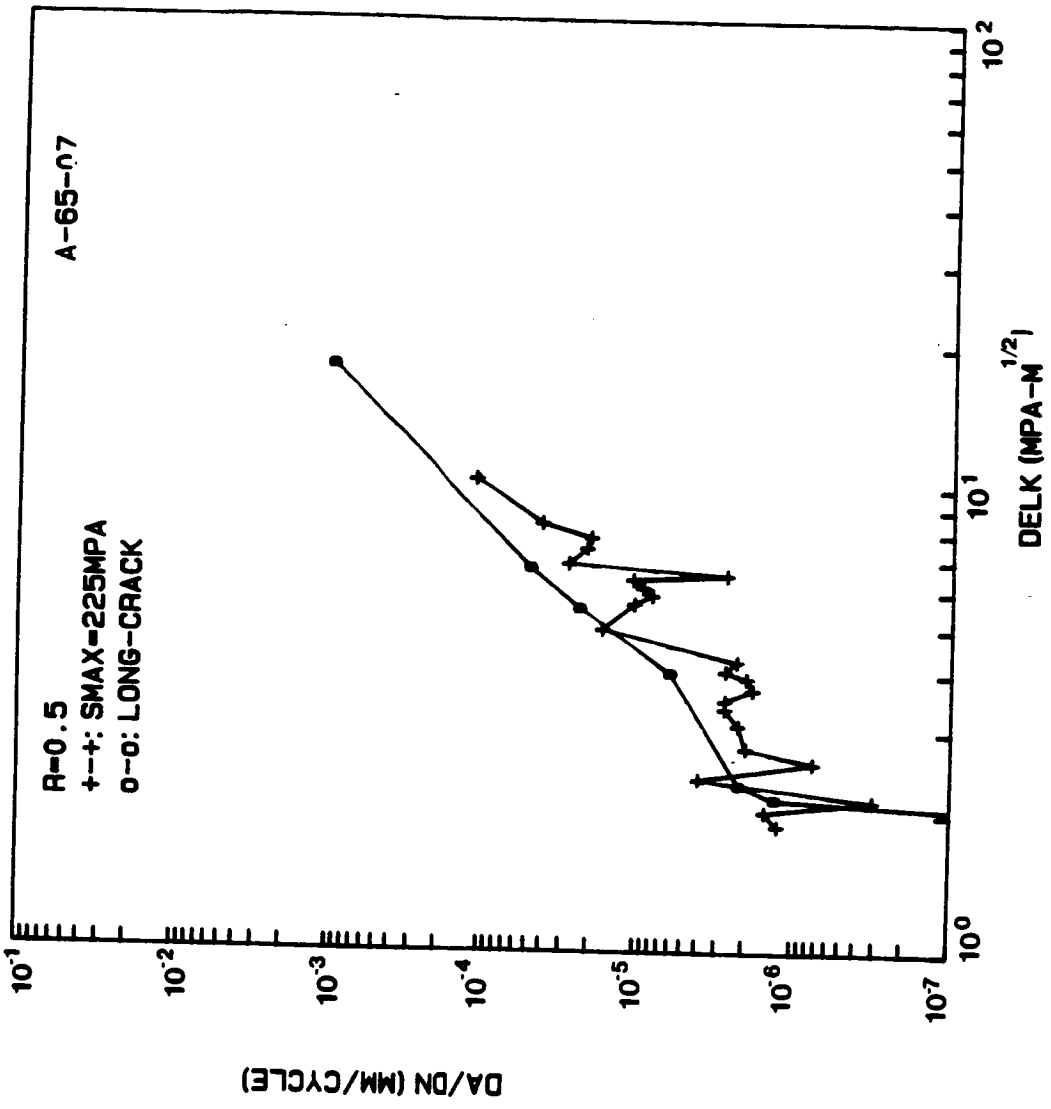
A-65-07
R=0.5
+-+: SMAX=225MPA
o-o: LONG-CRACK
DA/DN (MM/CYCLE)
DELK (MPA-M^1/2)
10^-1
10^-2
10^-3
10^-4
10^-5
10^-6
10^-7
10^0
10^1
10^2

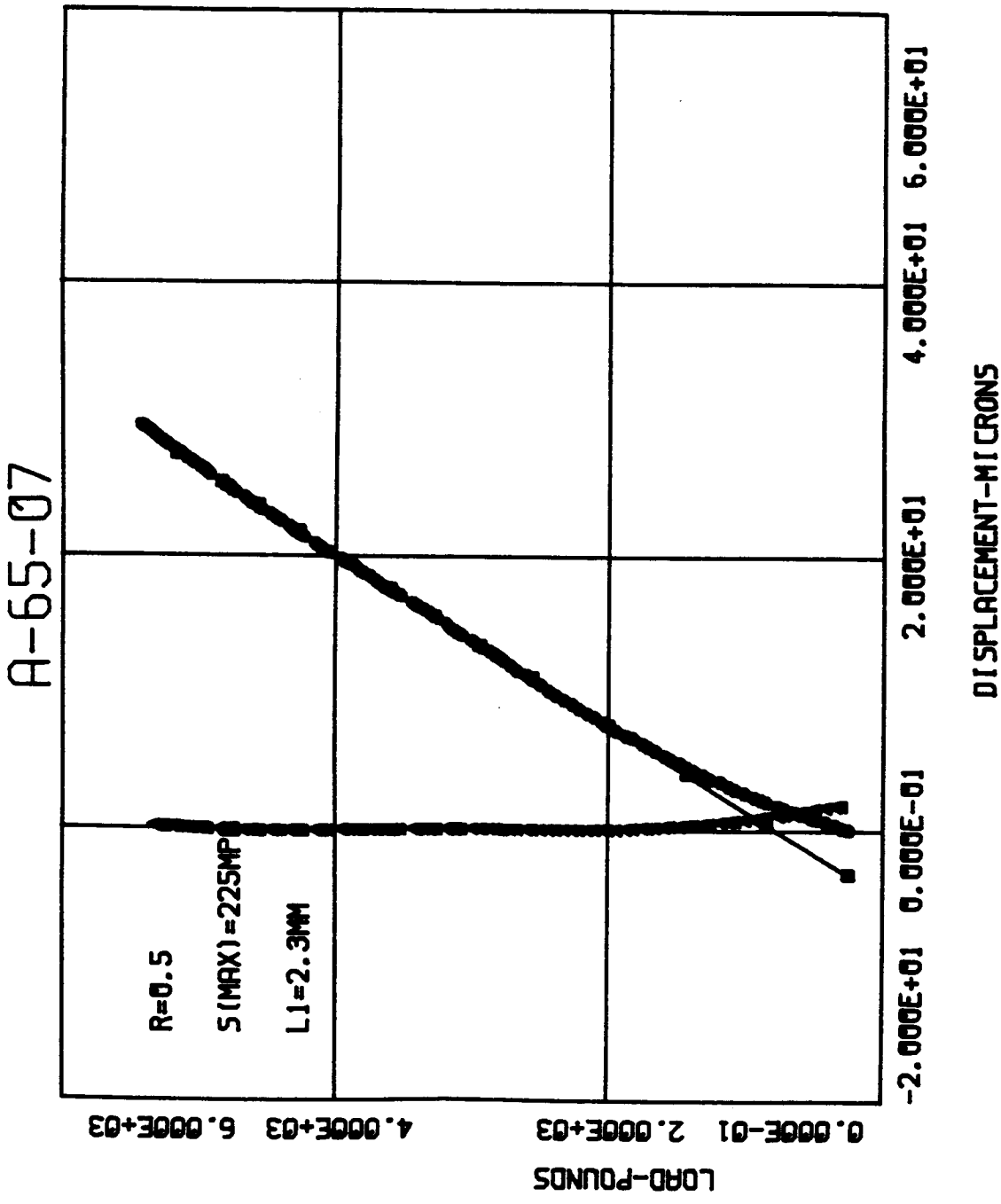
A-65-07
R=0.5
S(MAX)=225MP
L1=2.3MM
LOAD-POUNDS
0.0000E-01
2.0000E+03
4.0000E+03
6.0000E+03
-2.000E+01
0.000E-01
2.000E+01
4.000E+01
6.000E+01
DISPLACEMENT-MICRONS

A-65-07

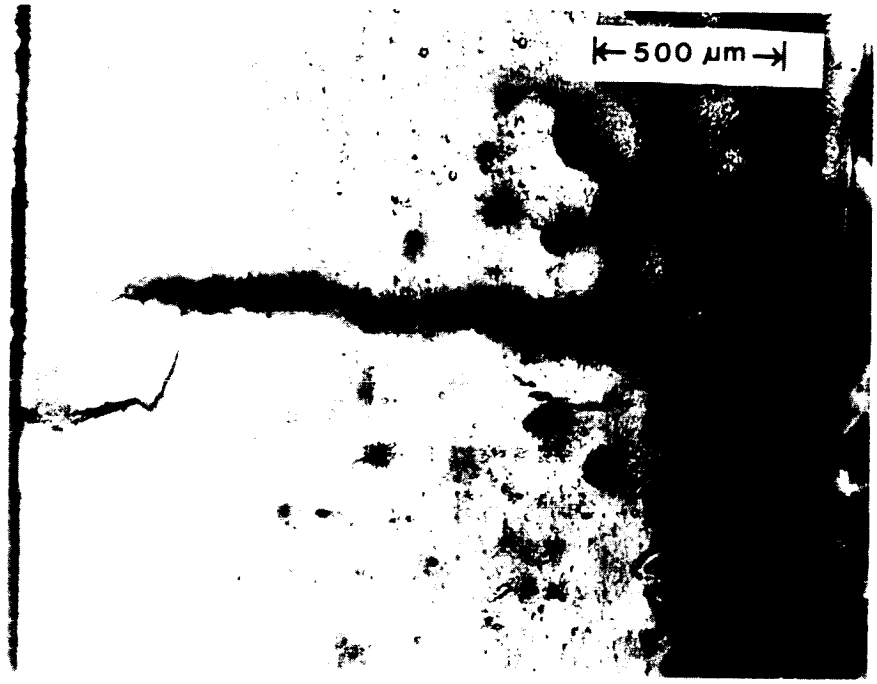

A-65-07

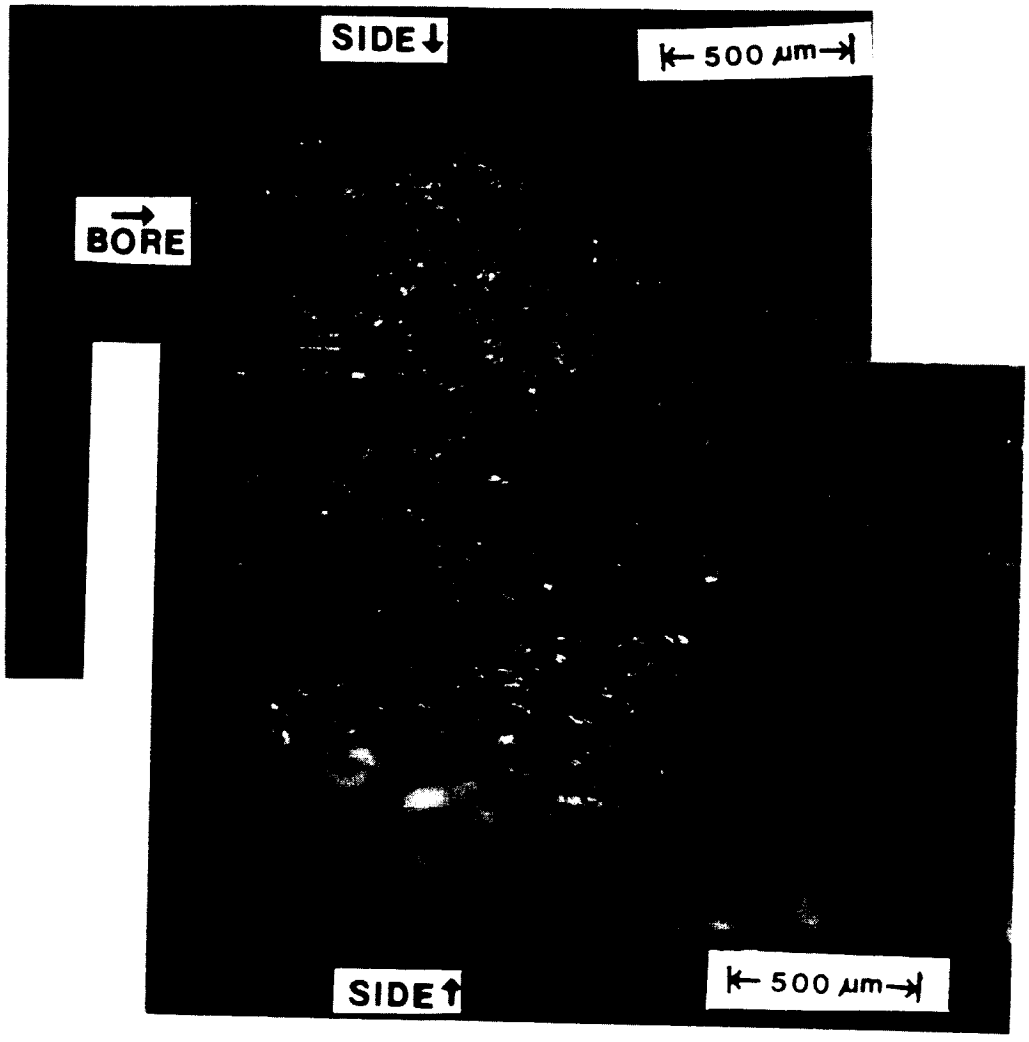

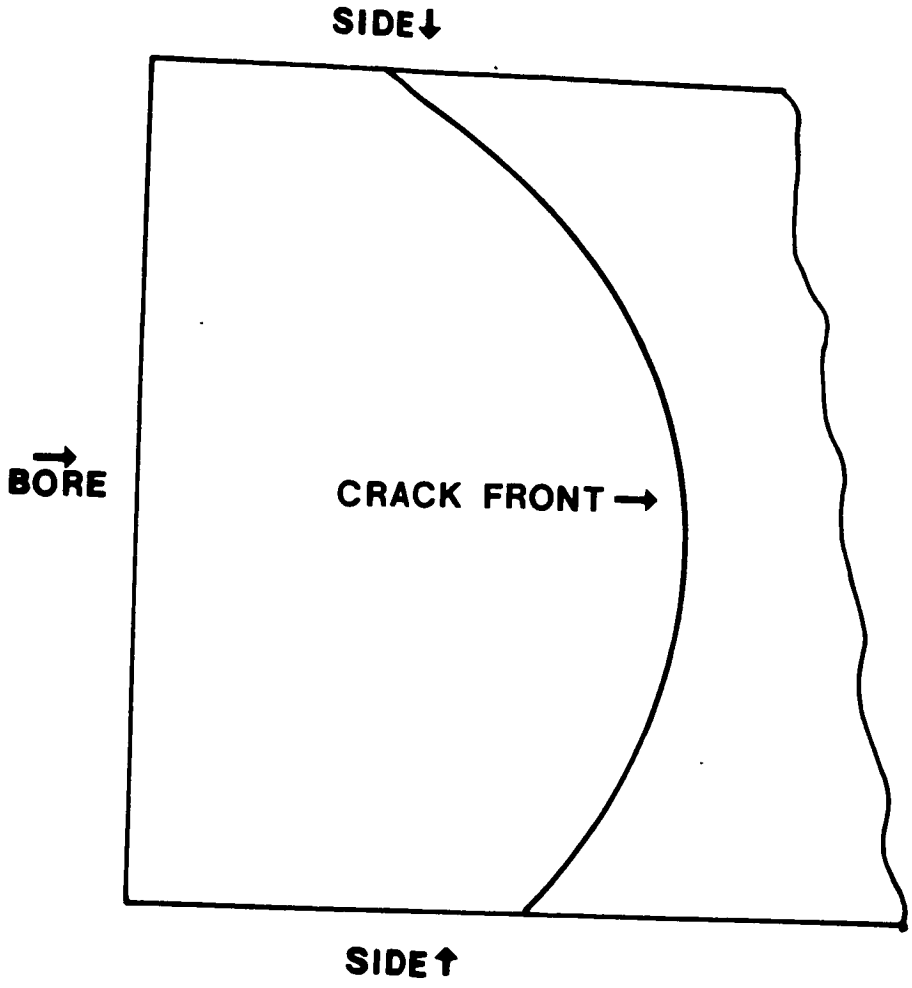

Tracing of Crack Front for A-65-07

TEST DATA

SPECIMEN NUMBER: A-71-05

DATE: 5/28/85

PARTICIPANT'S NAME: Joo-Jin Lee

John Cieslowski

TEST TEMPERATURE: 27°C

RELATIVE HUMIDITY: 65 %

WAVEFORM TYPE: Sinusoidal wave, 20 Hz

LOADING SEQUENCE TYPE: Constant amplitude

R-RATIO = 0.5

S max = 205 MPa

S min = 102.5 MPa

FINAL LENGTH OF CRACK: 2.3 mm

COMMENTS:

L1 was initiated at 1.2 mm down from the center line.

AGARD Short Crack DATA CHART

Record of crack lengths and map

Page 1 of 4 Loading Type Const. Amplitude R=0.5

Specimen no A-71-05 Peak Stress 205 MPa

0.1mm grid

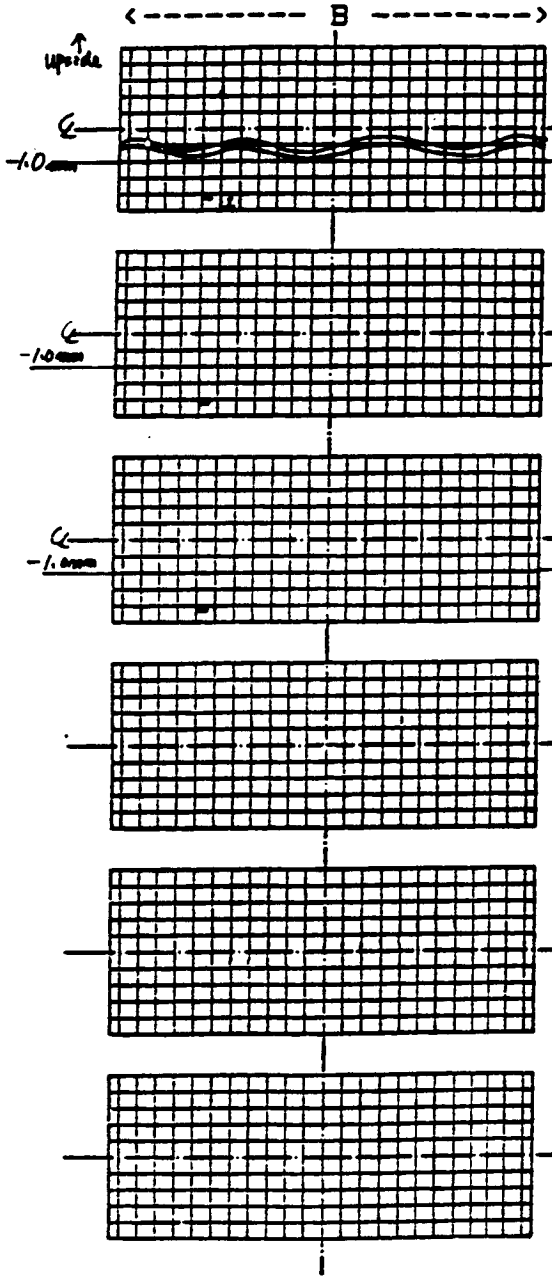

20 k Cycles
L1 .044 mm
L2 mm
L3 mm
L4 mm
L5 mm

25 k Cycles
L1 .044 mm
L2 mm
L3 mm
L4 mm
L5 mm

30 k Cycles
L1 .049 mm
L2 mm
L3 mm
L4 mm
L5 mm

Cycles
L1 mm
L2 mm
L3 mm
L4 mm
L5 mm

Cycles
L1 mm
L2 mm
L3 mm
L4 mm
L5 mm

Cycles
L1 mm
L2 mm
L3 mm
L4 mm
L5 mm

AGARD Short Crack DATA CHART

Record of crack lengths and map

Page 2 of 4 Loading Type R=0.5
Specimen no A-71-05 Peak Stress 205 MPa

0.1mm grid

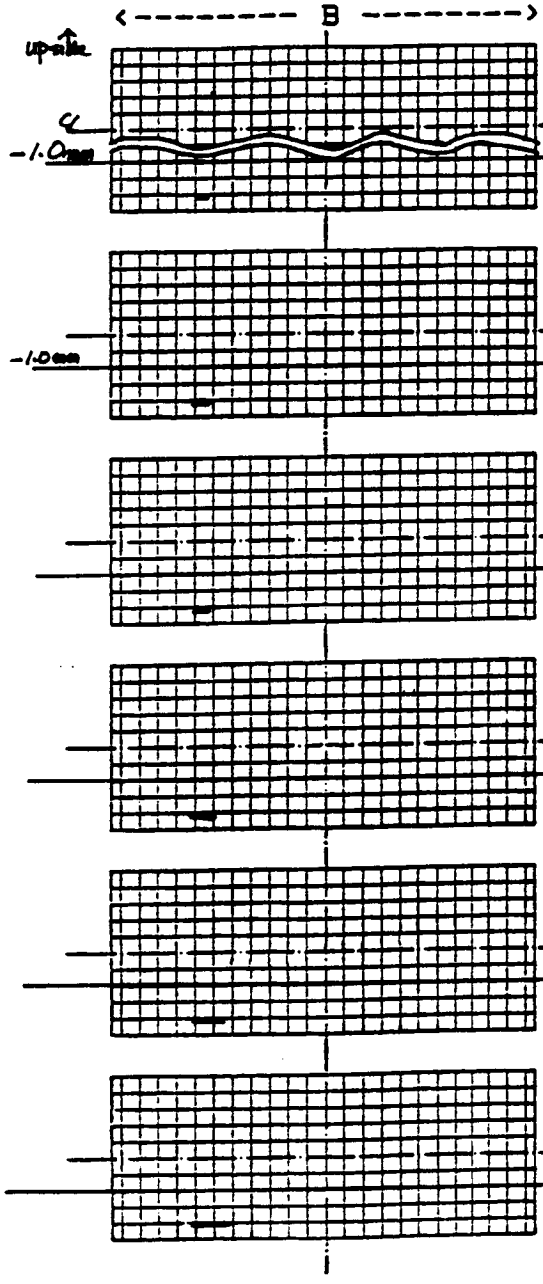

35k Cycles
L1 .055 mm
L2 ____ mm
L3 ____ mm
L4 ____ mm
L5 ____ mm

40k Cycles
L1 .065 mm
L2 ____ mm
L3 ____ mm
L4 ____ mm
L5 ____ mm

45k Cycles
L1 .065 mm
L2 ____ mm
L3 ____ mm
L4 ____ mm
L5 ____ mm

50k Cycles
L1 .109 mm
L2 ____ mm
L3 ____ mm
L4 ____ mm
L5 ____ mm

55k Cycles
L1 .147 mm
L2 ____ mm
L3 ____ mm
L4 ____ mm
L5 ____ mm

60k Cycles
L1 .202 mm
L2 ____ mm
L3 ____ mm
L4 ____ mm
L5 ____ mm

AGARD Short Crack DATA CHART

Record of crack lengths and map

Page 3 of 4. Loading Type R=0.5

Specimen no A-71-05 Peak Stress 205 MPa

0.1mm grid

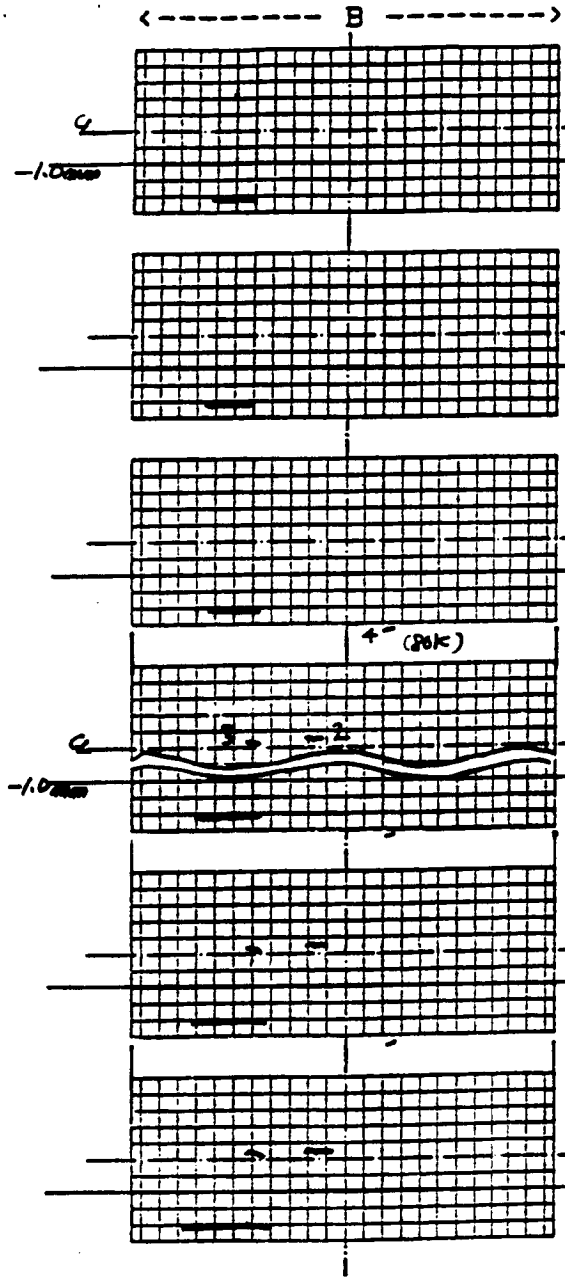

65k Cycles
L1 .213 mm
L2 ____ mm
L3 ____ mm
L4 ____ mm
L5 ____ mm

70k Cycles
L1 .218 mm
L2 ____ mm
L3 ____ mm
L4 ____ mm
L5 ____ mm

75k Cycles
L1 .273 mm
L2 ____ mm
L3 ____ mm
L4 ____ mm
L5 ____ mm

80k Cycles
L1 .337 mm
L2 .093 mm
L3 .065 mm
L4 .049 mm
L5 ____ mm

85k Cycles
L1 .382 mm
L2 .112 mm
L3 .070 mm
L4 .054 mm
L5 ____ mm

90k Cycles
L1 .469 mm
L2 .169 mm
L3 .076 mm
L4 .055 mm
L5 ____ mm

AGARD Short Crack DATA CHART

Record of crack lengths and map

Page 4 of 4 Loading Type R=0.5

Specimen no A-71-05 Peak Stress 205 MPa

0.1mm grid

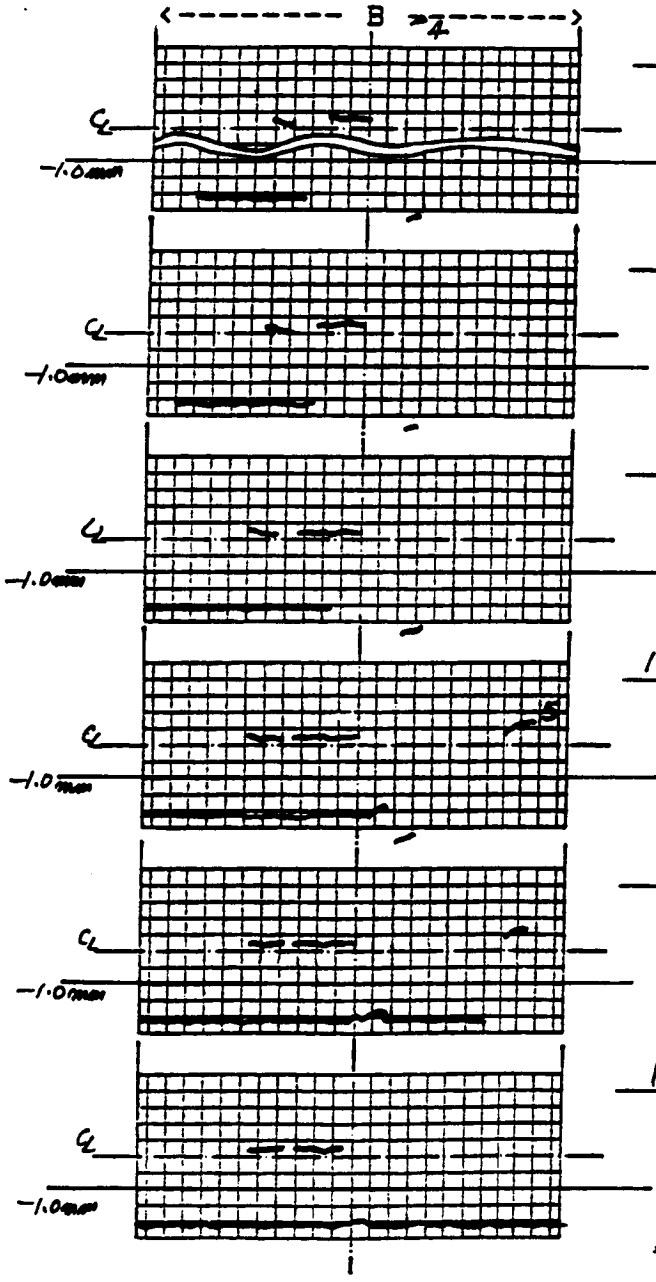

95 K Cycles
L1 .572 mm
L2 .213 mm
L3 .104 mm
L4 .055 mm
L5 mm

100K Cycles
L1 .703 mm
L2 .245 mm
L3 .120 mm
L4 .087 mm
L5 mm

105K Cycles
L1 .965 mm
L2 .283 mm
L3 .164 mm
L4 .087 mm
L5 mm

110K Cycles
L1 1.281 mm
L2 .332 mm
L3 .196 mm
L4 .114 mm
L5 .169 mm

115K Cycles
L1 1.848 mm
L2 .316 mm
L3 * mm
L4 . * mm
L5 * mm

117K Cycles
L1 Thru mm
L2 .251 mm
L3 .174 mm
L4 ** mm
L5 ** mm

* Crack tip was not clear

** Couldn't find the crack

** DA/DN DATA **

SPECIMEN' NO. = A-71-05.L1
NO. OF DATA = 19
R= 0.50
SMAX=205.0 MPa
Surface crack

	CYCLE(X1000)	CRK L. 2a(mm)	AVG. a(mm)	DELK(MPa-M)	DADN(mm/CYCLE)
0	25	0.044	0.000	0.00	0.000 X1.E-6
1	30	0.049	0.023	1.95	0.500 X1.E-6
2	35	0.055	0.026	2.06	0.600 X1.E-6
3	40	0.065	0.030	2.21	1.000 X1.E-6
4	50	0.109	0.043	2.63	2.200 X1.E-6
5	55	0.147	0.064	3.15	3.800 X1.E-6
6	60	0.202	0.087	3.64	5.500 X1.E-6
7	65	0.213	0.104	3.94	1.100 X1.E-6
8	70	0.218	0.108	4.01	0.500 X1.E-6
9	75	0.273	0.123	4.25	5.500 X1.E-6
10	80	0.337	0.152	4.69	6.400 X1.E-6
11	85	0.382	0.180	5.05	4.500 X1.E-6
12	90	0.469	0.213	5.45	8.700 X1.E-6
13	95	0.572	0.260	5.97	10.300 X1.E-6
14	100	0.703	0.319	6.54	13.100 X1.E-6
15	105	0.965	0.417	7.39	26.200 X1.E-6
16	110	1.281	0.561	8.45	31.600 X1.E-6
17	115	1.848	0.782	9.83	56.700 X1.E-6
18	117	2.250	1.025	11.20	100.500 X1.E-6

** DA/DN DATA **

SPECIMEN' NO. = A-71-05.L2
NO. OF DATA = 7
R= 0.50
SMAX=205.0 MPa
surface crack

	CYCLE(X1000)	CRK L. 2a(mm)	AVG. a(mm)	DELK(MPa-M)	DADN(mm/CYCLE)
0	80	0.093	0.000	0.00	0.000 X1.E-6
1	85	0.112	0.051	2.84	1.900 X1.E-6
2	90	0.169	0.070	3.29	5.700 X1.E-6
3	95	0.213	0.095	3.79	4.400 X1.E-6
4	100	0.245	0.115	4.12	3.200 X1.E-6
5	105	0.283	0.132	4.39	3.800 X1.E-6
6	110	0.337	0.155	4.72	5.400 X1.E-6

** DA/DN DATA **

SPECIMEN' NO. = A-71-05.L3
NO. OF DATA = 7
R= 0.50
SMAX=205.0 MPa
surface crack

	CYCLE(X1000)	CRK L. 2a(mm)	Center AVG. a(mm)	DELK(MPa-M)	DADN(mm/CYCLE)
0	80	0.065	0.000	0.00	0.000 X1.E-6
1	85	0.070	0.034	2.33	0.500 X1.E-6
2	90	0.076	0.036	2.42	0.600 X1.E-6
3	95	0.104	0.045	2.67	2.800 X1.E-6
4	100	0.120	0.056	2.96	1.600 X1.E-6
5	105	0.164	0.071	3.31	4.400 X1.E-6
6	110	0.196	0.090	3.69	3.200 X1.E-6

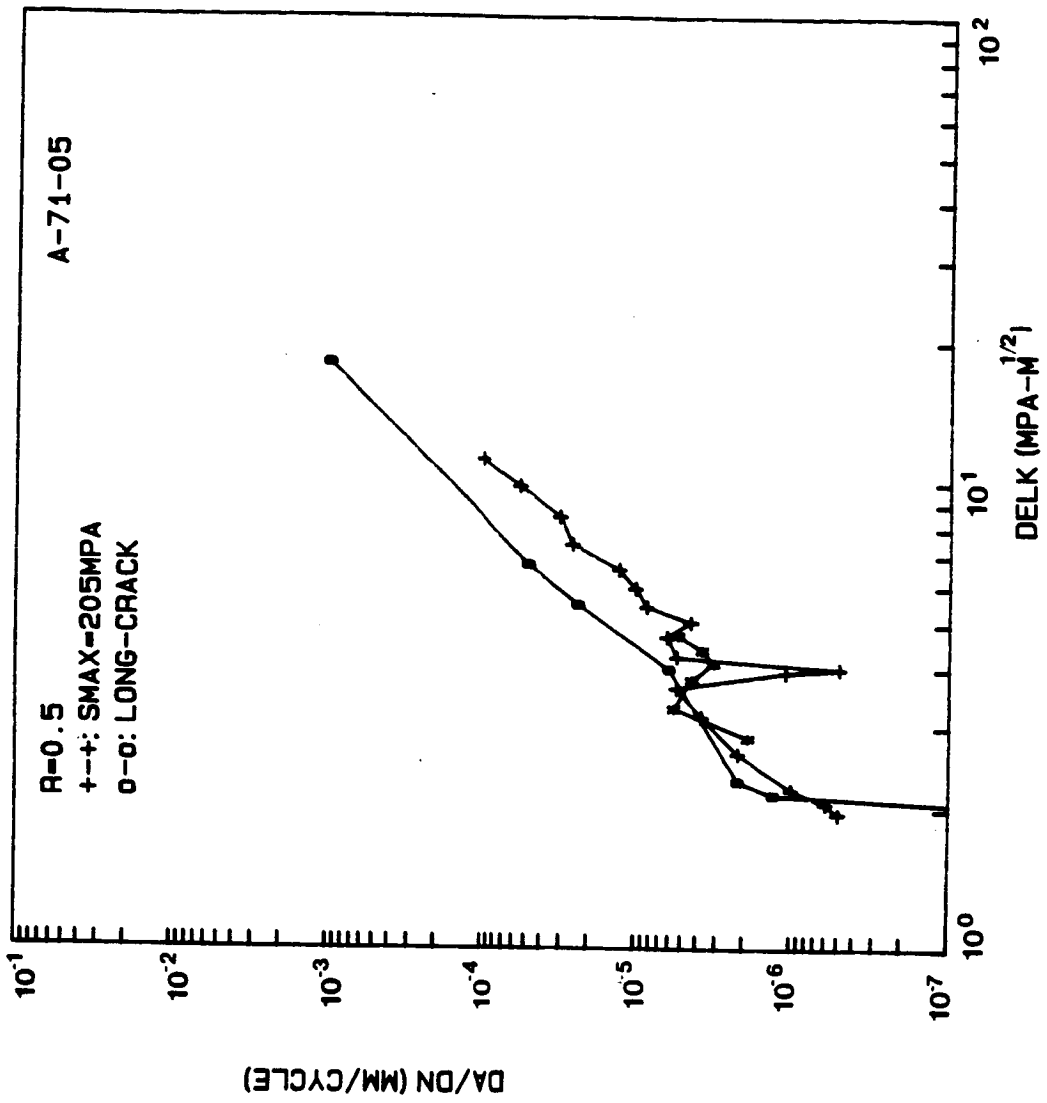
A-71-05
R=0.5
+--+: SMAX=205MPA
o--o: LONG-CRACK
DA/DN (MM/CYCLE)
DELK (MPA-M^1/2)
10^-1
10^-2
10^-3
10^-4
10^-5
10^-6
10^-7
10^0
10^1
10^2

A-71-05

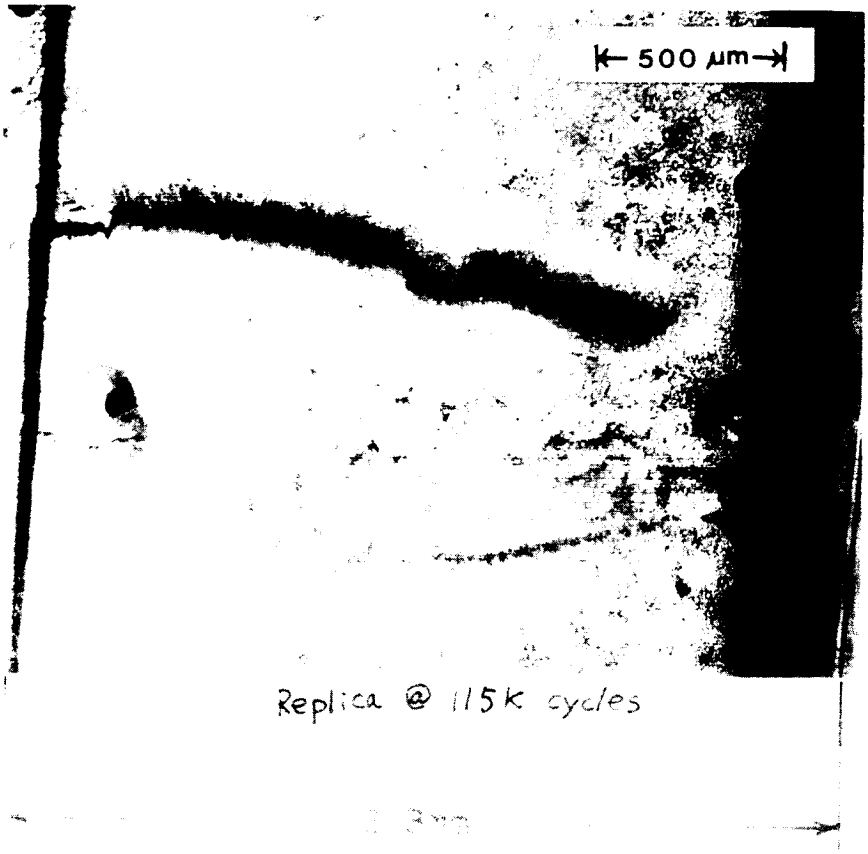

A-71-05

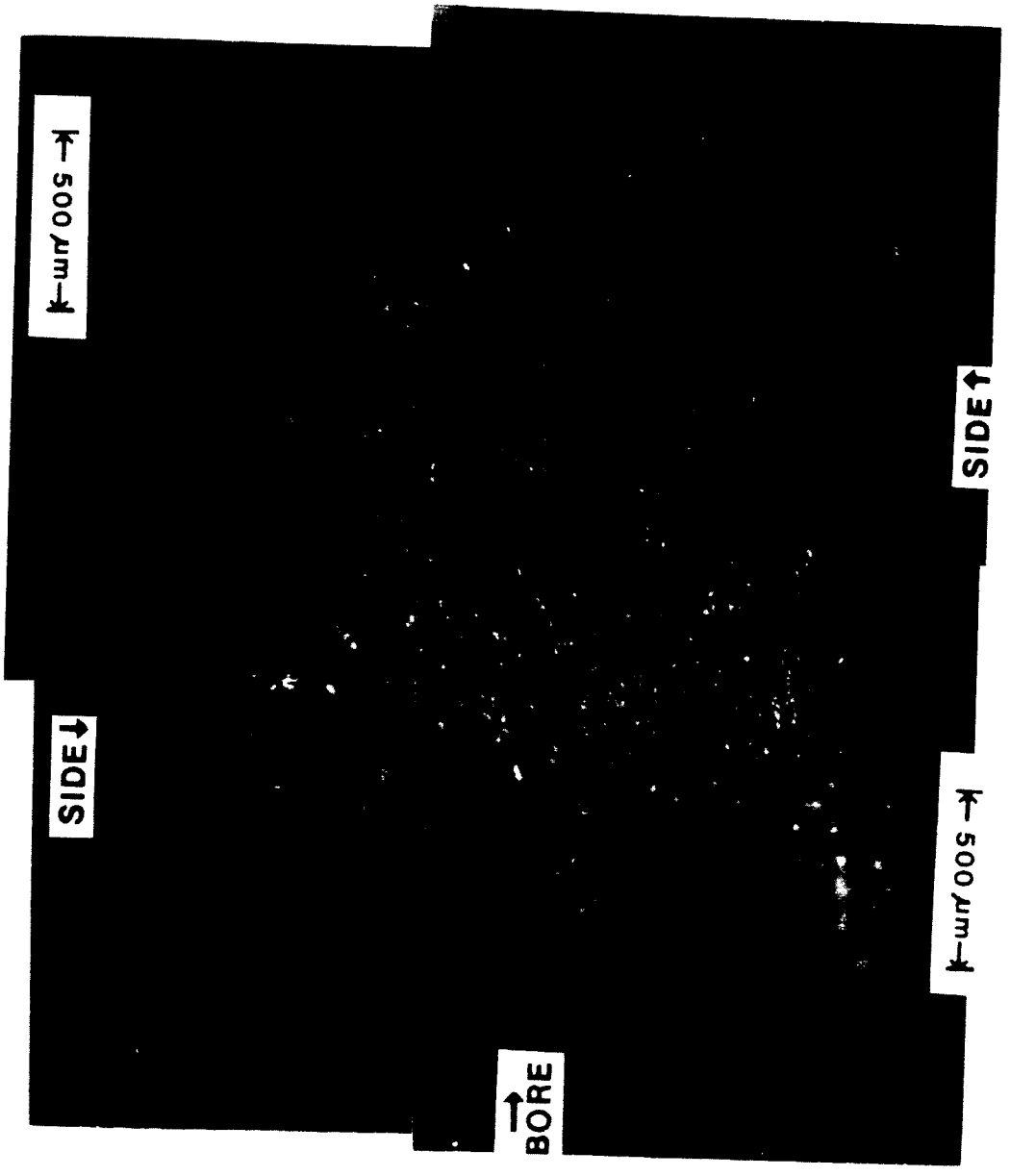

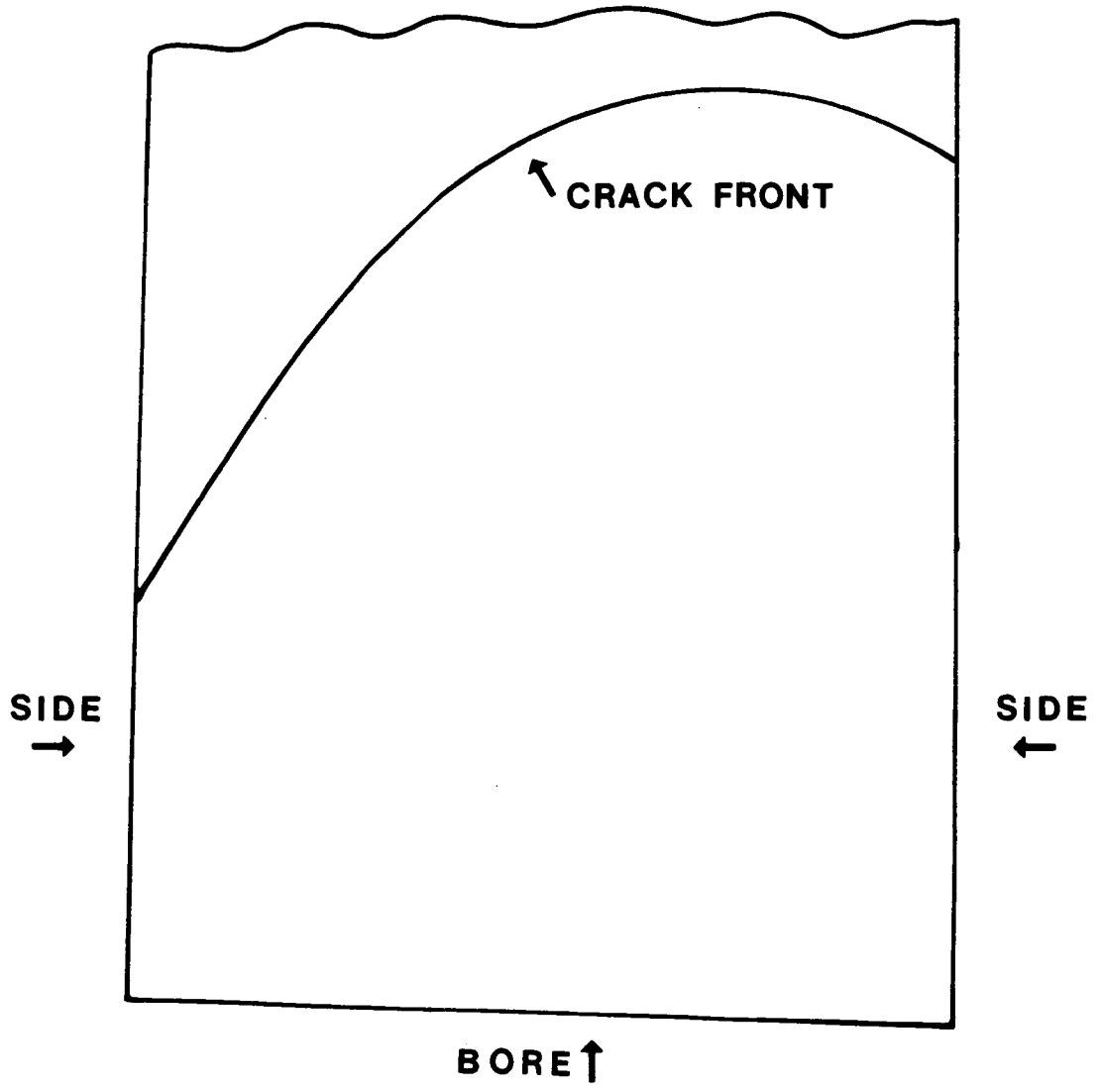

Tracing of Crack Front for A-71-05

TEST DATA

SPECIMEN NUMBER: A-68-22

DATE: 5/27/85

PARTICIPANT'S NAME: Joo-Jin Lee

John Cieslowski

TEST TEMPERATURE: 25°C

RELATIVE HUMIDITY: 53 %

WAVEFORM TYPE: Sinusoidal wave, 20 Hz

LOADING SEQUENCE TYPE: Constant amplitude

R-RATIO = 0.5

S max = 205 MPa

S min = 102.5 MPa

FINAL LENGTH OF CRACK: 0.545 mm (L1)

COMMENTS:

AGARD Short Crack DATA CHART

Record of crack lengths and map

Page 1 of 2

Specimen no A-68-22

Loading Type Const. Amplitude R=0.5

Peak Stress 205 MPa

0.1mm grid

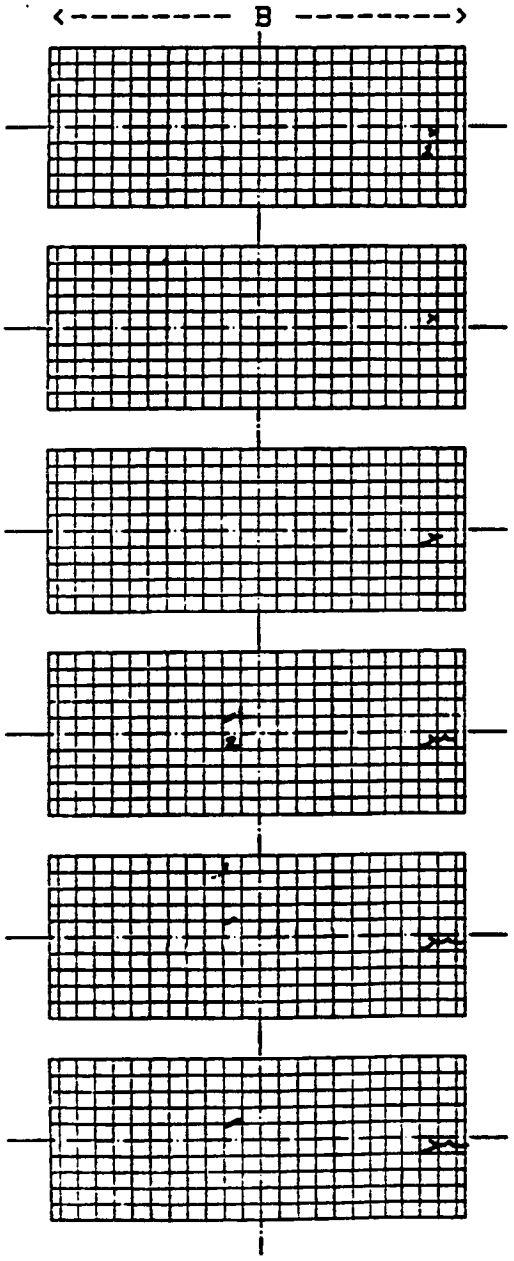

35k Cycles
L1 .049 mm
L2 ____ mm
L3 ____ mm
L4 ____ mm
L5 ____ mm

40k Cycles
L1 .055 mm
L2 ____ mm
L3 ____ mm
L4 ____ mm
L5 ____ mm

45k Cycles
L1 .104 mm
L2 ____ mm
L3 ____ mm
L4 ____ mm
L5 ____ mm

50k Cycles
L1 .174 mm
L2 .055 mm
L3 ____ mm
L4 ____ mm
L5 ____ mm

55k Cycles
L1 .196 mm
L2 .059 mm
L3 ____ mm
L4 ____ mm
L5 ____ mm

60k Cycles
L1 .213 mm
L2 .082 mm
L3 ____ mm
L4 ____ mm
L5 ____ mm

AGARD Short Crack DATA CHART

Record of crack lengths and map

Page 2 of 2 Loading Type R=0.5

Specimen no A-68-22 Peak Stress 205 MPa

0.1mm grid

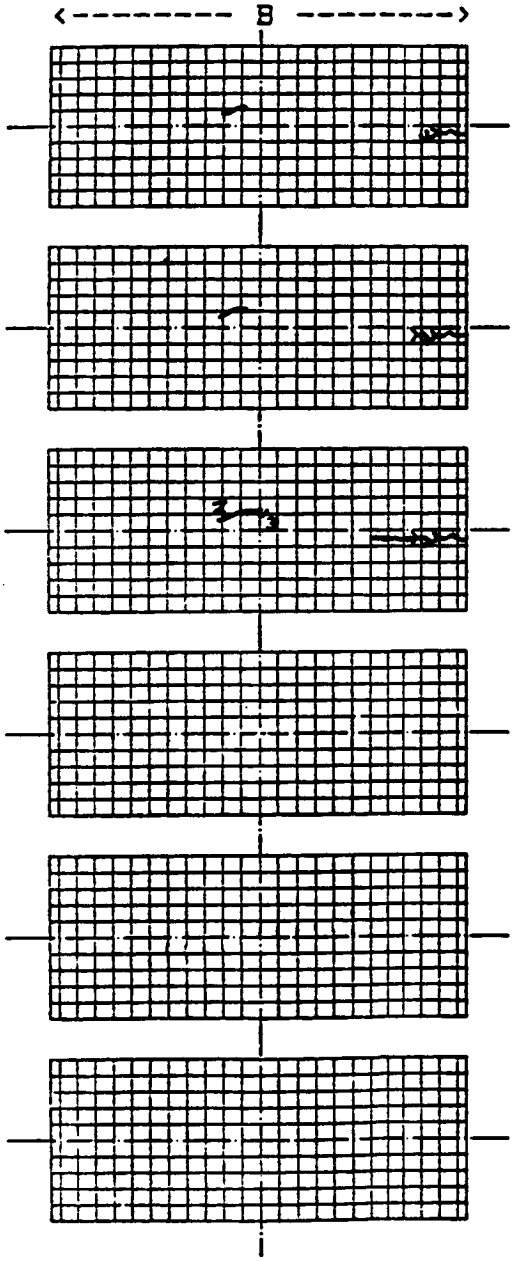

65k Cycles
L1 .251 mm
L2 .120 mm
L3 _____ mm
L4 _____ mm
L5 _____ mm

70k Cycles
L1 .300 mm
L2 .153 mm
L3 _____ mm
L4 _____ mm
L5 _____ mm

75k Cycles
L1 .545 mm
L2 .234 mm
L3 .038 mm
L4 _____ mm
L5 _____ mm

_____ Cycles
L1 _____ mm
L2 _____ mm
L3 _____ mm
L4 _____ mm
L5 _____ mm

_____ Cycles
L1 _____ mm
L2 _____ mm
L3 _____ mm
L4 _____ mm
L5 _____ mm

_____ Cycles
L1 _____ mm
L2 _____ mm
L3 _____ mm
L4 _____ mm
L5 _____ mm

** DA/DN DATA **

SPECIMEN' NO. = A-68-22.L1
NO. OF DATA = 9
R= 0.50
SMAX=205.0 MPa
near edge → corner crack @ 53K

	CYCLE(X1000)	CRK L. 2a(mm)	AVG. a(mm)	DELK(MPa-M)	DADN(mm/CYCLE)
0	35	0.049	0.000	0.00	0.000 X1.E-6
1	40	0.055	0.052	2.81	1.200 X1.E-6
2	45	0.104	0.079	3.44	9.800 X1.E-6
3	50	0.174	0.139	4.45	14.000 X1.E-6
4	55	0.196	0.185	5.07	4.400 X1.E-6
5	60	0.213	0.205	5.31	3.400 X1.E-6
6	65	0.251	0.232	5.62	7.600 X1.E-6
7	70	0.300	0.275	6.06	9.800 X1.E-6
8	75	0.545	0.422	7.33	49.000 X1.E-6

** DA/DN DATA **

SPECIMEN' NO. = A-68-22.L2
NO. OF DATA = 6
R= 0.50
SMAX=205.0 MPa
surface crack

	CYCLE(X1000)	CRK L. 2a(mm)	AVG. a(mm)	DELK(MPa-M)	DADN(mm/CYCLE)
0	50	0.055	0.000	0.00	0.000 X1.E-6
1	55	0.059	0.029	2.15	0.400 X1.E-6
2	60	0.082	0.035	2.38	2.300 X1.E-6
3	65	0.120	0.050	2.82	3.800 X1.E-6
4	70	0.153	0.068	3.25	3.300 X1.E-6
5	75	0.234	0.097	3.81	8.100 X1.E-6

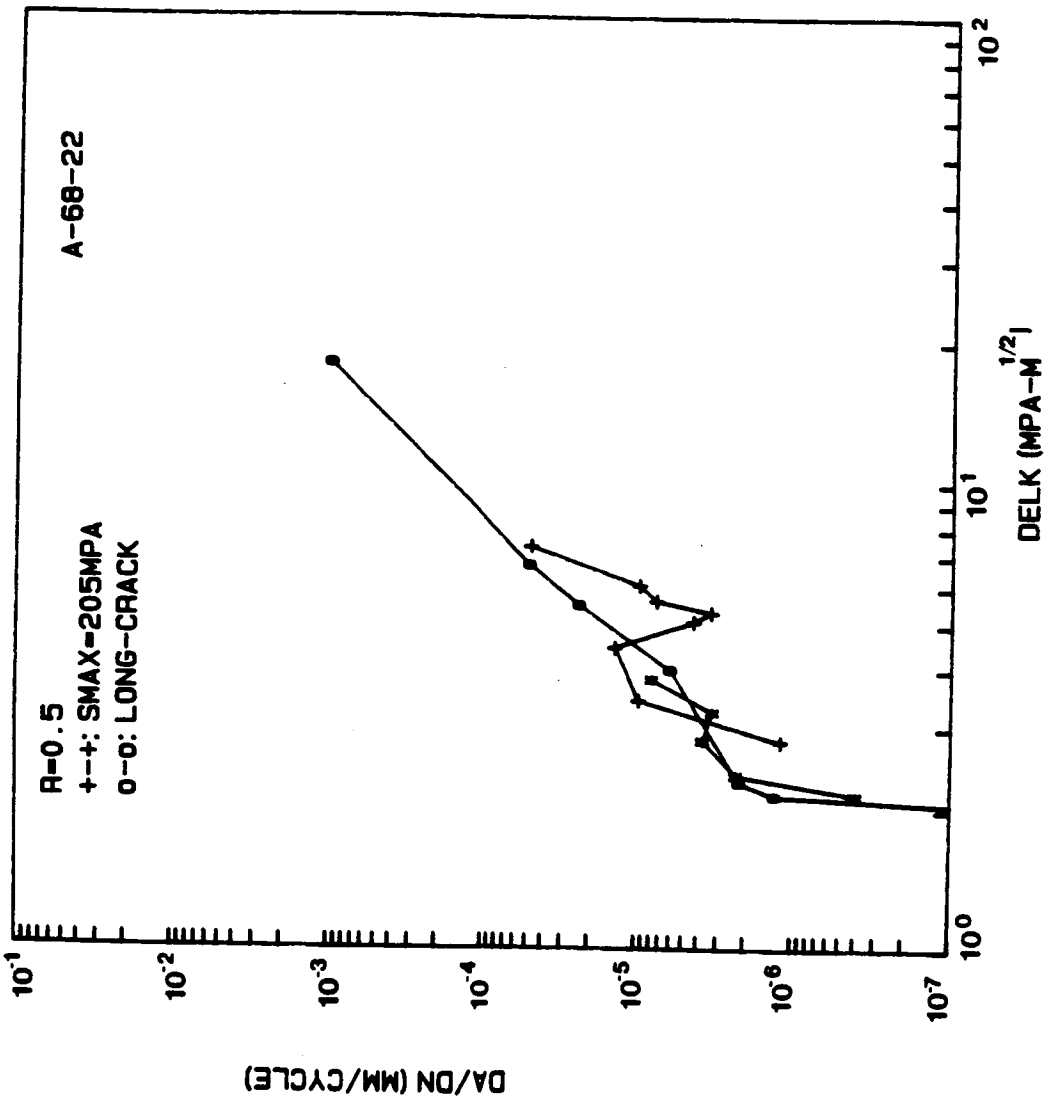
A-68-22
R=0.5
+--+: SMAX=205MPA
o-o: LONG-CRACK
DA/DN (MM/CYCLE)
DELK (MPA-M^1/2)
10^-1
10^-2
10^-3
10^-4
10^-5
10^-6
10^-7
10^0
10^1
10^2

A-68-22
R=0.5
S(MAX)=205MPa
L2=0.18MM
LOAD-POUNDS
0.000E-01
2.000E+03
4.000E+03
6.000E+03
-6.000E+00
-3.000E+00
0.000E-01
3.000E+00
6.000E+00
DISPLACEMENT-MICRONS

A-68-22
R=0.5
S(MAX)=205MPA
L1=0.52MM
LOAD-POUNDS
0.0000E-01
2.0000E+03
4.0000E+03
6.0000E+03
-6.000E+00
-3.000E+00
0.000E-01
3.000E+00
6.000E+00
DISPACEMENT-MICRONS

A-68-22

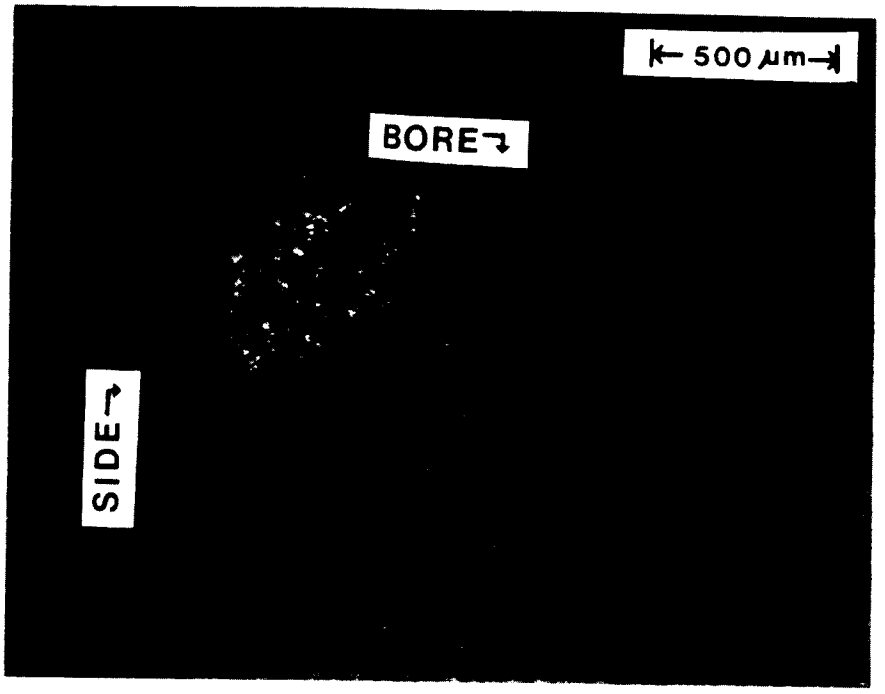

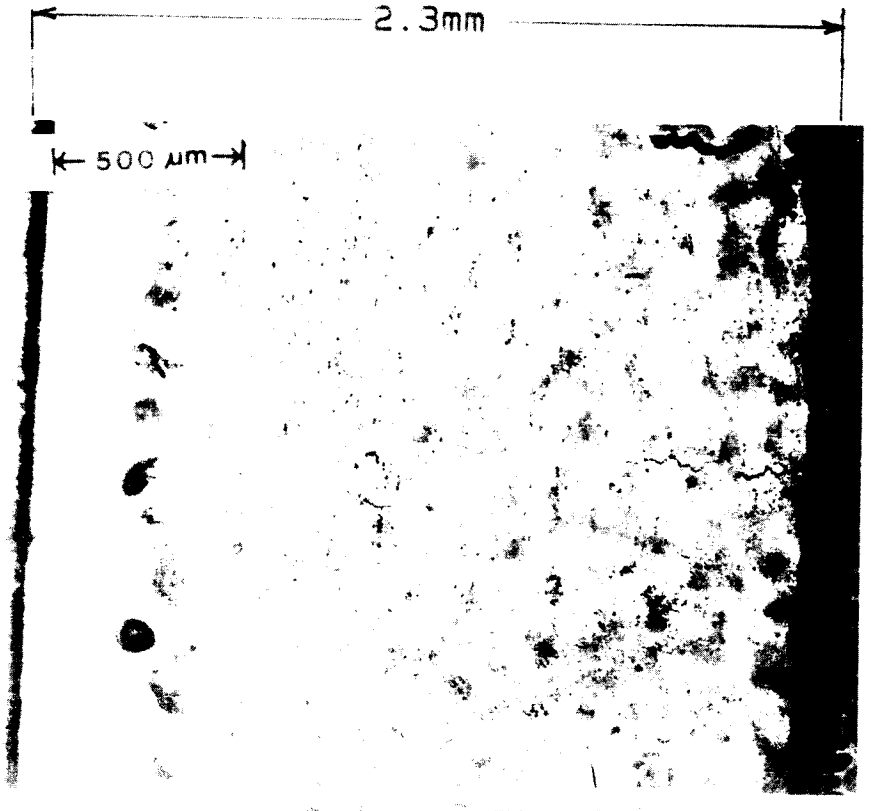

Replica @ 75× Scales

TEST DATA

SPECIMEN NUMBER: A-84-03

DATE: 5/30/85

PARTICIPANT'S NAME: Joo-Jin Lee

John Cieslowski

TEST TEMPERATURE: 27°C

RELATIVE HUMIDITY: 44%

WAVEFORM TYPE: Sinusoidal wave, 20 Hz

LOADING SEQUENCE TYPE: Constant amplitude

R-RATIO = 0.5

S max = 195 MPa

S min = 97.5 MPa

FINAL LENGTH OF CRACK:

COMMENTS:

Crack was grown to break up the specimen during cycling from 750k ~ 760k.

AGARD Short Crack DATA CHART

Record of crack lengths and map

Page 1 of 1 Loading Type Const. Amplitude R=0.5

Specimen no A-84-03 Peak Stress 195 MPa

0.1mm grid

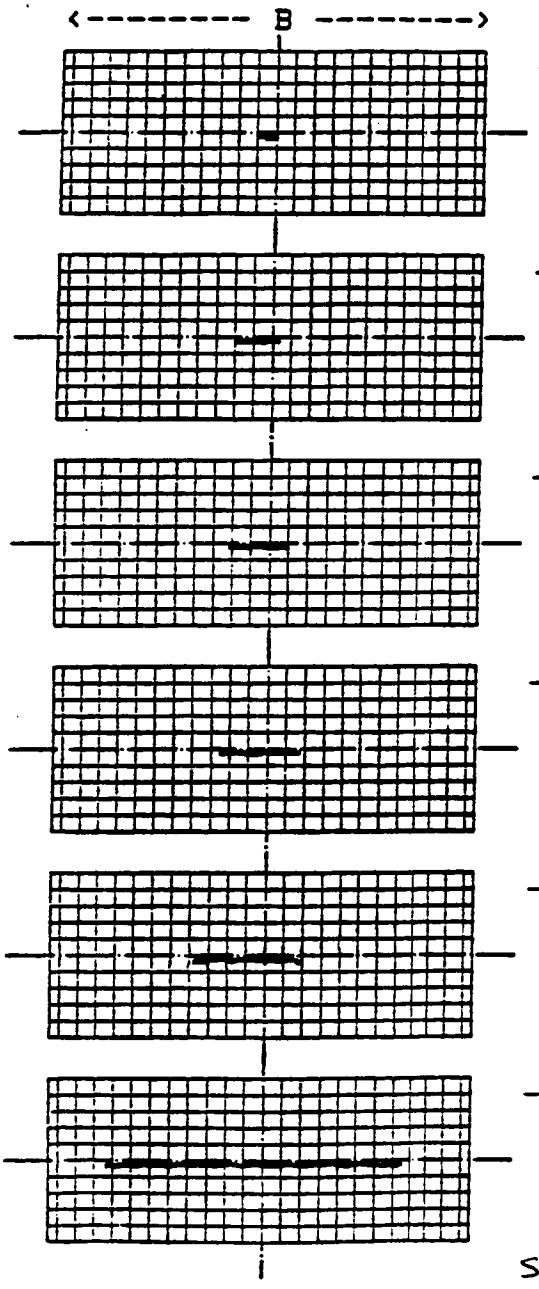

690 K Cycles
L1 .098 mm
L2 ____ mm
L3 ____ mm
L4 ____ mm
L5 ____ mm

710 K Cycles
L1 .229 mm
L2 ____ mm
L3 ____ mm
L4 ____ mm
L5 ____ mm

720 K Cycles
L1 .316 mm
L2 ____ mm
L3 ____ mm
L4 ____ mm
L5 ____ mm

730 K Cycles
L1 .425 mm
L2 ____ mm
L3 ____ mm
L4 ____ mm
L5 ____ mm

740 K Cycles
L1 .561 mm
L2 ____ mm
L3 ____ mm
L4 ____ mm
L5 ____ mm

750 K Cycles
L1 1.55 mm
L2 ____ mm
L3 ____ mm
L4 ____ mm
L5 ____ mm

Specimen was broken during cycling

** DA/DN DATA **

SPECIMEN' NO. = A-84-03.L1
NO. OF DATA = 6
R= 0.50
SMAX=195.0 MPa
Surface crack

	CYCLE(X1000)	CRK L. 2a(mm)	AVG. a(mm)	DELK(MPa-M)	DADN(mm/CYCLE)
0	690	0.098	0.000	0.00	0.000 X1.E-6
1	710	0.229	0.082	3.36	3.275 X1.E-6
2	720	0.316	0.136	4.24	4.350 X1.E-6
3	730	0.425	0.185	4.87	5.450 X1.E-6
4	740	0.561	0.247	5.54	6.800 X1.E-6
5	750	1.550	0.528	7.82	49.450 X1.E-6

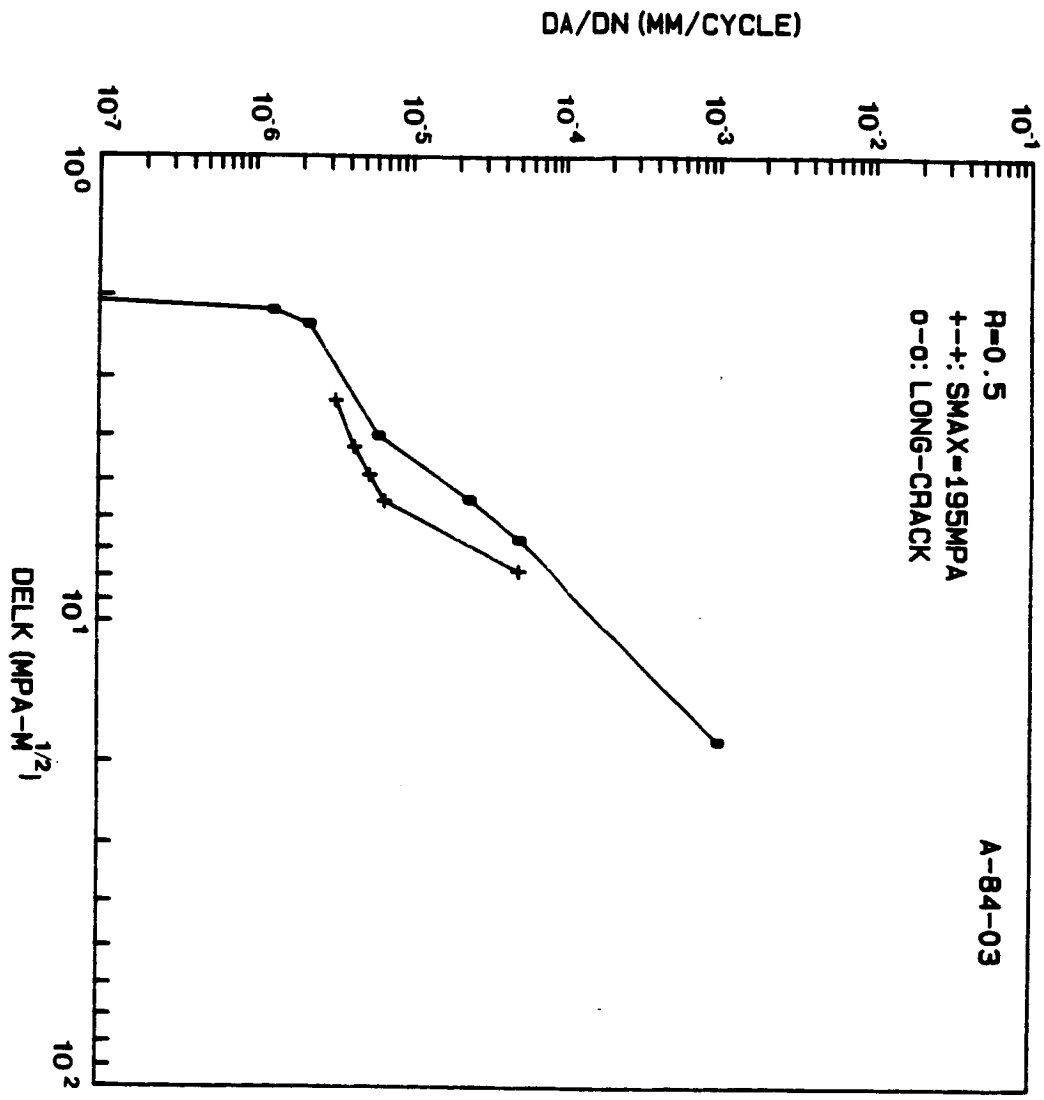
DA/DN (MM/CYCLE)
10^{-1}
10^{-2}
10^{-3}
10^{-4}
10^{-5}
10^{-6}
10^{-7}
R=0.5
+-+: SMAX=195MPA
o-o: LONG-CRACK
A-84-03
10^{0}
10^{1}
10^{2}
DELK (MPA-M$^{1/2}$)

A-84-03

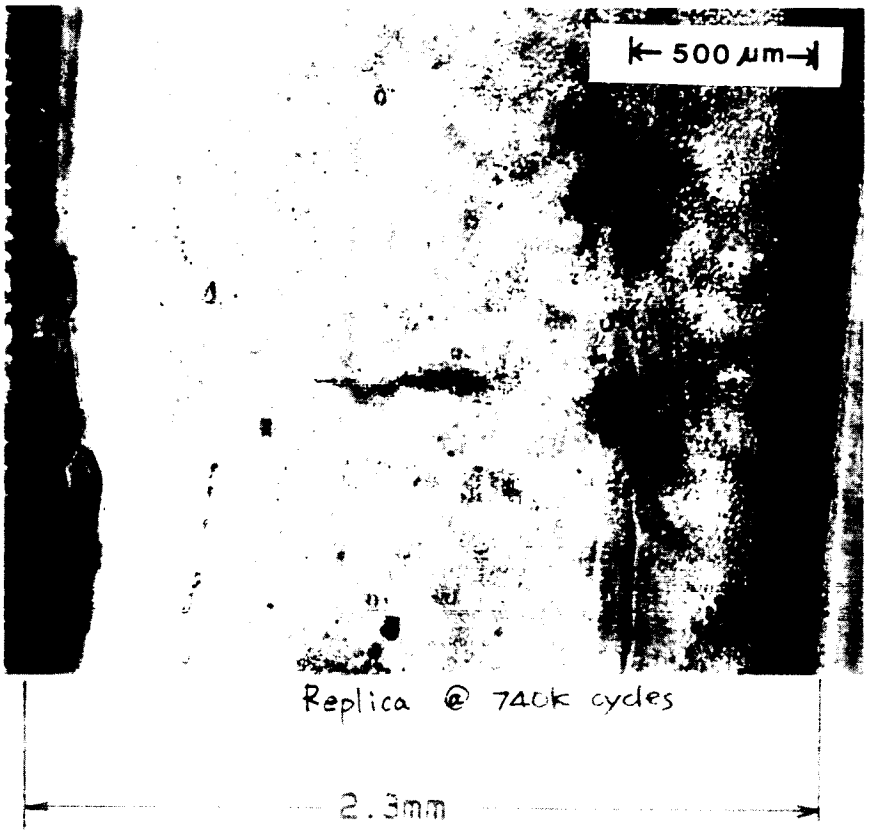

TEST DATA

SPECIMEN NUMBER: A-59-13

DATE: 5/29/85

PARTICIPANT'S NAME: Joo-Jin Lee

John Cieslowski

TEST TEMPERATURE: 26°C

RELATIVE HUMIDITY: 50 %

WAVEFORM TYPE: Sinusoidal wave, 20 Hz

LOADING SEQUENCE TYPE: Constant amplitude

R-RATIO = 0.5

S max = 195 MPa

S min = 97.5 MPa

FINAL LENGTH OF CRACK: 0.403 mm (L1)

COMMENTS:

AGARD Short Crack DATA CHART

Record of crack lengths and map

Page 1 of 1 — Loading Type Const. Amplitude R=0.5

Specimen no A-59-13 — Peak Stress 195 MPa

0.1mm grid

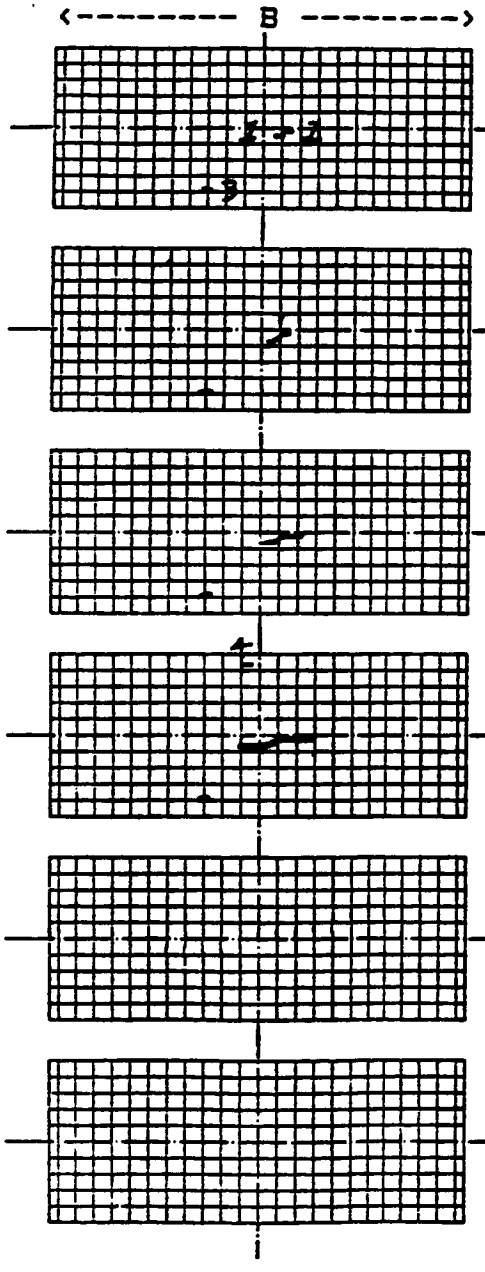

130 K Cycles
L1 .060 mm
L2 .038 mm
L3 .027 mm
L4 ____ mm
L5 ____ mm

150K Cycles
L1 .136 mm
L2 Lt mm
L3 .027 mm
L4 ____ mm
L5 ____ mm

160K Cycles
L1 .218 mm
L2 ____ mm
L3 .044 mm
L4 ____ mm
L5 ____ mm

170K Cycles
L1 .403 mm
L2 ____ mm
L3 * mm
L4 .055 mm
L5 ____ mm

____ Cycles
L1 ____ mm
L2 ____ mm
L3 ____ mm
L4 ____ mm
L5 ____ mm

____ Cycles
L1 ____ mm
L2 ____ mm
L3 ____ mm
L4 ____ mm
L5 ____ mm

* Crack tip was not clear

** DA/DN DATA **

SPECIMEN NO. = A-59-13.L1
STRESS RATIO=0.5
MAX.STRESS=195.0 MPa
NO.OF DATA= 3
surface crack

	CYCLE(X1000)	CRK L 2a(mm)	AVG. a(mm)	DELK(MPa-M)	DADN(mm/CYCLE)
0	130	0.060	0.00	0.00	0.000 X1.E-6
1	150	0.136	0.05	2.65	1.900 X1.E-6
2	160	0.218	0.09	3.48	4.100 X1.E-6
3	170	0.403	0.16	4.49	9.250 X1.E-6

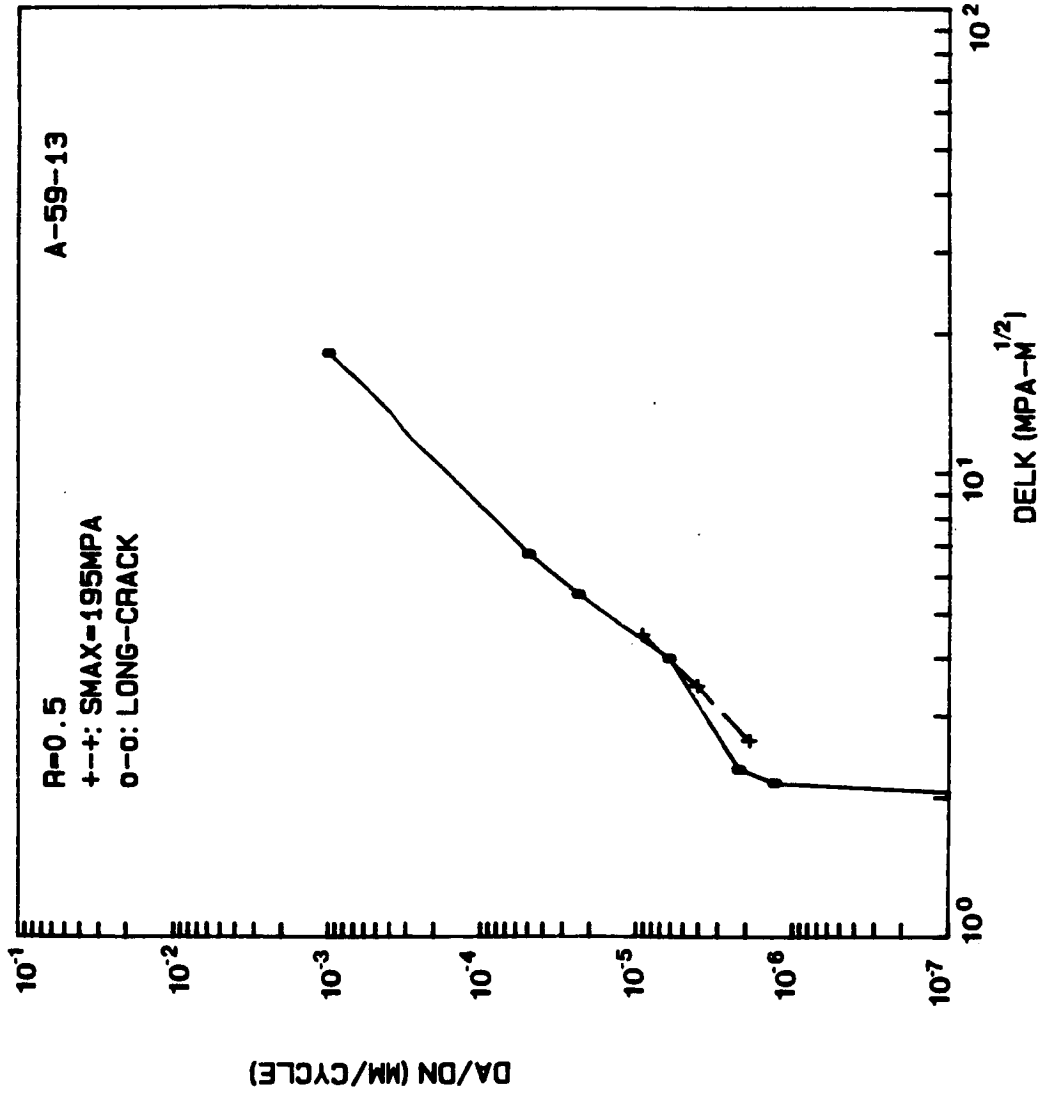
A-59-13
R=0.5
+--+: SMAX=195MPA
o-o: LONG-CRACK
DA/DN (MM/CYCLE)
DELK (MPA-M^1/2)
10^-1
10^-2
10^-3
10^-4
10^-5
10^-6
10^-7
10^0
10^1
10^2

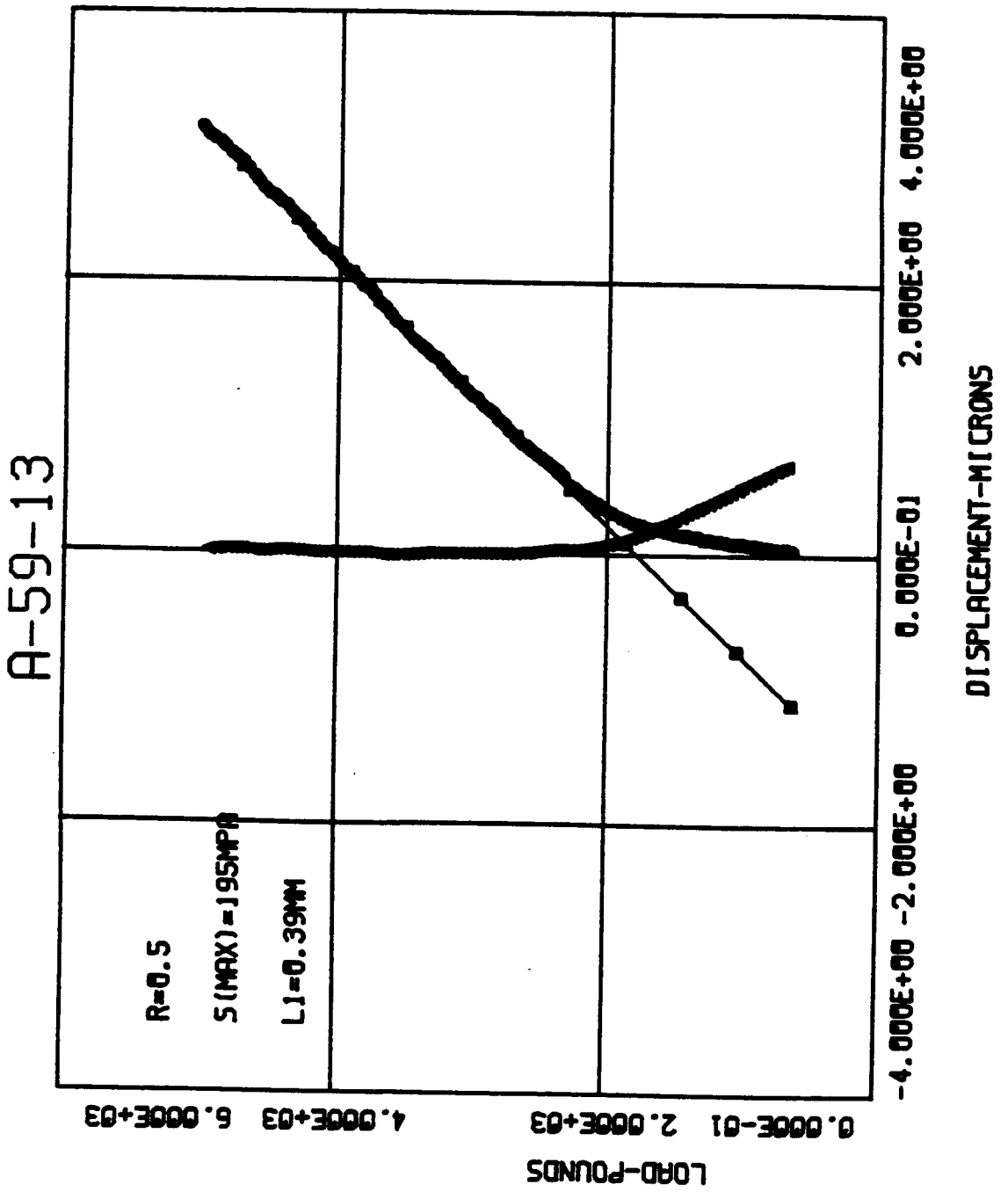
A-59-13
R=0.5
S(MAX)=195MPA
LI=0.39MM
LOAD-POUNDS
0.0000E-01
2.0000E+03
4.0000E+03
6.0000E+03
-4.000E+00
-2.000E+00
0.000E-01
2.000E+00
4.000E+00
DISPLACEMENT-MICRONS

A-59-13

Replica @ 170K cycles

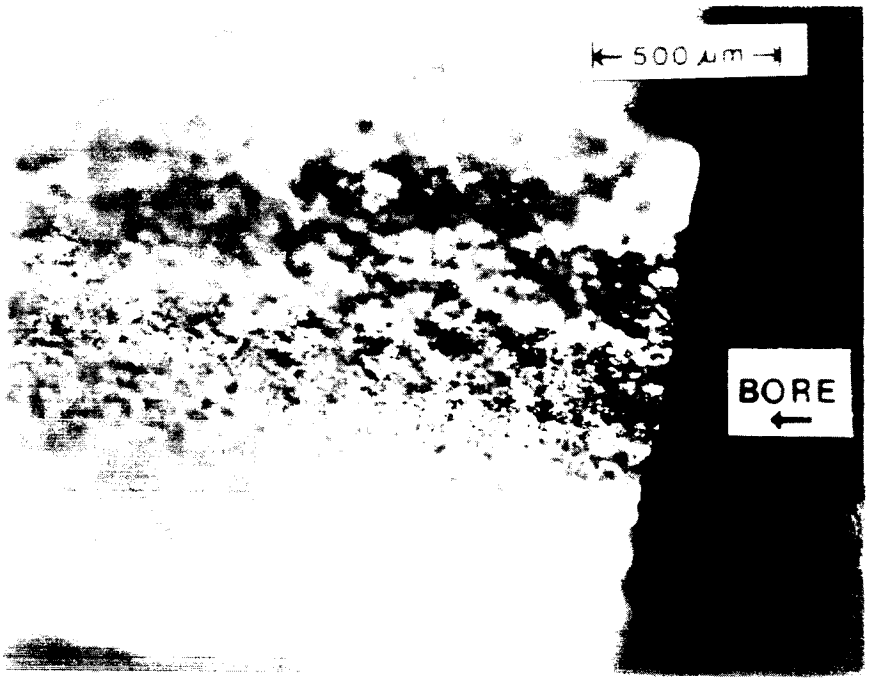

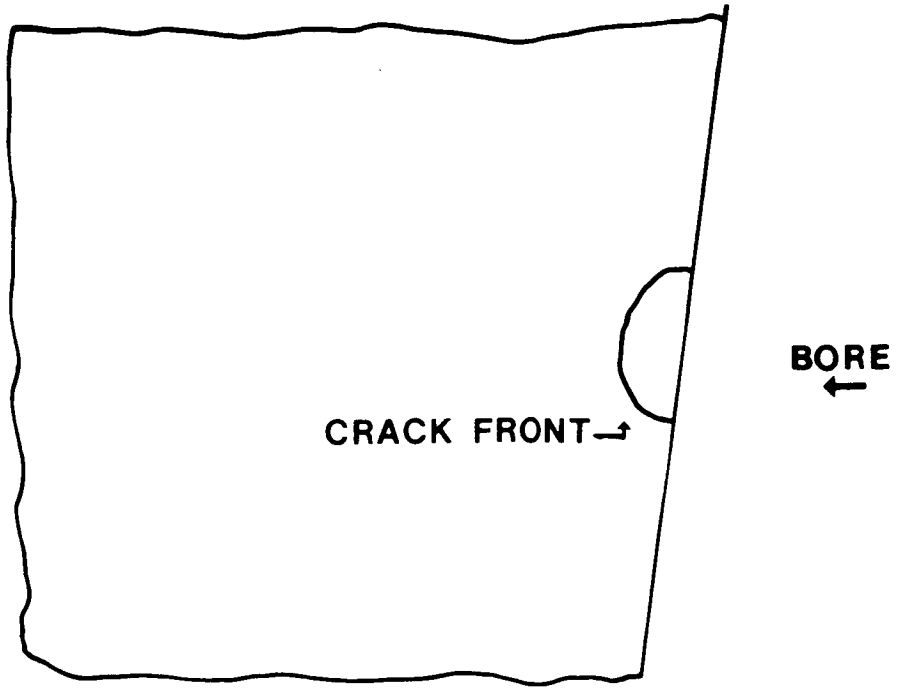

Tracing of Crack Front for A-59-13

TEST DATA

SPECIMEN NUMBER: A-52-03

DATE: 6/4/85

PARTICIPANT'S NAME: Joo-Jin Lee

John Cieslowski

TEST TEMPERATURE: 26° C

RELATIVE HUMIDITY: 60 %

WAVEFORM TYPE: Sinusoidal wave, 20 Hz

LOADING SEQUENCE TYPE: Constant amplitude

R-RATIO = 0.0

S max = 145 MPa

S min = 0 MPa

FINAL LENGTH OF CRACK: 2.3 mm (L3)

COMMENTS:

AGARD Short Crack DATA CHART

Record of crack lengths and map

Page 1 of 5 Loading Type Constant Amplitude R=0.0

Specimen no A-52-03 Peak Stress 145 MPa

0.1mm grid

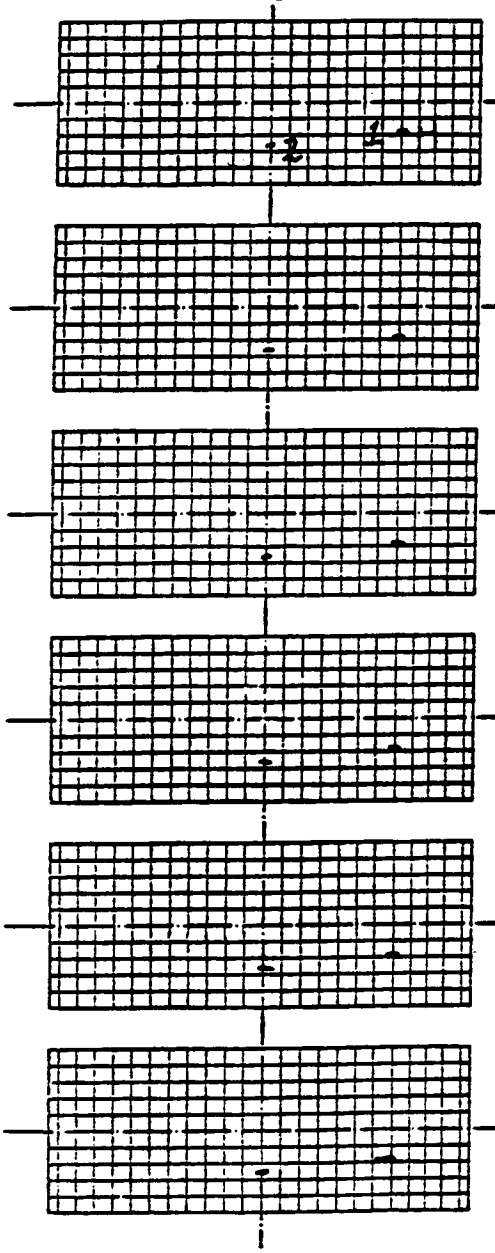

6K Cycles
L1 .033 mm
L2 .027 mm
L3 ____ mm
L4 ____ mm
L5 ____ mm

8K Cycles
L1 .033 mm
L2 * mm
L3 ____ mm
L4 ____ mm
L5 ____ mm

10K Cycles
L1 .033 mm
L2 .027 mm
L3 ____ mm
L4 ____ mm
L5 ____ mm

12K Cycles
L1 * mm
L2 * mm
L3 ____ mm
L4 ____ mm
L5 ____ mm

14K Cycles
L1 .065 mm
L2 .065 mm
L3 ____ mm
L4 ____ mm
L5 ____ mm

16K Cycles
L1 .071 mm
L2 .065 mm
L3 ____ mm
L4 ____ mm
L5 ____ mm

* Crack tip was not clear.

AGARD Short Crack DATA CHART

Record of crack lengths and map

Page 2 of 5 Loading Type R=0.0

Specimen no A-52-03 Peak Stress 145 MPa

0.1mm grid

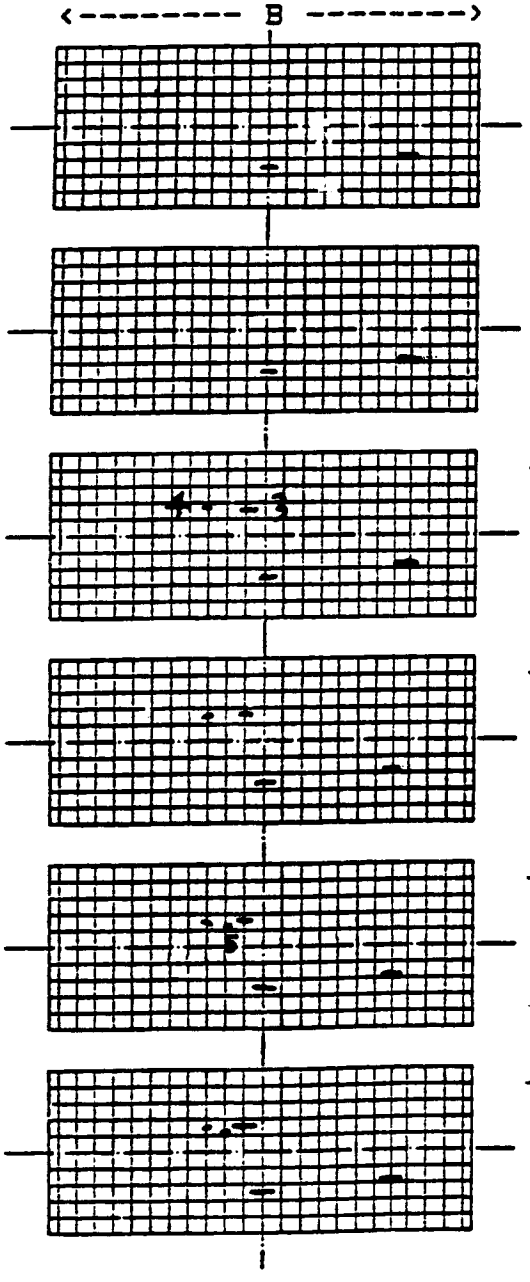

18K Cycles
L1 .093 mm
L2 .071 mm
L3 mm
L4 mm
L5 mm

20K Cycles
L1 .098 mm
L2 .076 mm
L3 mm
L4 mm
L5 mm

22K Cycles
L1 .104 mm
L2 .087 mm
L3 .071 mm
L4 .027 mm
L5 mm

24K Cycles
L1 .104 mm
L2 .098 mm
L3 .076 mm
L4 .027 mm
L5 mm

26K Cycles
L1 .104 mm
L2 .109 mm
L3 .087 mm
L4 .033 mm
L5 .027 mm

28K Cycles
L1 .114 mm
L2 .109 mm
L3 .120 mm
L4 .033 mm
L5 .027 mm

AGARD Short Crack DATA CHART

Record of crack lengths and map

Page 3 of 5 Loading Type R=0.0

Specimen no A-52-03 Peak Stress 145 MPa

0.1mm grid

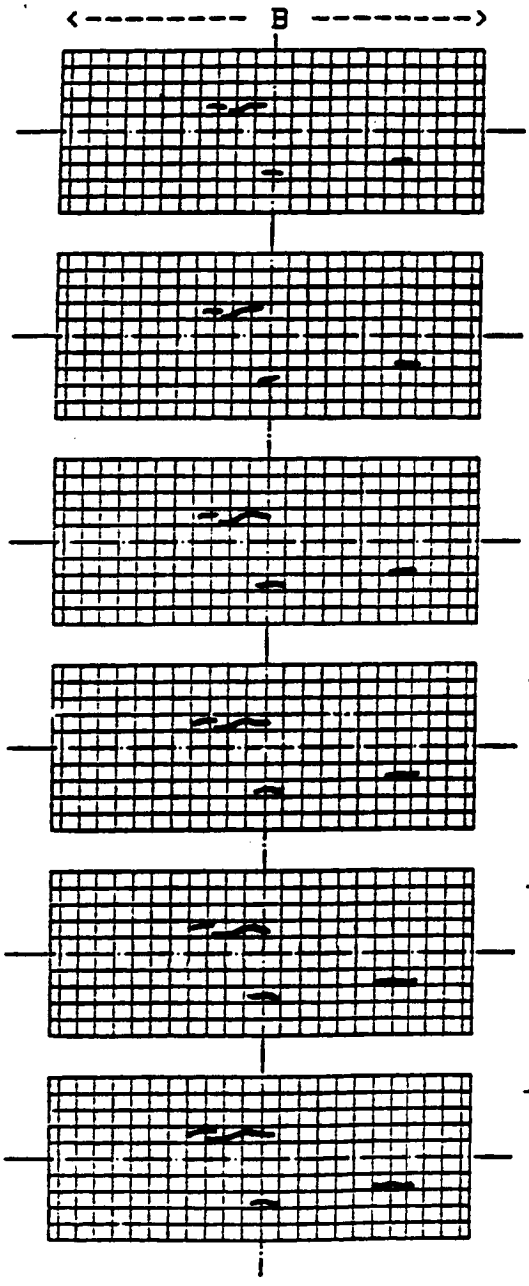

30K Cycles
L1 .114 mm
L2 .109 mm
L3 .196 mm
L4 .092 mm
L5 L3 mm

32K Cycles
L1 .153 mm
L2 .120 mm
L3 .196 mm
L4 .104 mm
L5 mm

34K Cycles
L1 .174 mm
L2 .158 mm
L3 .245 mm
L4 .104 mm
L5 mm

36K Cycles
L1 .185 mm
L2 .142 mm
L3 .256 mm
L4 .104 mm
L5 mm

38K Cycles
L1 .239 mm
L2 .153 mm
L3 .278 mm
L4 .104 mm
L5 mm

40K Cycles
L1 .239 mm
L2 .158 mm
L3 .343 mm
L4 .131 mm
L5 mm

AGARD Short Crack DATA CHART

Record of crack lengths and map

Page 4 of 5 Loading Type R=0.0

Specimen no A-52-03 Peak Stress 145 MPa

0.1mm grid

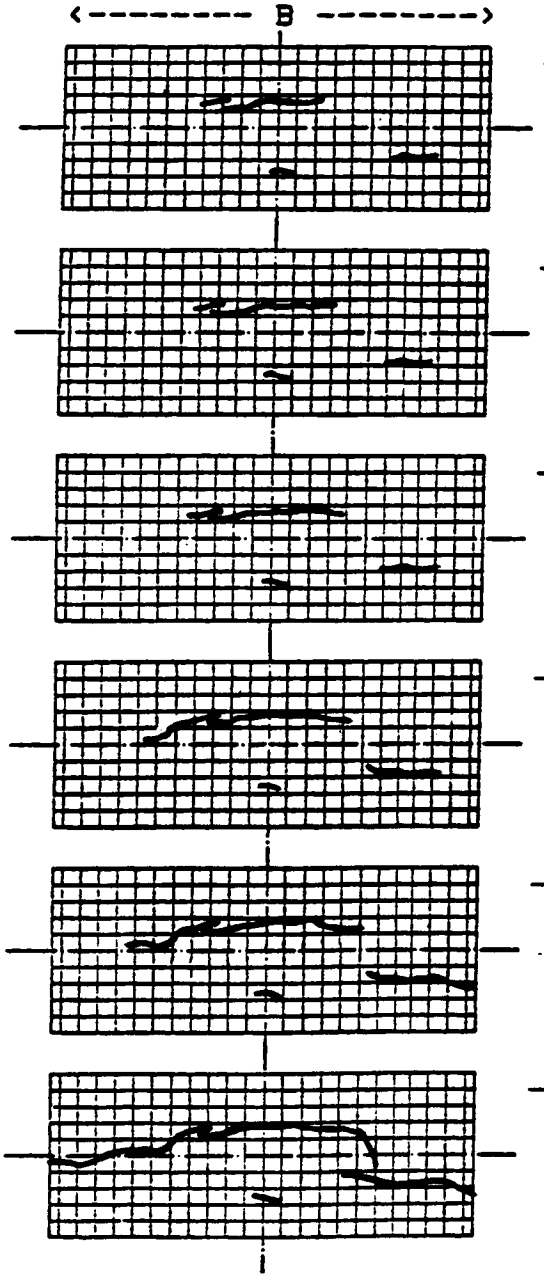

42 K Cycles
L1 .267 mm
L2 .147 mm
L3 .534 mm
L4 ____ mm
L5 ____ mm

44 K Cycles
L1 .265 mm
L2 .147 mm
L3 .665 mm
L4 .164 mm
L5 ____ mm

46 K Cycles
L1 .338 mm
L2 .147 mm
L3 .834 mm
L4 L3 mm
L5 ____ mm

48 K Cycles
L1 .425 mm
L2 .131 mm
L3 1122 mm
L4 ____ mm
L5 ____ mm

50 K Cycles
L1 .665 mm
L2 .131 mm
L3 1.264 mm
L4 ____ mm
L5 ____ mm

52 K Cycles
L1 .735 mm
L2 .136 mm
L3 1.777 mm
L4 ____ mm
L5 ____ mm

AGARD Short Crack DATA CHART

Record of crack lengths and map

Page 5 of 5 Loading Type R=0.0

Specimen no A-SZ-03 Peak Stress 145 MPa

0.1mm grid

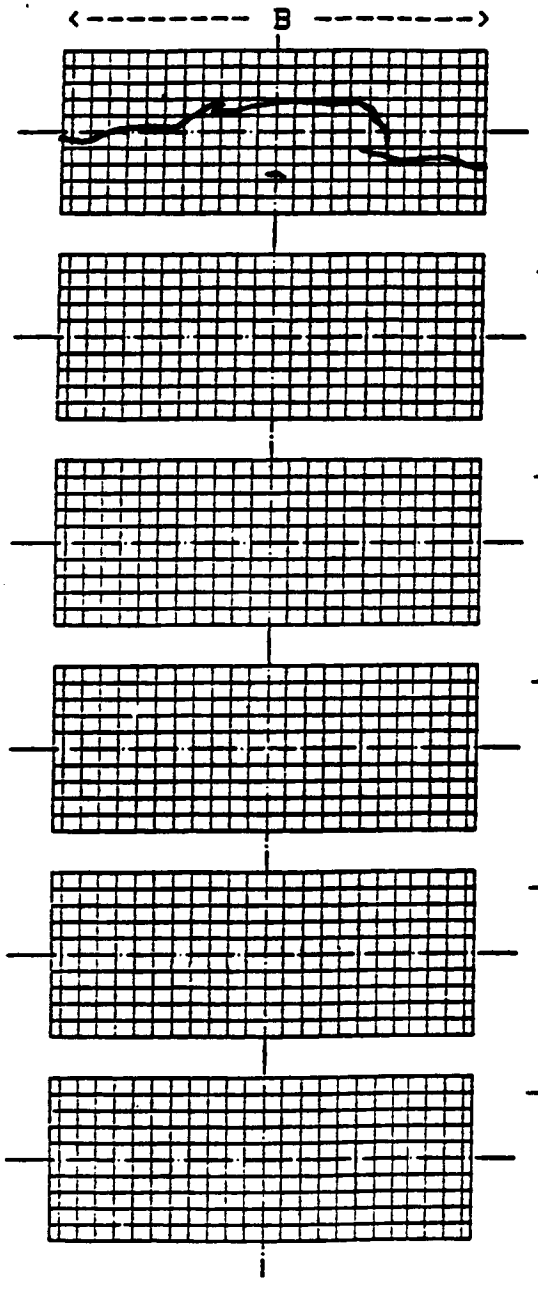

53K Cycles
L1 4 mm
L2 .131 mm
L3 Thru mm
L4 mm
L5 mm

Cycles
L1 mm
L2 mm
L3 mm
L4 mm
L5 mm

Cycles
L1 mm
L2 mm
L3 mm
L4 mm
L5 mm

Cycles
L1 mm
L2 mm
L3 mm
L4 mm
L5 mm

Cycles
L1 mm
L2 mm
L3 mm
L4 mm
L5 mm

Cycles
L1 mm
L2 mm
L3 mm
L4 mm
L5 mm

** DA/DN DATA **

SPECIMEN NO. = A-52-03.L3
NO. OF DATA = 16
R= 0.00
SMAX=145.0 MPa
surface crack

	CYCLE(X1000)	CRK L. 2a(mm)	AVG. a(mm)	DELK(MPa-M)	DADN(mm/CYCLE)
0	22	0.071	0.000	0.00	0.000 X1.E-6
1	24	0.076	0.037	3.44	1.250 X1.E-6
2	26	0.087	0.041	3.61	2.750 X1.E-6
3	28	0.120	0.052	4.04	8.250 X1.E-6
4	30	0.196	0.079	4.92	19.000 X1.E-6
5	34	0.245	0.110	5.73	6.125 X1.E-6
6	36	0.256	0.125	6.07	2.750 X1.E-6
7	38	0.278	0.133	6.24	5.500 X1.E-6
8	40	0.343	0.155	6.68	16.250 X1.E-6
9	42	0.534	0.219	7.81	47.750 X1.E-6
10	44	0.665	0.300	9.00	32.750 X1.E-6
11	46	0.834	0.375	9.96	42.250 X1.E-6
12	48	1.127	0.490	11.24	73.250 X1.E-6
13	50	1.264	0.598	12.30	34.250 X1.E-6
14	52	1.777	0.760	13.72	128.250 X1.E-6
15	53	2.250	1.007	15.71	236.500 X1.E-6

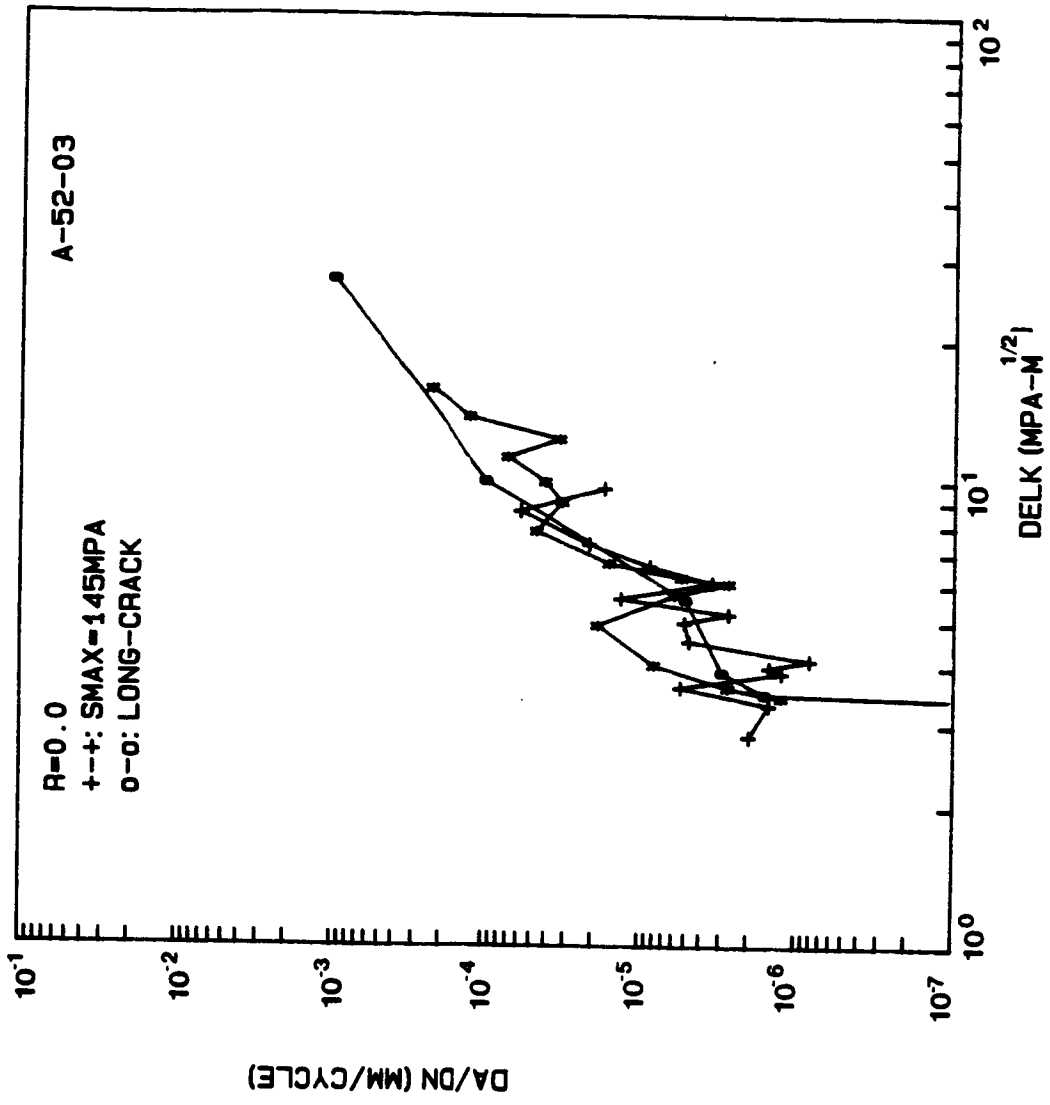
A-52-03
R=0.0
+-+: SMAX=145MPA
o-o: LONG-CRACK
DA/DN (MM/CYCLE)
DELK (MPA-M^1/2)
10^-1
10^-2
10^-3
10^-4
10^-5
10^-6
10^-7
10^0
10^1
10^2

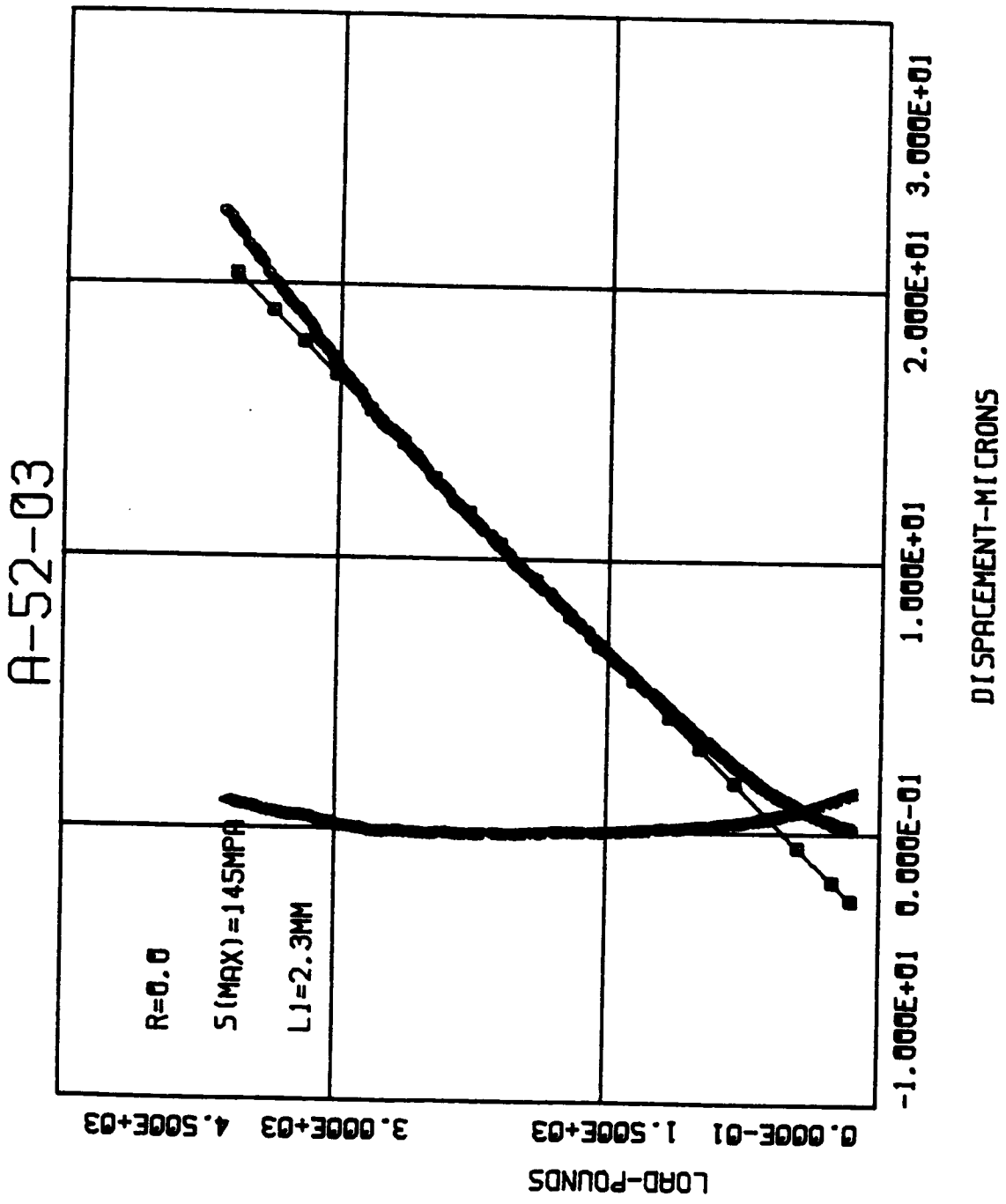
A-52-03
R=0.0
S(MAX)=145MPA
L1=2.3MM
LOAD-POUNDS
0.000E-01
1.500E+03
3.000E+03
4.500E+03
-1.000E+01
0.000E-01
1.000E+01
2.000E+01
3.000E+01
DISPACEMENT-MICRONS

ORIGINAL PAGE IS
OF POOR QUALITY

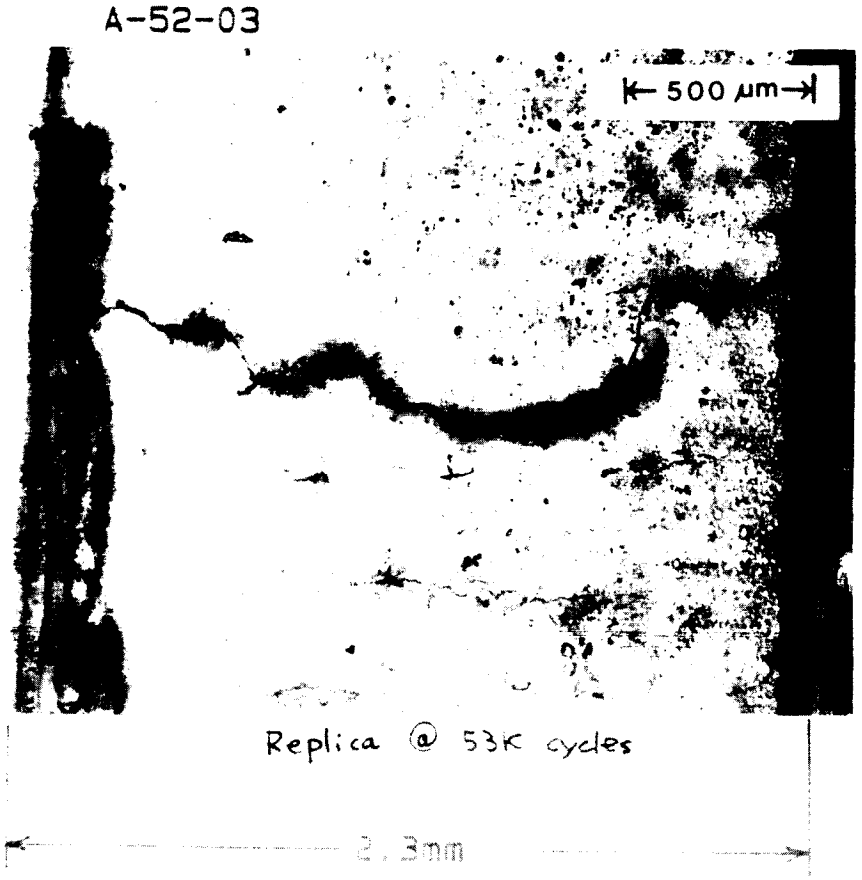

A-52-03

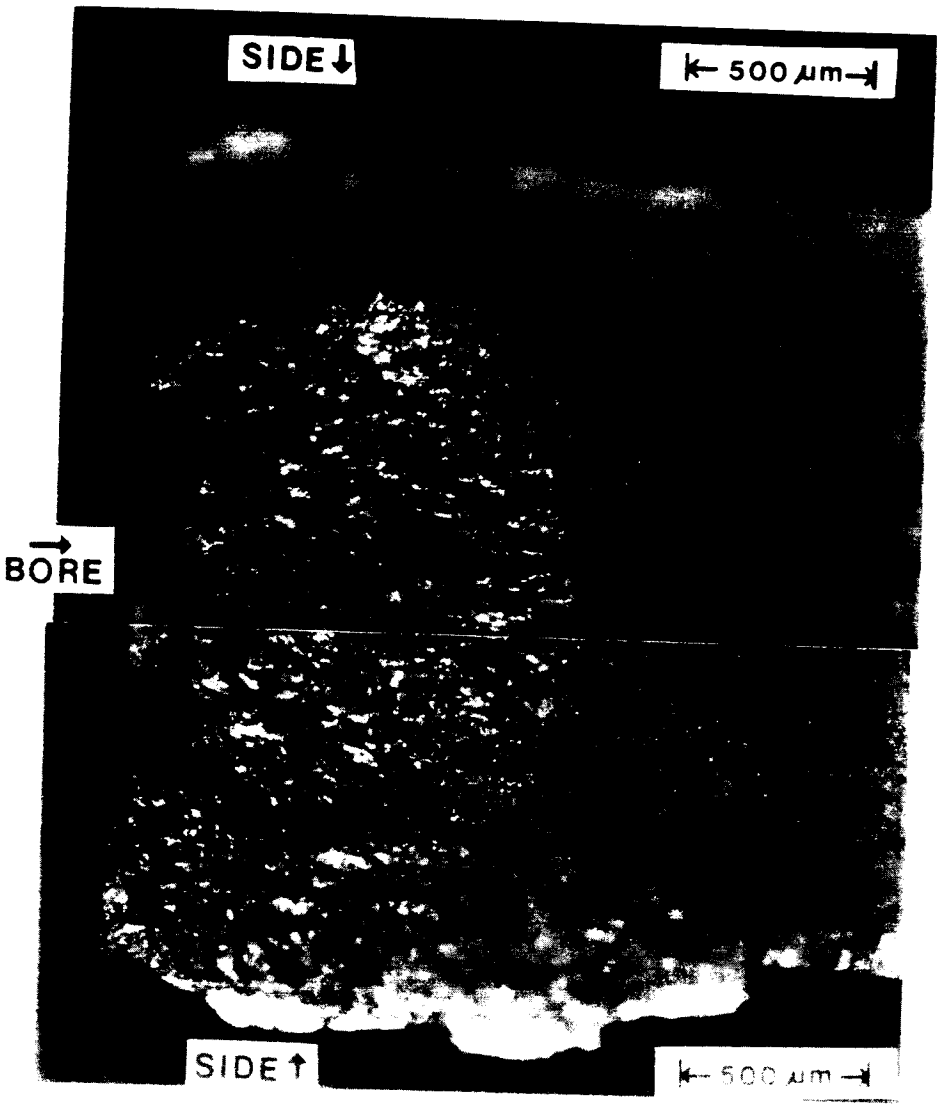

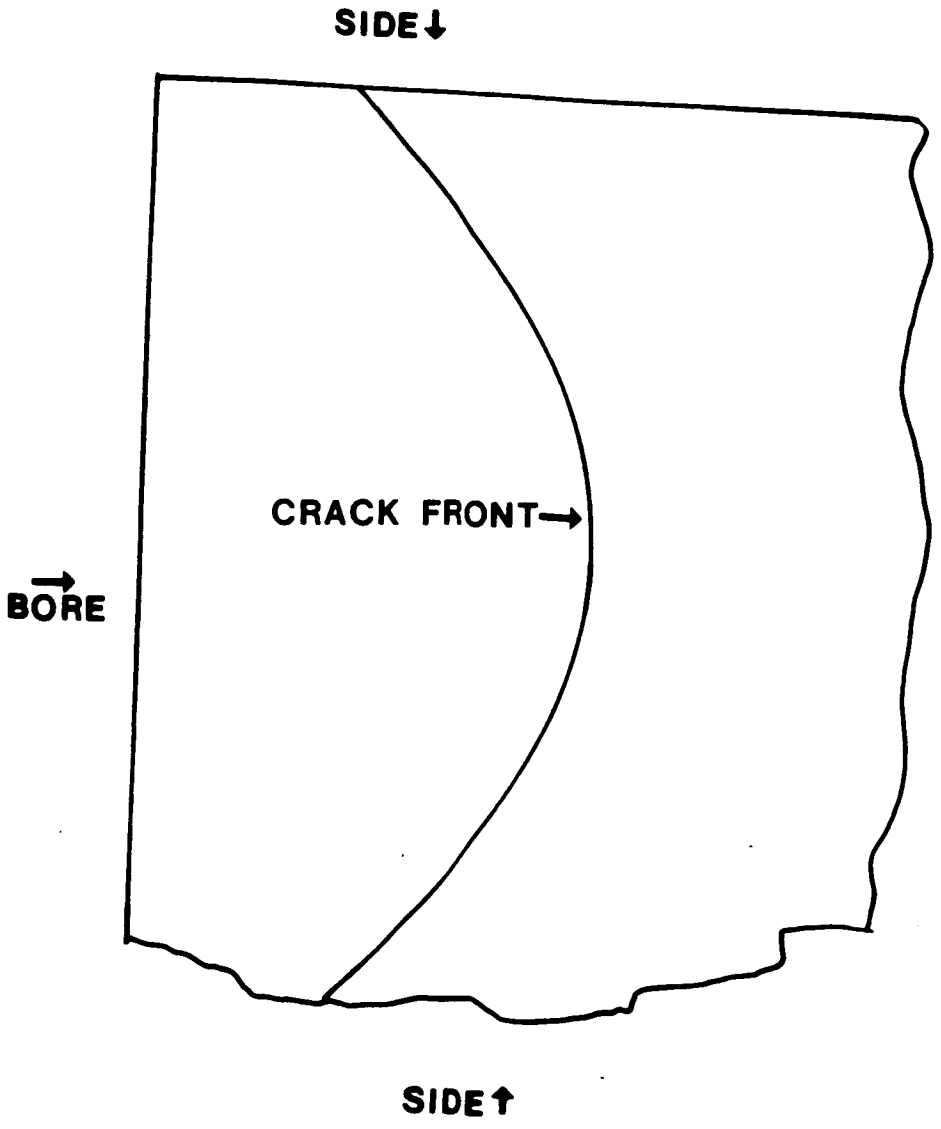

Tracing of Crack Front for A-52-03

TEST DATA

SPECIMEN NUMBER: A-51-16

DATE: 6/10/85

PARTICIPANT'S NAME: Joo-Jin Lee

John Cieslowski

TEST TEMPERATURE: 26° C

RELATIVE HUMIDITY: 54 %

WAVEFORM TYPE: Sinusoidal wave, 20 Hz

LOADING SEQUENCE TYPE: Constant amplitude

R-RATIO = 0.0

S max = 145 MPa

S min = 0. MPa

FINAL LENGTH OF CRACK: 0.245 mm (L2)

COMMENTS:

Photo of crack surface from broken specimen was not able to be taken (out of focus)

AGARD Short Crack DATA CHART

Record of crack lengths and map

Page 1 of 2 — Loading Type Const. Amplitude R = 0

Specimen no A-51-16 — Peak Stress 145 MPa

0.1mm grid

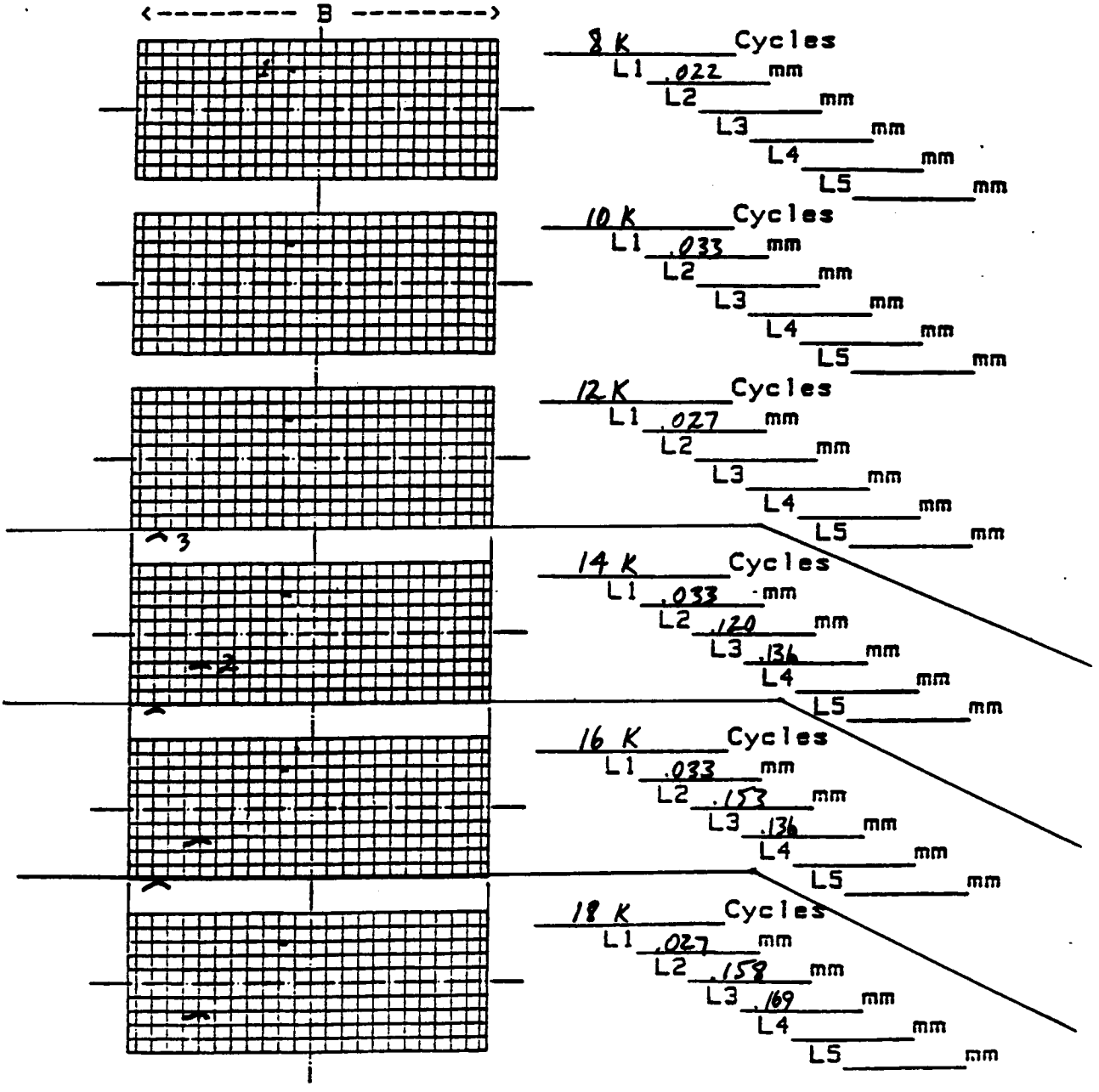

AGARD Short Crack DATA CHART

Record of crack lengths and map

Page 2 of 2 Loading Type Const. Amplitude R = 0

Specimen no A-51-16 Peak Stress 145 MPa

0.1mm grid

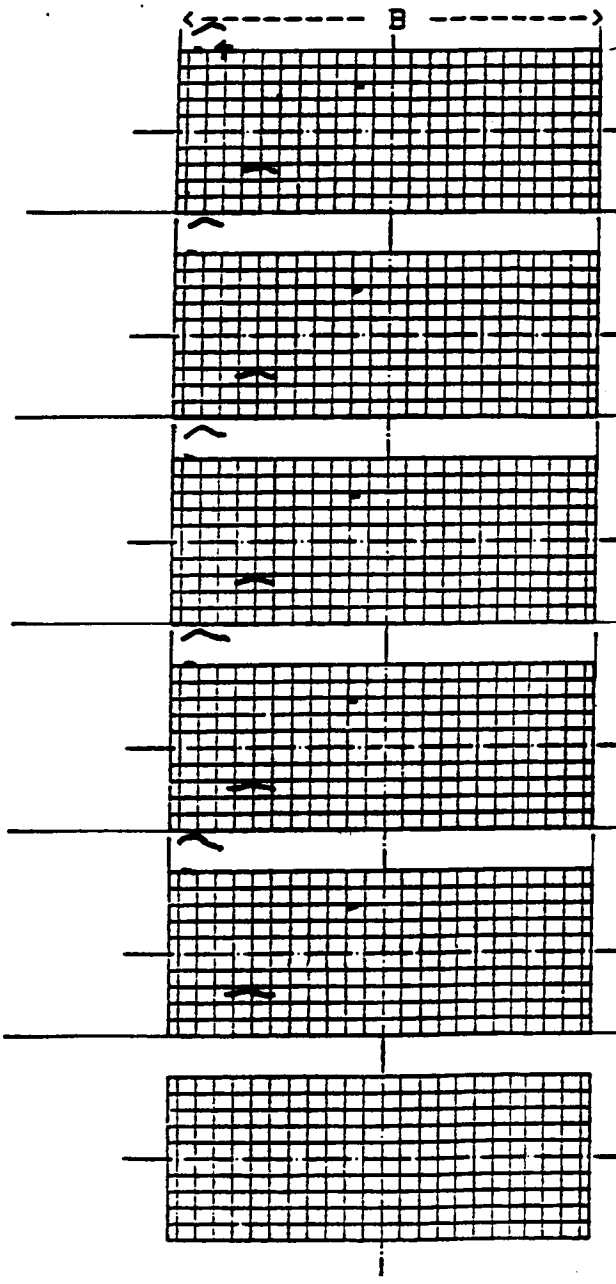

20 K Cycles
L1 .038 mm
L2 .190 mm
L3 .174 mm
L4 .027 mm
L5 mm

22 K Cycles
L1 .044 mm
L2 .213 mm
L3 .185 mm
L4 .033 mm
L5 mm

24 K Cycles
L1 .038 mm
L2 .201 mm
L3 .223 mm
L4 .044 mm
L5 mm

26 K Cycles
L1 .038 mm
L2 .240 mm
L3 .256 mm
L4 .060 mm
L5 mm

28 K Cycles
L1 .038 mm
L2 .245 mm
L3 .234 mm
L4 .082 mm
L5 mm

Cycles
L1 mm
L2 mm
L3 mm
L4 mm
L5 mm

** DA/DN DATA **

SPECIMEN' NO. = A-51-16.L2
NO. OF DATA = 7
R= 0.00
SMAX=145.0 MPa
surface crack

	CYCLE(X1000)	CRK L. 2a(mm)	AVG. a(mm)	DELK(MPa-M)	DADN(mm/CYCLE)
0	14	0.120	0.000	0.00	0.000 X1.E-6
1	16	0.153	0.068	4.60	8.250 X1.E-6
2	18	0.158	0.078	4.88	1.250 X1.E-6
3	20	0.180	0.084	5.07	5.500 X1.E-6
4	22	0.213	0.098	5.43	8.250 X1.E-6
5	26	0.240	0.113	5.80	3.375 X1.E-6
6	28	0.245	0.121	5.98	1.250 X1.E-6

** DA/DN DATA **

SPECIMEN' NO. = A-51-16.L3
NO. OF DATA = 6
R= 0.00
SMAX=145.0 MPa
near edge

	CYCLE(X1000)	CRK L. 2a(mm)	AVG. a(mm)	DELK(MPa-M)	DADN(mm/CYCLE)
0	14	0.136	0.000	0.00	0.000 X1.E-6
1	18	0.169	0.153	6.57	8.250 X1.E-6
2	20	0.174	0.171	6.94	2.500 X1.E-6
3	22	0.185	0.179	7.08	5.500 X1.E-6
4	24	0.223	0.204	7.50	19.000 X1.E-6
5	26	0.256	0.239	8.06	16.500 X1.E-6

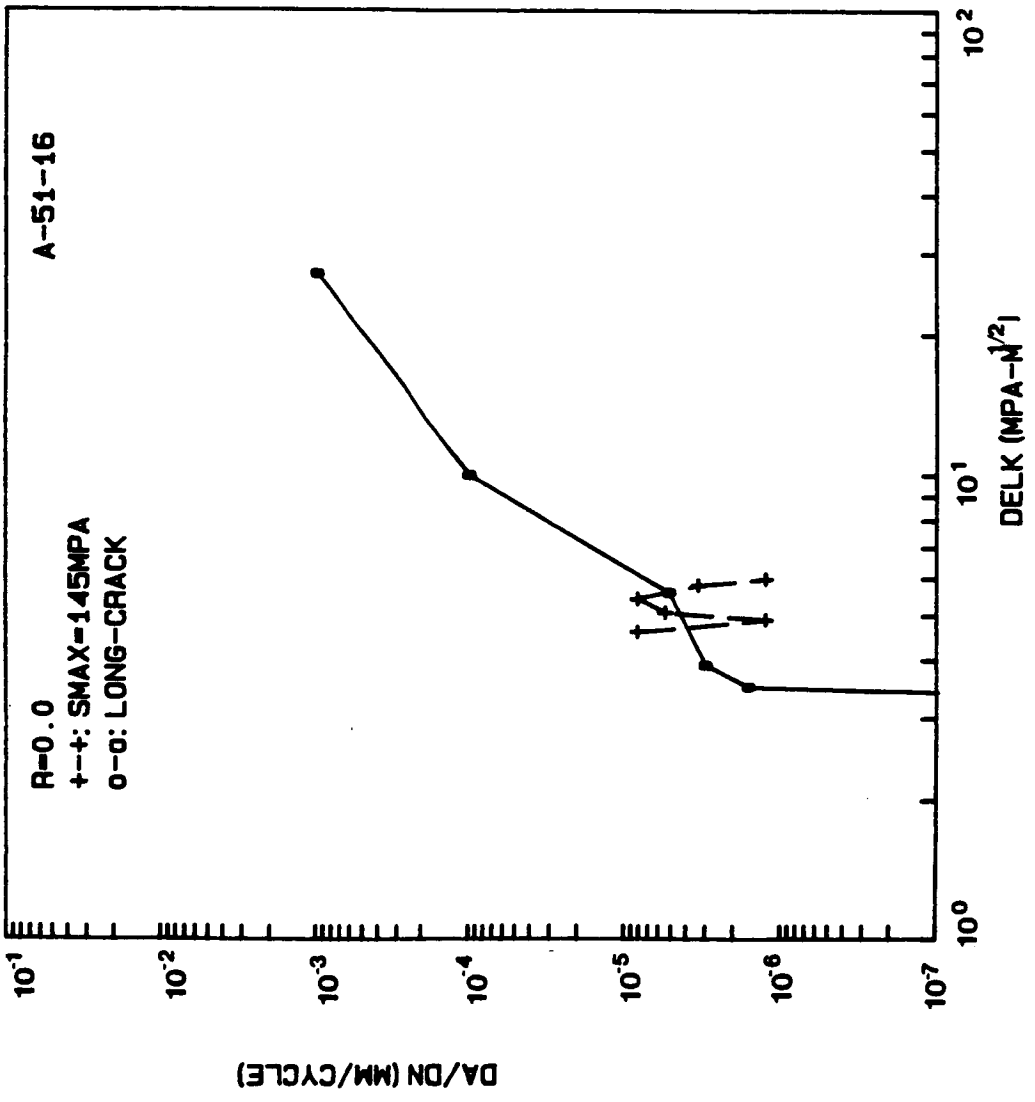
A-51-16
R=0.0
+--+: SMAX=145MPA
o-o: LONG-CRACK
DA/DN (MM/CYCLE)
DELK (MPA-M^1/2)
10^-1
10^-2
10^-3
10^-4
10^-5
10^-6
10^-7
10^0
10^1
10^2

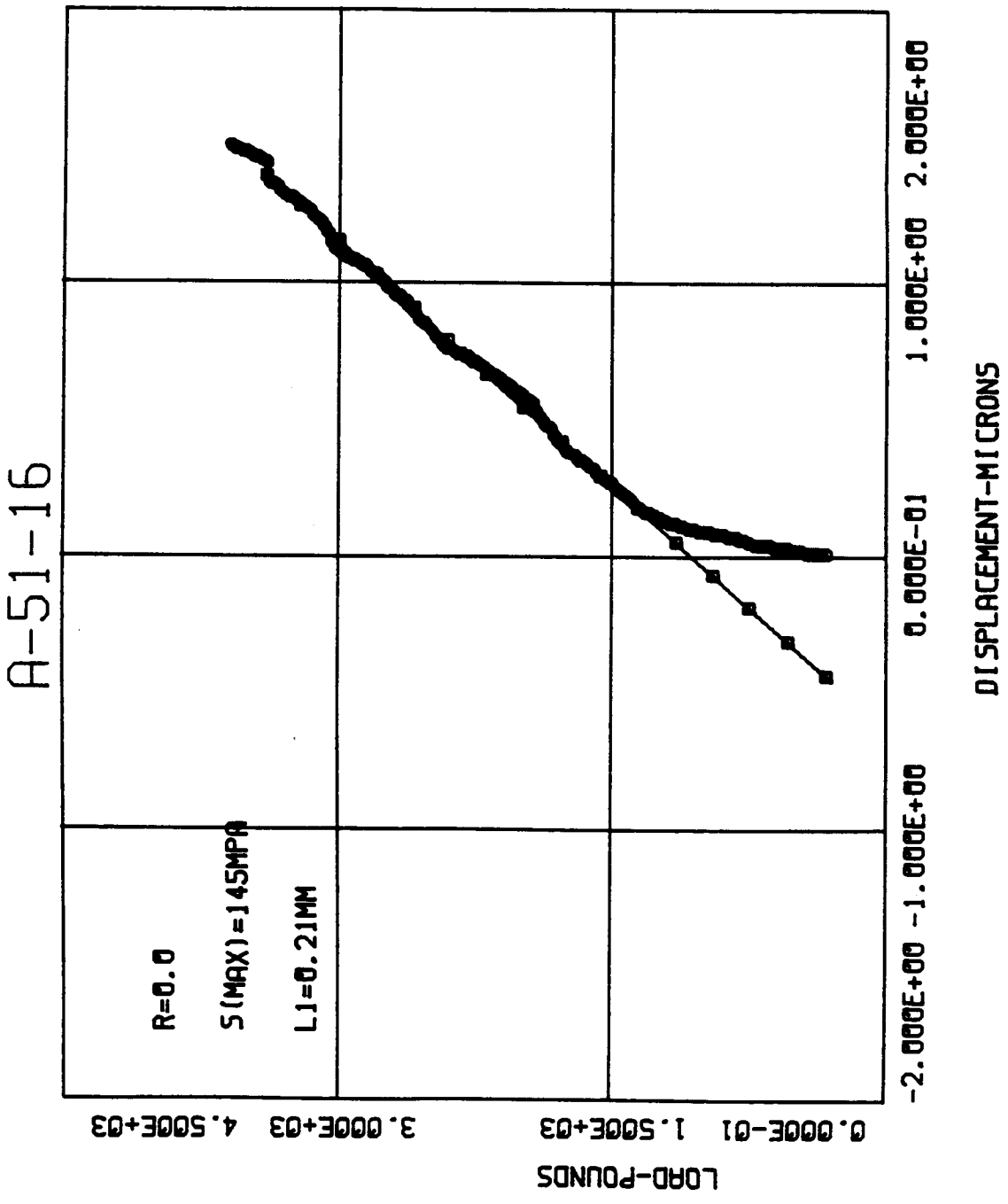
A-51-16
R=0.0
S(MAX)=145MPA
L1=0.21MM
LOAD-POUNDS
0.000E-01
1.500E+03
3.000E+03
4.500E+03
-2.000E+00
-1.000E+00
0.000E-01
1.000E+00
2.000E+00
DISPLACEMENT-MICRONS

A-51-16

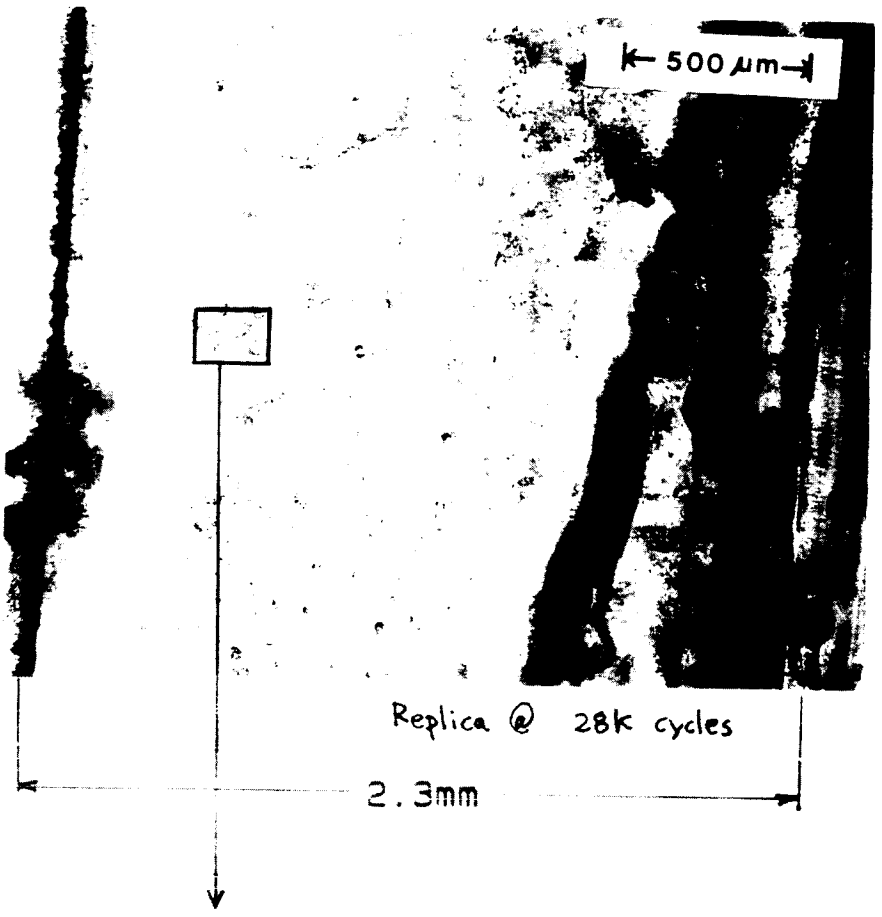

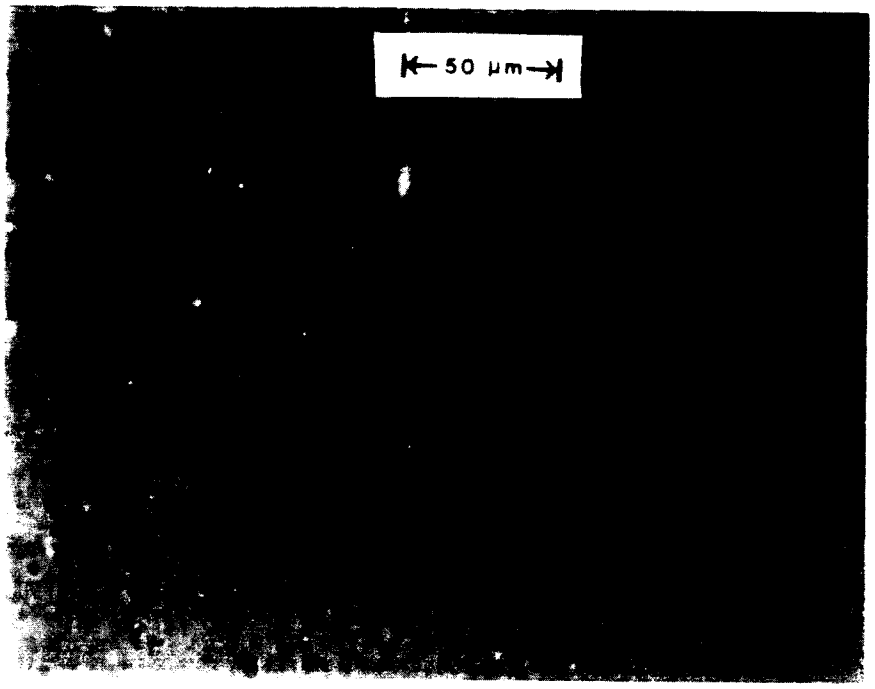

TEST DATA

SPECIMEN NUMBER: A - 82 -16

DATE: 6/14/85

PARTICIPANT'S NAME: Joo-Jin Lee

John Cieslowski

TEST TEMPERATURE: 28°C

RELATIVE HUMIDITY: 40 %

WAVEFORM TYPE: Sinusoidal wave, 20 Hz

LOADING SEQUENCE TYPE: Constant amplitude

R-RATIO = 0.0

S max = 120 MPa

S min = 0 MPa

FINAL LENGTH OF CRACK: 2.3 mm

COMMENTS:

AGARD Short Crack DATA CHART

Record of crack lengths and map

Page 1 of 3 — Loading Type Constant Amplitude R=0.0

Specimen no A-52-16 — Peak Stress 120 MPa

0.1mm grid

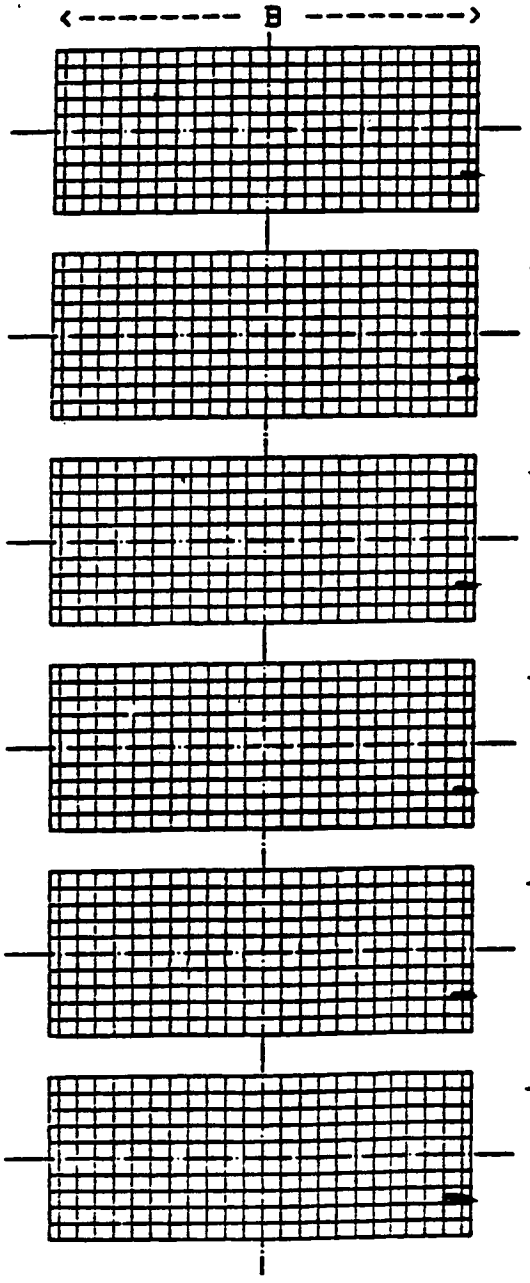

60K Cycles
L1 .093 mm
L2 ____ mm
L3 ____ mm
L4 ____ mm
L5 ____ mm

65K Cycles
L1 .098 mm
L2 ____ mm
L3 ____ mm
L4 ____ mm
L5 ____ mm

70K Cycles
L1 .098 mm
L2 ____ mm
L3 ____ mm
L4 ____ mm
L5 ____ mm

75K Cycles
L1 .109 mm
L2 ____ mm
L3 ____ mm
L4 ____ mm
L5 ____ mm

80K Cycles
L1 * mm
L2 ____ mm
L3 ____ mm
L4 ____ mm
L5 ____ mm

85K Cycles
L1 .153 mm
L2 ____ mm
L3 ____ mm
L4 ____ mm
L5 ____ mm

* crack tip is not clear

AGARD Short Crack DATA CHART

Record of crack lengths and map

Page 2 of 3 Loading Type R = 0

Specimen no A-82-16 Peak Stress 120 MPa

0.1mm grid

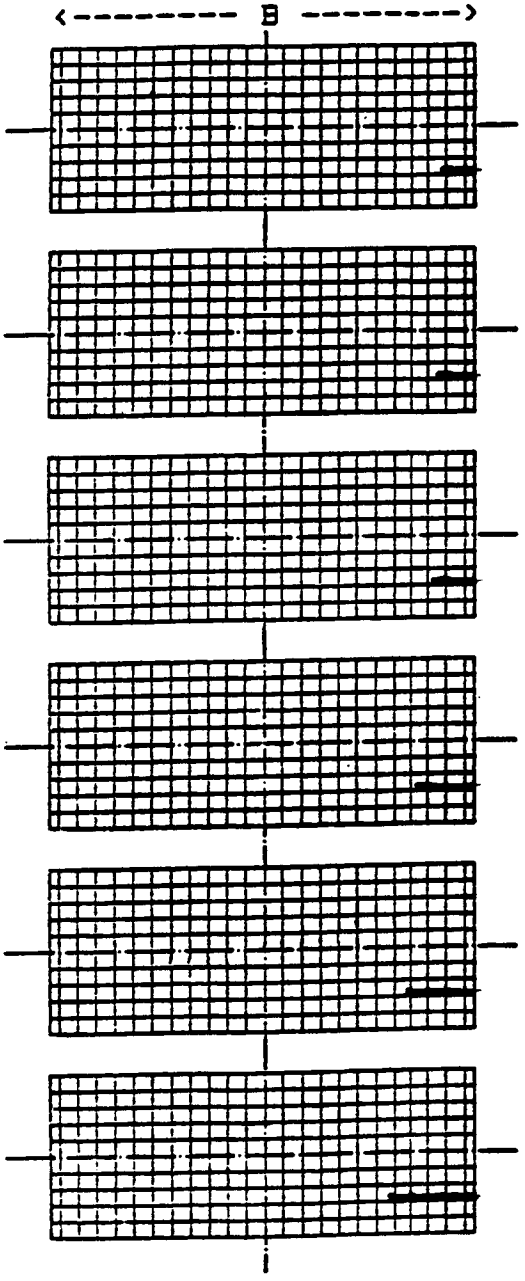

90K Cycles
L1 .174 mm
L2 ____ mm
L3 ____ mm
L4 ____ mm
L5 ____ mm

95K Cycles
L1 .196 mm
L2 ____ mm
L3 ____ mm
L4 ____ mm
L5 ____ mm

100K Cycles
L1 .223 mm
L2 ____ mm
L3 ____ mm
L4 ____ mm
L5 ____ mm

105K Cycles
L1 .273 mm
L2 ____ mm
L3 ____ mm
L4 ____ mm
L5 ____ mm

110K Cycles
L1 .360 mm
L2 ____ mm
L3 ____ mm
L4 ____ mm
L5 ____ mm

115K Cycles
L1 .469 mm
L2 ____ mm
L3 ____ mm
L4 ____ mm
L5 ____ mm

AGARD Short Crack DATA CHART

Record of crack lengths and map

Page 3 of 3 Loading Type R=0

Specimen no 4-82-16 Peak Stress 120 MPa

0.1mm grid

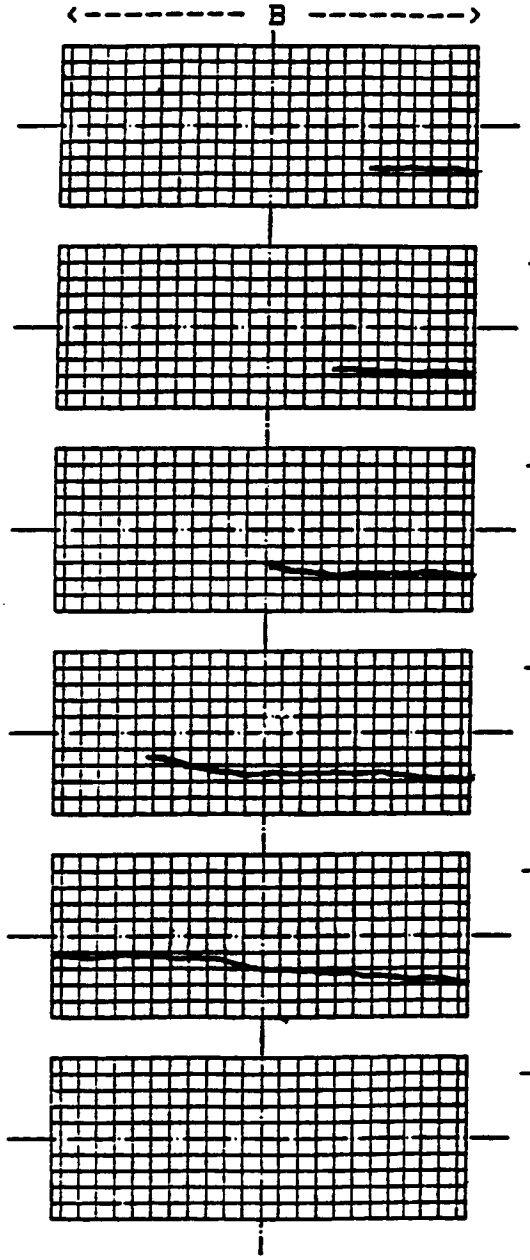

120 K Cycles
L1 .605 mm
L2 _____ mm
L3 _____ mm
L4 _____ mm
L5 _____ mm

125 K Cycles
L1 .796 mm
L2 _____ mm
L3 _____ mm
L4 _____ mm
L5 _____ mm

130 K Cycles
L1 1.123 mm
L2 _____ mm
L3 _____ mm
L4 _____ mm
L5 _____ mm

135 K Cycles
L1 1.837 mm
L2 _____ mm
L3 _____ mm
L4 _____ mm
L5 _____ mm

138.4 K Cycles
L1 THRU mm
L2 _____ mm
L3 _____ mm
L4 _____ mm
L5 _____ mm

_____ Cycles
L1 _____ mm
L2 _____ mm
L3 _____ mm
L4 _____ mm
L5 _____ mm

** DA/DN DATA **

SPECIMEN' NO. = A-82-16.L1
NO. OF DATA = 15
R= 0.00
SMAX=120.0 MPa
Corner crack

	CYCLE(X1000)	CRK L. 2a(mm)	AVG. a(mm)	DELK(MPa-M)	DADN(mm/CYCLE)
0	60	0.093	0.000	0.00	0.000 X1.E-6
1	65	0.098	0.095	4.38	1.000 X1.E-6
2	75	0.109	0.104	4.55	1.100 X1.E-6
3	85	0.153	0.131	5.08	4.400 X1.E-6
4	90	0.174	0.163	5.62	4.200 X1.E-6
5	95	0.196	0.185	5.94	4.400 X1.E-6
6	100	0.223	0.209	6.28	5.400 X1.E-6
7	105	0.273	0.248	6.77	10.000 X1.E-6
8	110	0.360	0.316	7.55	17.400 X1.E-6
9	115	0.469	0.414	8.51	21.800 X1.E-6
10	120	0.605	0.537	9.53	27.200 X1.E-6
11	125	0.796	0.700	10.72	38.200 X1.E-6
12	130	1.123	0.959	12.30	65.400 X1.E-6
13	135	1.837	1.480	14.87	142.800 X1.E-6
14	138	2.250	2.043	17.32	137.667 X1.E-6

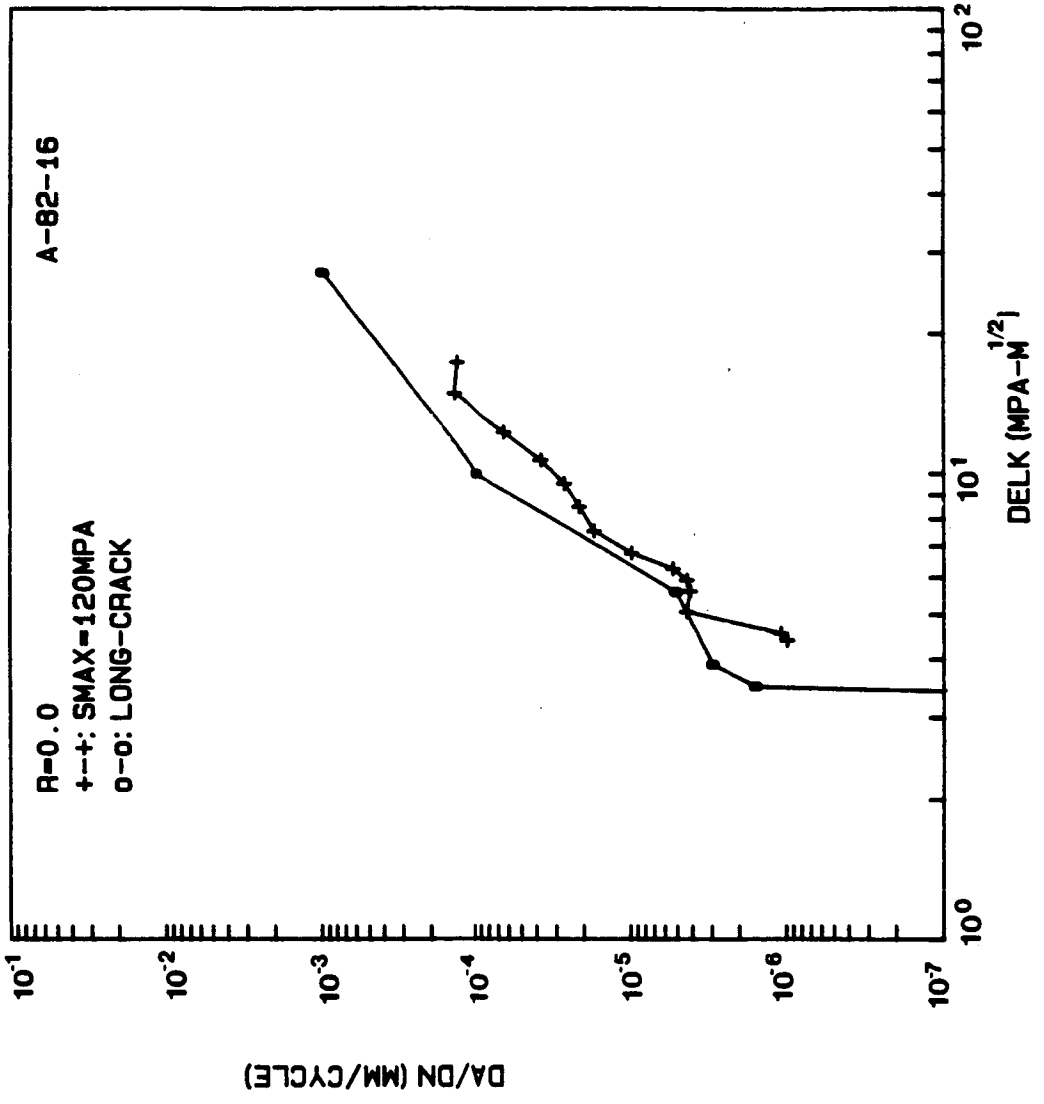
A-82-16
R=0.0
+--+: SMAX=120MPA
o-o: LONG-CRACK
DA/DN (MM/CYCLE)
DELK (MPA-M^1/2)
10^-1
10^-2
10^-3
10^-4
10^-5
10^-6
10^-7
10^0
10^1
10^2

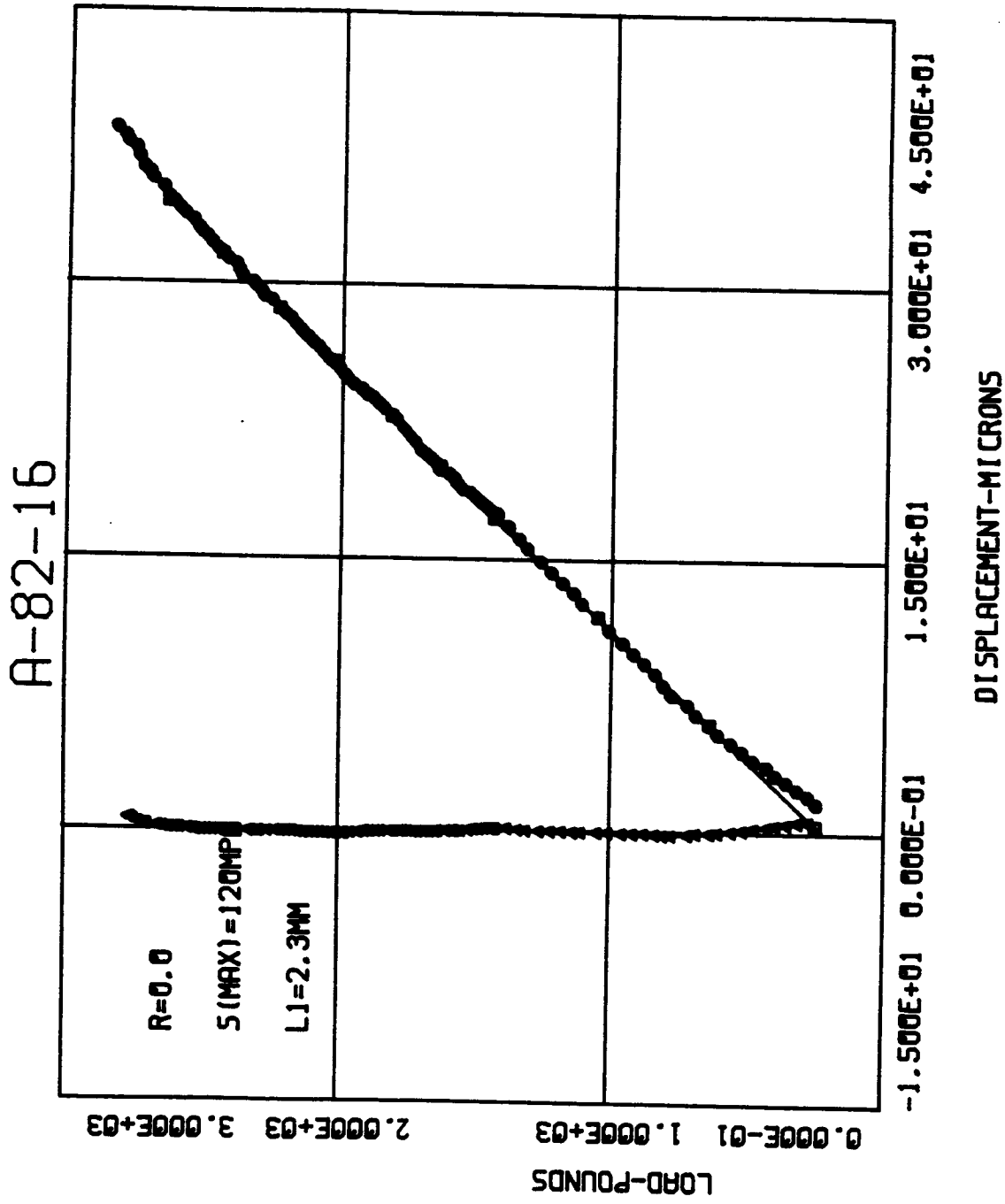
A-82-16
R=0.0
S(MAX)=120MP
L1=2.3MM
LOAD-POUNDS
0.000E-01
1.000E+03
2.000E+03
3.000E+03
-1.500E+01
0.000E-01
1.500E+01
3.000E+01
4.500E+01
DISPLACEMENT-MICRONS

A-82-16

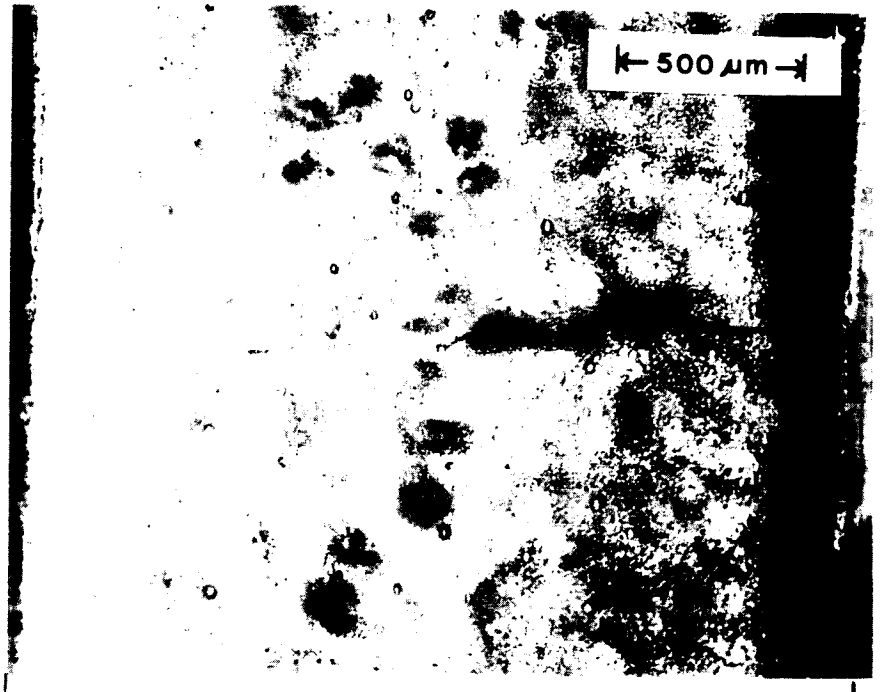

[illegible] 38.4K cycles

A-82-16

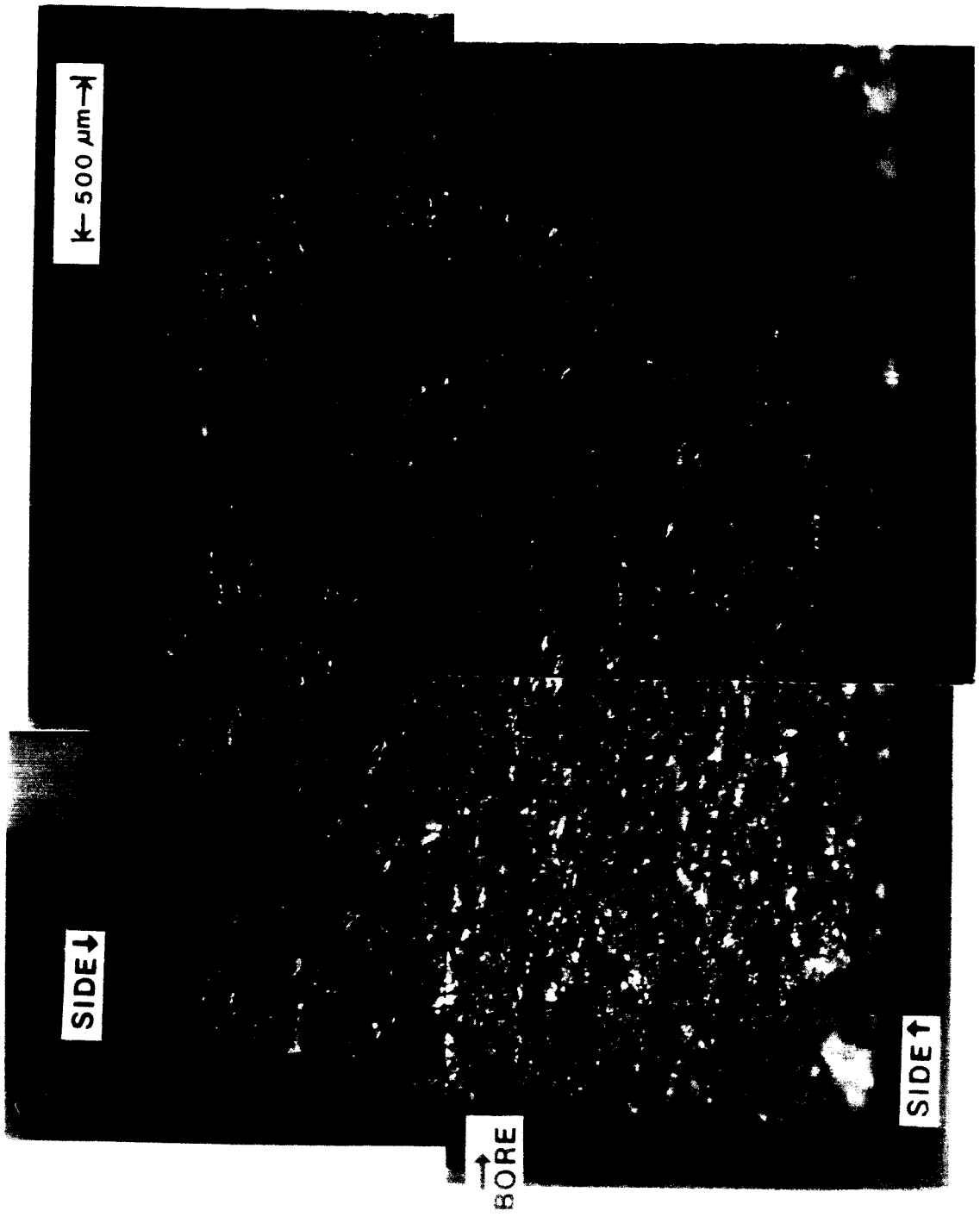

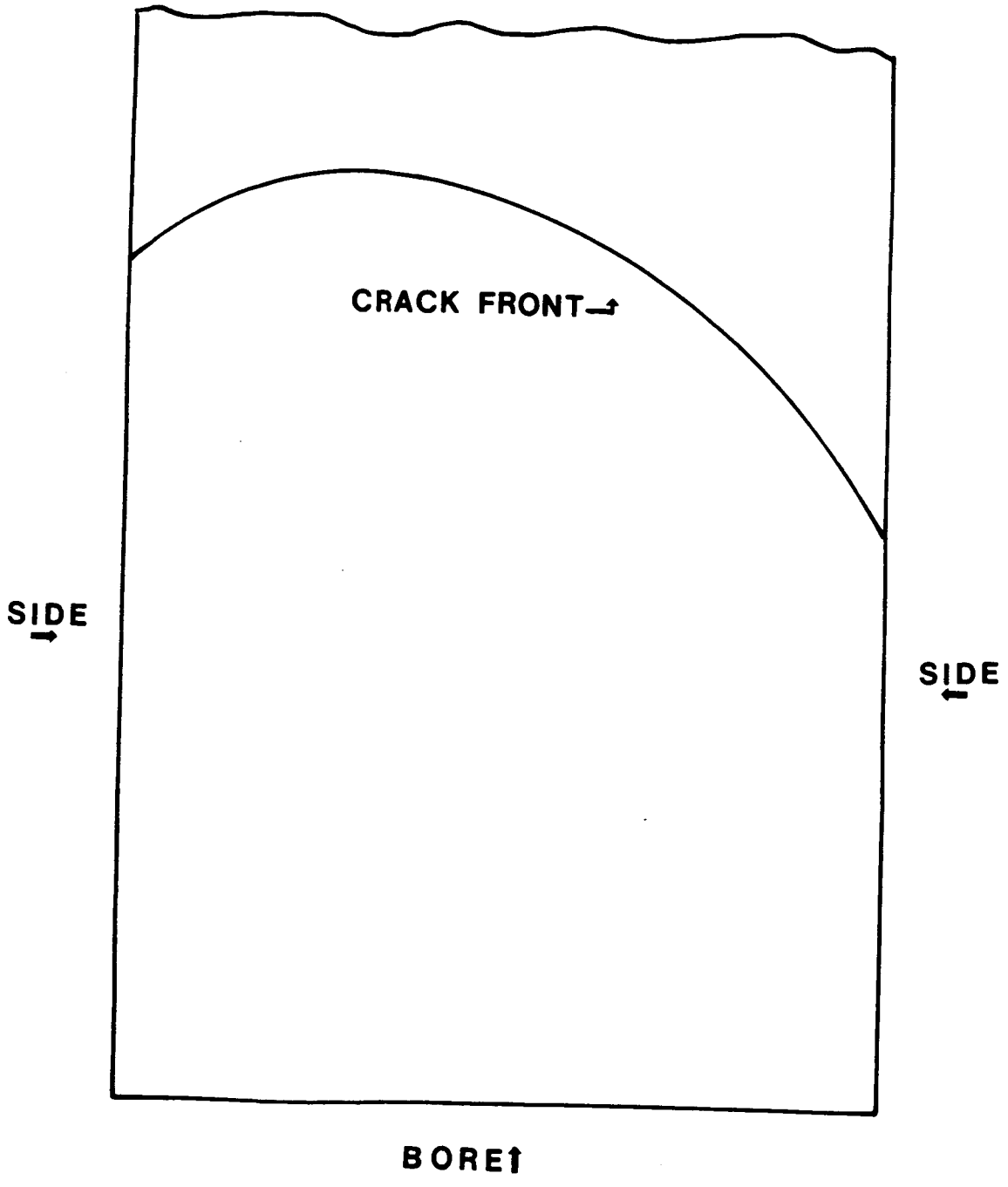

Tracing of Crack Front for A-82-16

TEST DATA

SPECIMEN NUMBER: A-59-30

DATE: 6/11/85

PARTICIPANT'S NAME: Joo-Jin Lee

John Cieslowski

TEST TEMPERATURE: -6°C

RELATIVE HUMIDITY: 60 %

WAVEFORM TYPE: Sinusoidal wave, 20 Hz

LOADING SEQUENCE TYPE: Constant amplitude

R-RATIO = 0.0

S max = 120 MPa

S min = 0 MPa

FINAL LENGTH OF CRACK: No crack

COMMENTS:

No crack was found at 660k cycles.

(Predicted life was 130k).

TEST DATA

SPECIMEN NUMBER: A-57-14

DATE: 6/20/85

PARTICIPANT'S NAME: Joo-Jin Lee

John Cieslowski

TEST TEMPERATURE: 27° C

RELATIVE HUMIDITY: 35%

WAVEFORM TYPE: Sinusoidal wave, 20 Hz

LOADING SEQUENCE TYPE: Constant amplitude

R-RATIO = 0.0

S max = 110 MPa

S min = 0 MPa

FINAL LENGTH OF CRACK: 2.2mm (Thru thickness)

COMMENTS:

L2 and L3 was found at 0.5mm down from the center line.

AGARD Short Crack DATA CHART

Record of crack lengths and map

Page 1 of -1 Loading Type Const. Amplitude R=0

Specimen no A-57-14 Peak Stress 110 MPa

0.1mm grid

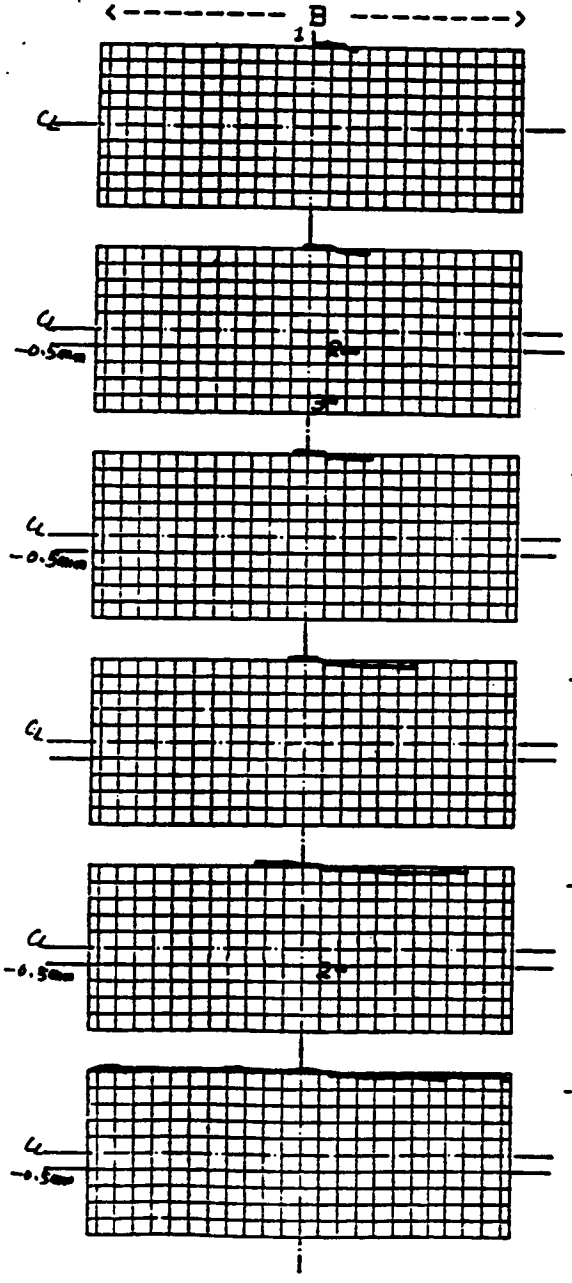

80k Cycles
L1 .225 mm
L2 ____ mm
L3 ____ mm
L4 ____ mm
L5 ____ mm

90k Cycles
L1 .355 mm
L2 .060 mm
L3 0.025 mm
L4 ____ mm
L5 ____ mm

100k Cycles
L1 .430 mm
L2 * mm
L3 * mm
L4 ____ mm
L5 ____ mm

110k Cycles
L1 .700 mm
L2 * mm
L3 * mm
L4 ____ mm
L5 ____ mm

120k Cycles
L1 1.17 mm
L2 .065 mm
L3 ____ mm
L4 ____ mm
L5 ____ mm

130k Cycles
L1 2.20 mm
L2 ____ mm
L3 ____ mm
L4 ____ mm
L5 ____ mm

* Crack was not found

** DA/DN DATA **

SPECIMEN' NO. = A-57-14.L1
NO. OF DATA = 6
R= 0.00
SMAX=110.0 MPa
Surface crack

	CYCLE(X1000)	CRK L. 2a(mm)	AVG. a(mm)	DELK(MPa-M)	DADN(mm/CYCLE)
0	80	0.225	0.000	0.00	0.000 X1.E-6
1	90	0.355	0.145	4.92	6.500 X1.E-6
2	100	0.430	0.196	5.64	3.750 X1.E-6
3	110	0.700	0.282	6.65	13.500 X1.E-6
4	120	1.170	0.468	8.35	23.500 X1.E-6
5	130	2.190	0.840	10.91	51.000 X1.E-6

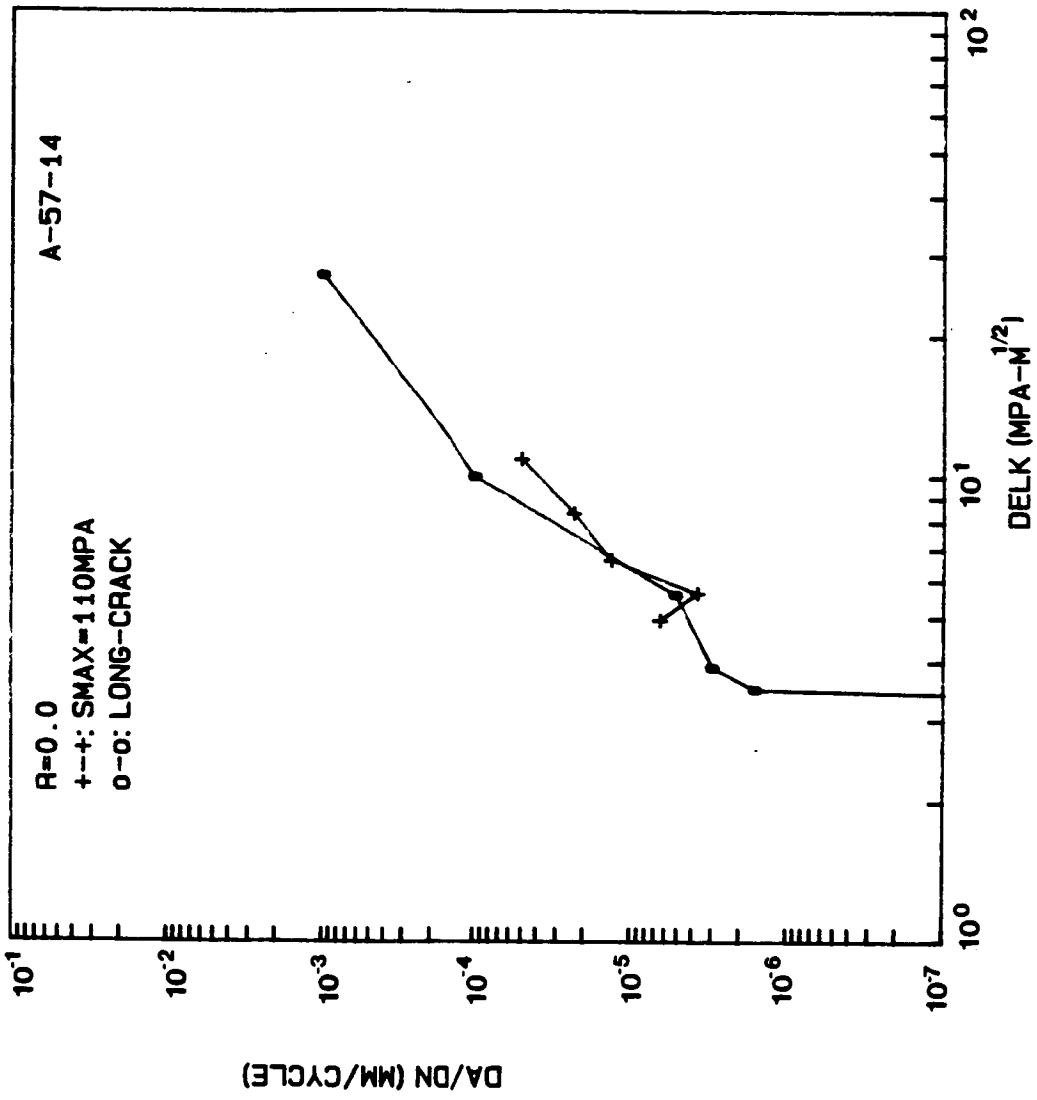
A-57-14
R=0.0
+--+: SMAX=110MPA
o-o: LONG-CRACK
DA/DN (MM/CYCLE)
DELK (MPA-M^1/2)
10^-1
10^-2
10^-3
10^-4
10^-5
10^-6
10^-7
10^0
10^1
10^2

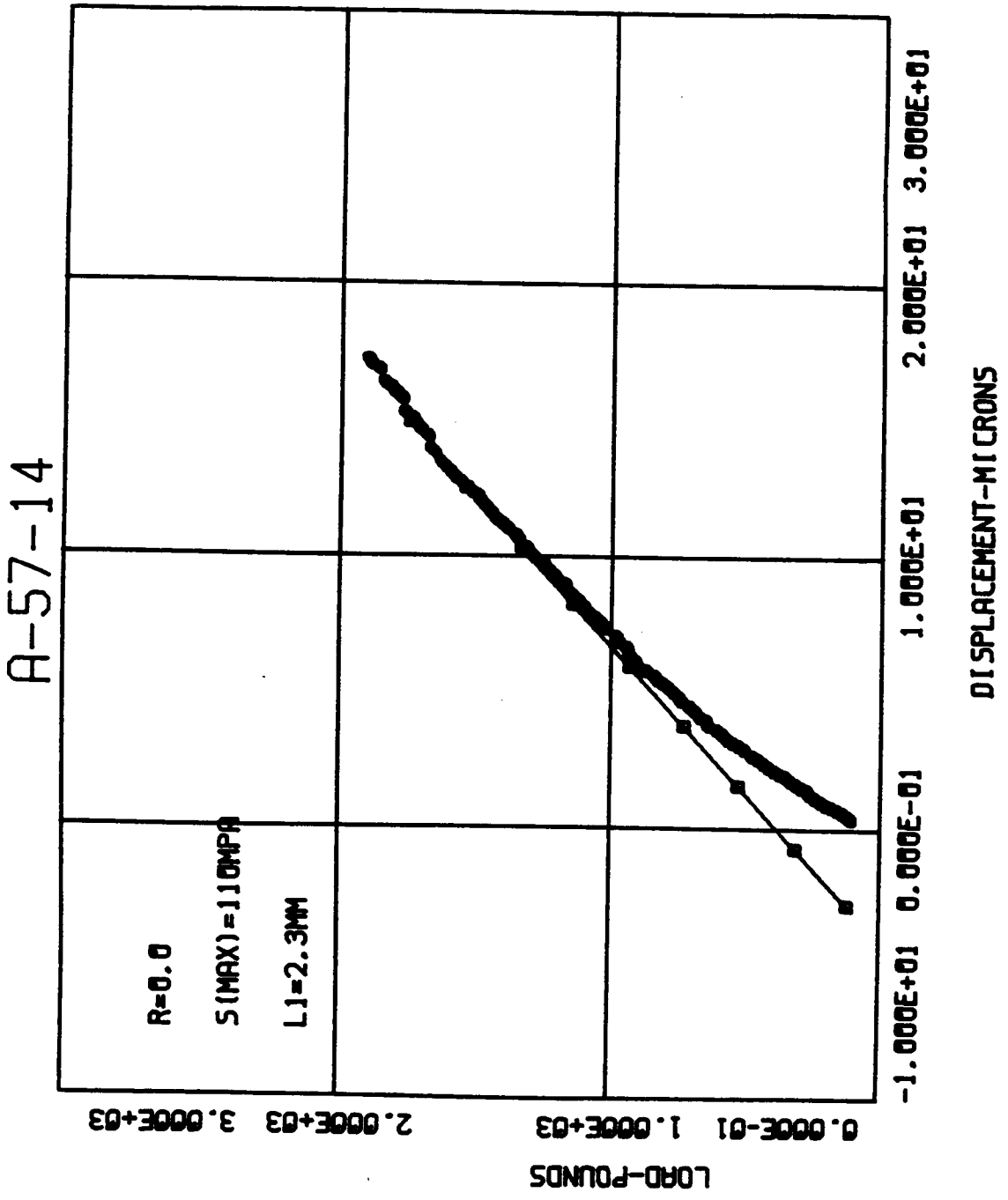
A-57-14
R=0.0
S(MAX)=110MPA
L1=2.3MM
LOAD-POUNDS
0.000E-01
1.000E+03
2.000E+03
3.000E+03
-1.000E+01
0.000E-01
1.000E+01
2.000E+01
3.000E+01
DISPLACEMENT-MICRONS

A-57-14

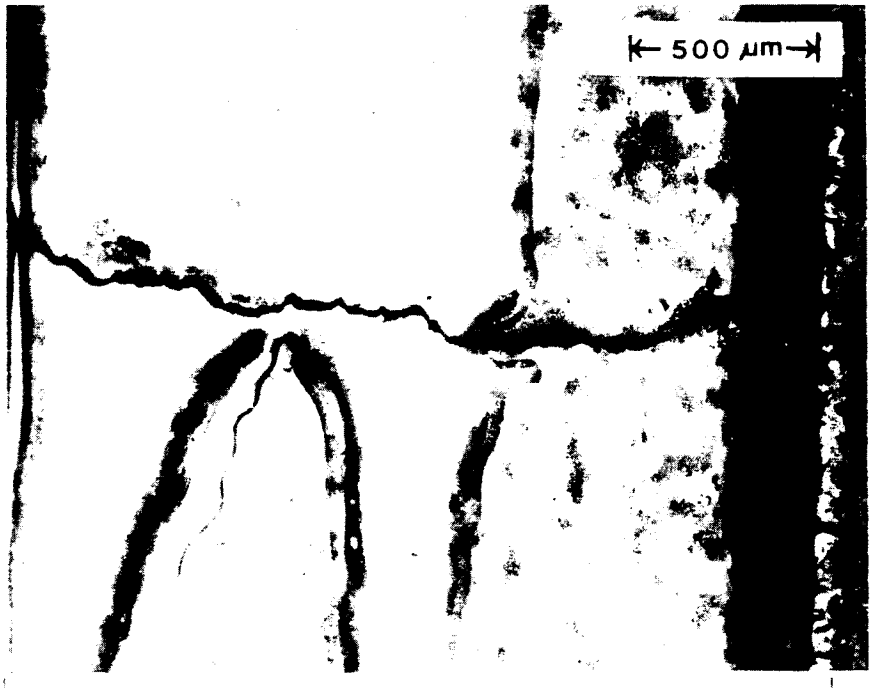

Replica @ 130K cycles

A-57-14

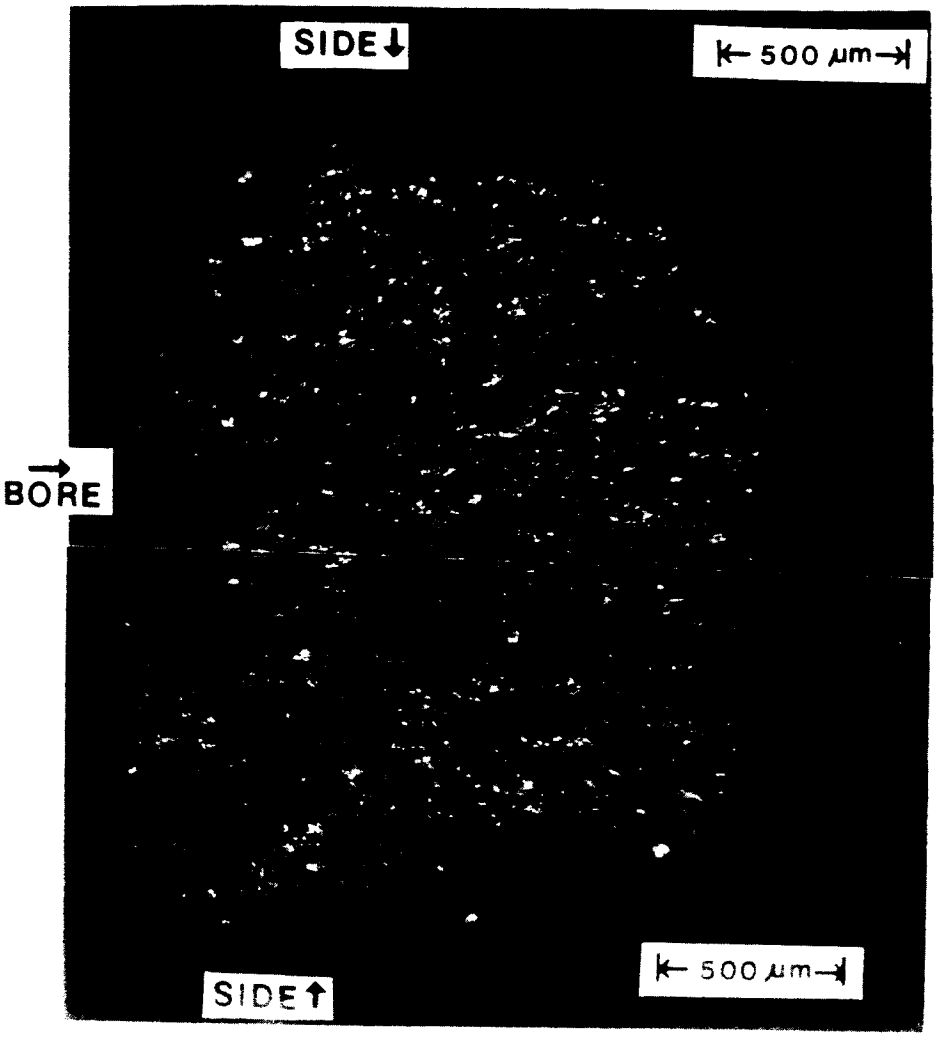

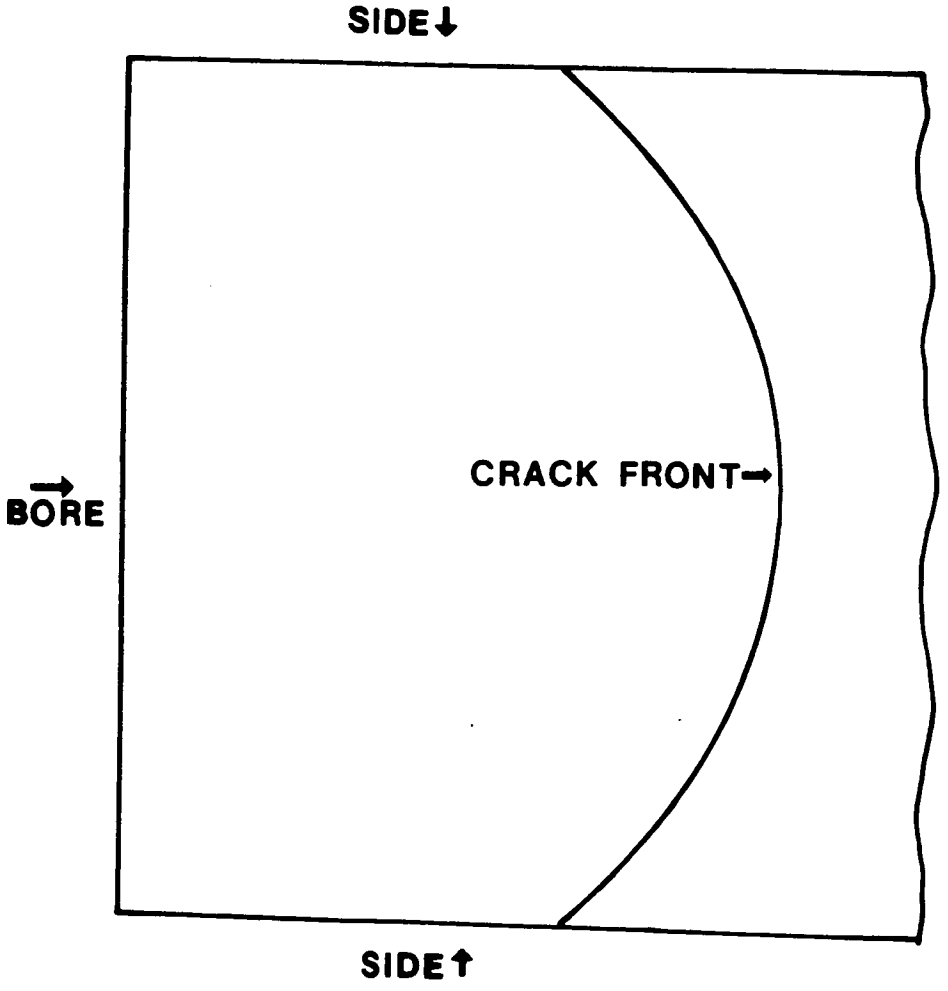

Tracing of Crack Front for A-57-14

TEST DATA

SPECIMEN NUMBER: A-80-28

DATE: 6/15/85

PARTICIPANT'S NAME: Joo-Jin Lee

John Cieslowski

TEST TEMPERATURE: 27°C

RELATIVE HUMIDITY: 54 %

WAVEFORM TYPE: Sinusoidal wave, 20 Hz

LOADING SEQUENCE TYPE: Constant amplitude

R-RATIO = 0.0

S max = 110 MPa

S min = 0 MPa

FINAL LENGTH OF CRACK: 0.371 mm

COMMENTS:

AGARD Short Crack DATA CHART

Record of crack lengths and map

Page 1 of 2 Loading Type Const. Amplitude R=0

Specimen no A-80-28 Peak Stress 110 MPa

0.1mm grid

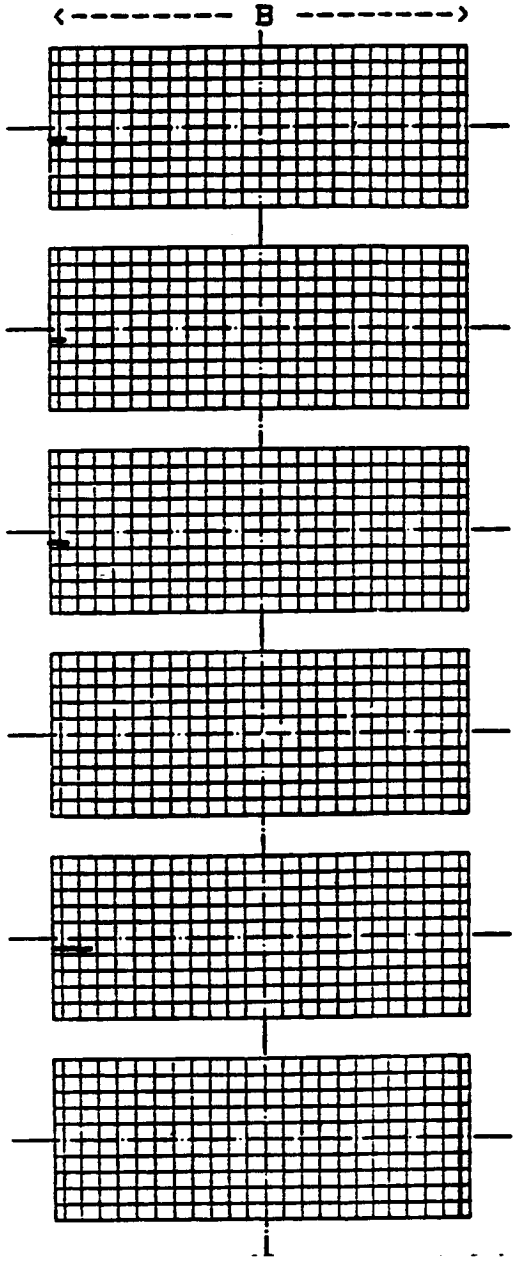

100 K Cycles
L1 .092 mm
L2 ____ mm
L3 ____ mm
L4 ____ mm
L5 ____ mm

110 K Cycles
L1 .087 mm
L2 ____ mm
L3 ____ mm
L4 ____ mm
L5 ____ mm

120 K Cycles
L1 .114 mm
L2 ____ mm
L3 ____ mm
L4 ____ mm
L5 ____ mm

130 K Cycles
L1 * mm
L2 ____ mm
L3 ____ mm
L4 ____ mm
L5 ____ mm

140 K Cycles
L1 .229 mm
L2 ____ mm
L3 ____ mm
L4 ____ mm
L5 ____ mm

150 K Cycles
L1 * mm
L2 ____ mm
L3 ____ mm
L4 ____ mm
L5 ____ mm

* Replica was not clear

AGARD Short Crack DATA CHART

Record of crack lengths and map

Page 2 of 2 Loading Type R=0

Specimen no A-80-29 Peak Stress 110 MPa

0.1mm grid

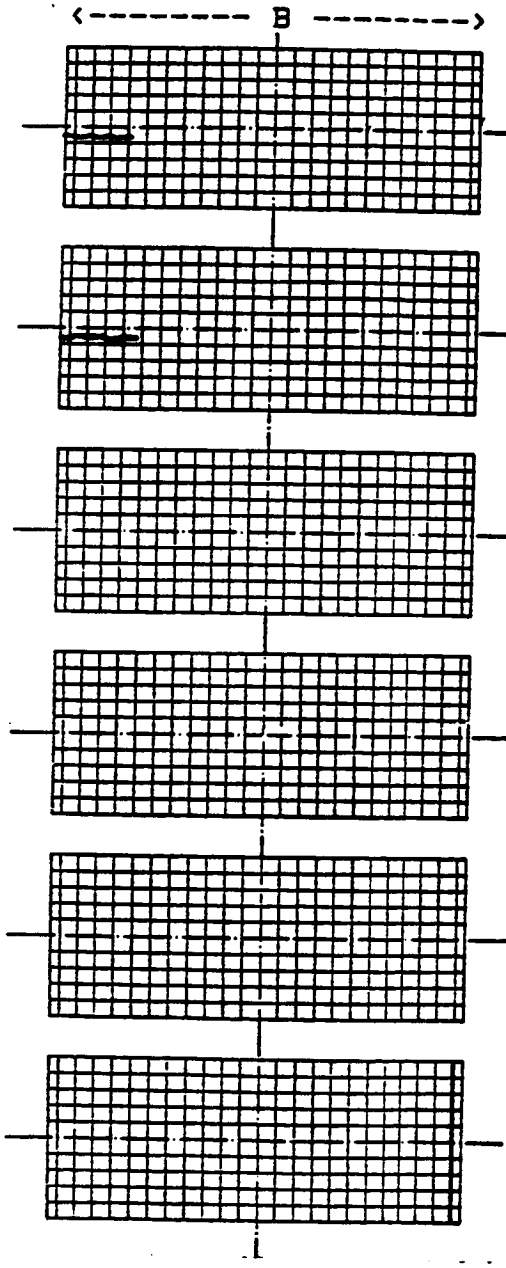

160K Cycles
L1 .371 mm
L2 mm
L3 mm
L4 mm
L5 mm

150K Cycles
L1 .414 mm
L2 mm
L3 mm
L4 mm
L5 mm

Cycles
L1 mm
L2 mm
L3 mm
L4 mm
L5 mm

Cycles
L1 mm
L2 mm
L3 mm
L4 mm
L5 mm

Cycles
L1 mm
L2 mm
L3 mm
L4 mm
L5 mm

Cycles
L1 mm
L2 mm
L3 mm
L4 mm
L5 mm

** DA/DN DATA **

SPECIMEN' NO. = A-80-28.L1
NO. OF DATA = 5
R= 0.00
SMAX=110.0 MPa
corner crack

	CYCLE(X1000)	CRK L. 2a(mm)	AVG. a(mm)	DELK(MPa-M)	DADN(mm/CYCLE)
0	100	0.082	0.000	0.00	0.000 X1.E-6
1	110	0.087	0.084	3.79	0.500 X1.E-6
2	120	0.114	0.100	4.11	2.700 X1.E-6
3	140	0.229	0.171	5.26	5.750 X1.E-6
4	160	0.371	0.300	6.76	7.100 X1.E-6

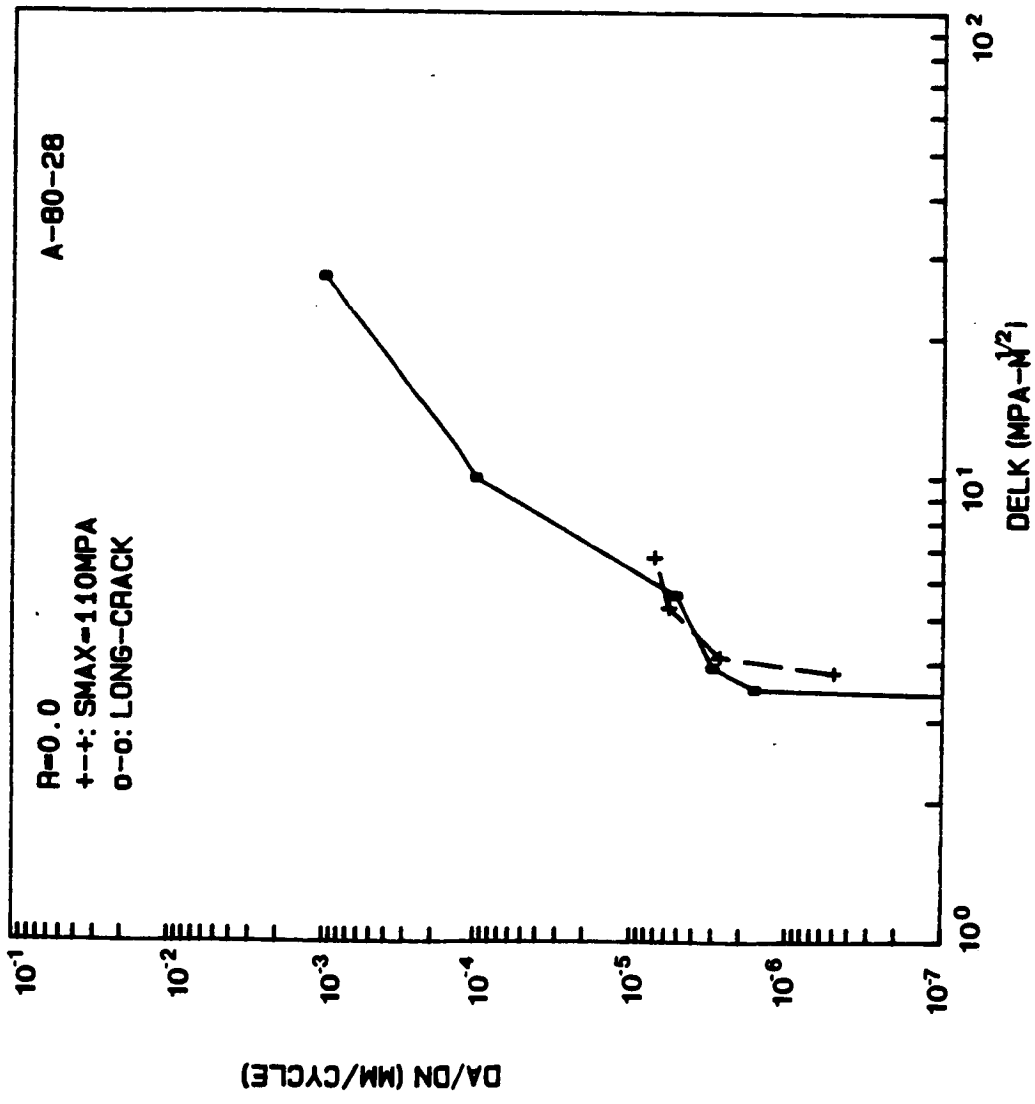
A-80-28
R=0.0
+--+: SMAX=110MPA
o-o: LONG-CRACK
DA/DN (MM/CYCLE)
DELK (MPA-M^1/2)
10^-1
10^-2
10^-3
10^-4
10^-5
10^-6
10^-7
10^0
10^1
10^2

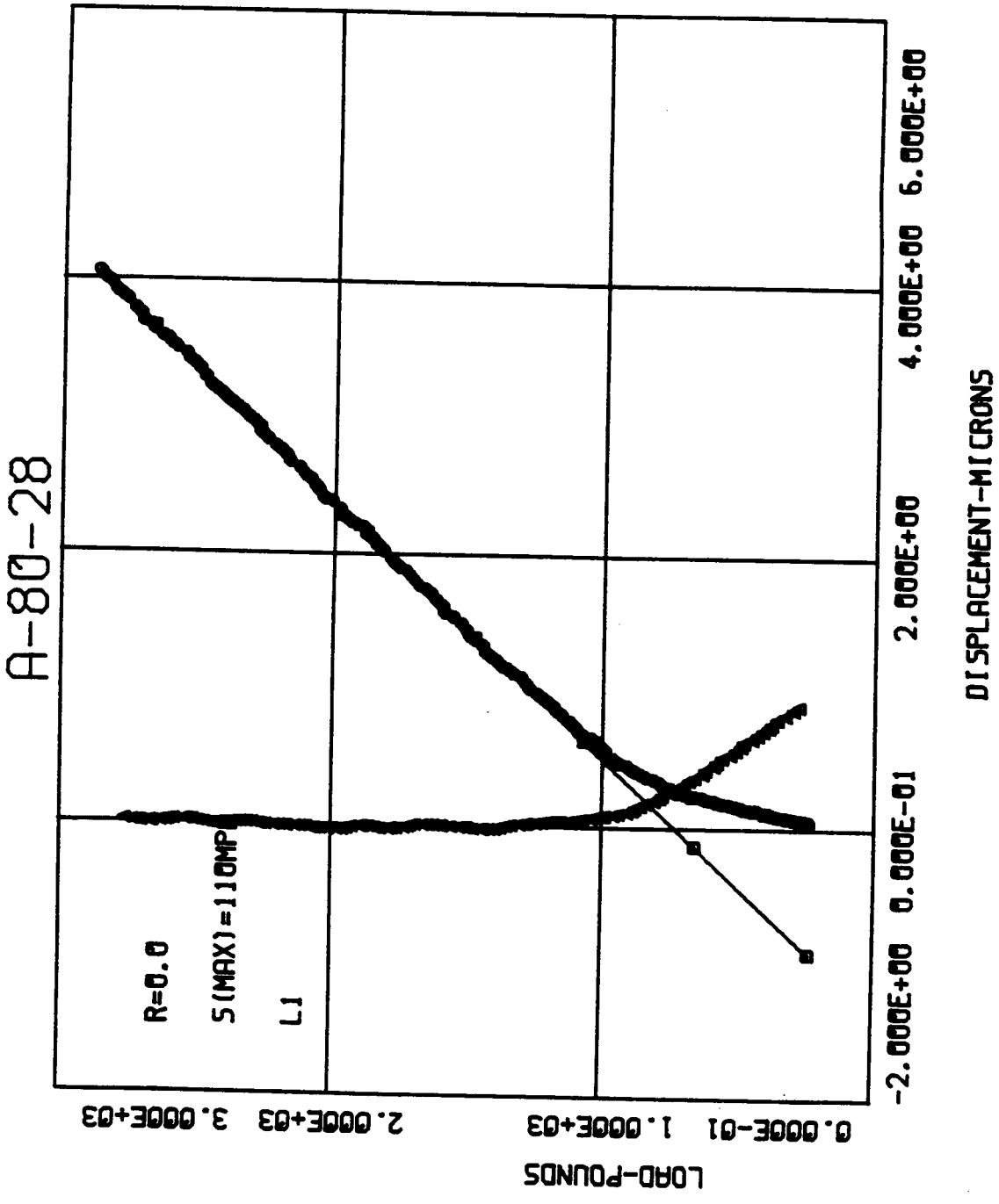
A-80-28
R=0.0
S(MAX)=110MP
L1
LOAD-POUNDS
0.000E-01
1.000E+03
2.000E+03
3.000E+03
-2.000E+00
0.000E-01
2.000E+00
4.000E+00
6.000E+00
DISPLACEMENT-MICRONS

A-80-28

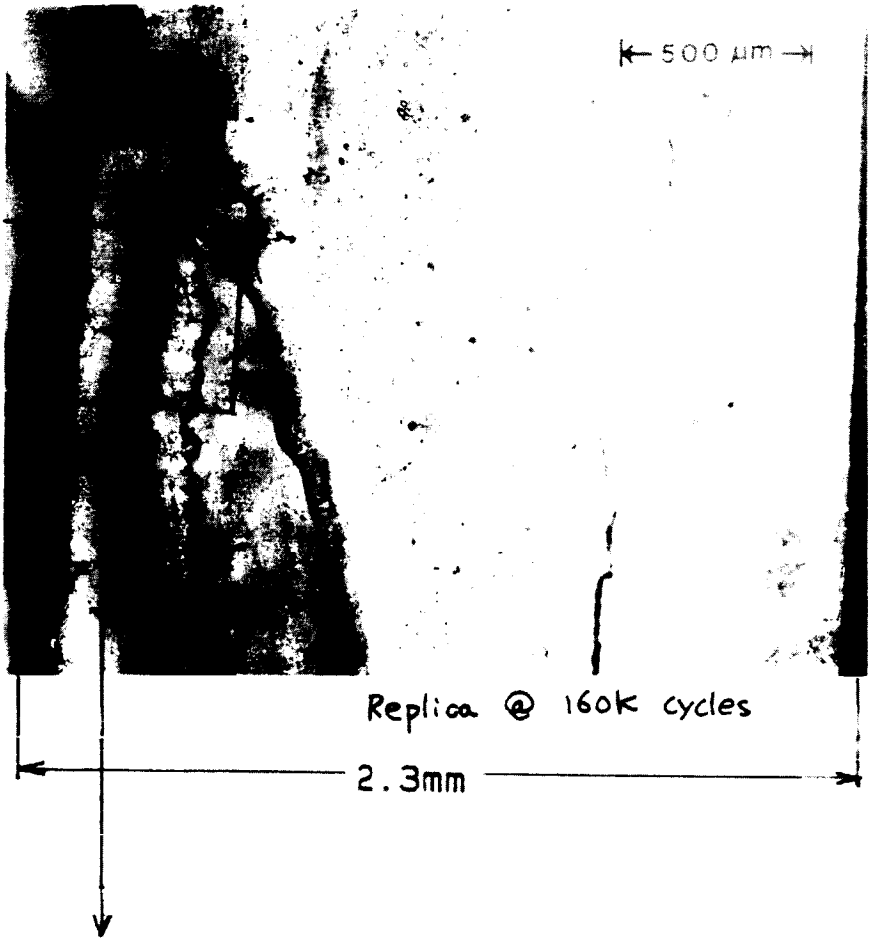

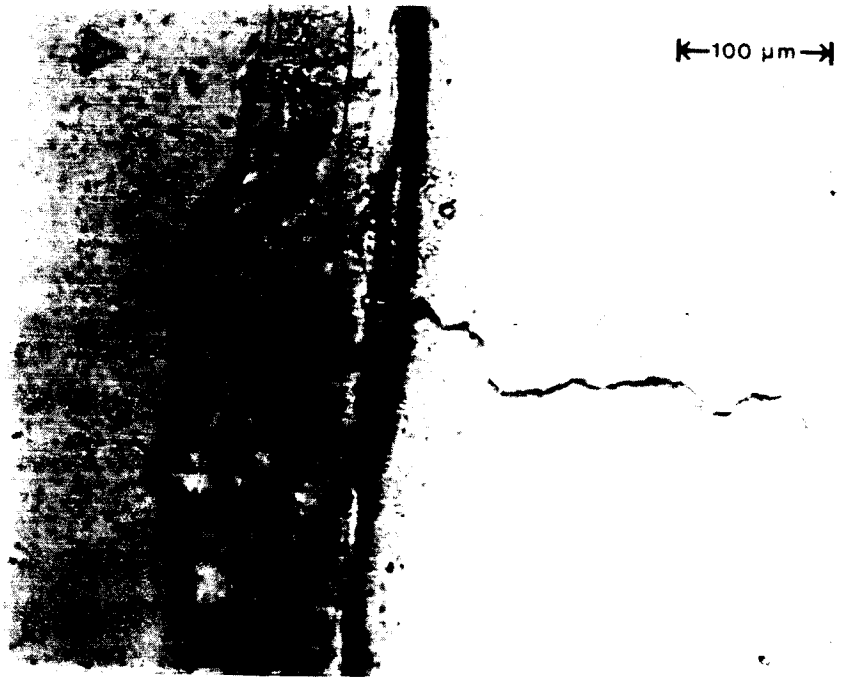

A-80-28

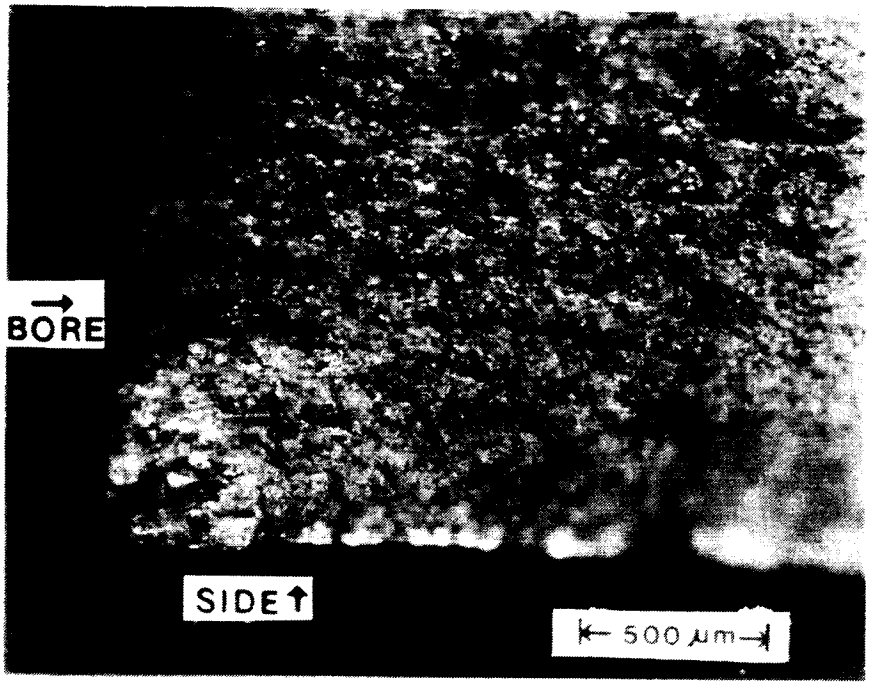

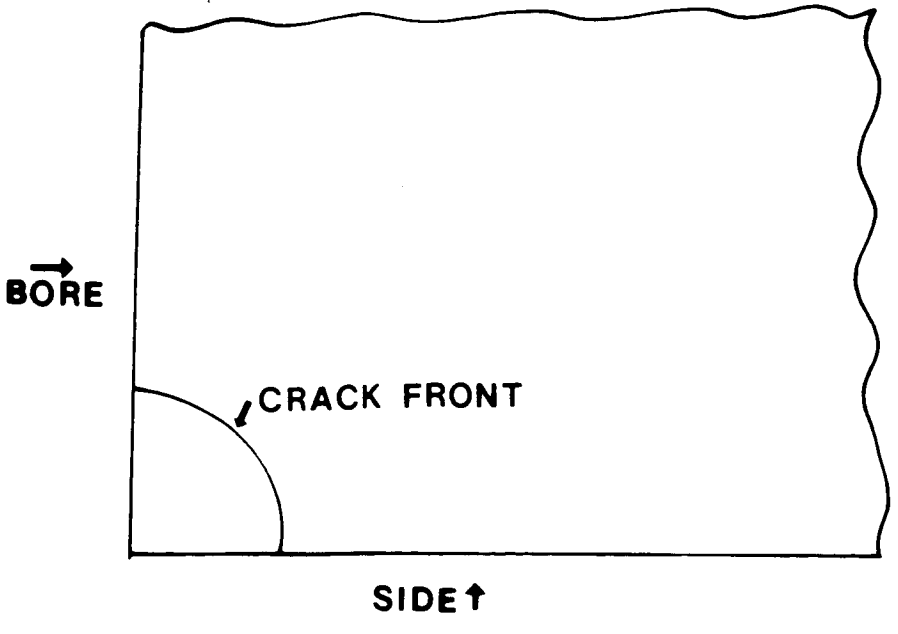

Tracing of Crack Front for A-80-28

TEST DATA

SPECIMEN NUMBER: A-55-27

DATE: 6/25/85

PARTICIPANT'S NAME: Joo-Jin Lee

John Cieslowski

TEST TEMPERATURE: 26° C

RELATIVE HUMIDITY: 44%

WAVEFORM TYPE: Sinusoidal wave, 20 Hz

LOADING SEQUENCE TYPE: Constant amplitude

R-RATIO = -1.0

S max = 105 MPa

S min = -105 MPa

FINAL LENGTH OF CRACK: 2.3mm (Thru thickness) - L1

COMMENTS:

Photo of crack surface was not available.
(out of focus)

AGARD Short Crack DATA CHART

Record of crack lengths and map

Page 1 of 2 Loading Type Const. Amplitude R=-1

Specimen no A-55-27 Peak Stress: 105 MPa

0.1mm grid

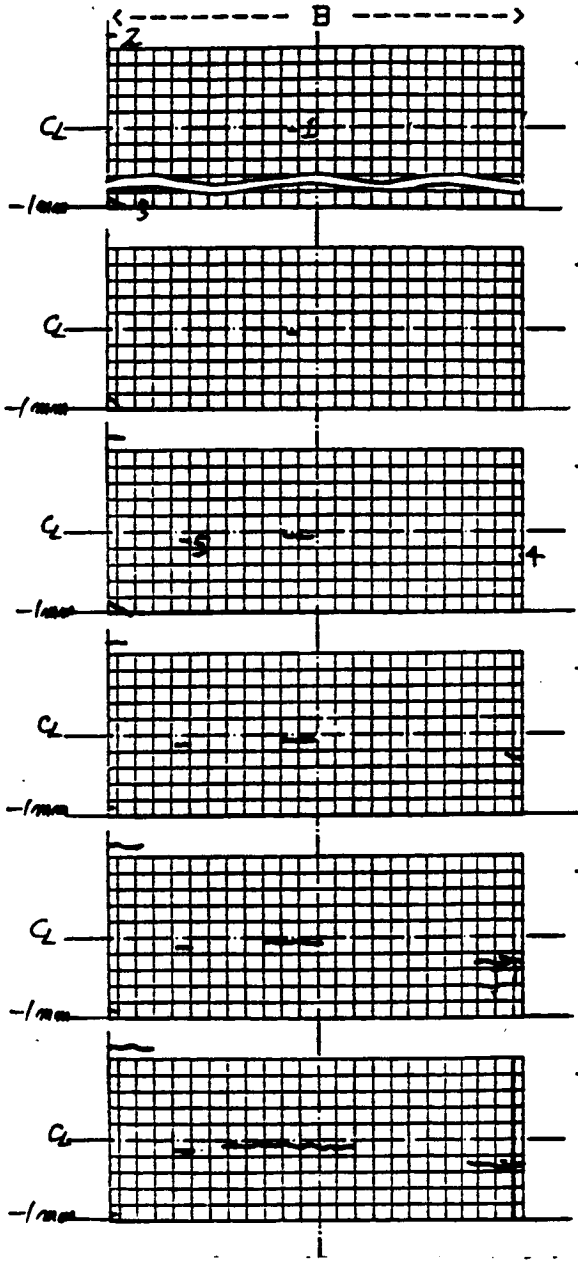

4 K Cycles
L1 .032 mm
L2 .055 mm
L3 .076 mm
L4 ____ mm
L5 ____ mm

6K Cycles
L1 .049 mm
L2 * mm
L3 * mm
L4 ____ mm
L5 ____ mm

8K Cycles
L1 .136 mm
L2 .093 mm
L3 * mm
L4 .120 mm
L5 .065 mm

10 K Cycles
L1 .191 mm
L2 .136 mm
L3 .136 mm
L4 .087 mm
L5 .087 mm

12 K Cycles
L1 .322 mm
L2 .190 mm
L3 * mm
L4 .251 mm
L5 .098 mm

14 K Cycles
L1 .758 mm
L2 .229 mm
L3 * mm
L4 .294 mm
L5 .120 mm

* Crack was not clear

AGARD Short Crack DATA CHART

Record of crack lengths and map

Page 2 of 2 Loading Type R=-1

Specimen no A-55-27 Peak Stress 105 MPa

0.1mm grid

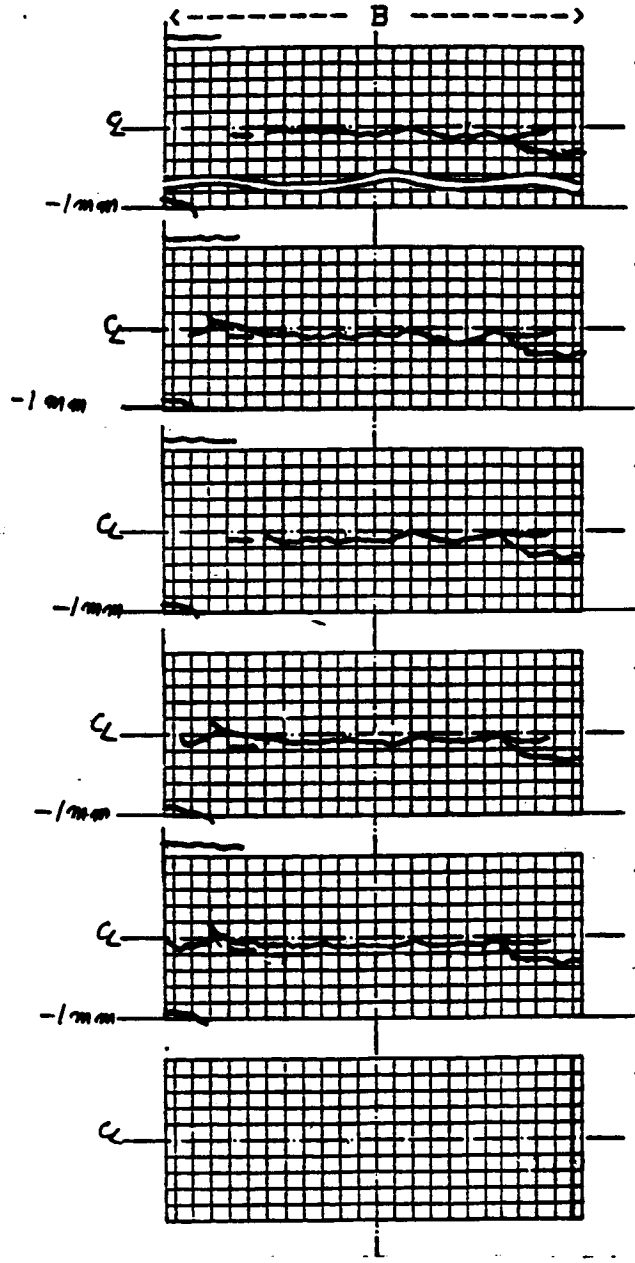

16K Cycles
L1 1.76 mm
L2 .300 mm
L3 * mm
L4 L1 mm
L5 .136 mm

17K Cycles
L1 2.110 mm
L2 .403 mm
L3 * mm
L4 mm
L5 .153 mm

19K Cycles
L1 2.115 mm
L2 .414 mm
L3 .267 mm
L4 mm
L5 .158 mm

20K Cycles
L1 2.175 mm
L2 .414 mm
L3 .267 mm
L4 mm
L5 .158 mm

20.5K Cycles
L1 THRU mm
L2 .431 mm
L3 .220 mm
L4 mm
L5 .169 mm

Cycles
L1 mm
L2 mm
L3 mm
L4 mm
L5 mm

* Crack was not clear

** DA/DN DATA **

SPECIMEN' NO. = A-55-27.L1
NO. OF DATA = 10
R=-1.00
SMAX=105.0 MPa
surface crack

	CYCLE(X1000)	CRK L. 2a(mm)	AVG. a(mm)	DELK(MPa-M)	DADN(mm/CYCLE)
0	4	0.032	0.000	0.00	0.000 X1.E-6
1	6	0.049	0.020	3.74	4.250 X1.E-6
2	8	0.136	0.046	5.55	21.750 X1.E-6
3	10	0.191	0.082	7.23	13.750 X1.E-6
4	12	0.322	0.128	8.88	32.750 X1.E-6
5	14	0.758	0.270	12.43	109.000 X1.E-6
6	16	1.760	0.629	18.23	250.500 X1.E-6
7	17	2.110	0.967	22.31	175.000 X1.E-6

** DA/DN DATA **

SPECIMEN' NO. = A-55-27.L2
NO. OF DATA = 9
R=-1.00
SMAX=105.0 MPa
corner crack

	CYCLE(X1000)	CRK L. 2a(mm)	AVG. a(mm)	DELK(MPa-M)	DADN(mm/CYCLE)
0	4	0.055	0.000	0.00	0.000 X1.E-6
1	8	0.093	0.074	6.80	9.500 X1.E-6
2	10	0.136	0.114	8.35	21.500 X1.E-6
3	12	0.180	0.158	9.68	22.000 X1.E-6
4	14	0.229	0.204	10.87	24.500 X1.E-6
5	16	0.300	0.264	12.20	35.500 X1.E-6
6	17	0.403	0.352	13.84	103.000 X1.E-6
7	18	0.414	0.408	14.79	11.000 X1.E-6
8	20	0.431	0.422	15.01	8.500 X1.E-6

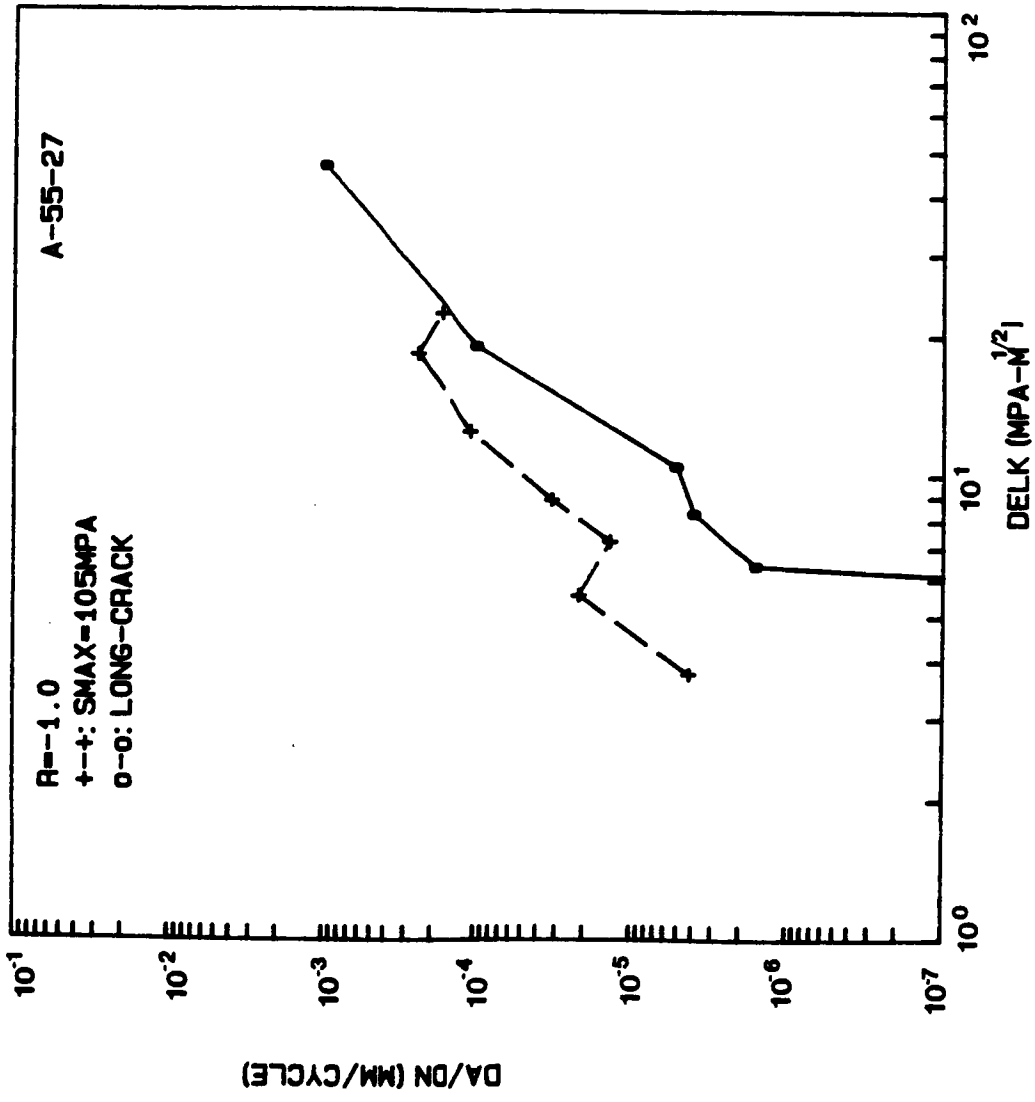
A-55-27
R=-1.0
+-+: SMAX=105MPA
o-o: LONG-CRACK
DA/DN (MM/CYCLE)
DELK (MPA-M^1/2)
10^-1
10^-2
10^-3
10^-4
10^-5
10^-6
10^-7
10^0
10^1
10^2

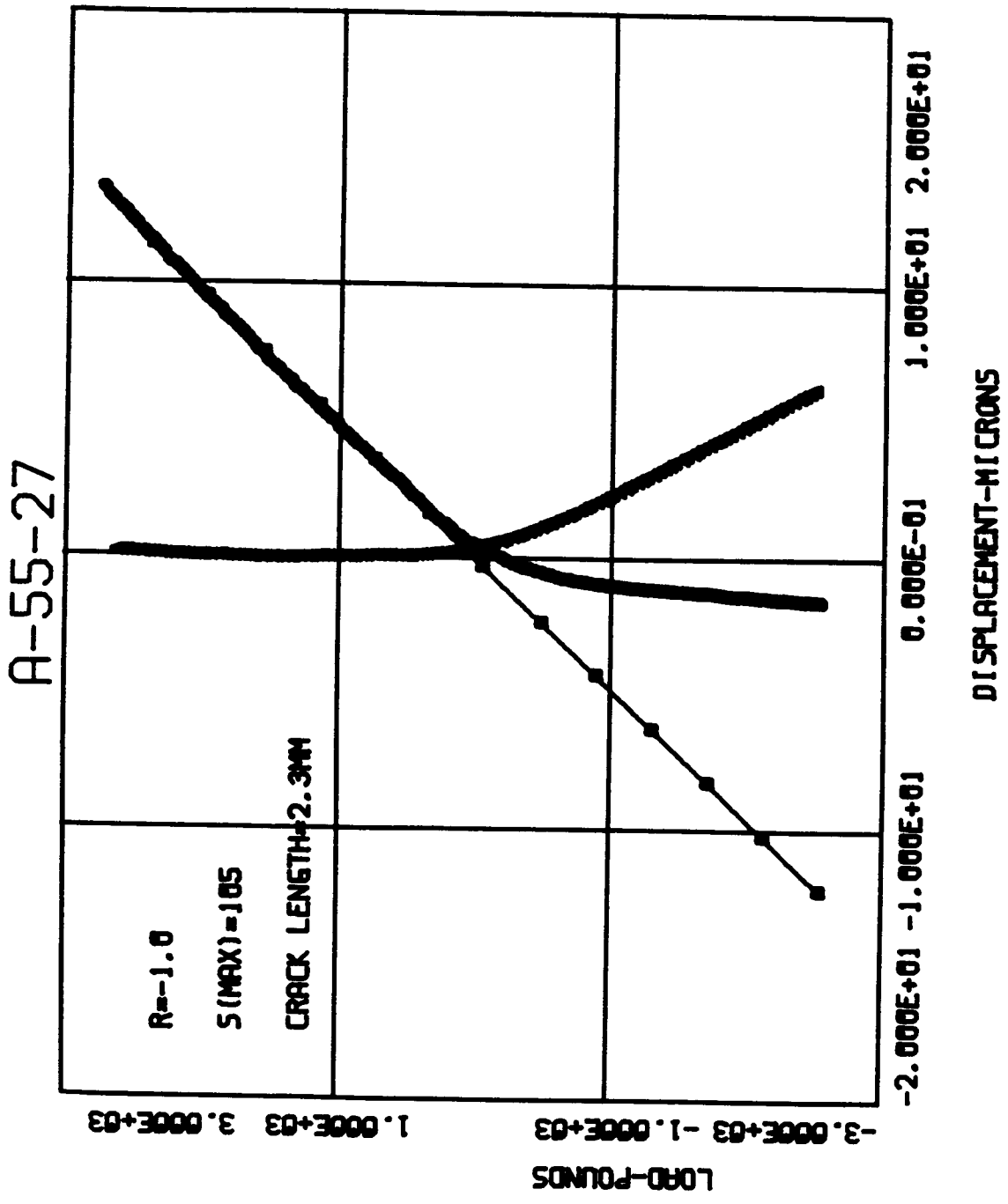
A-55-27
R=-1.0
S(MAX)=105
CRACK LENGTH=2.3MM
LOAD-POUNDS
3.000E+03
1.000E+03
-1.000E+03
-3.000E+03
-2.000E+01
-1.000E+01
0.000E-01
1.000E+01
2.000E+01
DISPLACEMENT-MICRONS

A-55-27

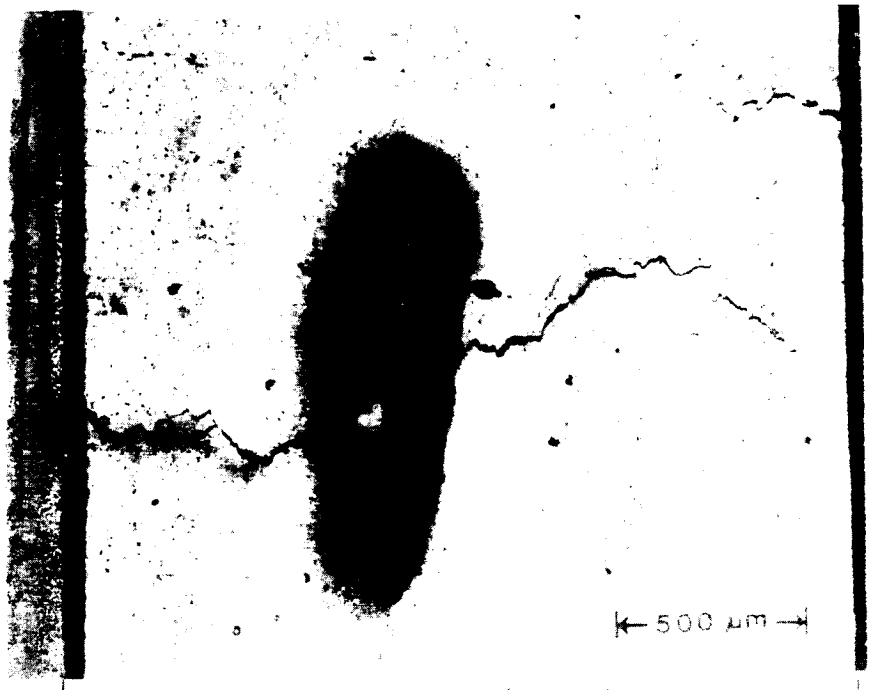

2.3mm

TEST DATA

SPECIMEN NUMBER: A-67-08

DATE: 6/20/85

PARTICIPANT'S NAME: Joo-Jin Lee

John Cieslowski

TEST TEMPERATURE: 27°C

RELATIVE HUMIDITY: 35 %

WAVEFORM TYPE: Sinusoidal wave, 20 Hz

LOADING SEQUENCE TYPE: Constant amplitude

R-RATIO = -1.0

S max = 105MPa

S min = -105 MPa

FINAL LENGTH OF CRACK: 0.398 mm (L1)

COMMENTS:

L3 was found at 1mm above the center line.

AGARD Short Crack DATA CHART

Record of crack lengths and map

Page 1 of 1 Loading Type Const. Amplitude R=-1

Specimen no A-67-08 Peak Stress 105 MPa

0.1mm grid

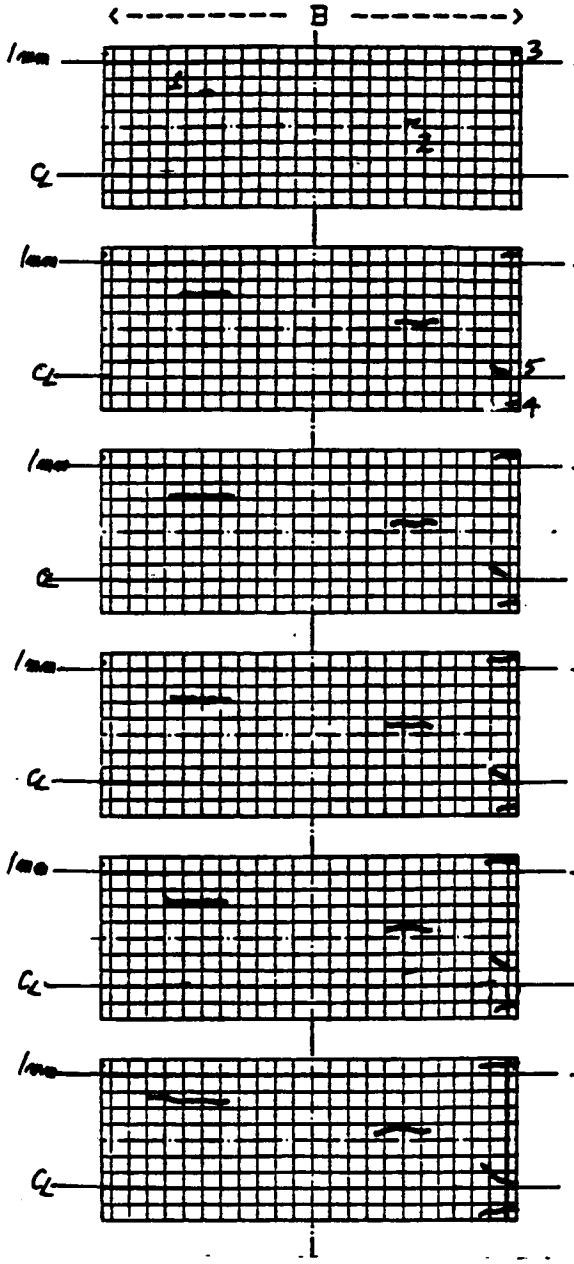

7K Cycles
L1 .092 mm
L2 .055 mm
L3 .044 mm
L4 mm
L5 mm

9K Cycles
L1 .267 mm
L2 .207 mm
L3 .104 mm
L4 .065 mm
L5 .076 mm

10K Cycles
L1 .279 mm
L2 .223 mm
L3 .120 mm
L4 .076 mm
L5 .065 mm

11K Cycles
L1 .300 mm
L2 .262 mm
L3 .158 mm
L4 .104 mm
L5 .093 mm

12K Cycles
L1 .322 mm
L2 .262 mm
L3 .164 mm
L4 .104 mm
L5 .076 mm

14K Cycles
L1 .398 mm
L2 .289 mm
L3 .191 mm
L4 .191 mm
L5 .218 mm

** DA/DN DATA **

SPECIMEN' NO. = A-67-08.L1
NO. OF DATA = 6
R=-1.00
SMAX=105.0 MPa
surface crack

	CYCLE(X1000)	CRK L. 2a(mm)	AVG. a(mm)	DELK(MPa-M)	DADN(mm/CYCLE)
0	7	0.082	0.000	0.00	0.000 X1.E-6
1	9	0.267	0.087	7.45	46.250 X1.E-6
2	10	0.278	0.136	9.13	.5.500 X1.E-6
3	11	0.300	0.145	9.37	11.000 X1.E-6
4	12	0.322	0.155	9.69	11.000 X1.E-6
5	14	0.398	0.180	10.35	19.000 X1.E-6

** DA/DN DATA **

SPECIMEN' NO. = A-67-08.L3
NO. OF DATA = 6
R=-1.00
SMAX=105.0 MPa
corner crack

	CYCLE(X1000)	CRK L. 2a(mm)	Corner AVG. a(mm)	DELK(MPa-M)	DADN(mm/CYCLE)
0	7	0.044	0.000	0.00	0.000 X1.E-6
1	9	0.104	0.074	6.80	30.000 X1.E-6
2	10	0.120	0.112	8.26	16.000 X1.E-6
3	11	0.158	0.139	9.13	38.000 X1.E-6
4	12	0.164	0.161	9.76	6.000 X1.E-6
5	14	0.191	0.177	10.20	13.500 X1.E-6

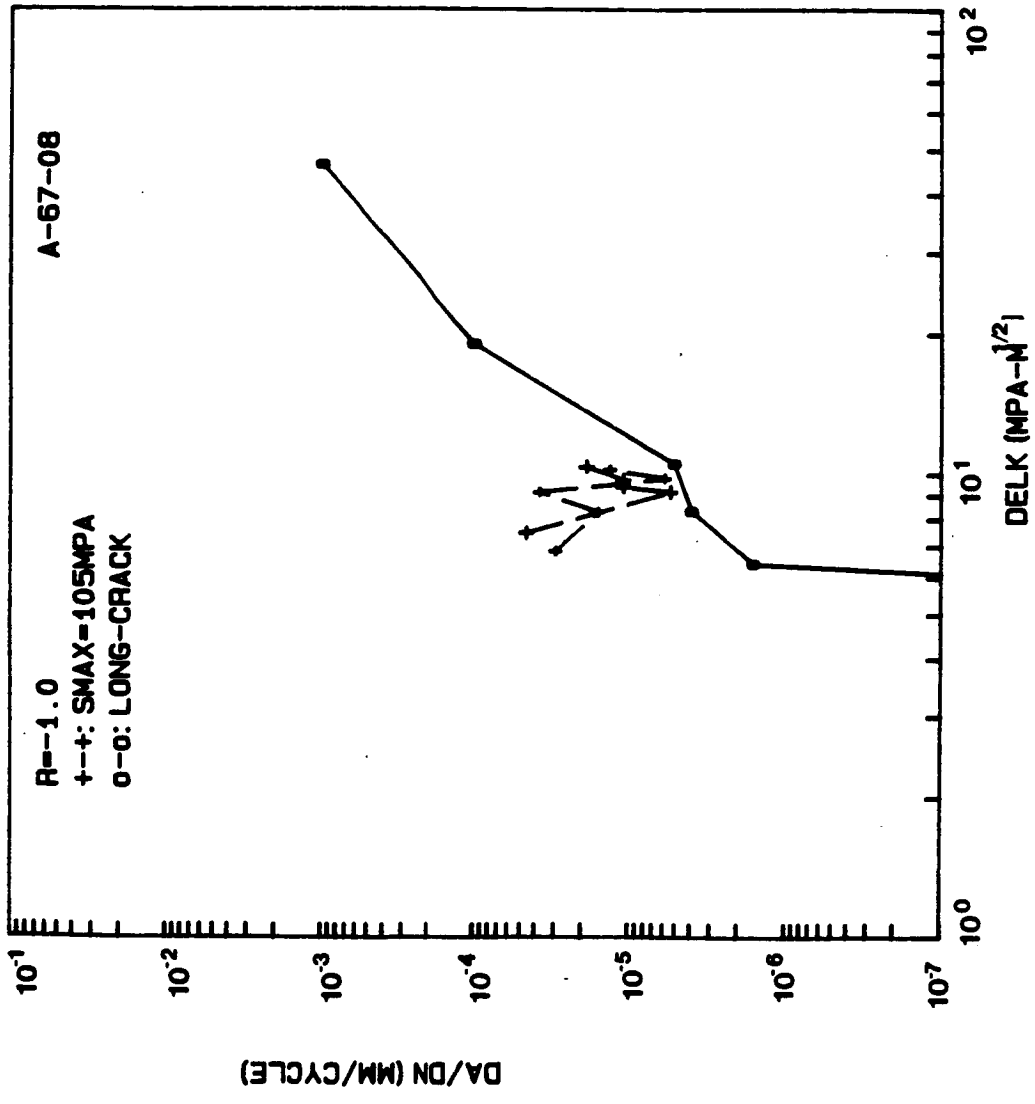
A-67-08
R=-1.0
+-+: SMAX=105MPA
o-o: LONG-CRACK
DA/DN (MM/CYCLE)
DELK (MPA-M^1/2)
10^-1
10^-2
10^-3
10^-4
10^-5
10^-6
10^-7
10^0
10^1
10^2

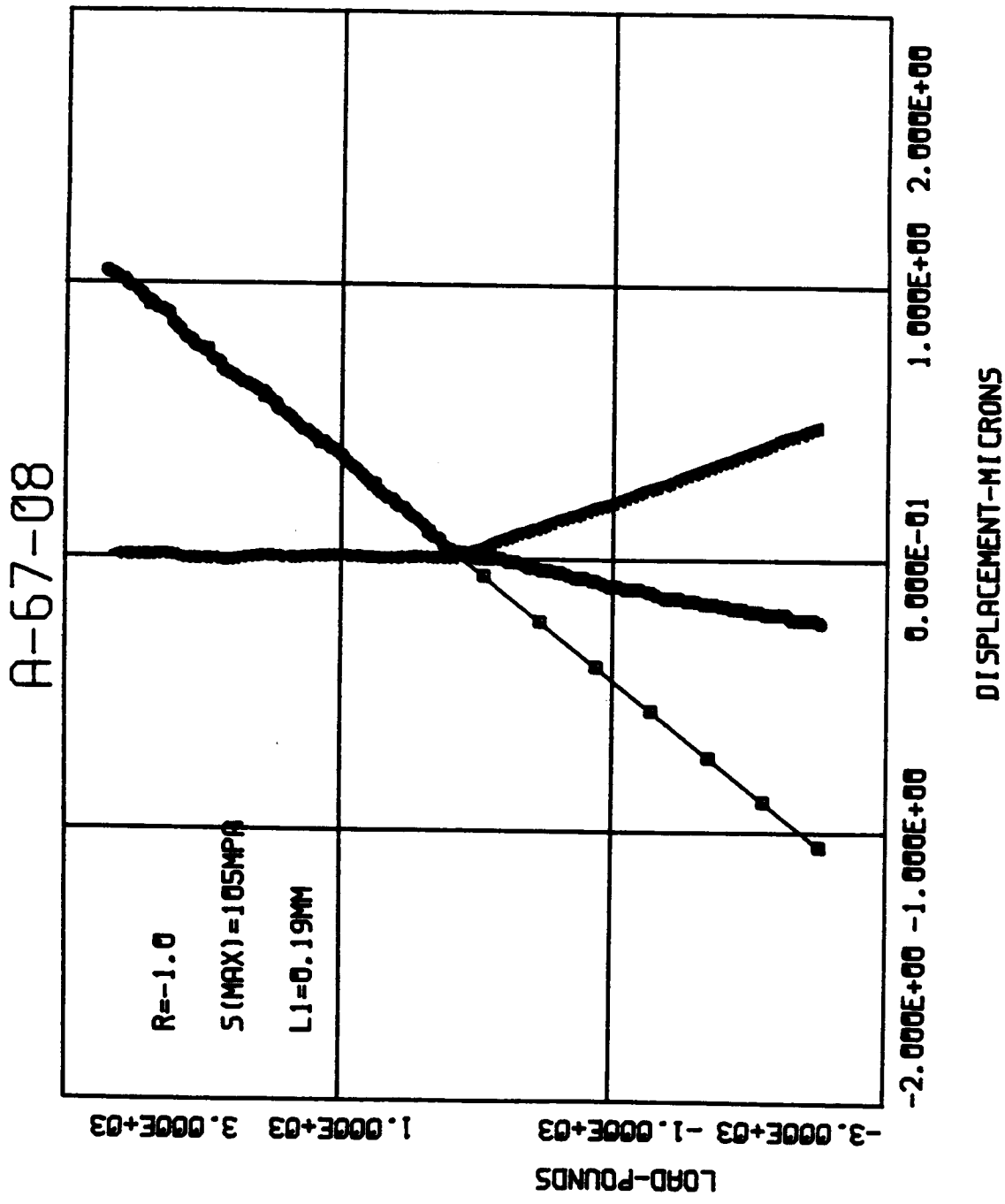
A-67-08
R=-1.0
S(MAX)=105MPA
L1=0.19MM
LOAD-POUNDS
-3.000E+03
-1.000E+03
1.000E+03
3.000E+03
-2.000E+00
-1.000E+00
0.000E-01
1.000E+00
2.000E+00
DISPLACEMENT-MICRONS

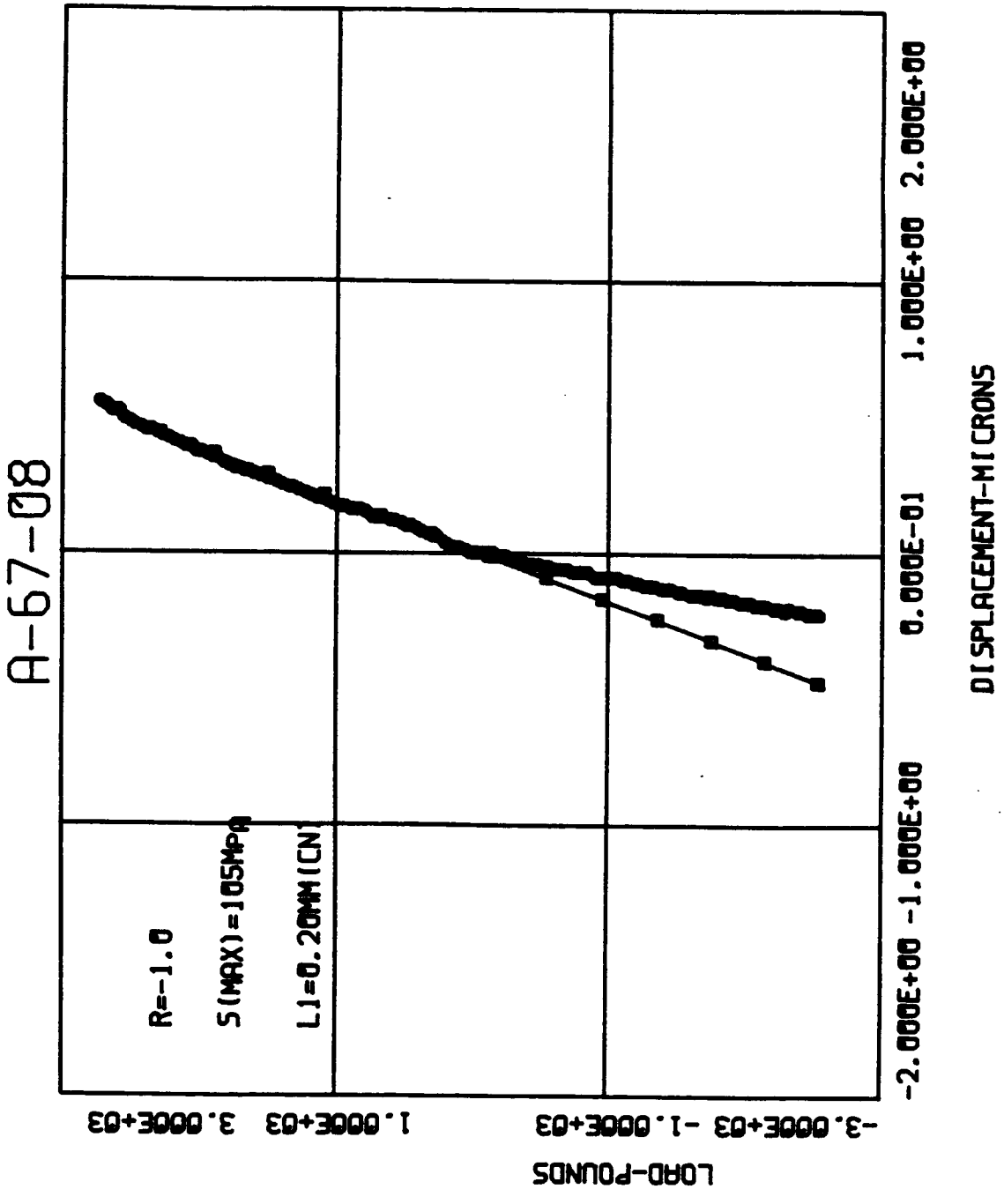
A-67-08
R=-1.0
S(MAX)=105MPa
L1=0.20MM(CN)
LOAD-POUNDS
3.0000E+03
1.0000E+03
-1.0000E+03
-3.0000E+03
-2.000E+00
-1.000E+00
0.000E-01
1.000E+00
2.000E+00
DISPLACEMENT-MICRONS

A-67-08

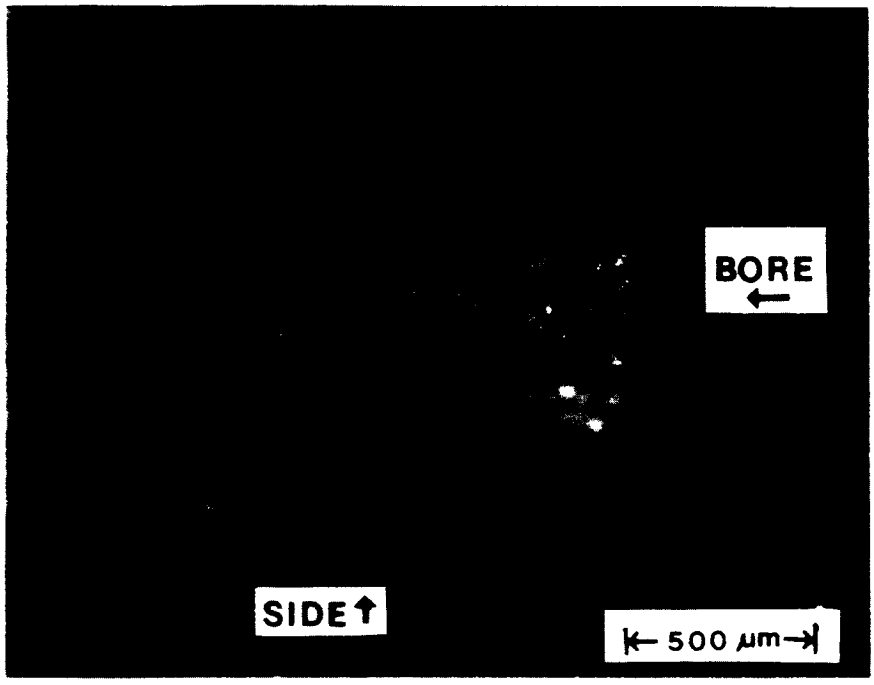

A-67-08

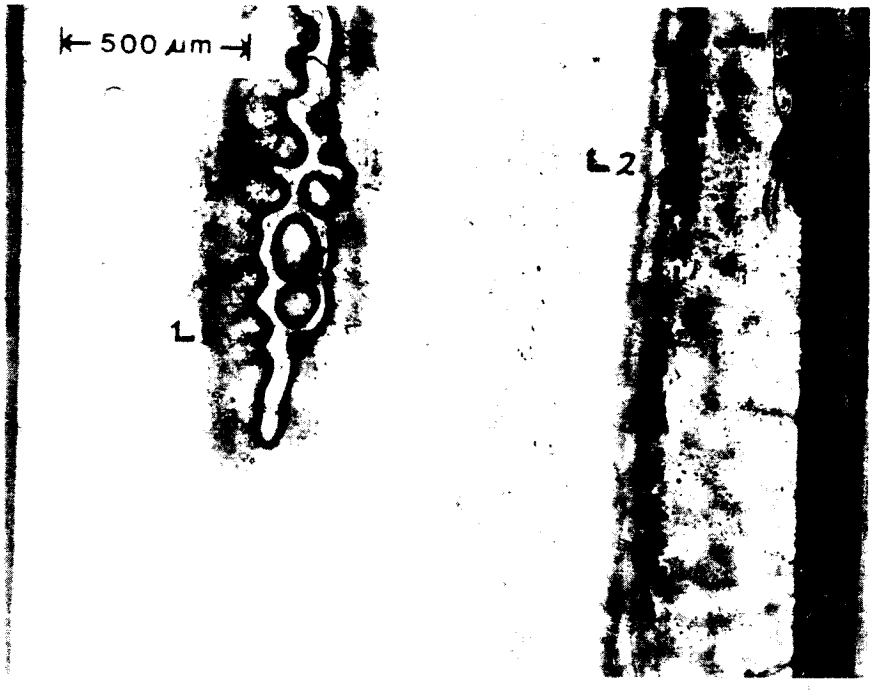

TEST DATA

SPECIMEN NUMBER: A-65-24

DATE: 7/8/85

PARTICIPANT'S NAME: Joo-Jin Lee

John Cieslowski

TEST TEMPERATURE: 27°C

RELATIVE HUMIDITY: 54 %

WAVEFORM TYPE: Sinusoidal wave, 20 Hz

LOADING SEQUENCE TYPE: Constant amplitude

R-RATIO = −1

S max = 80MPa

S min = −80MPa

FINAL LENGTH OF CRACK: 2.3mm (Thru thickness) - L1

COMMENTS:

L2 was found at 0.7mm down the center line.

L4 was found at 0.8 mm above the center line.

AGARD Short Crack DATA CHART

Record of crack lengths and map

Page 1 of 3 Loading Type Const. Amplitude R = -1

Specimen no A-65-24 Peak Stress 80 MPa

0.1mm grid

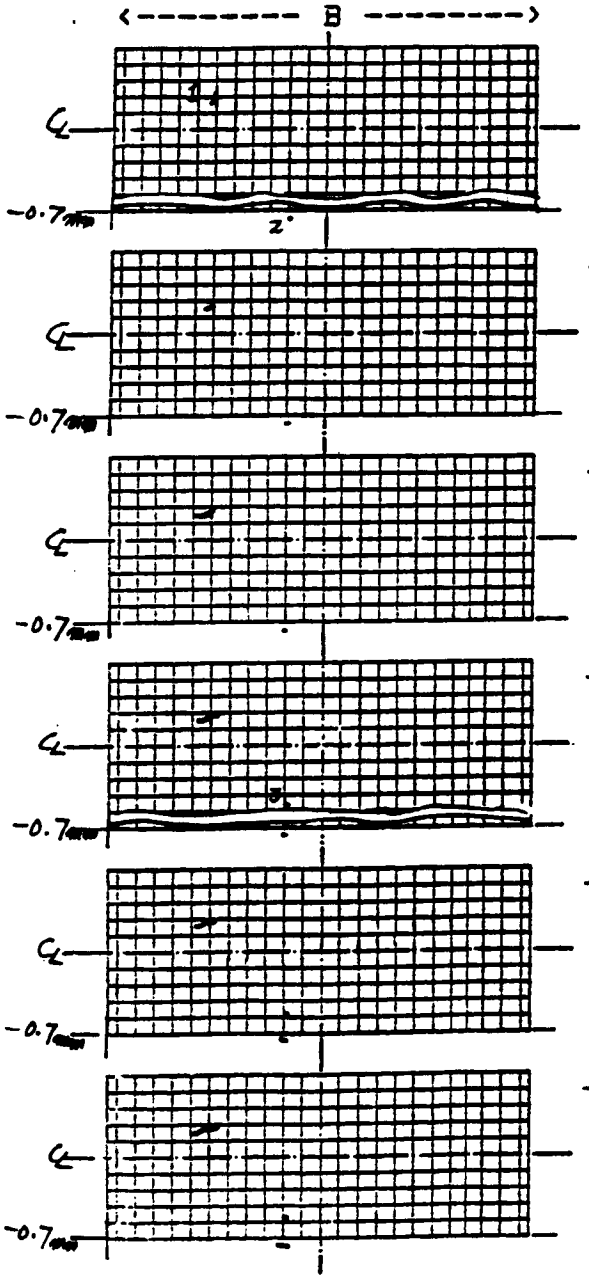

40K Cycles
L1 .033 mm
L2 .016 mm
L3 ____ mm
L4 ____ mm
L5 ____ mm

45K Cycles
L1 .049 mm
L2 .022 mm
L3 ____ mm
L4 ____ mm
L5 ____ mm

50K Cycles
L1 .093 mm
L2 .033 mm
L3 ____ mm
L4 ____ mm
L5 ____ mm

55K Cycles
L1 .109 mm
L2 .033 mm
L3 .016 mm
L4 ____ mm
L5 ____ mm

60K Cycles
L1 .109 mm
L2 .039 mm
L3 .027 mm
L4 ____ mm
L5 ____ mm

65K Cycles
L1 .131 mm
L2 .055 mm
L3 .033 mm
L4 ____ mm
L5 ____ mm

AGARD Short Crack DATA CHART

Record of crack lengths and map

Page 2 of 3 Loading Type R = -1

Specimen no A-65-24 Peak Stress 80 MPa

0.1mm grid

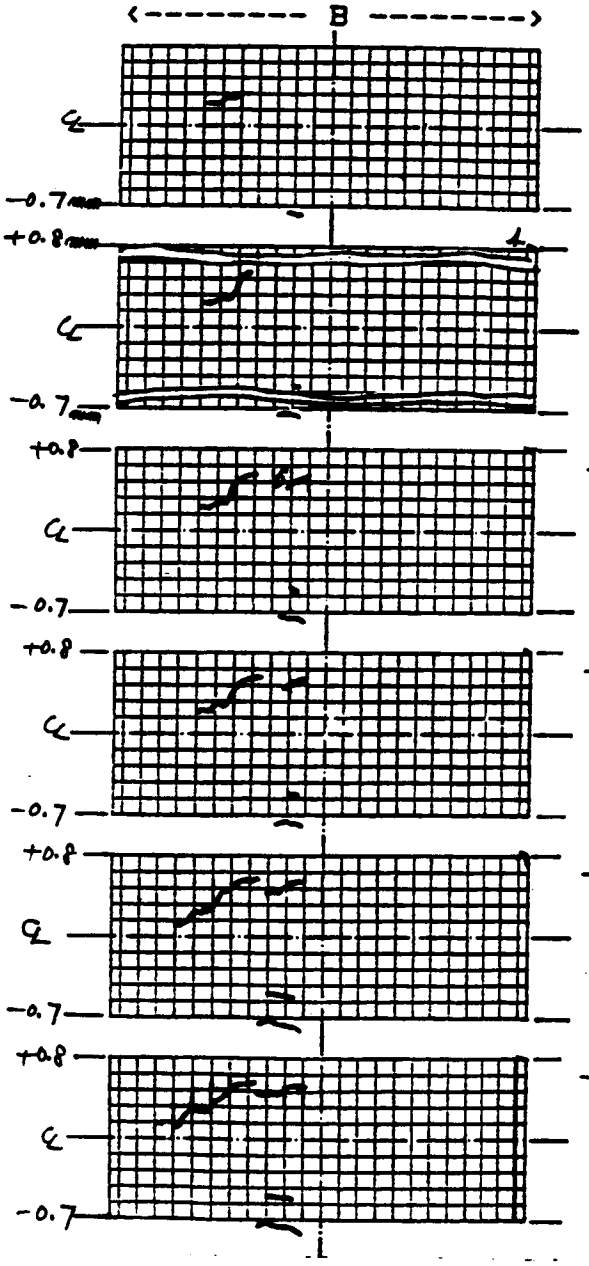

70 K Cycles
L1 .191 mm
L2 .087 mm
L3 * mm
L4 mm
L5 mm

75 K Cycles
L1 .251 mm
L2 .136 mm
L3 .060 mm
L4 .038 mm
L5 mm

80 K Cycles
L1 .338 mm
L2 .158 mm
L3 .060 mm
L4 .038 mm
L5 .125 mm

85 K Cycles
L1 .382 mm
L2 .158 mm
L3 .060 mm
L4 .038 mm
L5 .131 mm

90 K Cycles
L1 .409 mm
L2 .229 mm
L3 .147 mm
L4 .044 mm
L5 .185 mm

95 K Cycles
L1 .480 mm
L2 .240 mm
L3 .170 mm
L4 * mm
L5 .278 mm

* Crack was not clear

AGARD Short Crack DATA CHART

Record of crack lengths and map

Page 3 of 3 Loading Type R=-1

Specimen no A-65-24 Peak Stress 80 MPa

0.1mm grid

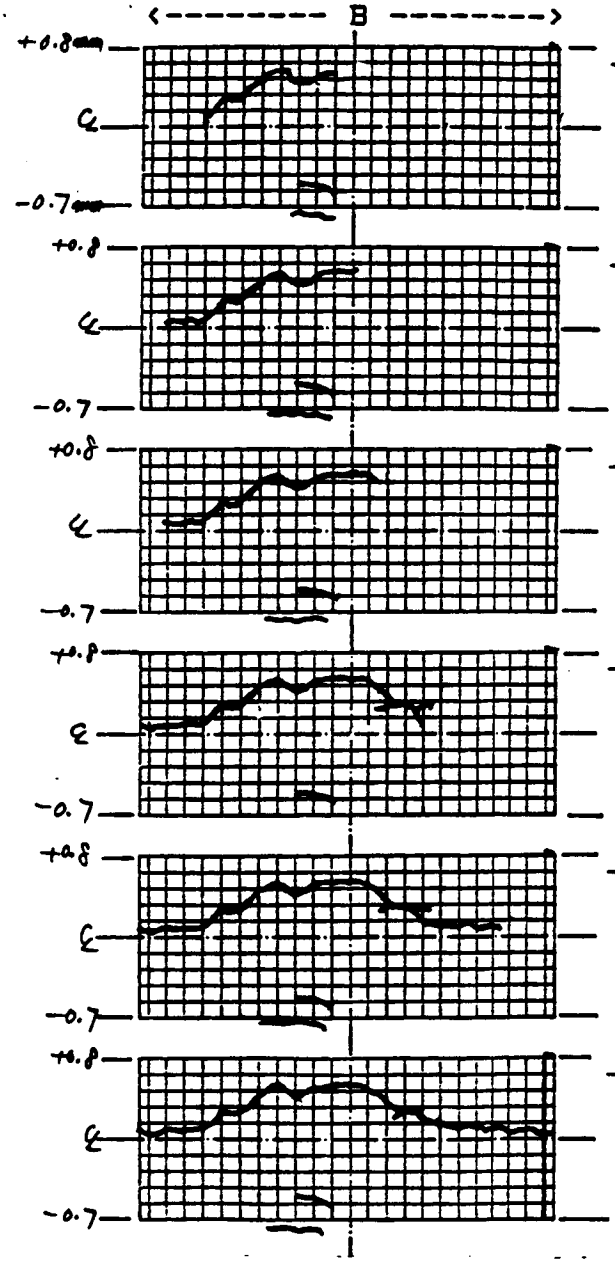

100K Cycles
L1 .698 mm
L2 .245 mm
L3 .174 mm
L4 .044 mm
L5 L1 mm

105K Cycles
L1 1.046 mm
L2 .321 mm
L3 .196 mm
L4 .060 mm
L5 mm

110K Cycles
L1 1.117 mm
L2 .332 mm
L3 .213 mm
L4 .049 mm
L5 mm

115K Cycles
L1 1.613 mm
L2 * mm
L3 * mm
L4 .055 mm
L5 mm

120K Cycles
L1 2.027 mm
L2 .343 mm
L3 .223 mm
L4 .055 mm
L5 mm

125K Cycles
L1 THRU mm
L2 .343 mm
L3 .229 mm
L4 .055 mm
L5 mm

* Crack was not clear

** DA/DN DATA **

SPECIMEN' NO. = A-65-24.L1
NO. OF DATA = 17
R=-1.00
SMAX= 80.0 MPa
surface crack

	CYCLE(X1000)	CRK L. 2a(mm)	AVG. a(mm)	DELK(MPa-M)	DADN(mm/CYCLE)
0	40	0.033	0.000	0.00	0.000 X1.E-6
1	45	0.044	0.019	2.78	1.100 X1.E-6
2	50	0.093	0.034	3.67	4.900 X1.E-6
3	55	0.109	0.050	4.41	1.600 X1.E-6
4	65	0.131	0.060	4.78	1.100 X1.E-6
5	70	0.191	0.080	5.47	6.000 X1.E-6
6	75	0.251	0.111	6.32	6.000 X1.E-6
7	80	0.338	0.147	7.20	8.700 X1.E-6
8	85	0.382	0.180	7.88	4.400 X1.E-6
9	90	0.409	0.198	8.23	2.700 X1.E-6
10	95	0.480	0.222	8.67	7.100 X1.E-6
11	100	0.698	0.294	9.85	21.800 X1.E-6
12	105	1.046	0.436	11.77	34.800 X1.E-6
13	110	1.117	0.541	12.97	7.100 X1.E-6
14	115	1.613	0.683	14.41	49.600 X1.E-6
15	120	2.027	0.910	16.49	41.400 X1.E-6

** DA/DN DATA **

SPECIMEN' NO. = A-65-24.L2
NO. OF DATA = 14
R=-1.00
SMAX= 80.0 MPa
surface crack

	CYCLE(X1000)	CRK L. 2a(mm)	AVG. a(mm)	DELK(MPa-M)	DADN(mm/CYCLE)
0	40	0.016	0.000	0.00	0.000 X1.E-6
1	45	0.022	0.009	1.97	0.600 X1.E-6
2	50	0.033	0.014	2.36	1.100 X1.E-6
3	60	0.038	0.018	2.67	0.250 X1.E-6
4	65	0.055	0.023	3.05	1.700 X1.E-6
5	70	0.087	0.036	3.73	3.200 X1.E-6
6	75	0.136	0.056	4.62	4.900 X1.E-6
7	80	0.158	0.073	5.25	2.200 X1.E-6
8	90	0.229	0.097	5.95	3.550 X1.E-6
9	95	0.240	0.117	6.50	1.100 X1.E-6
10	100	0.245	0.121	6.60	0.500 X1.E-6
11	105	0.321	0.141	7.07	7.600 X1.E-6
12	110	0.332	0.163	7.55	1.100 X1.E-6
13	120	0.343	0.169	7.66	0.550 X1.E-6

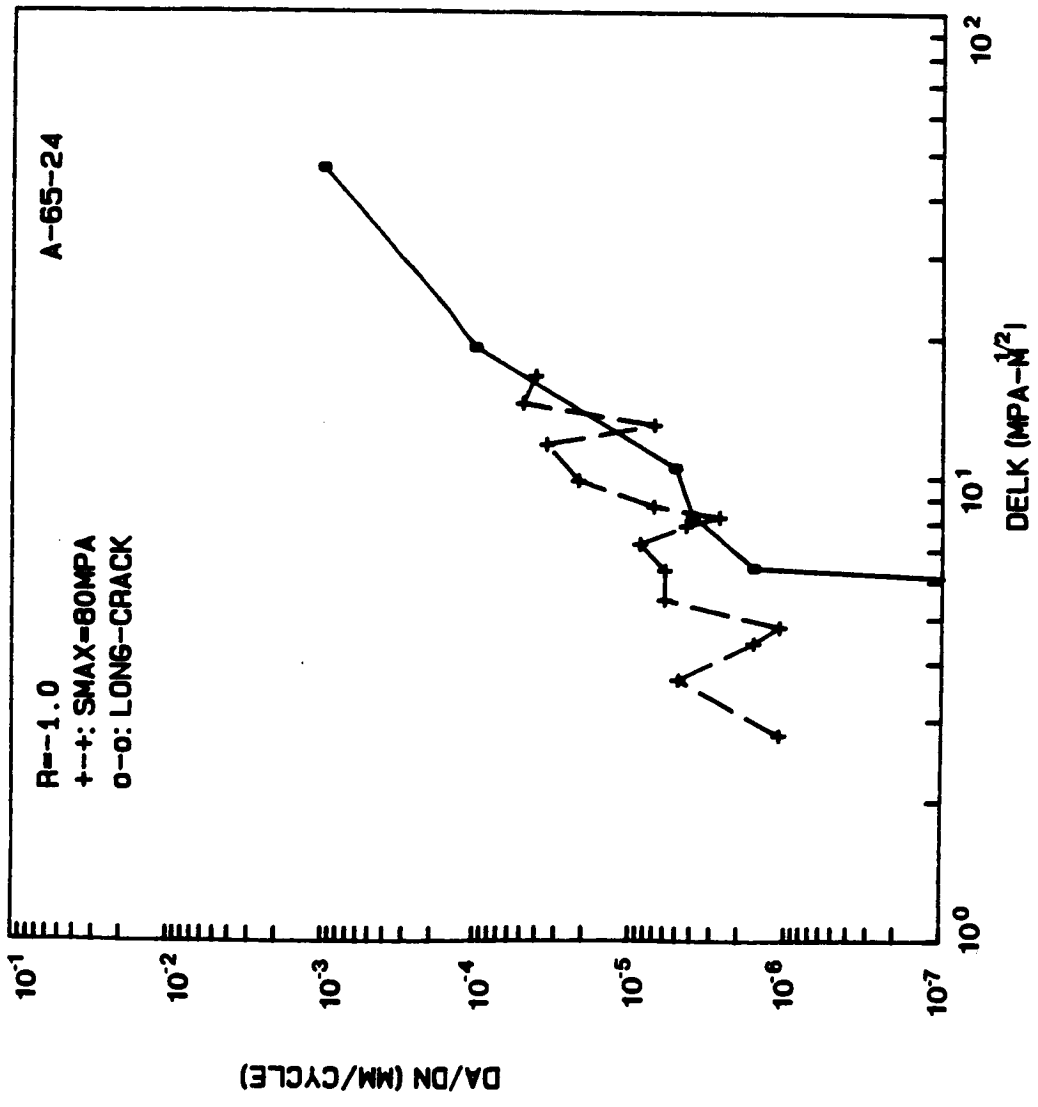
A-65-24
R=-1.0
+--+: SMAX=80MPA
o-o: LONG-CRACK
DA/DN (MM/CYCLE)
DELK (MPA-M^1/2)
10^-1
10^-2
10^-3
10^-4
10^-5
10^-6
10^-7
10^0
10^1
10^2

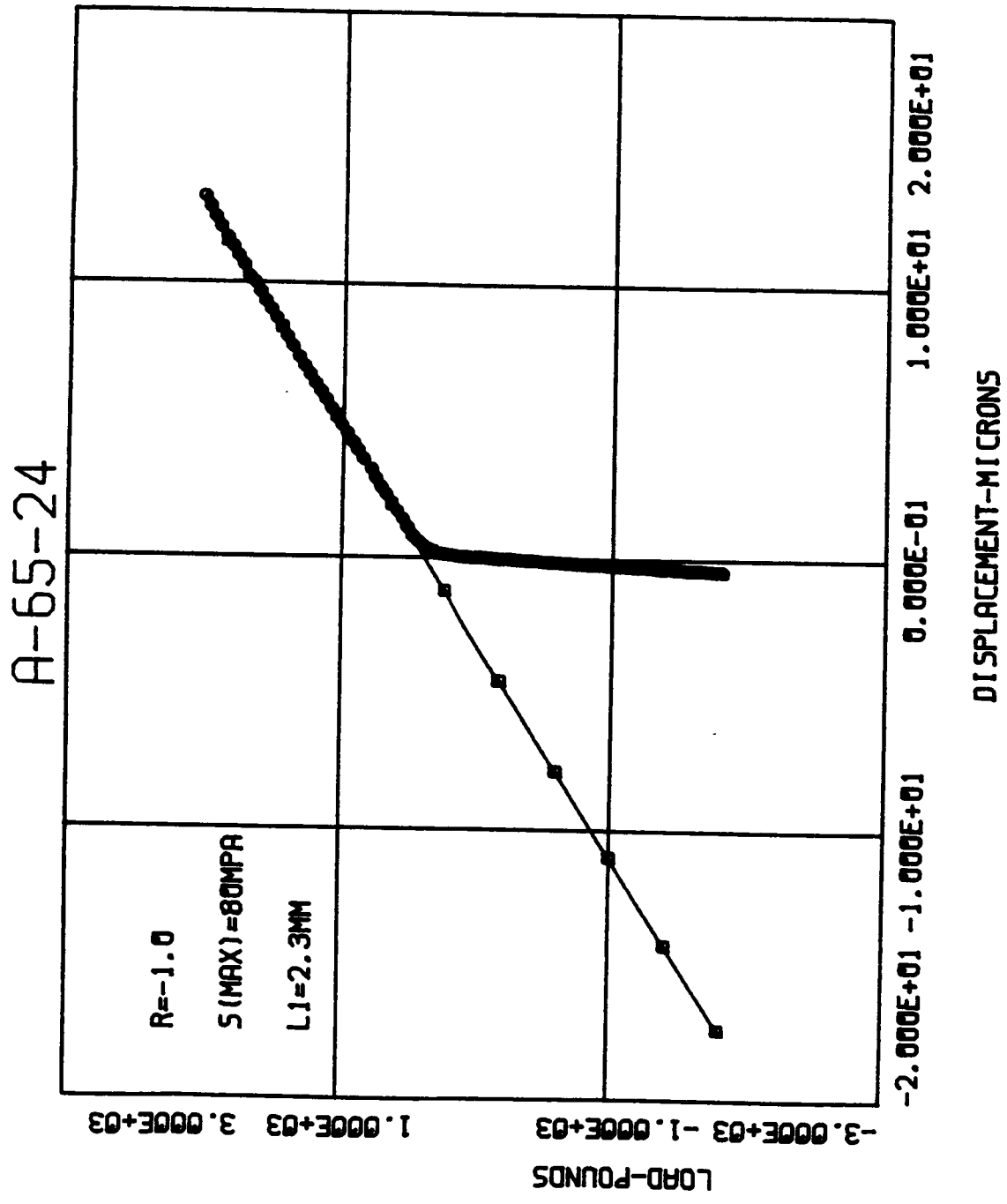
A-65-24
R=-1.0
S(MAX)=80MPA
L1=2.3MM
LOAD-POUNDS
3.000E+03
1.000E+03
-1.000E+03
-3.000E+03
-2.000E+01
-1.000E+01
0.000E-01
1.000E+01
2.000E+01
DISPLACEMENT-MICRONS

A-65-24

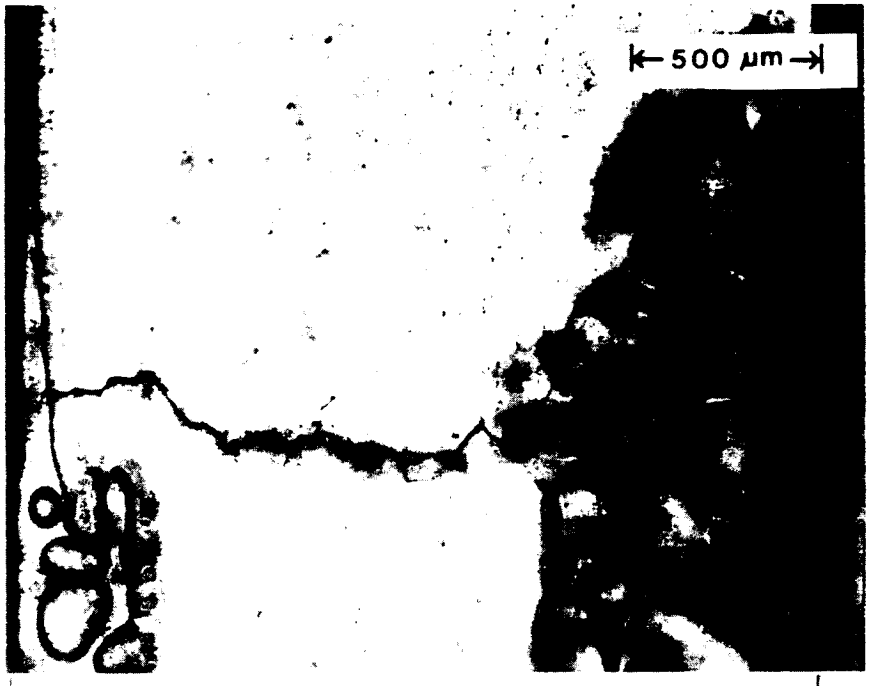

A-65-24

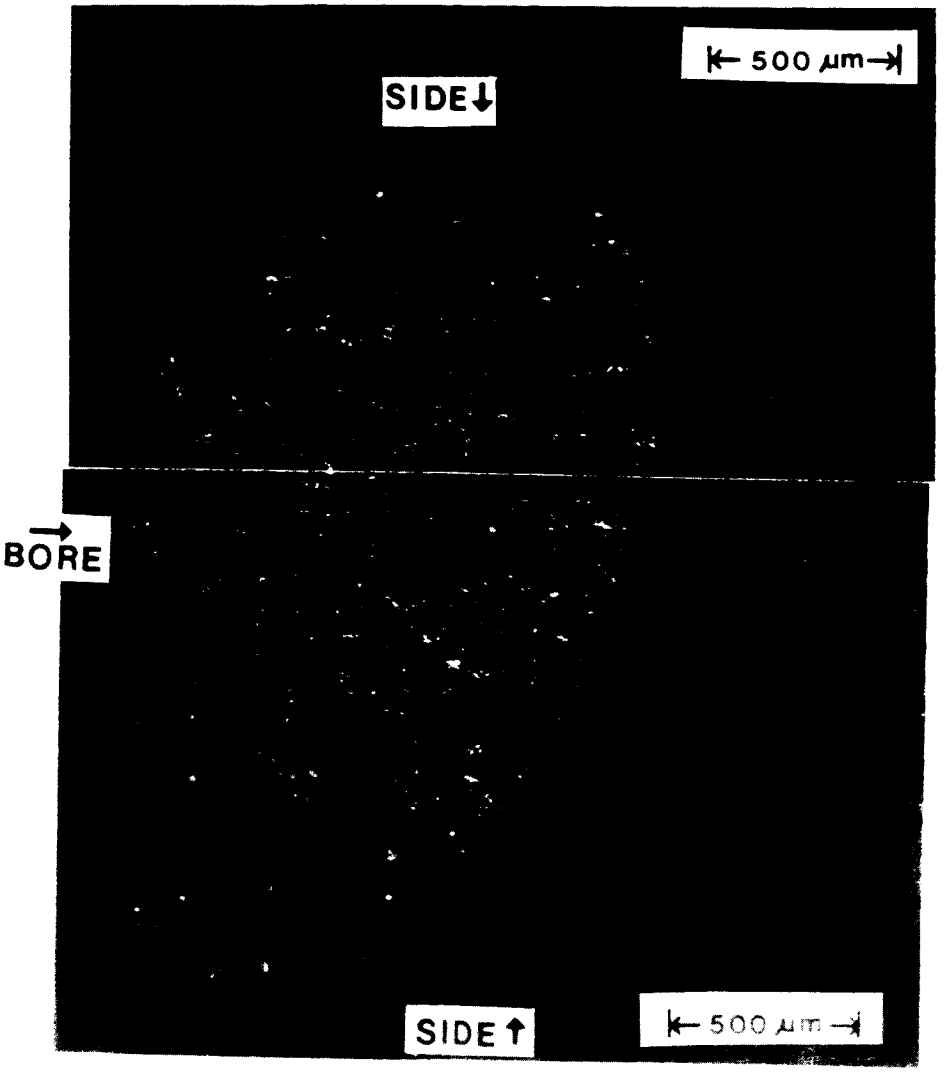

TEST DATA

SPECIMEN NUMBER: A-72-07

DATE: 7/2/85

PARTICIPANT'S NAME: Joo-Jin Lee

John Cieslowski

TEST TEMPERATURE: 27°C

RELATIVE HUMIDITY: 58 %

WAVEFORM TYPE: Sinusoidal wave, 20 Hz

LOADING SEQUENCE TYPE: Constant amplitude

R-RATIO = -1.0

S max = 80 MPa

S min = -80 MPa

FINAL LENGTH OF CRACK: 0.05 mm

COMMENTS:

Specimen couldn't be broken statically to examine the fracture surface.

→ No photo of fracture surface is available.

AGARD Short Crack DATA CHART

Record of crack lengths and map

Page 1 of -1 Loading Type R = -1 Const. Amplitude

Specimen no A-72-07 Peak Stress 80 MPa

0.1mm grid

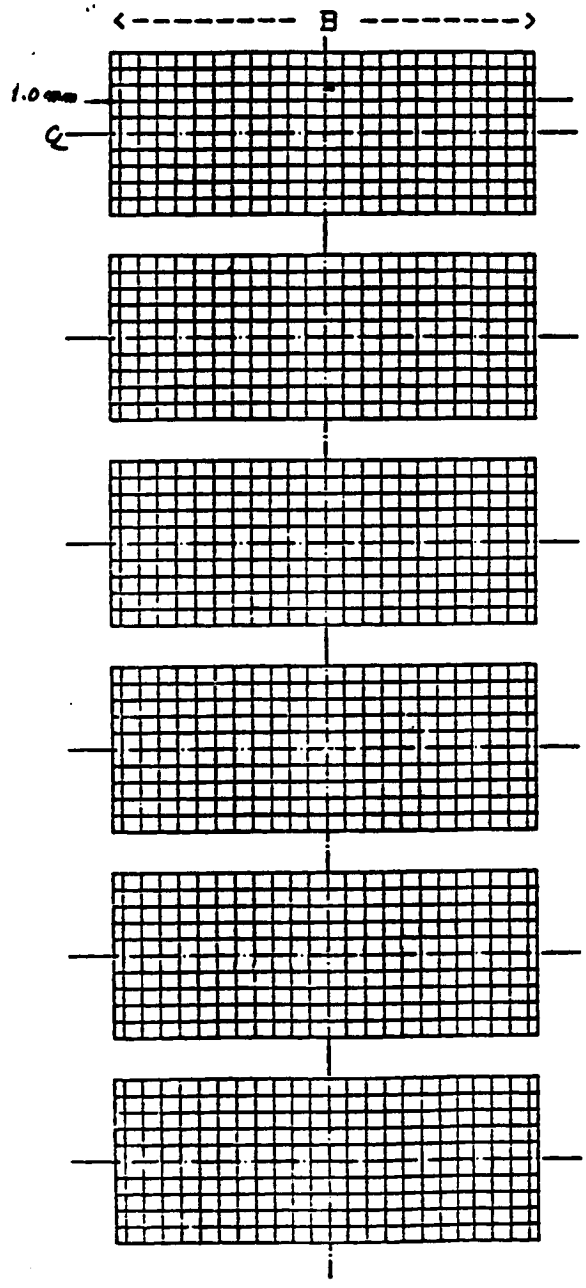

40k Cycles
L1 .050 mm
L2 _____ mm
L3 _____ mm
L4 _____ mm
L5 _____ mm

_____ Cycles
L1 _____ mm
L2 _____ mm
L3 _____ mm
L4 _____ mm
L5 _____ mm

_____ Cycles
L1 _____ mm
L2 _____ mm
L3 _____ mm
L4 _____ mm
L5 _____ mm

_____ Cycles
L1 _____ mm
L2 _____ mm
L3 _____ mm
L4 _____ mm
L5 _____ mm

_____ Cycles
L1 _____ mm
L2 _____ mm
L3 _____ mm
L4 _____ mm
L5 _____ mm

_____ Cycles
L1 _____ mm
L2 _____ mm
L3 _____ mm
L4 _____ mm
L5 _____ mm

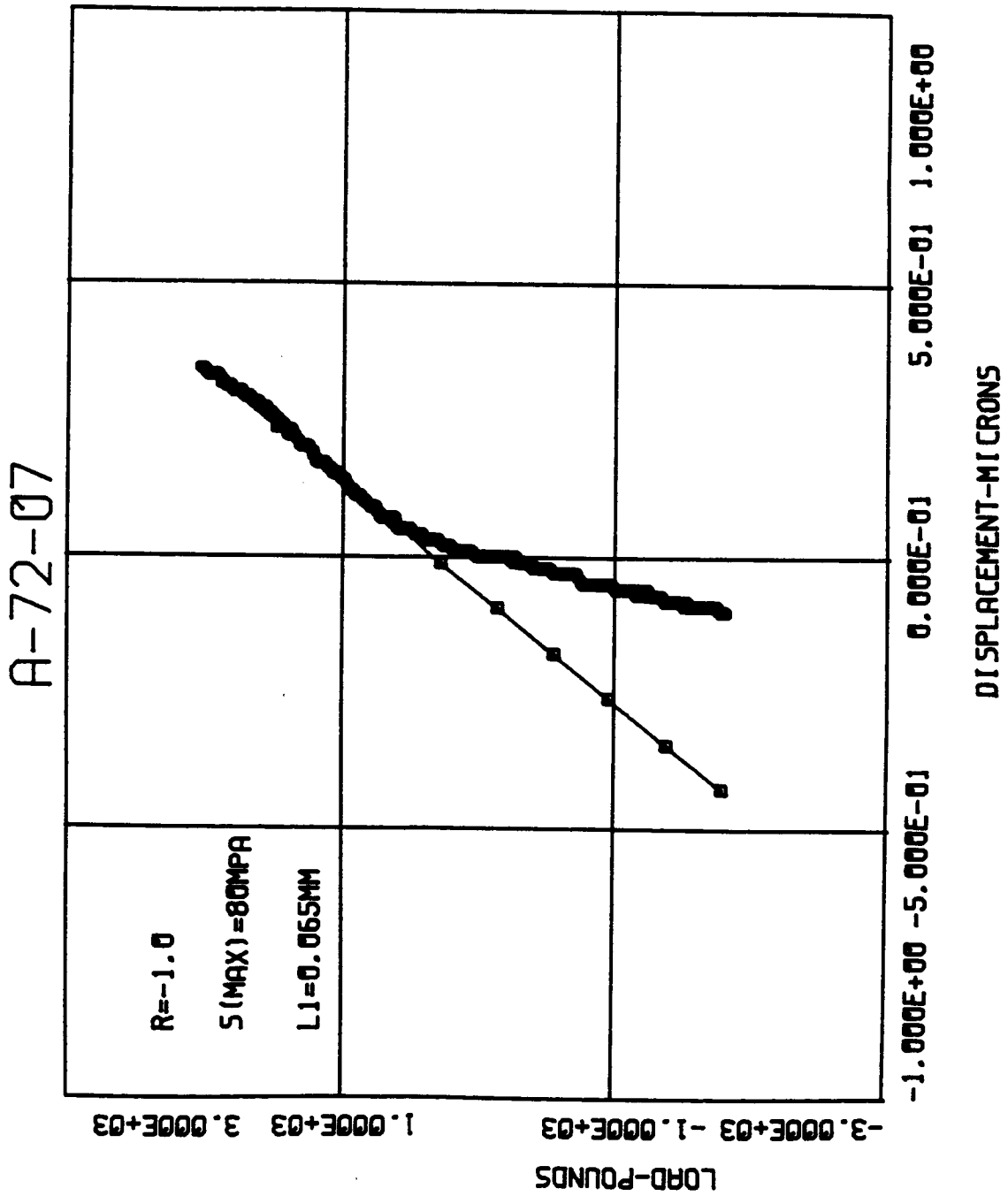
A-72-07
R=-1.0
S(MAX)=80MPA
L1=0.065MM
LOAD-POUNDS
-3.000E+03
-1.000E+03
1.000E+03
3.000E+03
-1.000E+00
-5.000E-01
0.000E-01
5.000E-01
1.000E+00
DISPLACEMENT-MICRONS

A-72-07

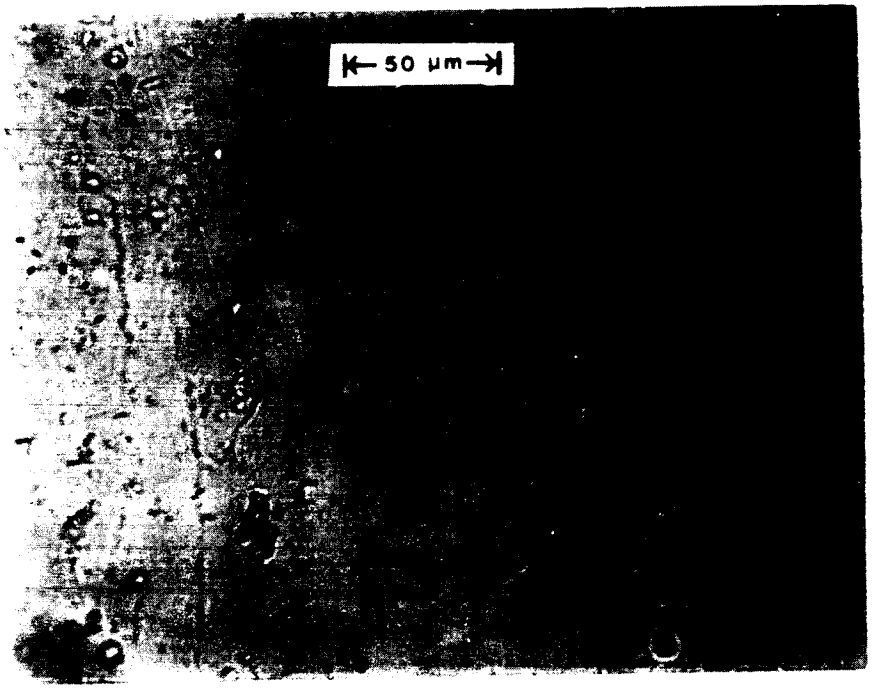

Replica

TEST DATA

SPECIMEN NUMBER: A-55-08

DATE: 7/9/85

PARTICIPANT'S NAME: Joo-Jin Lee

John Cieslowski

TEST TEMPERATURE: 27°C

RELATIVE HUMIDITY: 61 %

WAVEFORM TYPE: Sinusoidal wave, 20 Hz

LOADING SEQUENCE TYPE: Constant amplitude

R-RATIO = -1.0

S max = 70 MPa

S min = -70 MPa

FINAL LENGTH OF CRACK: 2.3 mm (Thru thickness) · L1

COMMENTS:

AGARD Short Crack DATA CHART

Record of crack lengths and map

Page 1 of 3 Loading Type Constant Amplitude R = -1

Specimen no A-55-08 Peak Stress 70 MPa

0.1mm grid

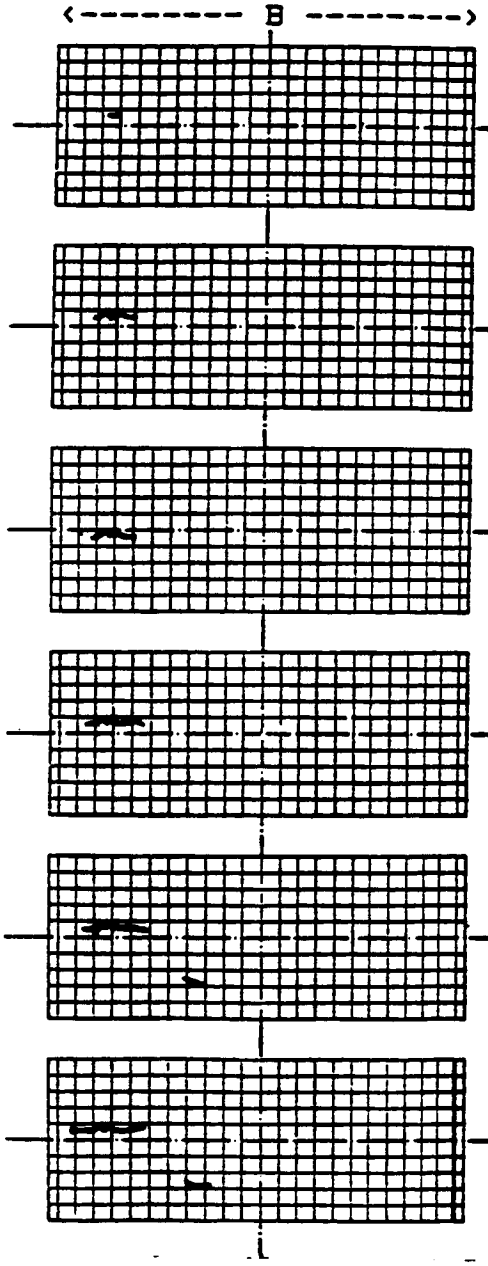

120K Cycles
L1 .265 mm
L2 ____ mm
L3 ____ mm
L4 ____ mm
L5 ____ mm

150K Cycles
L1 .213 mm
L2 ____ mm
L3 ____ mm
L4 ____ mm
L5 ____ mm

160K Cycles
L1 .202 mm
L2 ____ mm
L3 ____ mm
L4 ____ mm
L5 ____ mm

170K Cycles
L1 .316 mm
L2 ____ mm
L3 ____ mm
L4 ____ mm
L5 ____ mm

180K Cycles
L1 .338 mm
L2 .099 mm
L3 ____ mm
L4 ____ mm
L5 ____ mm

190K Cycles
L1 .420 mm
L2 .136 mm
L3 ____ mm
L4 ____ mm
L5 ____ mm

AGARD Short Crack DATA CHART

Record of crack lengths and map

Page 2 of 3 Loading Type R=-1

Specimen no A-55-09 Peak Stress 70 MPa

0.1mm grid

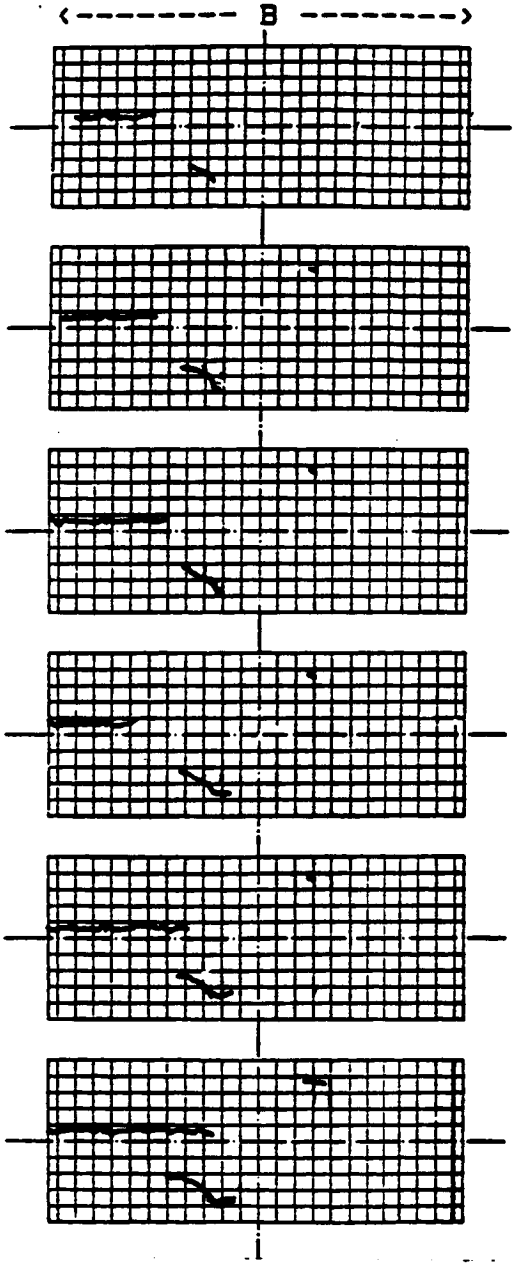

200 K Cycles
L1 .452 mm
L2 .158 mm
L3 ____ mm
L4 ____ mm
L5 ____ mm

210 K Cycles
L1 .512 mm
L2 .207 mm
L3 .033 mm
L4 ____ mm
L5 ____ mm

220 K Cycles
L1 .632 mm
L2 .218 mm
L3 .033 mm
L4 ____ mm
L5 ____ mm

230 K Cycles
L1 .659 mm
L2 .298 mm
L3 .033 mm
L4 ____ mm
L5 ____ mm

240 K Cycles
L1 .763 mm
L2 .305 mm
L3 .038 mm
L4 ____ mm
L5 ____ mm

250K Cycles
L1 .899 mm
L2 .349 mm
L3 .131 mm
L4 ____ mm
L5 ____ mm

AGARD Short Crack DATA CHART

Record of crack lengths and map

Page 3 of 3 Loading Type R=-1

Specimen no A-55-08 Peak Stress 70 MPa

0.1mm grid

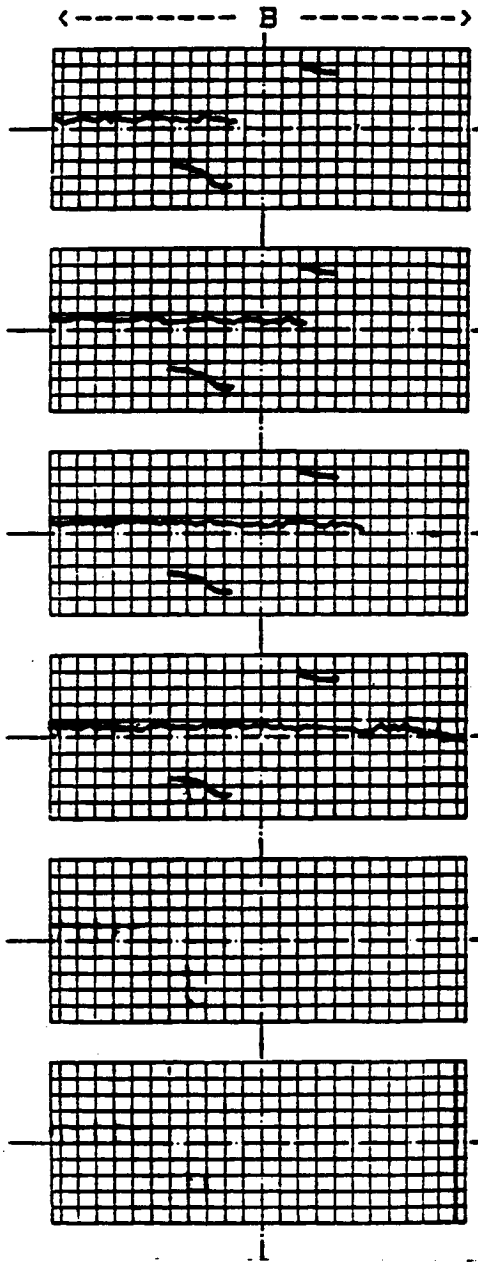

260 K Cycles
L1 1.079 mm
L2 .324 mm
L3 .170 mm
L4 _____ mm
L5 _____ mm

270 K Cycles
L1 1.363 mm
L2 .305 mm
L3 .170 mm
L4 _____ mm
L5 _____ mm

280 K Cycles
L1 1.700 mm
L2 .294 mm
L3 .201 mm
L4 .022 mm
L5 _____ mm

290K Cycles
L1 THRU mm
L2 .300 mm
L3 * mm
L4 L1 mm
L5 _____ mm

_____ Cycles
L1 _____ mm
L2 _____ mm
L3 _____ mm
L4 _____ mm
L5 _____ mm

_____ Cycles
L1 _____ mm
L2 _____ mm
L3 _____ mm
L4 _____ mm
L5 _____ mm

* Crack tip was not clear

** DA/DN DATA **

SPECIMEN' NO. = A-55-08.L1
NO. OF DATA = 15
R=-1.00
SMAX= 70.0 MPa
near edge → corner crack @ 220k

	CYCLE(X1000)	CRK L. 2a(mm)	AVG. a(mm)	DELK(MPa-M)	DADN(mm/CYCLE)
0	120	0.065	0.000	0.00	0.000 X1.E-6
1	150	0.213	0.069	4.48	2.467 X1.E-6
2	170	0.316	0.132	6.00	2.575 X1.E-6
3	180	0.338	0.163	6.61	1.100 X1.E-6
4	190	0.420	0.190	7.06	4.100 X1.E-6
5	200	0.452	0.218	7.52	1.600 X1.E-6
6	210	0.512	0.241	7.87	3.000 X1.E-6
7	220	0.632	0.286	8.51	6.000 X1.E-6
8	230	0.659	0.323	8.99	1.350 X1.E-6
9	240	0.763	0.355	9.39	5.200 X1.E-6
10	250	0.899	0.415	10.08	6.800 X1.E-6
11	260	1.079	0.495	10.90	9.000 X1.E-6
12	270	1.363	0.610	11.99	14.200 X1.E-6
13	280	1.700	0.766	13.29	16.850 X1.E-6
14	290	2.250	0.988	15.02	27.500 X1.E-6

** DA/DN DATA **

SPECIMEN' NO. = A-55-08.L2
NO. OF DATA = 8
R=-1.00
SMAX= 70.0 MPa
Surface Crack

	CYCLE(X1000)	CRK L. 2a(mm)	AVG. a(mm)	DELK(MPa-M)	DADN(mm/CYCLE)
0	180	0.098	0.000	0.00	0.000 X1.E-6
1	190	0.136	0.058	4.13	1.900 X1.E-6
2	200	0.158	0.073	4.59	1.100 X1.E-6
3	210	0.207	0.091	5.07	2.450 X1.E-6
4	220	0.218	0.106	5.44	0.550 X1.E-6
5	230	0.288	0.126	5.88	3.500 X1.E-6
6	240	0.305	0.148	6.32	0.850 X1.E-6
7	250	0.349	0.163	6.61	2.200 X1.E-6

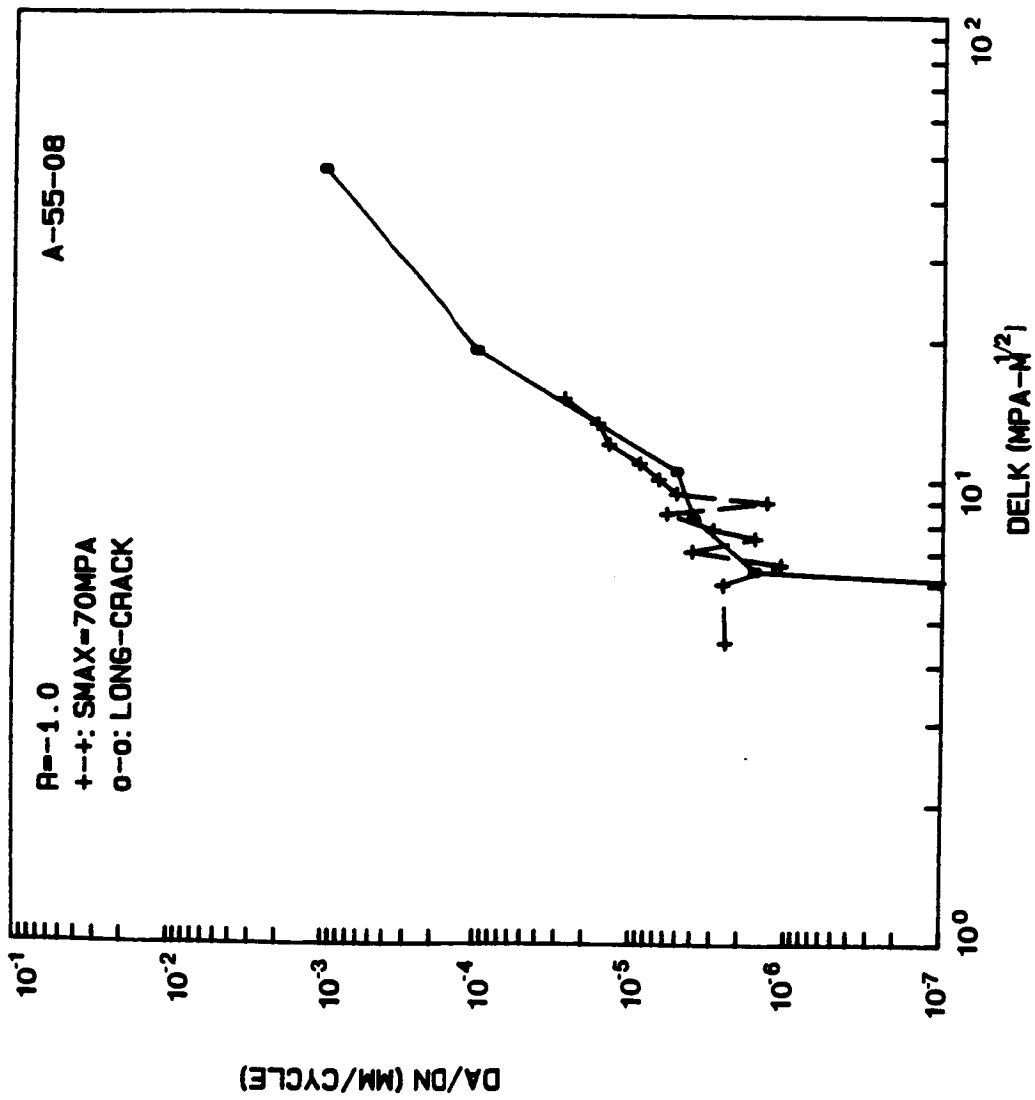
A-55-08
R=-1.0
+-+: SMAX=70MPA
o-o: LONG-CRACK
DA/DN (MM/CYCLE)
DELK (MPA-M^1/2)
10^-1
10^-2
10^-3
10^-4
10^-5
10^-6
10^-7
10^0
10^1
10^2

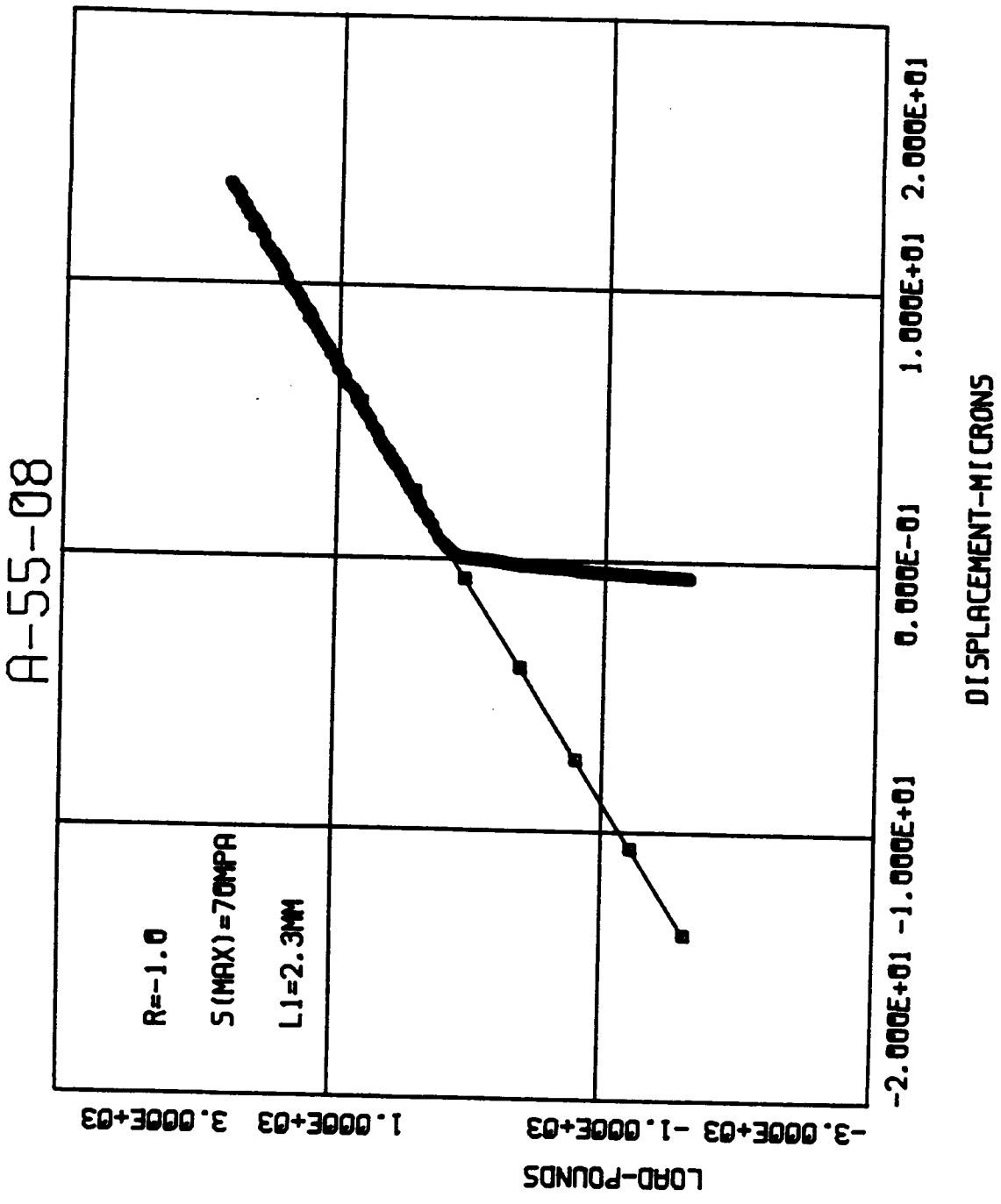
A-55-08
R=-1.0
S(MAX)=70MPA
L1=2.3MM
LOAD-POUNDS
-3.000E+03
-1.000E+03
1.000E+03
3.000E+03
-2.000E+01
-1.000E+01
0.000E-01
1.000E+01
2.000E+01
DISPLACEMENT-MICRONS

A-55-08

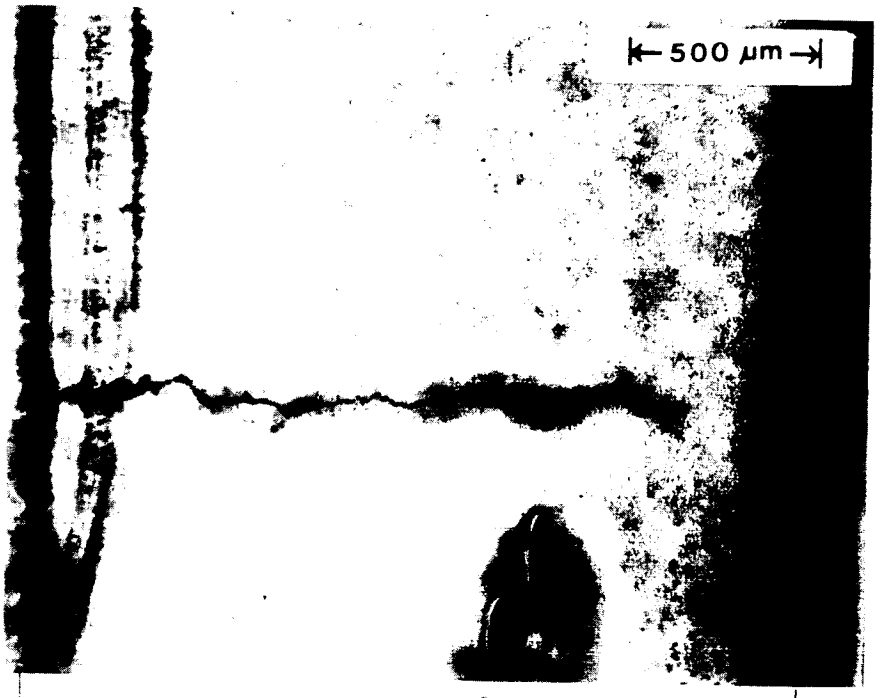

Replica @ 285K cycles

2.3mm

A-55-08

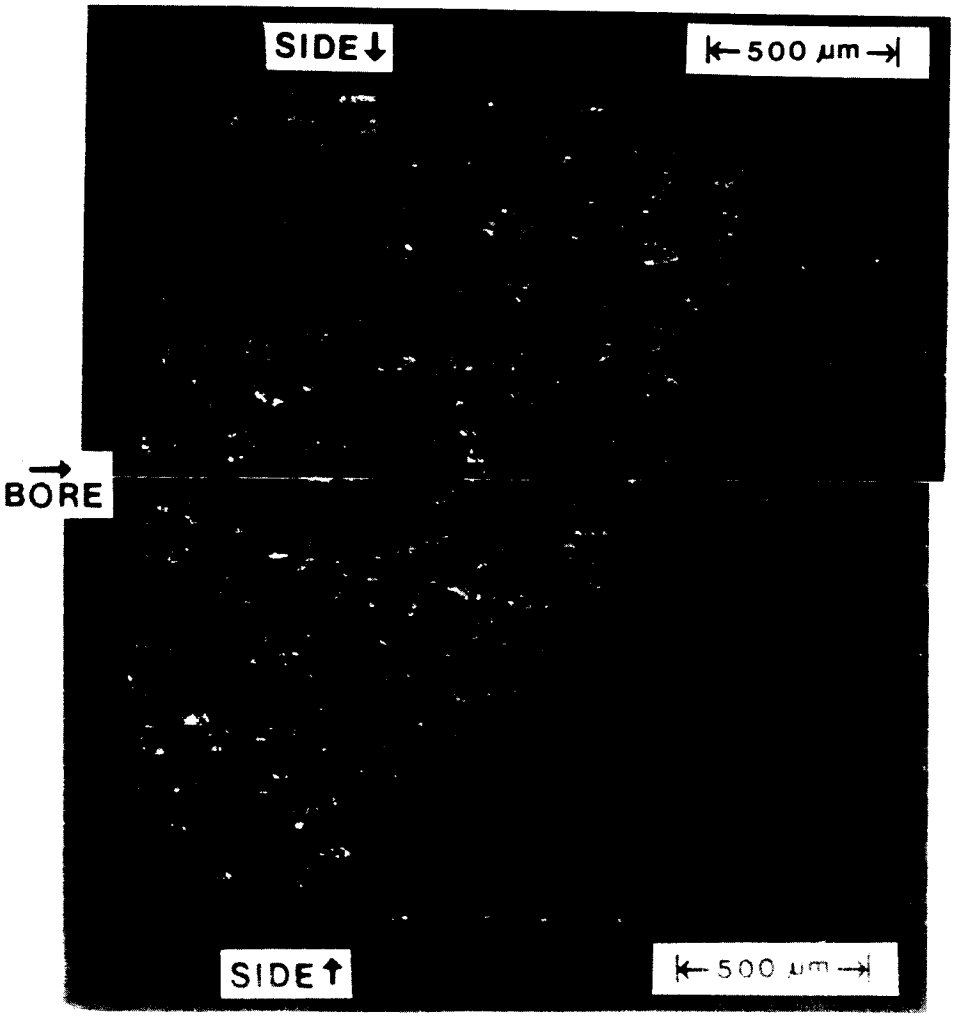

TEST DATA

SPECIMEN NUMBER: A-83-23

DATE: 6/26/85

PARTICIPANT'S NAME: Joo-Jin Lee

John Cieslowski

TEST TEMPERATURE: 26°C

RELATIVE HUMIDITY: 41 %

WAVEFORM TYPE: Sinusoidal wave, 20 Hz

LOADING SEQUENCE TYPE: Constant amplitude

R-RATIO = -1.0

S max = 70 MPa

S min = -70 MPa

FINAL LENGTH OF CRACK: 0.382 mm (L1)

COMMENTS:

AGARD Short Crack DATA CHART

Record of crack lengths and map

Page 1 of 2
Specimen no A-83-23

Loading Type const. Amplitude R=-1
Peak Stress 70 MPa

0.1mm grid

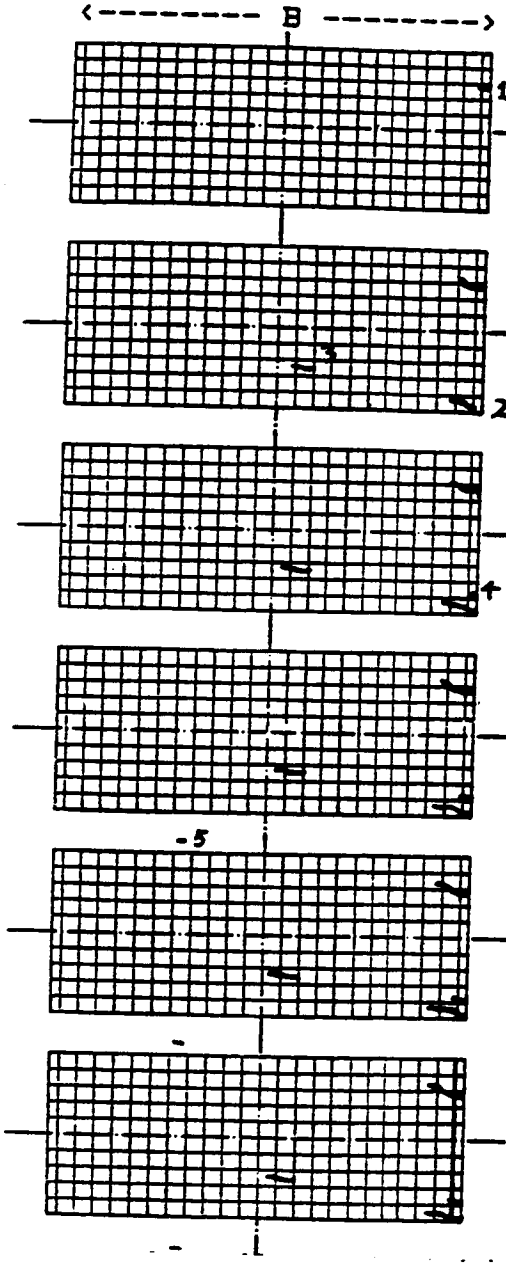

70K Cycles
L1 .044 mm
L2 ____ mm
L3 ____ mm
L4 ____ mm
L5 ____ mm

80 K Cycles
L1 .131 mm
L2 .147 mm
L3 .076 mm
L4 ____ mm
L5 ____ mm

90 K Cycles
L1 .169 mm
L2 .196 mm
L3 .147 mm
L4 .038 mm
L5 ____ mm

100 K Cycles
L1 .196 mm
L2 .207 mm
L3 .147 mm
L4 .055 mm
L5 .099 mm

110 K Cycles
L1 .196 mm
L2 .213 mm
L3 .169 mm
L4 .060 mm
L5 .055 mm

120 K Cycles
L1 .261 mm
L2 .240 mm
L3 .174 mm
L4 .060 mm
L5 .055 mm

C-4

AGARD Short Crack DATA CHART

Record of crack lengths and map

Page 2 of 2 Loading Type Const. Amplitude R=-1

Specimen no A-83-23 Peak Stress: 70 MPa

0.1mm grid

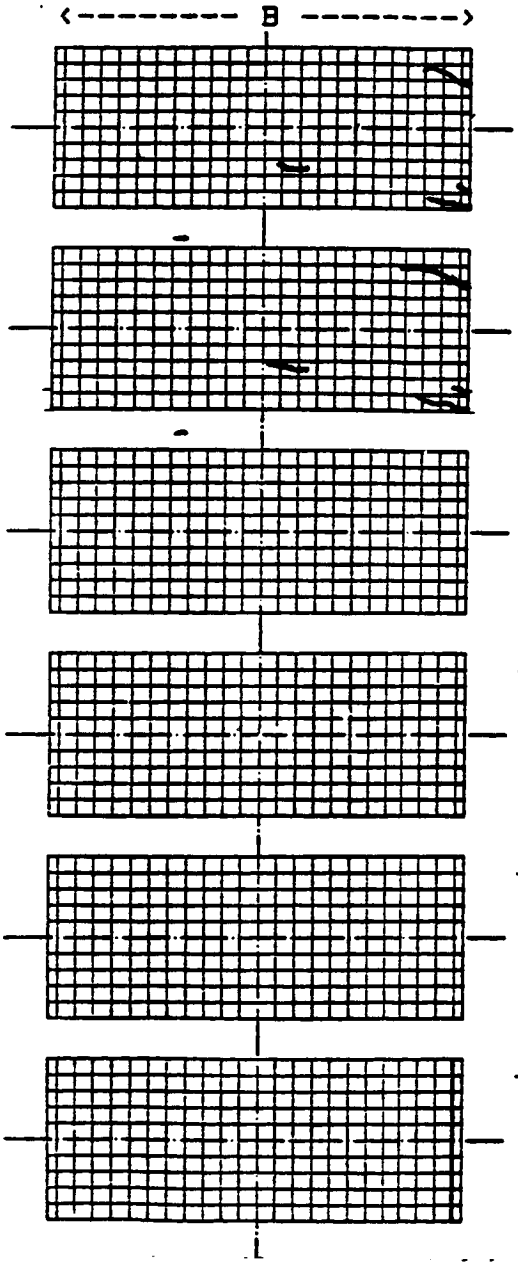

130 K Cycles
L1 .278 mm
L2 .240 mm
L3 .213 mm
L4 .060 mm
L5 .060 mm

140 K Cycles
L1 .382 mm
L2 .267 mm
L3 .229 mm
L4 .082 mm
L5 .065 mm

_____ Cycles
L1 _____ mm
L2 _____ mm
L3 _____ mm
L4 _____ mm
L5 _____ mm

_____ Cycles
L1 _____ mm
L2 _____ mm
L3 _____ mm
L4 _____ mm
L5 _____ mm

_____ Cycles
L1 _____ mm
L2 _____ mm
L3 _____ mm
L4 _____ mm
L5 _____ mm

_____ Cycles
L1 _____ mm
L2 _____ mm
L3 _____ mm
L4 _____ mm
L5 _____ mm

** DA/DN DATA **

SPECIMEN' NO. = A-83-23.L1
NO. OF DATA = 7
R=-1.00
SMAX= 70.0 MPa
Corner Crack

	CYCLE(X1000)	CRK L. 2a(mm)	AVG. a(mm)	DELK(MPa-M)	DADN(mm/CYCLE)
0	70	0.044	0.000	0.00	0.000 X1.E-6
1	80	0.131	0.087	4.91	8.700 X1.E-6
2	90	0.169	0.150	6.30	3.800 X1.E-6
3	100	0.196	0.183	6.89	2.700 X1.E-6
4	120	0.261	0.228	7.62	3.250 X1.E-6
5	130	0.278	0.269	8.20	1.700 X1.E-6
6	140	0.382	0.330	8.97	10.400 X1.E-6

** DA/DN DATA **

SPECIMEN' NO. = A-83-23.L2
NO. OF DATA = 6
R=-1.00
SMAX= 70.0 MPa
Corner Crack

	CYCLE(X1000)	CRK L. 2a(mm)	AVG. a(mm)	DELK(MPa-M)	DADN(mm/CYCLE)
0	80	0.147	0.000	0.00	0.000 X1.E-6
1	90	0.196	0.171	6.70	4.900 X1.E-6
2	100	0.207	0.201	7.20	1.100 X1.E-6
3	110	0.213	0.210	7.34	0.600 X1.E-6
4	120	0.240	0.227	7.59	2.700 X1.E-6
5	140	0.267	0.253	7.98	1.350 X1.E-6

** DA/DN DATA **

SPECIMEN' NO. = A-83-23.L3
NO. OF DATA = 6
R=-1.00
SMAX= 70.0 MPa
Surface Crack

	CYCLE(X1000)	CRK L. 2a(mm)	AVG. a(mm)	DELK(MPa-M)	DADN(mm/CYCLE)
0	80	0.076	0.000	0.00	0.000 X1.E-6
1	90	0.147	0.056	4.04	3.550 X1.E-6
2	110	0.169	0.079	4.75	0.550 X1.E-6
3	120	0.174	0.086	4.93	0.250 X1.E-6
4	130	0.213	0.097	5.21	1.950 X1.E-6
5	140	0.229	0.111	5.53	0.800 X1.E-6

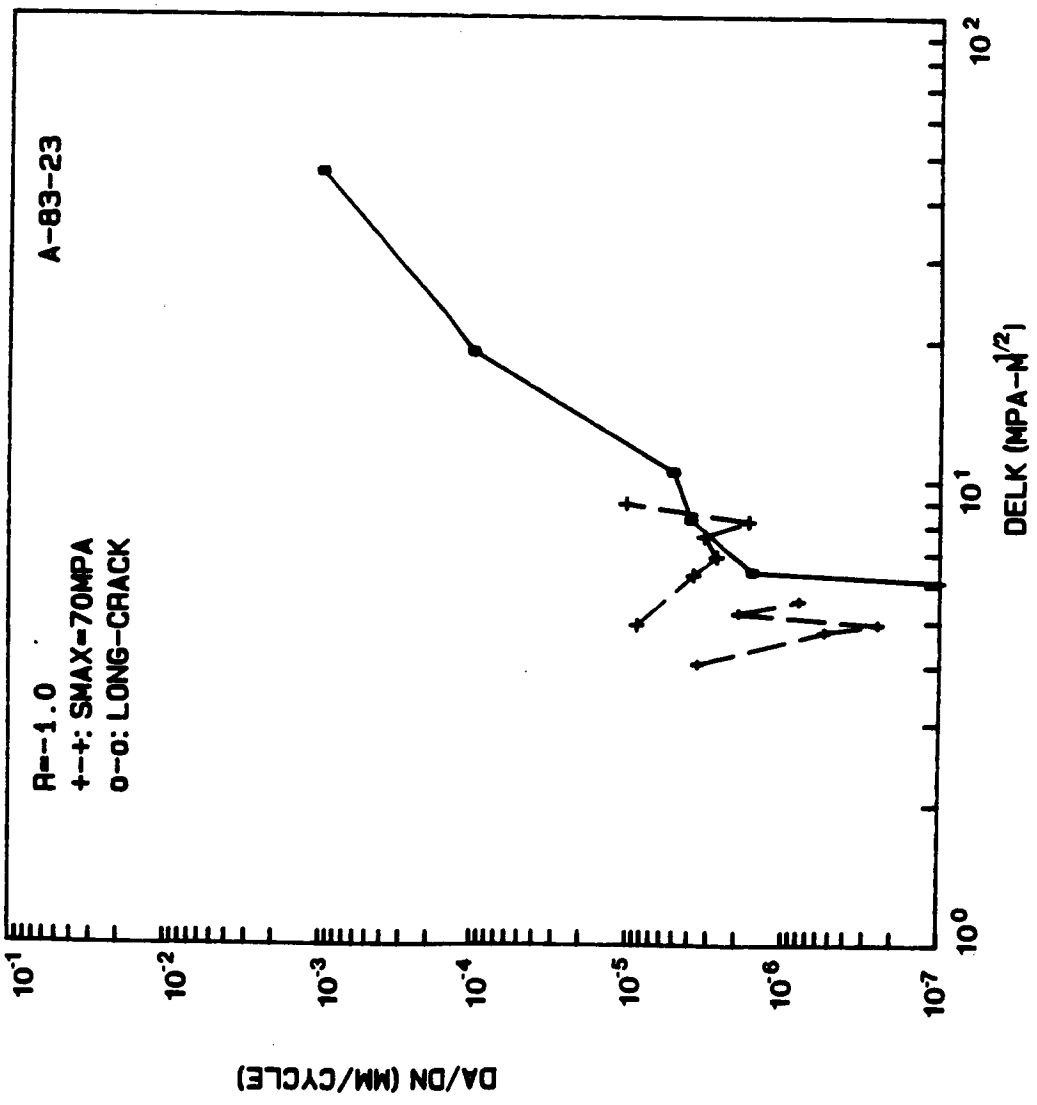
A-83-23
R=-1.0
+--+: SMAX=70MPA
o--o: LONG-CRACK
DA/DN (MM/CYCLE)
DELK (MPA-M^1/2)
10^-1
10^-2
10^-3
10^-4
10^-5
10^-6
10^-7
10^0
10^1
10^2

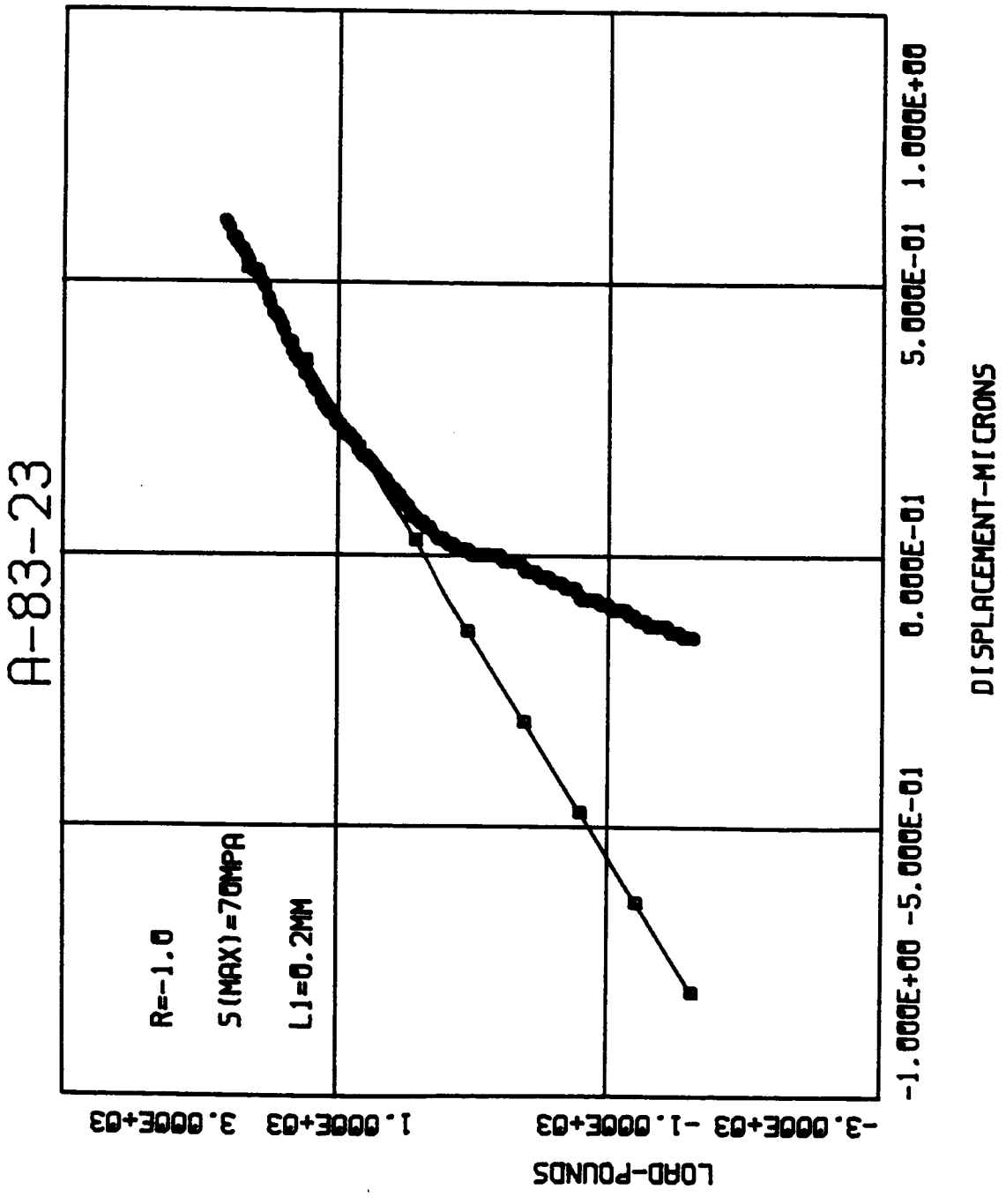
A-83-23
R=-1.0
S(MAX)=70MPA
LI=0.2MM
LOAD-POUNDS
-3.000E+03
-1.000E+03
1.000E+03
3.000E+03
-1.000E+00
-5.000E-01
0.000E-01
5.000E-01
1.000E+00
DISPLACEMENT-MICRONS

A-83-23

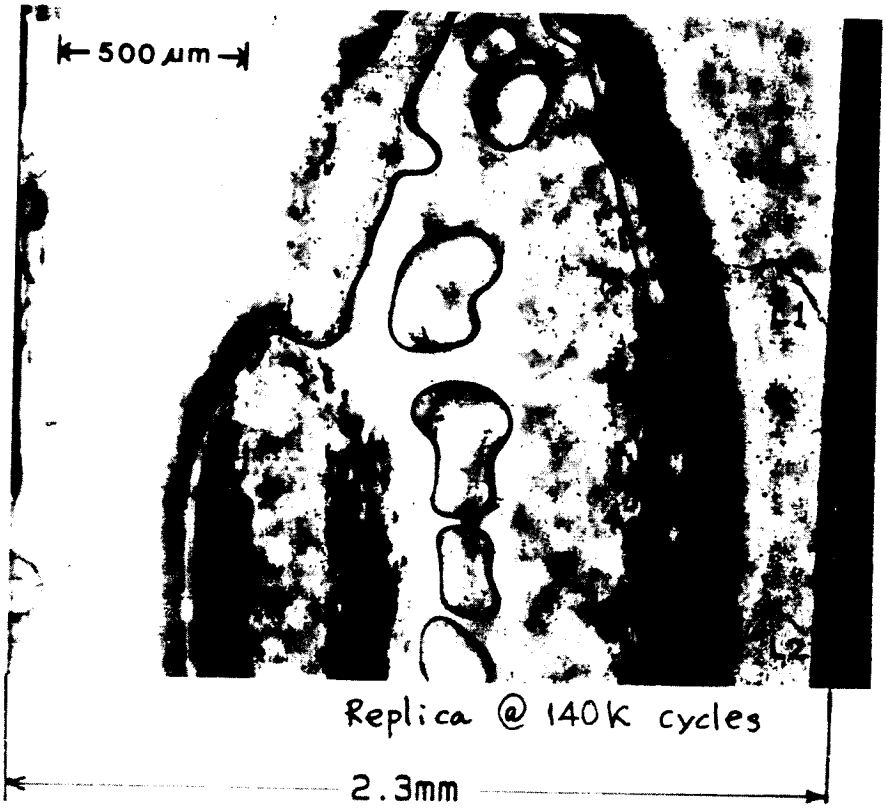

A-83-23

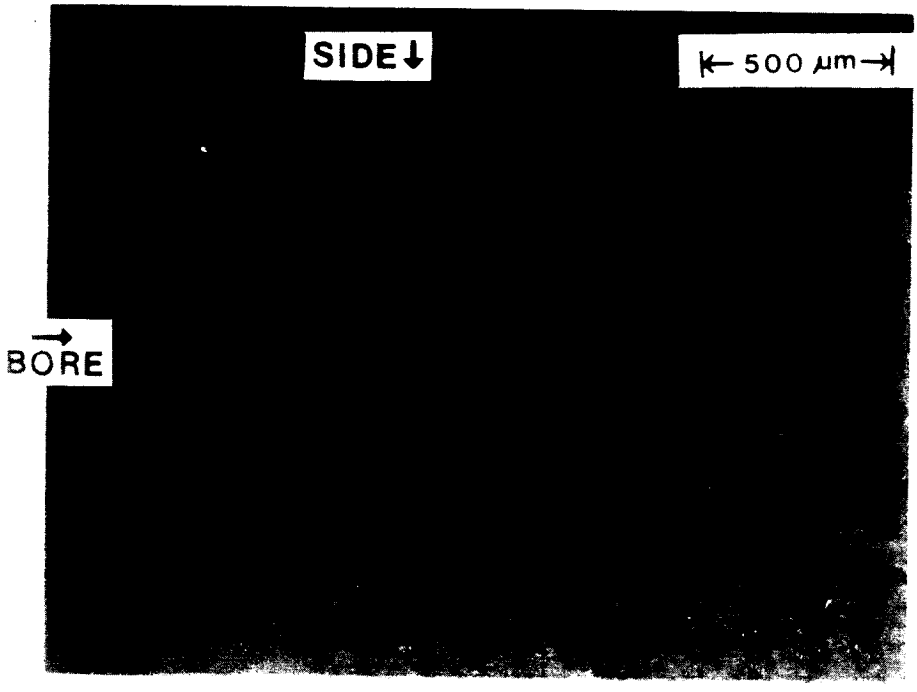

TEST DATA

SPECIMEN NUMBER: A-52-21

DATE: 7/12/85

PARTICIPANT'S NAME: Joo-Jin Lee

John Cieslowski

TEST TEMPERATURE: 27°C

RELATIVE HUMIDITY: 61 %

WAVEFORM TYPE: Sinusoidal wave, 20 Hz

LOADING SEQUENCE TYPE: Constant amplitude

R-RATIO = -2.0

S max = 75MPa

S min = -150MPa

FINAL LENGTH OF CRACK: 2.3mm (Thru thickness) - L1

COMMENTS:

AGARD Short Crack DATA CHART

Record of crack lengths and map

Page 1 of 2 Loading Type Const. Amplitude R=-2

Specimen no A-52-21 Peak Stress 75 MPa

0.1mm grid

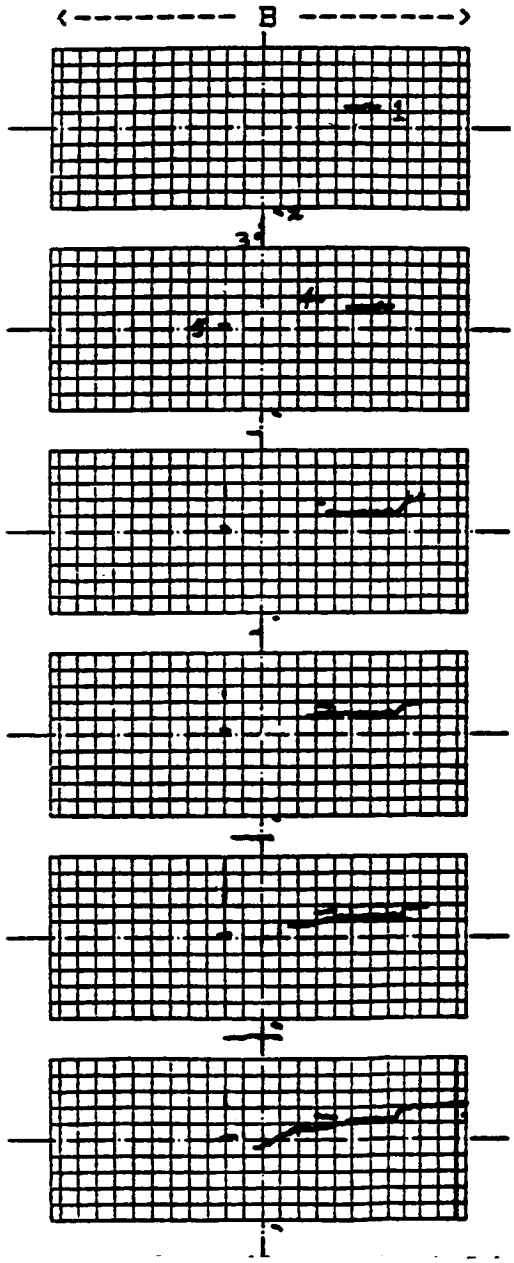

2K Cycles
L1 .180 mm
L2 .027 mm
L3 ____ mm
L4 ____ mm
L5 ____ mm

4K Cycles
L1 .267 mm
L2 .027 mm
L3 .033 mm
L4 .027 mm
L5 .033 mm

6K Cycles
L1 .419 mm
L2 .027 mm
L3 .076 mm
L4 .055 mm
L5 .033 mm

8K Cycles
L1 .605 mm
L2 .027 mm
L3 .076 mm
L4 .093 mm
L5 .049 mm

10K Cycles
L1 .796 mm
L2 .055 mm
L3 .293 mm
L4 .114 mm
L5 .060 mm

12K Cycles
L1 1.237 mm
L2 .055 mm
L3 .316 mm
L4 .109 mm
L5 .060 mm

AGARD Short Crack DATA CHART

Record of crack lengths and map

Page 2 of 2 Loading Type R=-2

Specimen no A-52-21 Peak Stress 75 MPa

0.1mm grid

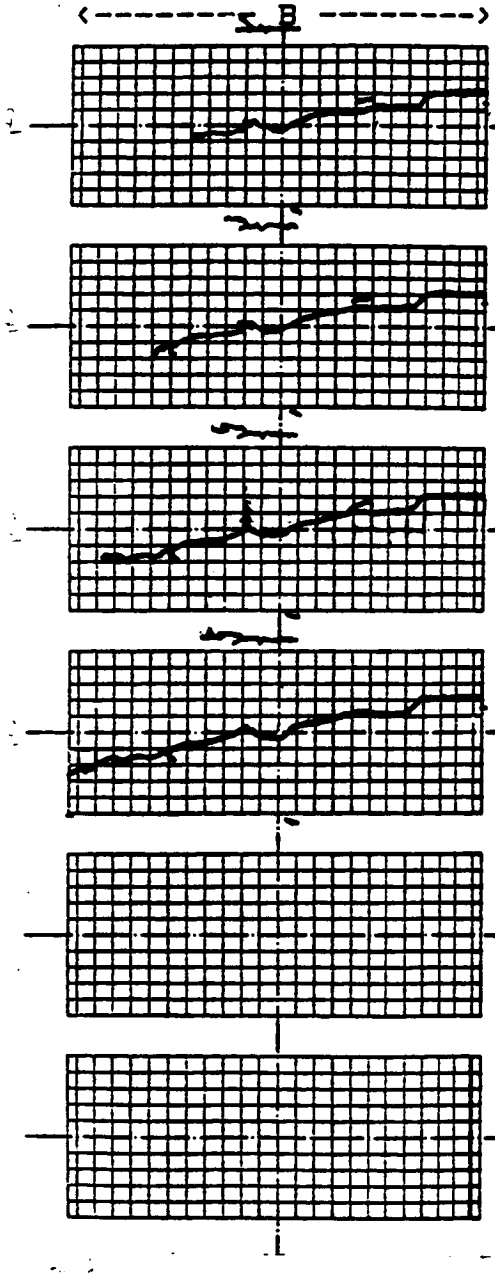

14K Cycles
L1 1.657 mm
L2 .071 mm
L3 .332 mm
L4 .109 mm
L5 L1 mm

16K Cycles
L1 1.853 mm
L2 .071 mm
L3 .436 mm
L4 .109 mm
L5 mm

18K Cycles
L1 2.131 mm
L2 .071 mm
L3 .495 mm
L4 L1 mm
L5 mm

20K Cycles
L1 THRU mm
L2 .071 mm
L3 .518 mm
L4 mm
L5 mm

Cycles
L1 mm
L2 mm
L3 mm
L4 mm
L5 mm

Cycles
L1 mm
L2 mm
L3 mm
L4 mm
L5 mm

** DA/DN DATA **

SPECIMEN' NO. = A-52-21.L1
NO. OF DATA = 10
R=-2.00
SMAX= 75.0 MPa
surface crack → corner crack @ 12k

	CYCLE(X1000)	CRK L. 2a(mm)	AVG. a(mm)	DELK(MPa-M)	DADN(mm/CYCLE)
0	2	0.180	0.000	0.00	0.000 X1.E-6
1	4	0.267	0.112	8.94	21.750 X1.E-6
2	6	0.419	0.171	10.85	38.000 X1.E-6
3	8	0.605	0.256	13.00	46.500 X1.E-6
4	10	0.796	0.350	14.99	47.750 X1.E-6
5	12	1.237→corner	0.508	17.73	110.250 X1.E-6
6	14	1.657	0.724	20.81	105.000 X1.E-6
7	16	1.853	0.877	22.79	49.000 X1.E-6
8	18	2.131	0.996	24.24	69.500 X1.E-6

** DA/DN DATA **

SPECIMEN' NO. = A-52-21.L3
NO. OF DATA = 8
R=-2.00
SMAX= 75.0 MPa
surface crack

	CYCLE(X1000)	CRK L. 2a(mm)	AVG. a(mm)	DELK(MPa-M)	DADN(mm/CYCLE)
0	4	0.033	0.000	0.00	0.000 X1.E-6
1	6	0.076	0.027	4.62	10.750 X1.E-6
2	10	0.283	0.090	8.09	25.875 X1.E-6
3	12	0.316	0.150	10.21	8.250 X1.E-6
4	14	0.332	0.162	10.57	4.000 X1.E-6
5	16	0.436	0.192	11.42	26.000 X1.E-6
6	18	0.495	0.233	12.45	14.750 X1.E-6
7	20	0.518	0.253	12.94	5.750 X1.E-6

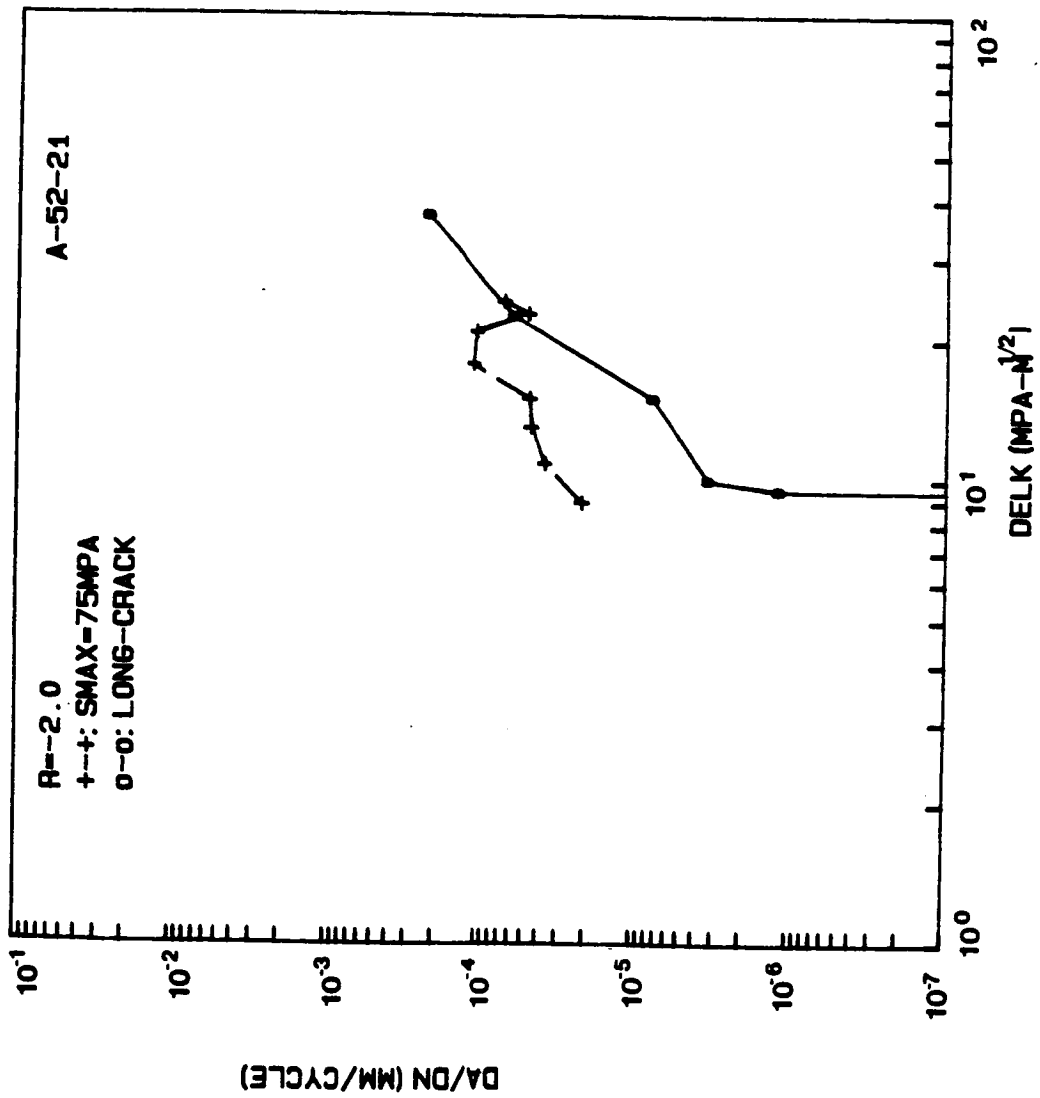
A-52-21
R=-2.0
+--+: SMAX=75MPA
o-o: LONG-CRACK
DA/DN (MM/CYCLE)
DELK (MPA-M^1/2)
10^-1
10^-2
10^-3
10^-4
10^-5
10^-6
10^-7
10^0
10^1
10^2

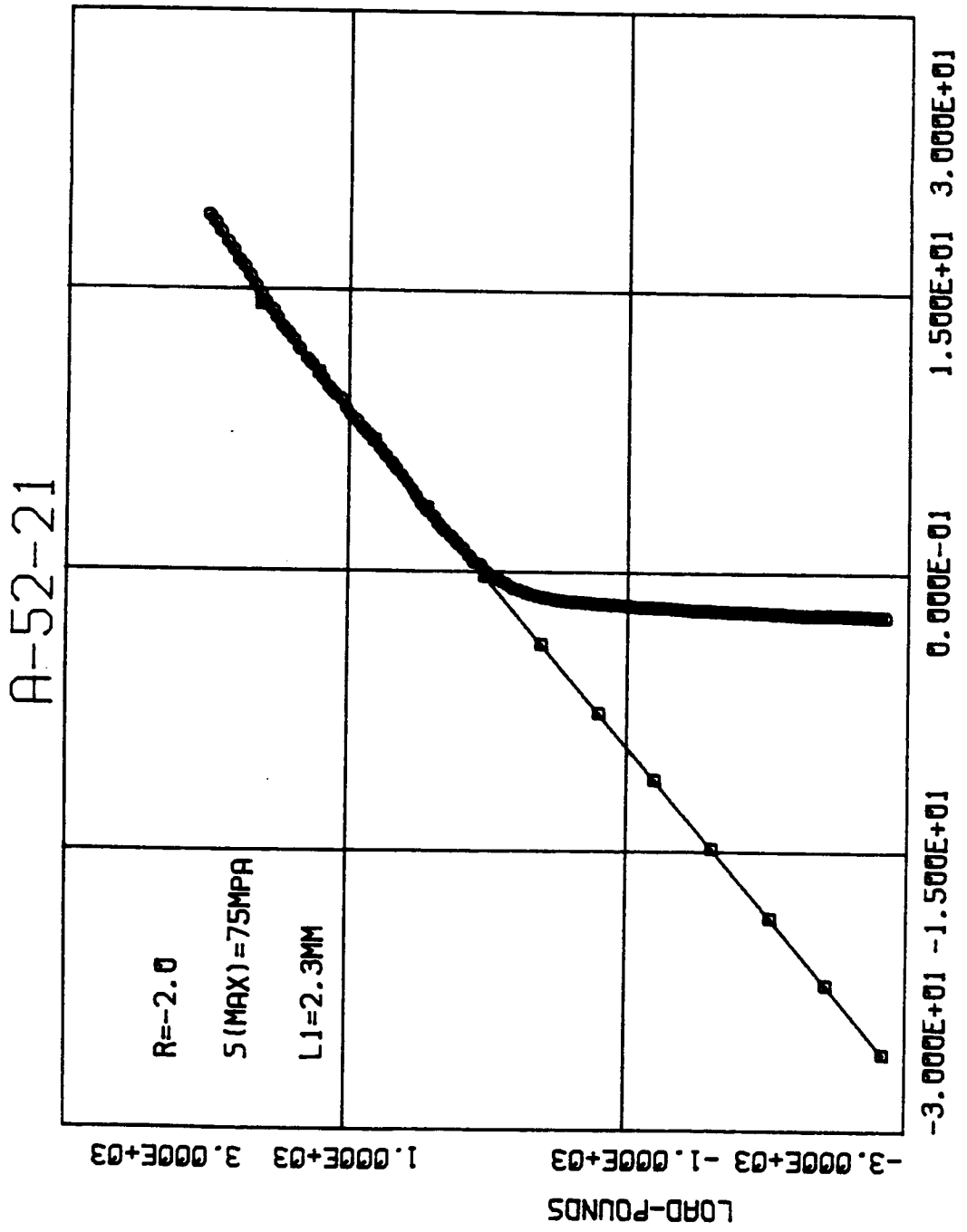
A-52-21
R=-2.0
S(MAX)=75MPA
L1=2.3MM
LOAD-POUNDS
-3.000E+03
-1.000E+03
1.000E+03
3.000E+03
-3.000E+01
-1.500E+01
0.000E-01
1.500E+01
3.000E+01
DISPLACEMENT-MICRONS

A-52-21

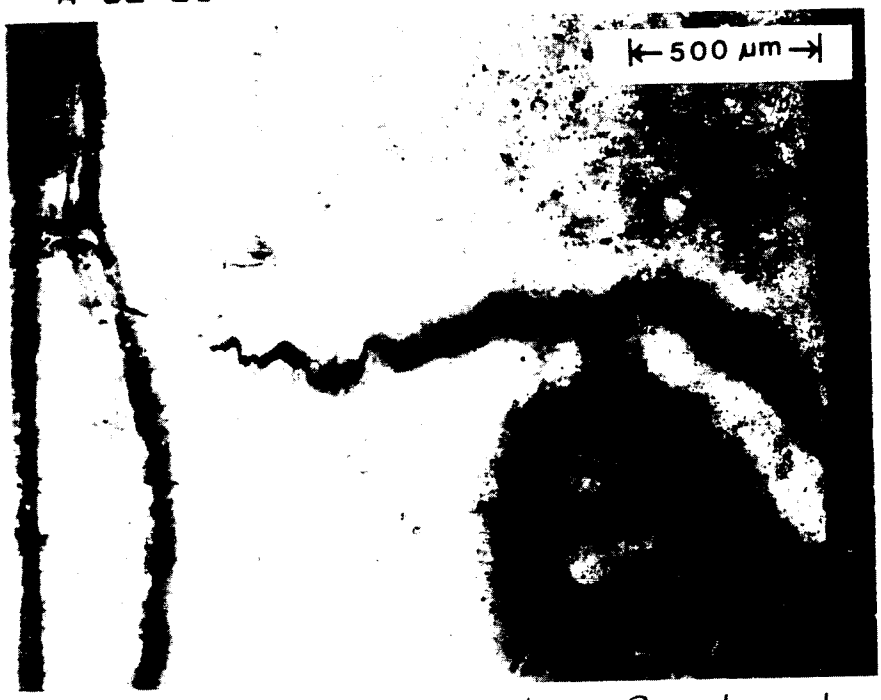

Replica @ 20K cycles

3mm

ORIGINAL PAGE IS
OF POOR QUALITY

A-52-21

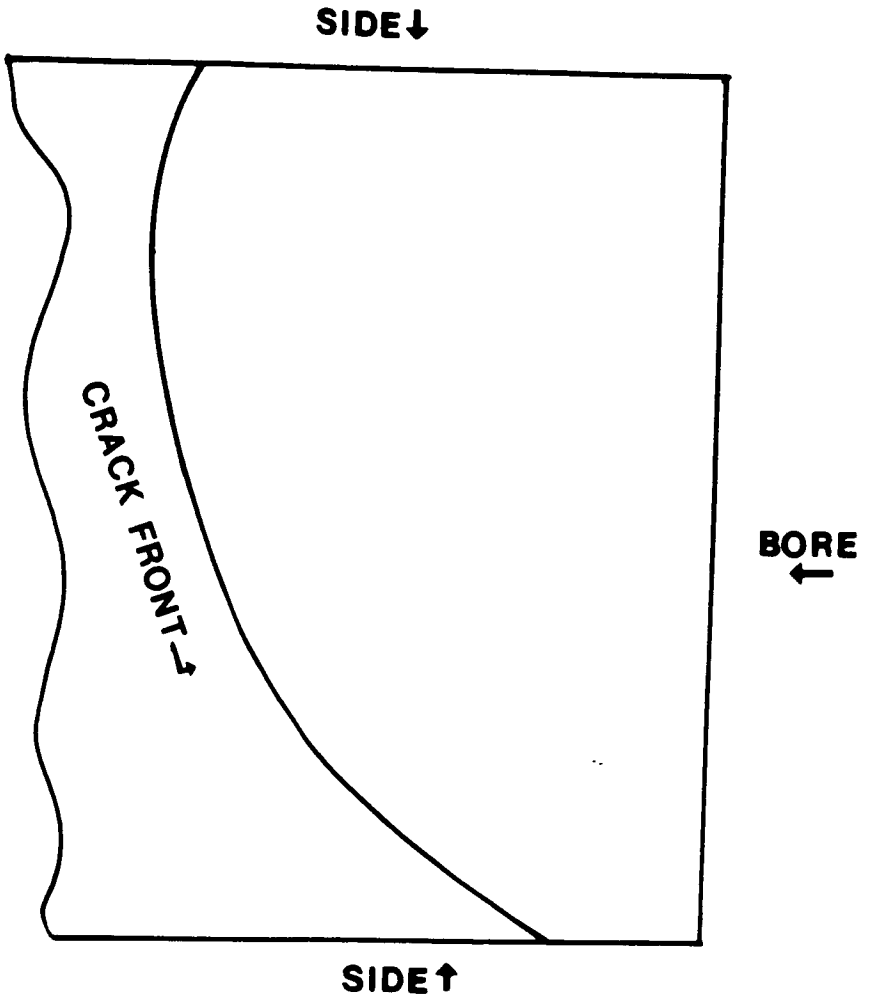

Tracing of Crack Front for A-52-21

TEST DATA

SPECIMEN NUMBER: A - 74 -20

DATE: 7/11/85

PARTICIPANT'S NAME: Joo-Jin Lee

John Cieslowski

TEST TEMPERATURE: 27°C

RELATIVE HUMIDITY: 54 %

WAVEFORM TYPE: Sinusoidal wave, 20 Hz

LOADING SEQUENCE TYPE: Constant amplitude

R-RATIO = -2

S max = 75MPa

S min = -150MPa

FINAL LENGTH OF CRACK: 0.035mm , 0.07mm , ...

COMMENTS:

- Many microcracks were found at 8k cycles.
- Crack Growth test was stopped to run ISDG measurement on 0.035mm crack.
- Specimen was not broken up statically.
- A photo was taken from the specimen surface. (showing 0.035mm crack and a indentation set)

* . No crack map was drawn.

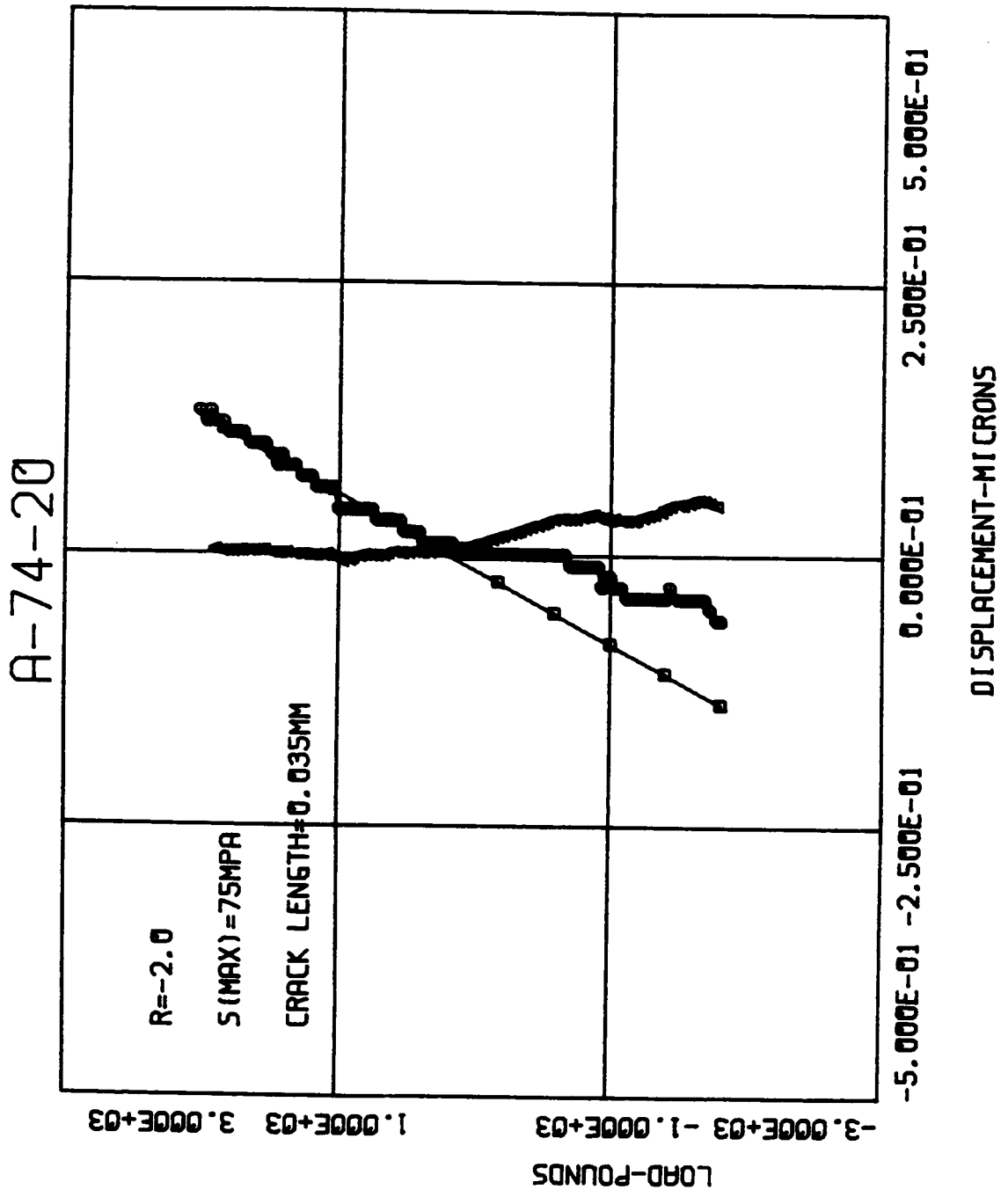
A-74-20
R=-2.0
S(MAX)=75MPA
CRACK LENGTH=0.035MM
LOAD-POUNDS
-3.000E+03
-1.000E+03
1.000E+03
3.000E+03
-5.000E-01
-2.500E-01
0.000E-01
2.500E-01
5.000E-01
DISPLACEMENT-MICRONS

TEST DATA

SPECIMEN NUMBER: A-75-16

DATE:

PARTICIPANT'S NAME: Joo-Jin Lee

John Cieslowski

TEST TEMPERATURE: 27° C

RELATIVE HUMIDITY: 68 %

WAVEFORM TYPE: Sinusoidal wave, 20 Hz

LOADING SEQUENCE TYPE: Constant amplitude

R-RATIO = -2.0

S max = 60MPa

S min = -120MPa

FINAL LENGTH OF CRACK: 2.175mm (Thru thickness) - L4

COMMENTS:

AGARD Short Crack DATA CHART

Record of crack lengths and map

Page 1 of 4 Loading Type Constant Amplitude R=-2

Specimen no A-75-16 Peak Stress 60 MPa

0.1mm grid

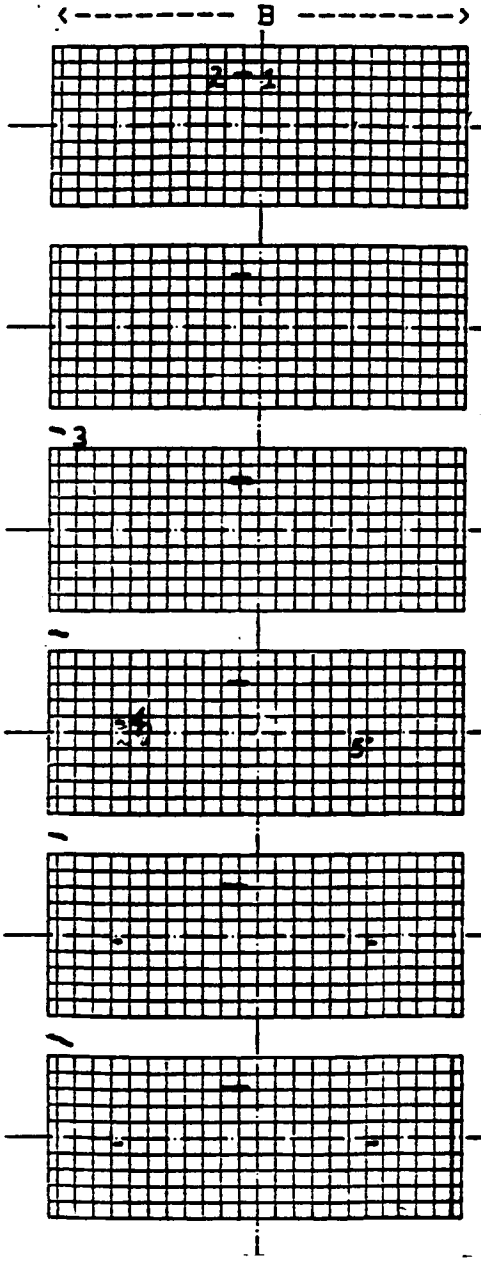

15K Cycles
L1 .027 mm
L2 .011 mm
L3 mm
L4 mm
L5 mm

20K Cycles
L1 .033 mm
L2 .016 mm
L3 mm
L4 mm
L5 mm

25K Cycles
L1 .087 mm
L2 L1 mm
L3 .087 mm
L4 mm
L5 mm

30K Cycles
L1 .087 mm
L2 mm
L3 .104 mm
L4 .038 mm
L5 .027 mm

35K Cycles
L1 .136 mm
L2 mm
L3 .109 mm
L4 .038 mm
L5 .055 mm

40K Cycles
L1 .153 mm
L2 mm
L3 .147 mm
L4 .038 mm
L5 .060 mm

AGARD Short Crack DATA CHART

Record of crack lengths and map

Page 2 of 4 Loading Type R=-2

Specimen no A-75-16 Peak Stress 60 MPa

0.1mm grid

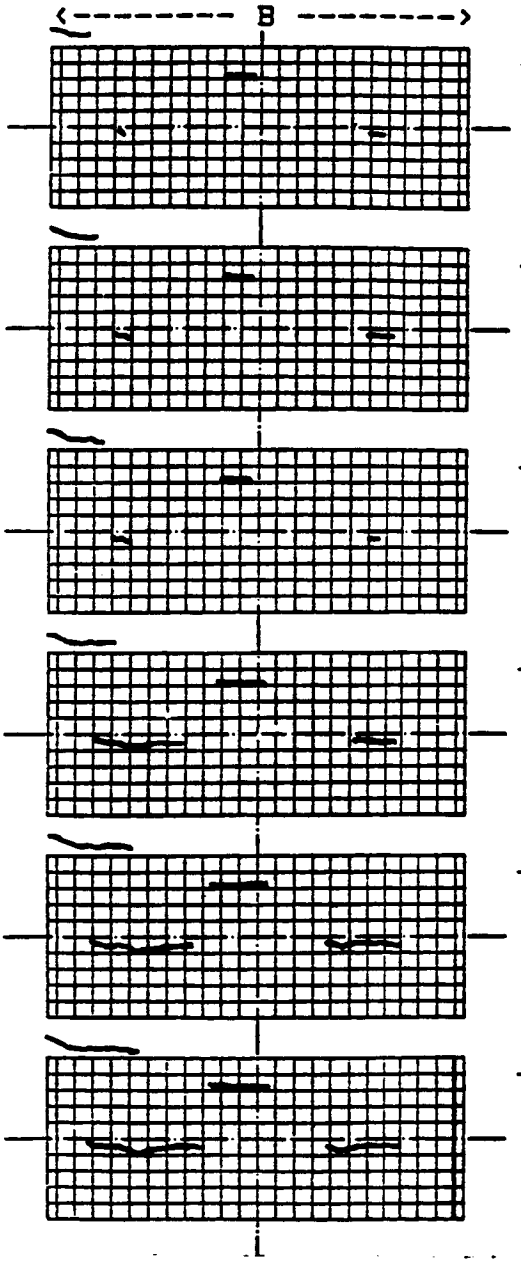

45K Cycles
L1 .158 mm
L2 mm
L3 .191 mm
L4 .055 mm
L5 .082 mm

50K Cycles
L1 .158 mm
L2 mm
L3 .251 mm
L4 .093 mm
L5 .153 mm

55K Cycles
L1 ** mm
L2 mm
L3 .305 mm
L4 .098 mm
L5 ** mm

60K Cycles
L1 .261 mm
L2 mm
L3 .371 mm
L4 .496 mm
L5 .234 mm

65K Cycles
L1 .278 mm
L2 mm
L3 .458 mm
L4 .545 mm
L5 .425 mm

70K Cycles
L1 .322 mm
L2 mm
L3 .491 mm
L4 .594 mm
L5 .676 mm

** not clear to measure

AGARD Short Crack DATA CHART

Record of crack lengths and map

Page 3 of 4 Loading Type R=-2

Specimen no A-75-16 Peak Stress 60 MPa

0.1mm grid

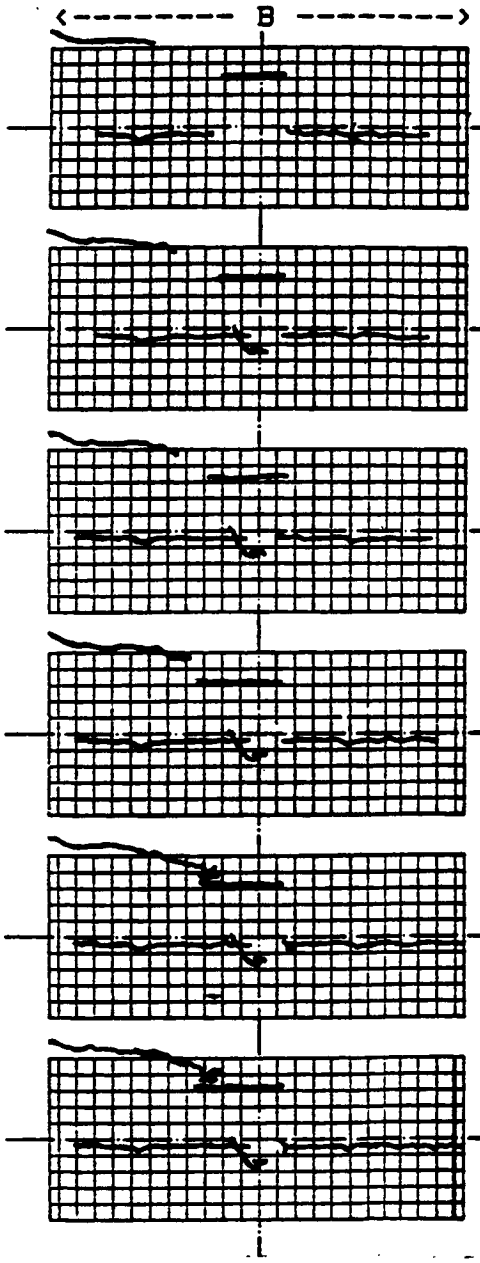

75K Cycles
L1 .349 mm
L2 mm
L3 .561 mm
L4 .632 mm
L5 .812 mm

80K Cycles
L1 .365 mm
L2 mm
L3 .676 mm
L4 .937 mm
L5 * mm

85K Cycles
L1 .425 mm
L2 mm
L3 .719 mm
L4 1.019 mm
L5 .845 mm

90K Cycles
L1 .431 mm
L2 mm
L3 .774 mm
L4 1.019 mm
L5 .850 mm

95K Cycles
L1 .458 mm
L2 mm
L3 .916 mm
L4 1.036 mm
L5 1.019 mm

100K Cycles
L1 .479 mm
L2 mm
L3 .953 mm
L4 1.068 mm
L5 1.036 mm

* not clear to measure

AGARD Short Crack DATA CHART

Record of crack lengths and map

Page 4 of 4 Loading Type R=-2
Specimen no A-75-16 Peak Stress 60 MPa

0.1mm grid

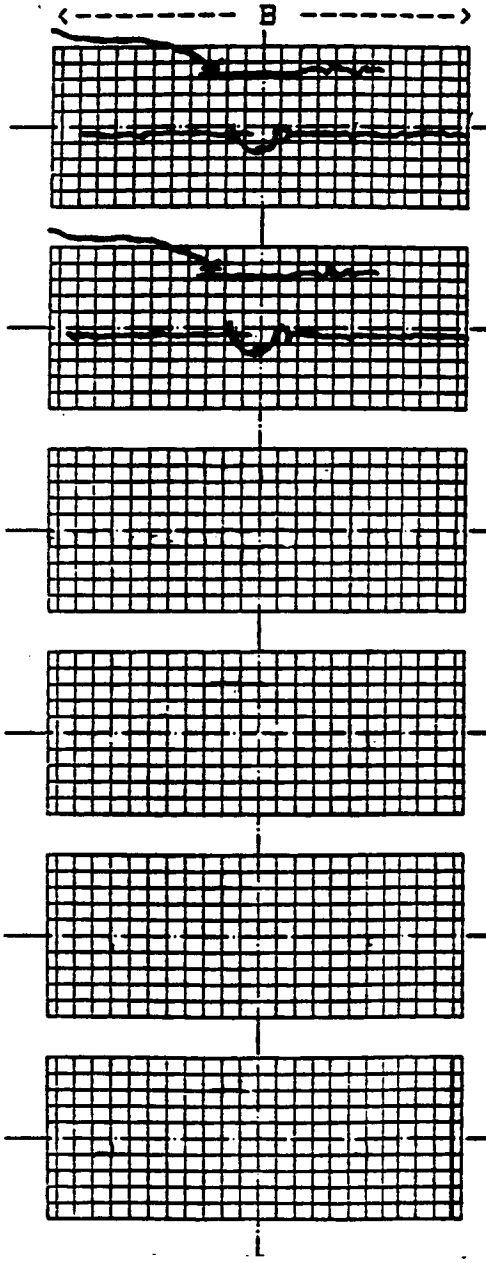

105K Cycles
L1 1.809 mm
L2 mm
L3 L1 mm
L4 2.104 mm
L5 L4 mm

110K Cycles
L1 1.809 mm
L2 mm
L3 mm
L4 2.175 mm
L5 mm

Cycles
L1 mm
L2 mm
L3 mm
L4 mm
L5 mm

Cycles
L1 mm
L2 mm
L3 mm
L4 mm
L5 mm

Cycles
L1 mm
L2 mm
L3 mm
L4 mm
L5 mm

Cycles
L1 mm
L2 mm
L3 mm
L4 mm
L5 mm

** DA/DN DATA **

SPECIMEN' NO. = A-75-16.L1
NO. OF DATA = 16
R=-2.00
SMAX= 60.0 MPa
surface crack

	CYCLE(X1000)	CRK L. 2a(mm)	AVG. a(mm)	DELK(MPa-M)	DADN(mm/CYCLE)
0	15	0.027	0.000	0.00	0.000 X1.E-6
1	20	0.033	0.015	2.77	0.600 X1.E-6
2	25	0.087	0.030	3.87	5.400 X1.E-6
3	35	0.136	0.056	5.19	2.450 X1.E-6
4	40	0.153	0.072	5.86	1.700 X1.E-6
5	45	0.158	0.078	6.06	0.500 X1.E-6
6	60	0.261	0.105	6.94	3.433 X1.E-6
7	65	0.278	0.135	7.78	1.700 X1.E-6
8	70	0.322	0.150	8.17	4.400 X1.E-6
9	75	0.349	0.168	8.59	2.700 X1.E-6
10	80	0.365	0.178	8.84	1.600 X1.E-6
11	85	0.425	0.197	9.25	6.000 X1.E-6
12	90	0.431	0.214	9.59	0.600 X1.E-6
13	95	0.458	0.222	9.76	2.700 X1.E-6
14	100	0.478	0.234	9.99	2.000 X1.E-6
15	105	1.809	0.572	14.96	133.100 X1.E-6

** DA/DN DATA **

SPECIMEN' NO. = A-75-16.L3
NO. OF DATA = 16
R=-2.00
SMAX= 60.0 MPa
corner crack

	CYCLE(X1000)	CRK L. 2a(mm)	AVG. a(mm)	DELK(MPa-M)	DADN(mm/CYCLE)
0	25	0.087	0.000	0.00	0.000 X1.E-6
1	30	0.104	0.095	6.58	3.400 X1.E-6
2	35	0.109	0.106	6.92	1.000 X1.E-6
3	40	0.147	0.128	7.53	7.600 X1.E-6
4	45	0.191	0.169	8.55	8.800 X1.E-6
5	50	0.251	0.221	9.65	12.000 X1.E-6
6	55	0.305	0.278	10.69	10.800 X1.E-6
7	60	0.371	0.338	11.66	13.200 X1.E-6
8	65	0.458	0.414	12.76	17.400 X1.E-6
9	70	0.491	0.475	13.54	6.600 X1.E-6
10	75	0.561	0.526	14.17	14.000 X1.E-6
11	80	0.676	0.618	15.22	23.000 X1.E-6
12	85	0.719	0.697	16.05	8.600 X1.E-6
13	90	0.774	0.747	16.53	11.000 X1.E-6
14	95	0.916	0.845	17.45	28.400 X1.E-6
15	100	0.953	0.934	18.23	7.400 X1.E-6

** DA/DN DATA **

SPECIMEN' NO. = A-75-16.L4
NO. OF DATA = 14
R=-2.00
SMAX= 60.0 MPa
surface crack

	CYCLE(X1000)	CRK L. 2a(mm)	AVG. a(mm)	DELK(MPa-M)	DADN(mm/CYCLE)
0	40	0.038	0.000	0.00	0.000 X1.E-6
1	45	0.055	0.023	3.43	1.700 X1.E-6
2	50	0.093	0.037	4.28	3.800 X1.E-6
3	55	0.098	0.048	4.83	0.500 X1.E-6
4	60	0.496	0.148	8.13	39.800 X1.E-6
5	65	0.545	0.260	10.48	4.900 X1.E-6
6	70	0.594	0.285	10.91	4.900 X1.E-6
7	75	0.632	0.306	11.29	3.800 X1.E-6
8	80	0.937	0.392	12.62	30.500 X1.E-6
9	85	1.019	0.489	13.94	8.200 X1.E-6
10	95	1.036	0.514	14.26	0.850 X1.E-6
11	100	1.068	0.526	14.41	3.200 X1.E-6
12	105	2.104	0.793	17.37	103.600 X1.E-6

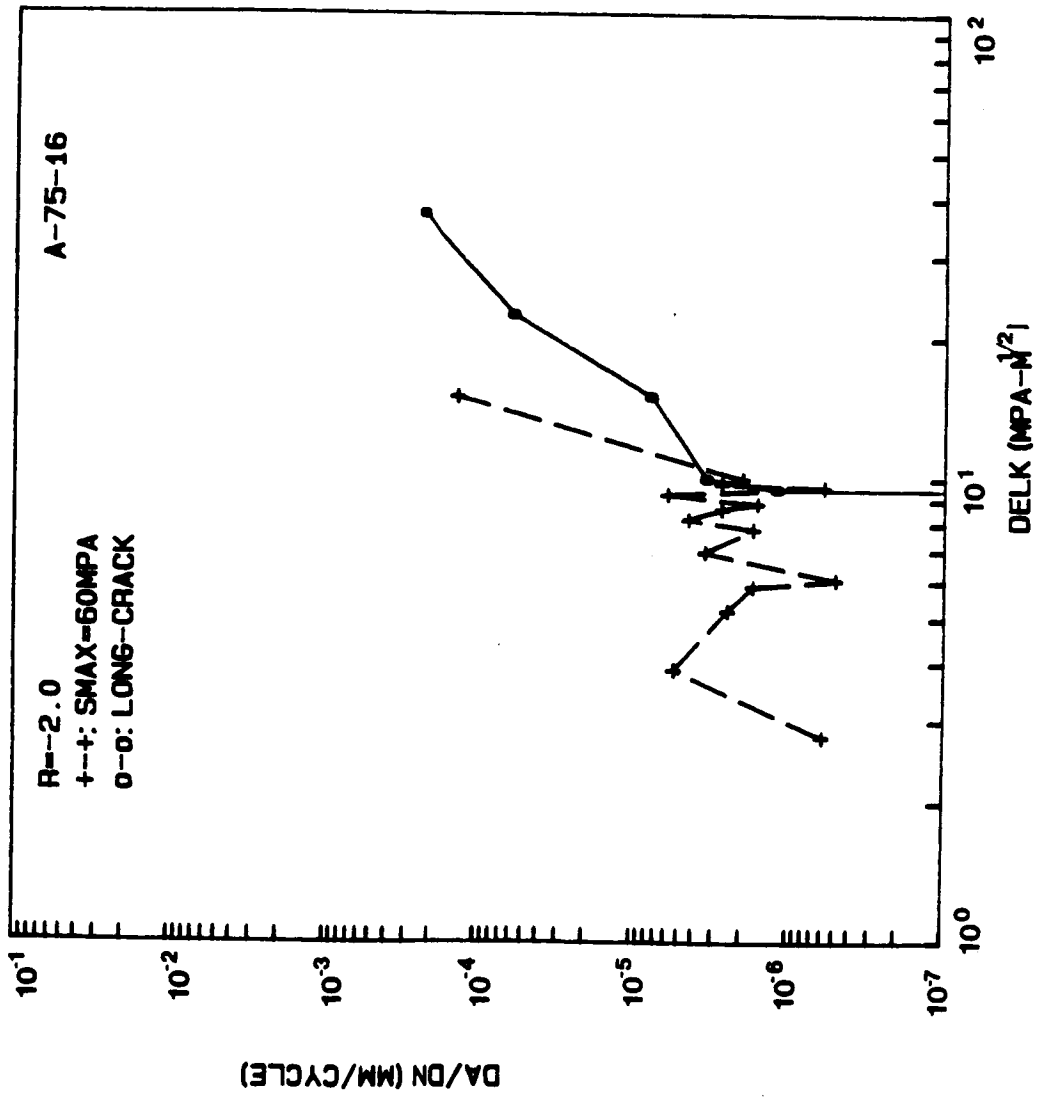
A-75-16
R=-2.0
+--+: SMAX=60MPA
o-o: LONG-CRACK
DA/DN (MM/CYCLE)
DELK (MPA-M^1/2)
10^-1
10^-2
10^-3
10^-4
10^-5
10^-6
10^-7
10^0
10^1
10^2

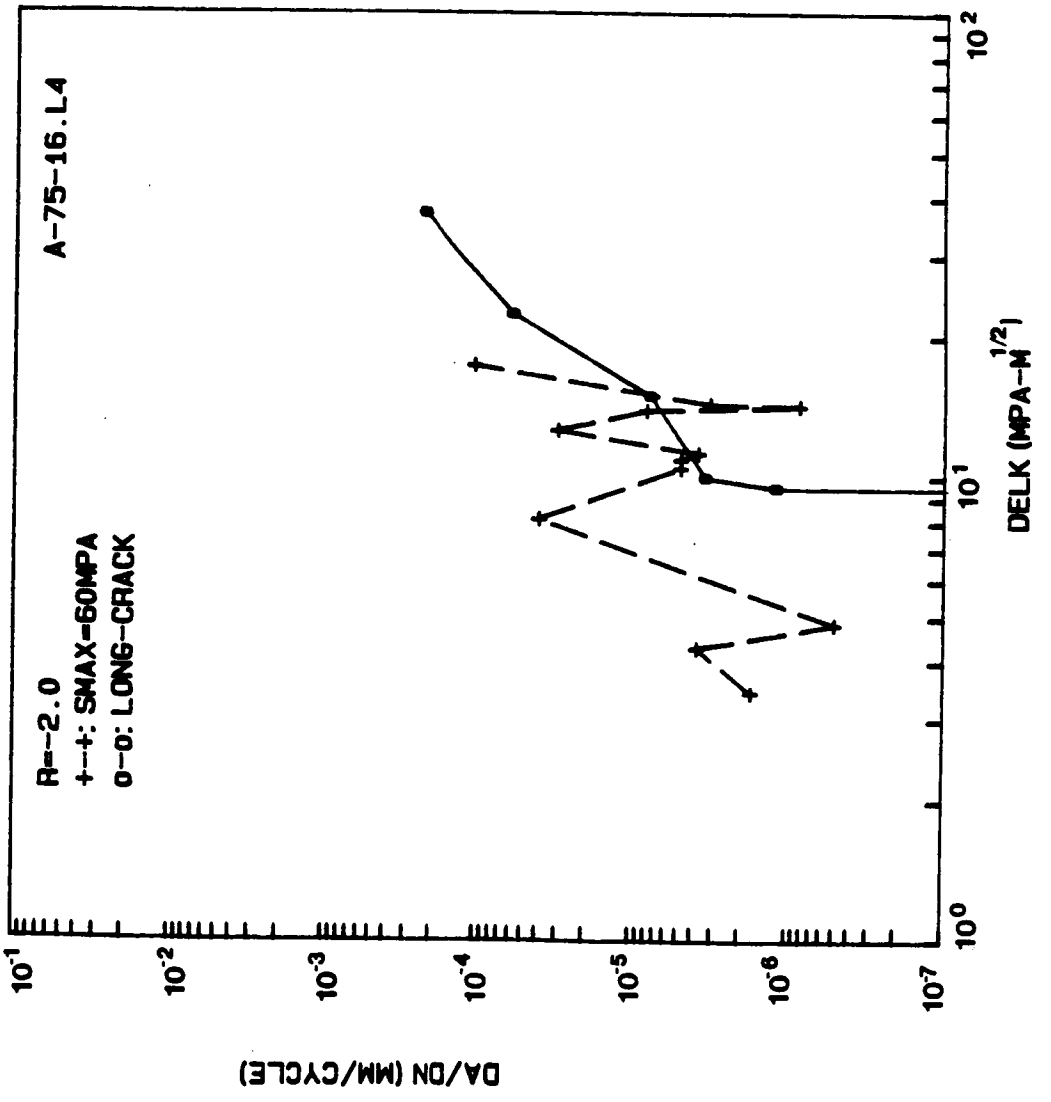
A-75-16.L4
R=-2.0
+--+: SMAX=60MPA
o-o: LONG-CRACK
DA/DN (MM/CYCLE)
DELK (MPA-M^1/2)
10^-1
10^-2
10^-3
10^-4
10^-5
10^-6
10^-7
10^0
10^1
10^2

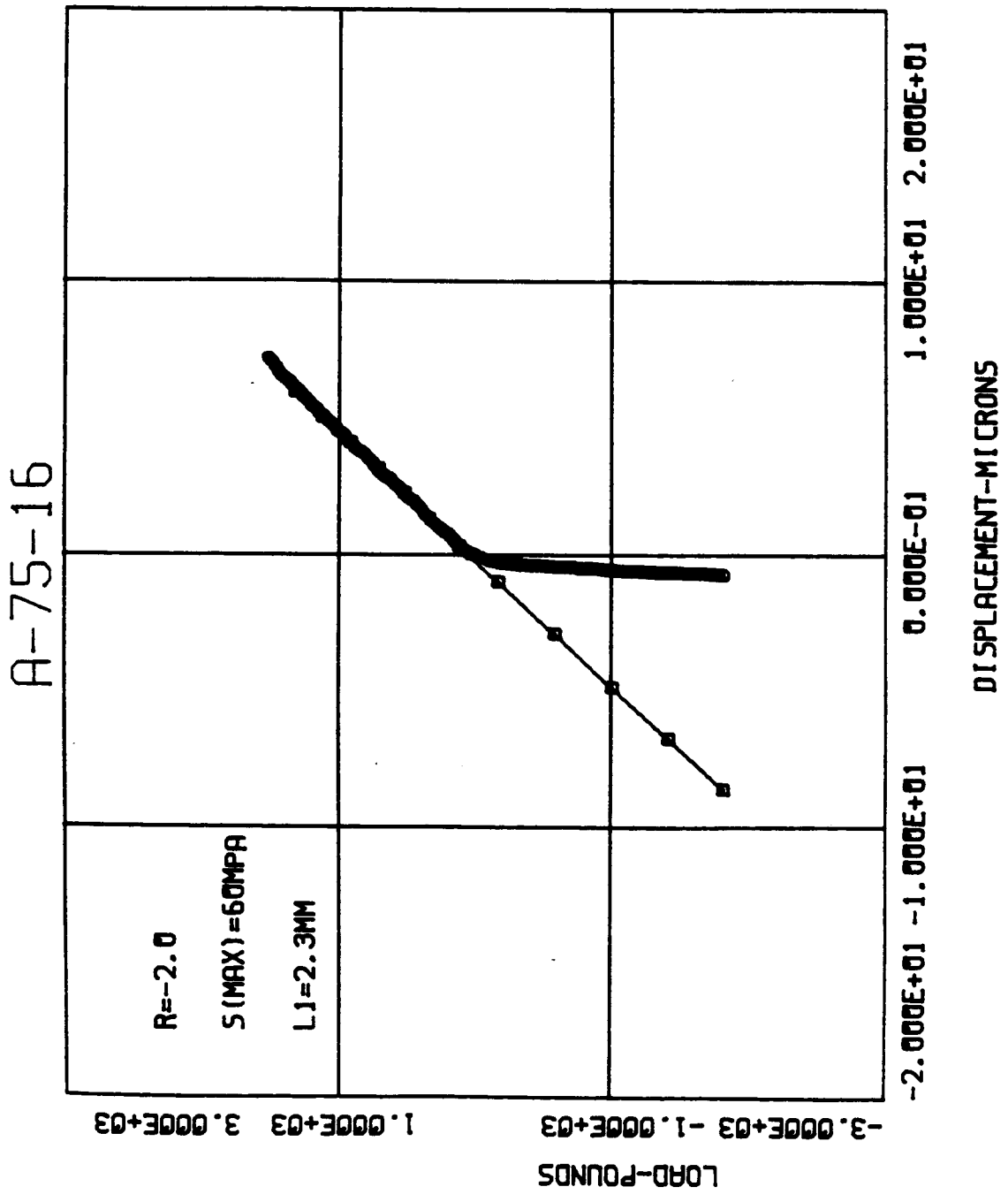
A-75-16
R=-2.0
S(MAX)=60MPA
LI=2.3MM
LOAD-POUNDS
-3.000E+03
-1.000E+03
1.000E+03
3.000E+03
-2.000E+01
-1.000E+01
0.000E-01
1.000E+01
2.000E+01
DISPLACEMENT-MICRONS

A-75-16

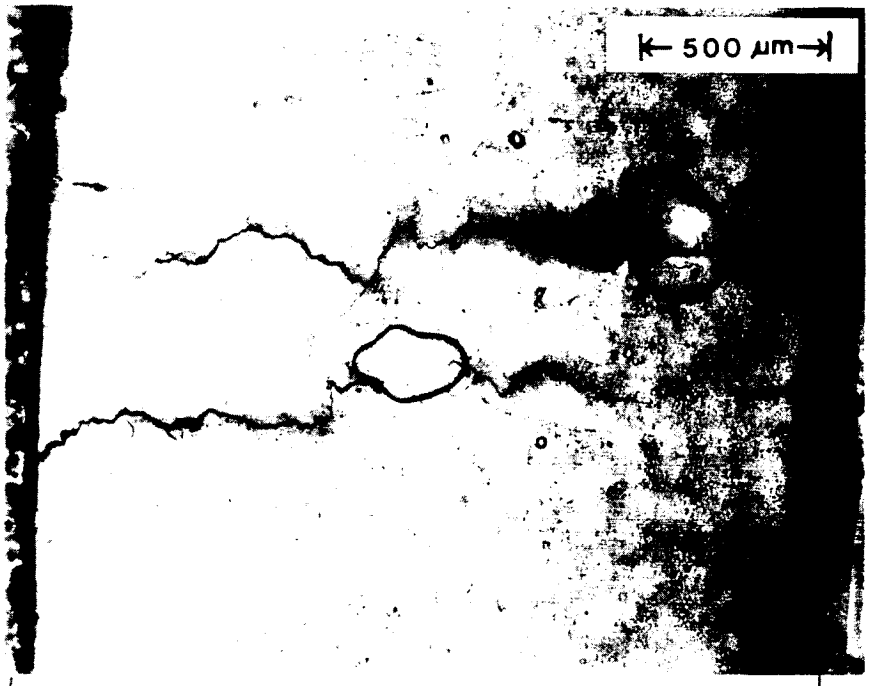

A-75-16

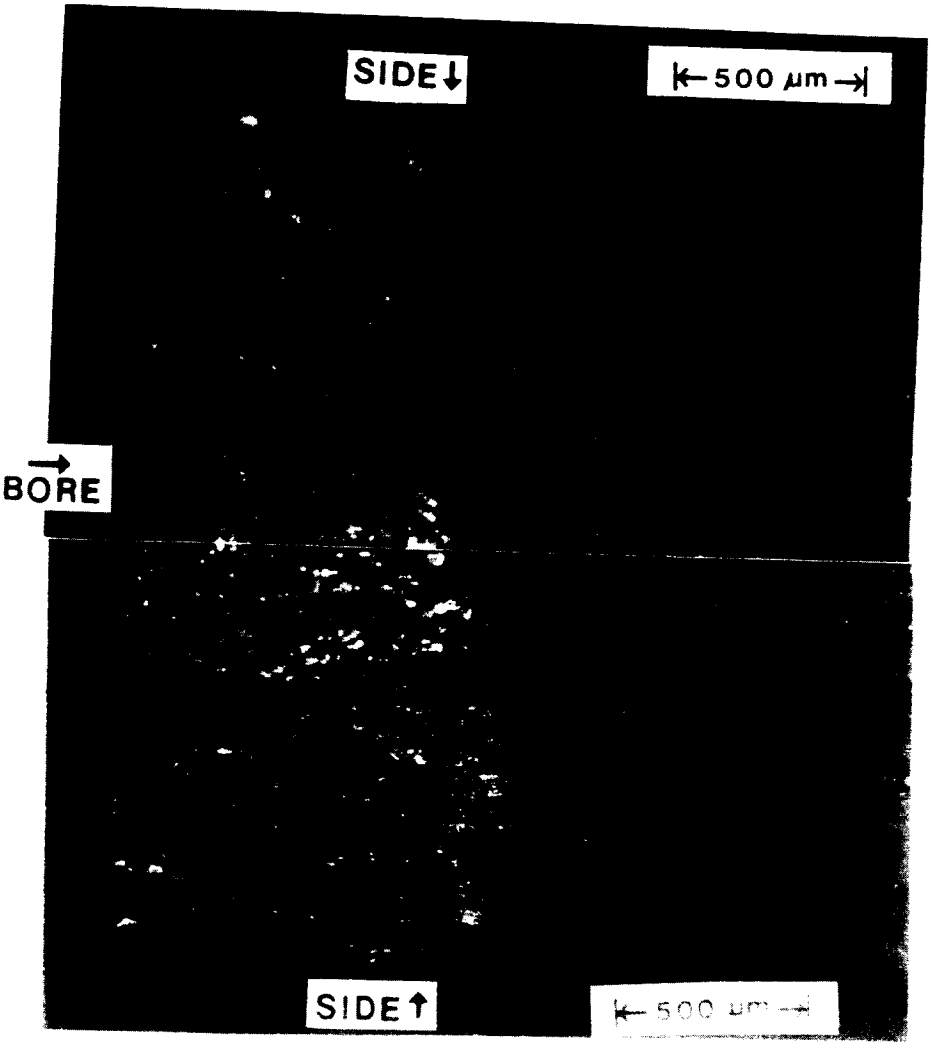

TEST DATA

SPECIMEN NUMBER: A-84-20

DATE: 7/11/85

PARTICIPANT'S NAME: Joo-Jin Lee

John Cieslowski

TEST TEMPERATURE: 27°C

RELATIVE HUMIDITY: 58 %

WAVEFORM TYPE: Sinusoidal wave, 20 Hz

LOADING SEQUENCE TYPE: Constant amplitude

R-RATIO = -2.0

S max = 60MPa

S min = -120MPa

FINAL LENGTH OF CRACK: 0.174 mm (CL2)

COMMENTS:

AGARD Short Crack DATA CHART

Record of crack lengths and map

Page 1 of 1 Loading Type _____

Specimen no A-84-20 Peak Stress 60 MPa

0.1mm grid

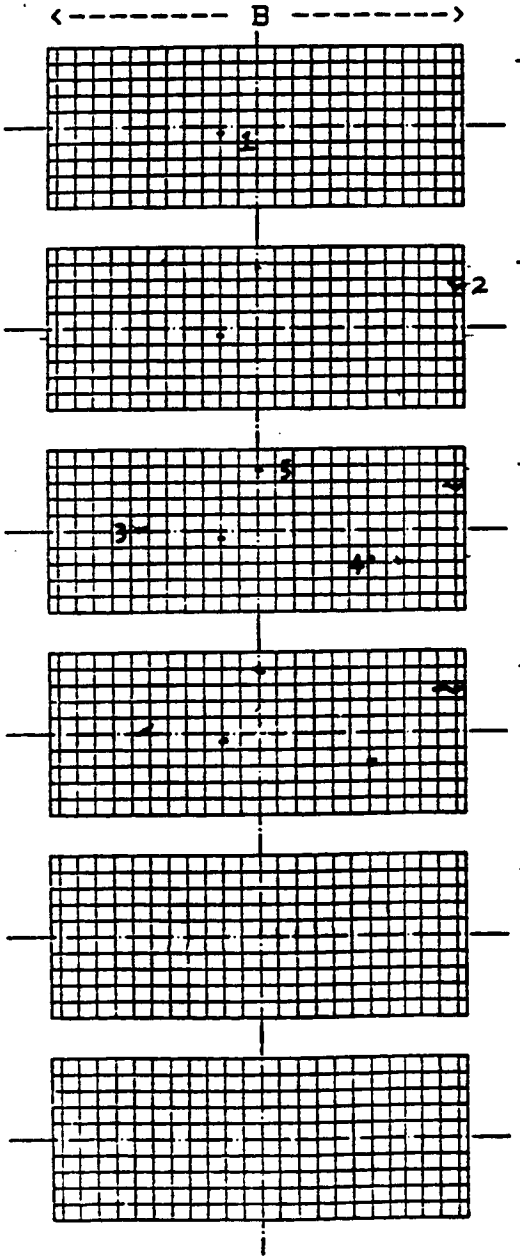

15K Cycles
L1 .016 mm
L2 _____ mm
L3 _____ mm
L4 _____ mm
L5 _____ mm

20K Cycles
L1 .022 mm
L2 .093 mm
L3 _____ mm
L4 _____ mm
L5 _____ mm

25K Cycles
L1 .022 mm
L2 .131 mm
L3 .038 mm
L4 .027 mm
L5 .022 mm

30K Cycles
L1 .027 mm
L2 .174 mm
L3 .055 mm
L4 .038 mm
L5 .033 mm

_____ Cycles
L1 _____ mm
L2 _____ mm
L3 _____ mm
L4 _____ mm
L5 _____ mm

_____ Cycles
L1 _____ mm
L2 _____ mm
L3 _____ mm
L4 _____ mm
L5 _____ mm

** DA/DN DATA **

SPECIMEN' NO. = A8420.L1
NO. OF DATA = 3
R=-2.00
SMAX= 60.0 MPa

SURFACE CRACK

	CYCLE(X1000)	CRK L. 2a(mm)	AVG. a(mm)	DELK(MPa-M)	DADN(mm/CYCLE)
0	15	0.016	0.000	0.00	0.000 X1.E-6
1	20	0.022	0.009	2.21	0.600 X1.E-6
2	30	0.027	0.012	2.51	0.250 X1.E-6

** DA/DN DATA **

SPECIMEN' NO. = A8420.L2
NO. OF DATA = 3
R=-2.00
SMAX= 60.0 MPa

CORNER CRACK

	CYCLE(X1000)	CRK L. 2a(mm)	AVG. a(mm)	DELK(MPa-M)	DADN(mm/CYCLE)
0	20	0.093	0.000	0.00	0.000 X1.E-6
1	25	0.131	0.112	7.08	7.600 X1.E-6
2	30	0.174	0.153	8.16	8.600 X1.E-6

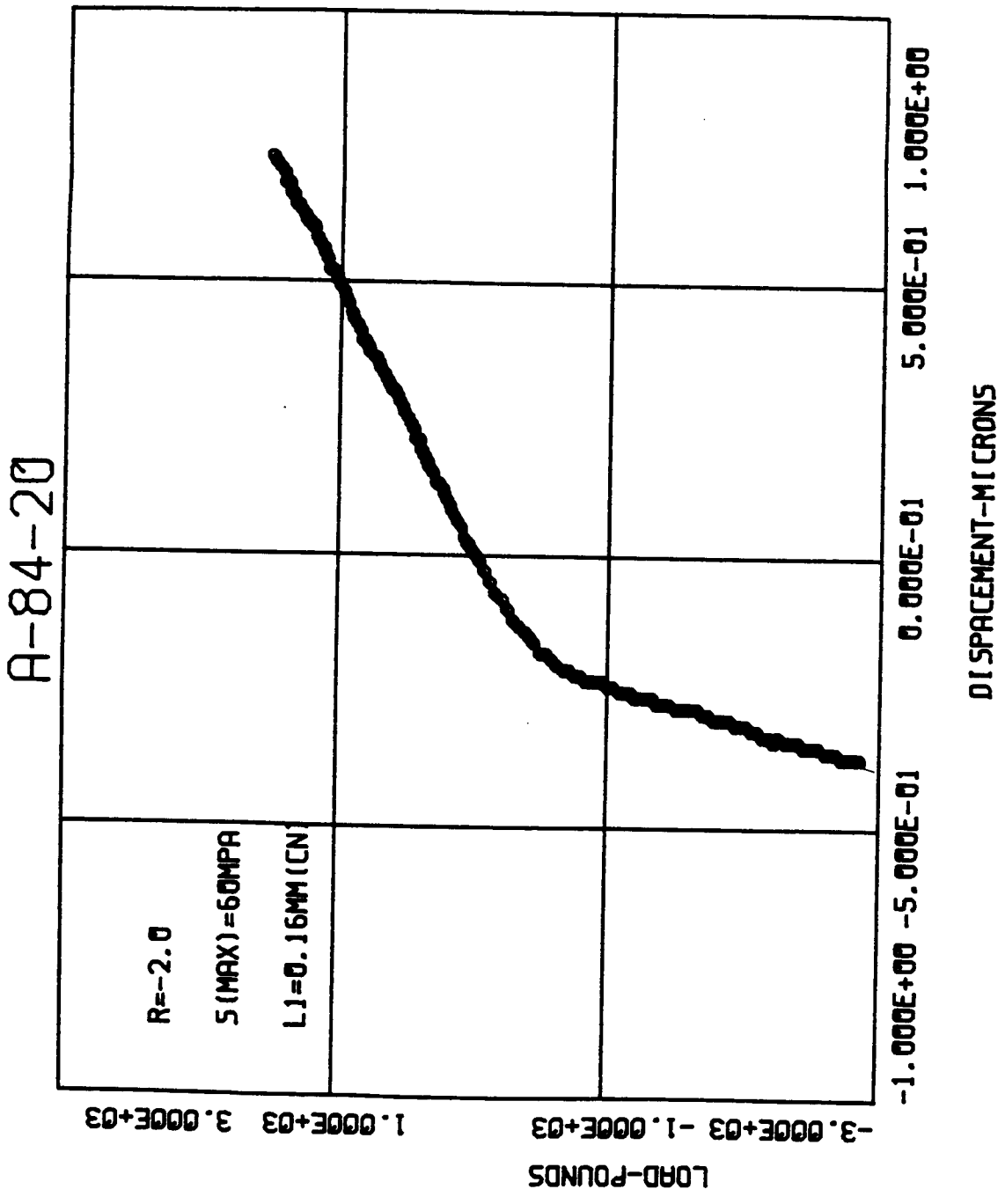
A-84-20
R=-2.0
S(MAX)=60MPA
L1=0.16MM(CN)
3.000E+03
1.000E+03
-1.000E+03
-3.000E+03
LOAD-POUNDS
-1.000E+00
-5.000E-01
0.000E-01
5.000E-01
1.000E+00
DISPACEMENT-MICRONS

A-84-20

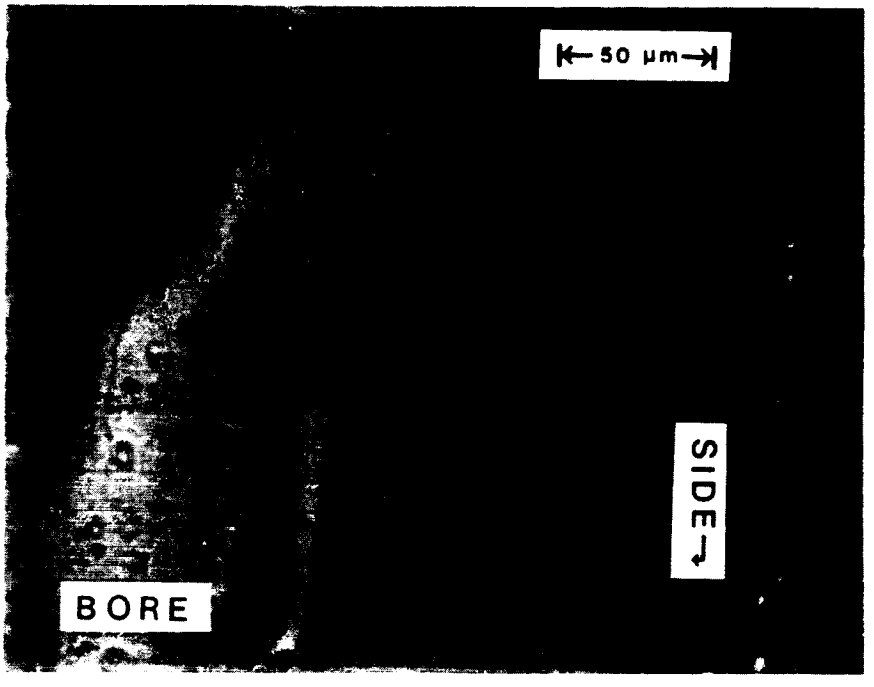

Replica @ 30k cycles

A-84-20

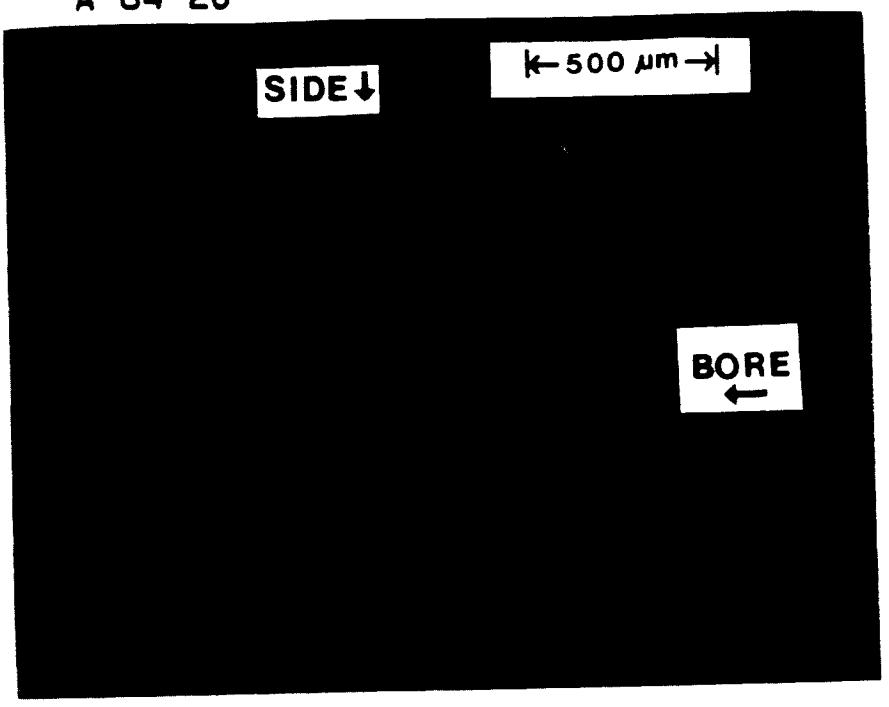

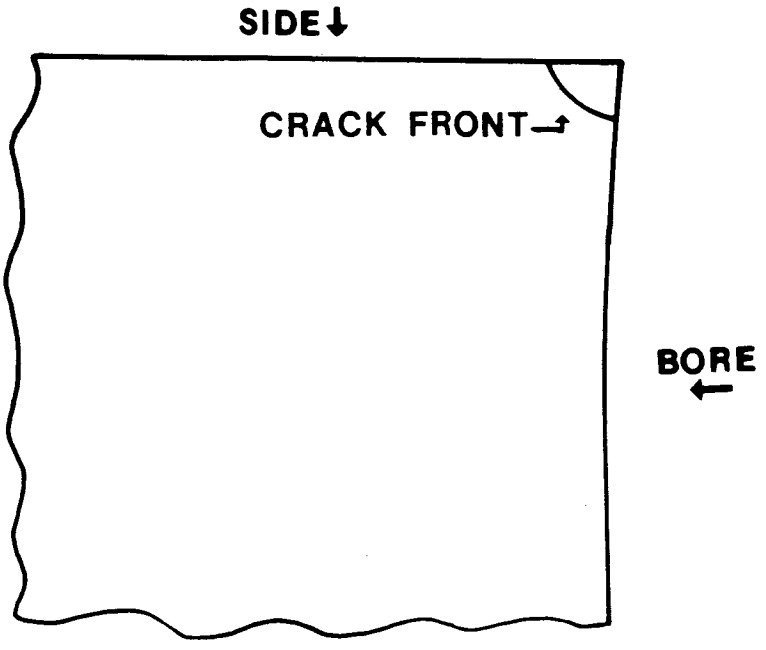

Tracing of Crack Front for A-84-20

TEST DATA

SPECIMEN NUMBER: A-80-11

DATE: 7/16/85

PARTICIPANT'S NAME: Joo-Jin Lee

John Cieslowski

TEST TEMPERATURE: 27°C

RELATIVE HUMIDITY: 68 %

WAVEFORM TYPE: Sinusoidal wave, 20 Hz

LOADING SEQUENCE TYPE: Constant amplitude

R-RATIO = -2.0

S max = 50MPa

S min = -100 MPa

FINAL LENGTH OF CRACK: 0.101 mm

COMMENTS:

AGARD Short Crack DATA CHART

Record of crack lengths and map

Page 1 of 1

Specimen no A-80-11

Loading Type const. Amplitude R=-2

Peak Stress 50 MPa

0.1mm grid

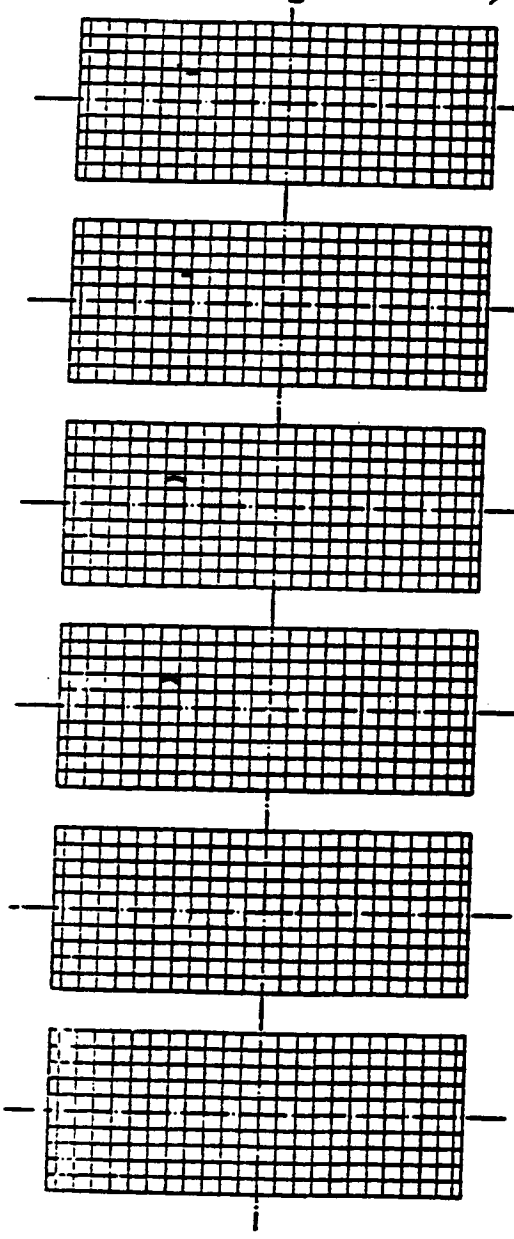

715k Cycles
L1 .050 mm
L2 mm
L3 mm
L4 mm
L5 mm

725k Cycles
L1 .055 mm
L2 mm
L3 mm
L4 mm
L5 mm

730k Cycles
L1 .100 mm
L2 mm
L3 mm
L4 mm
L5 mm

734k Cycles
L1 .108 mm
L2 mm
L3 mm
L4 mm
L5 mm

Cycles
L1 mm
L2 mm
L3 mm
L4 mm
L5 mm

Cycles
L1 mm
L2 mm
L3 mm
L4 mm
L5 mm

** DA/DN DATA **

SPECIMEN' NO. = A8011.L1
NO. OF DATA = 4
R=-2.00
SMAX= 50.0 MPa

SURFACE CRACK

	CYCLE(X1000)	CRK L. 2a(mm)	AVG. a(mm)	DELK(MPa-M)	DADN(mm/CYCLE)
0	715	0.050	0.000	0.00	0.000 X1.E-6
1	725	0.055	0.026	3.03	0.250 X1.E-6
2	730	0.100	0.039	3.65	4.500 X1.E-6
3	734	0.101	0.050	4.12	0.125 X1.E-6

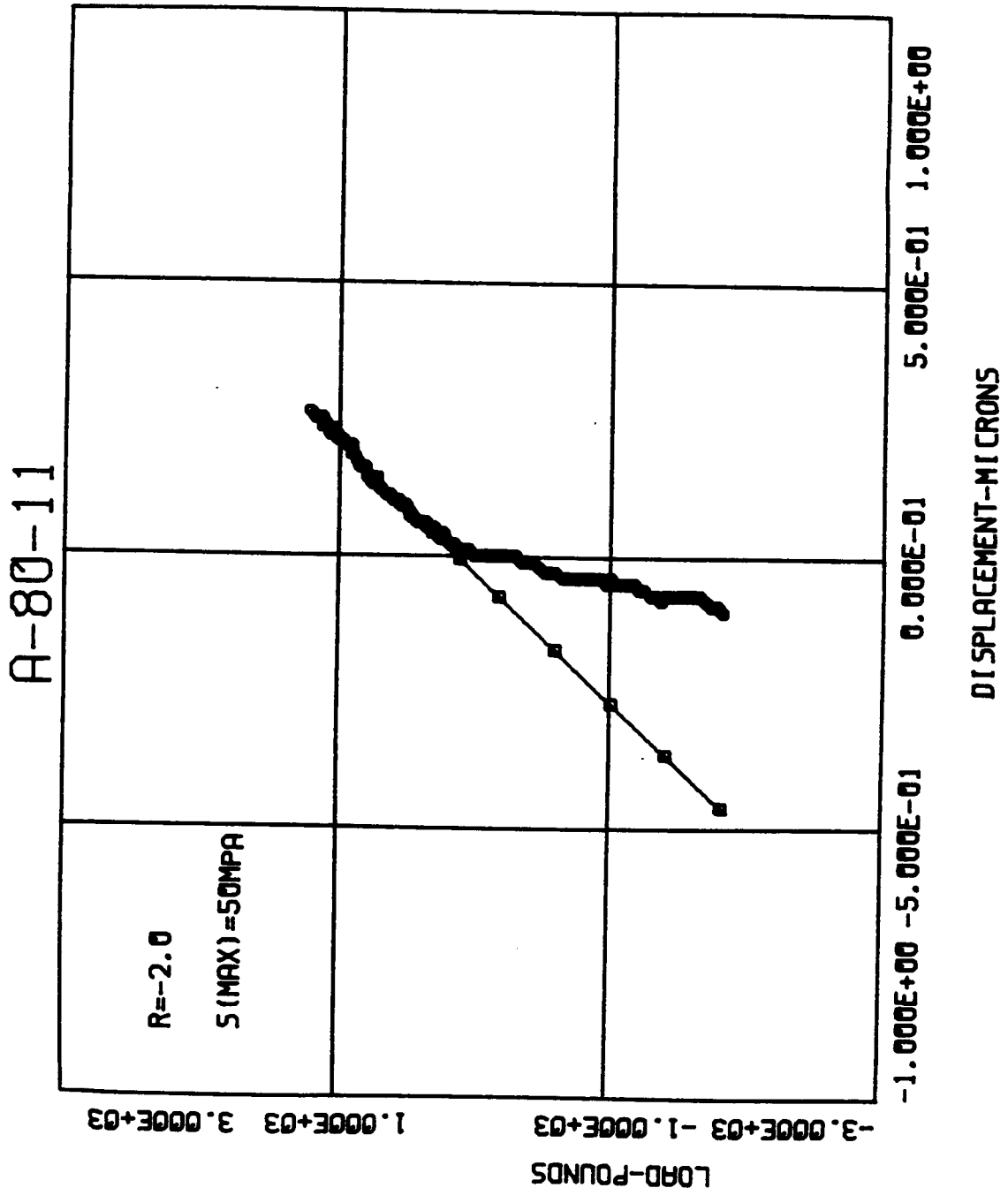
A-80-11
R=-2.0
S(MAX)=50MPA
LOAD-POUNDS
-3.000E+03
-1.000E+03
1.000E+03
3.000E+03
-1.000E+00
-5.000E-01
0.000E-01
5.000E-01
1.000E+00
DISPLACEMENT-MICRONS

A-80-11

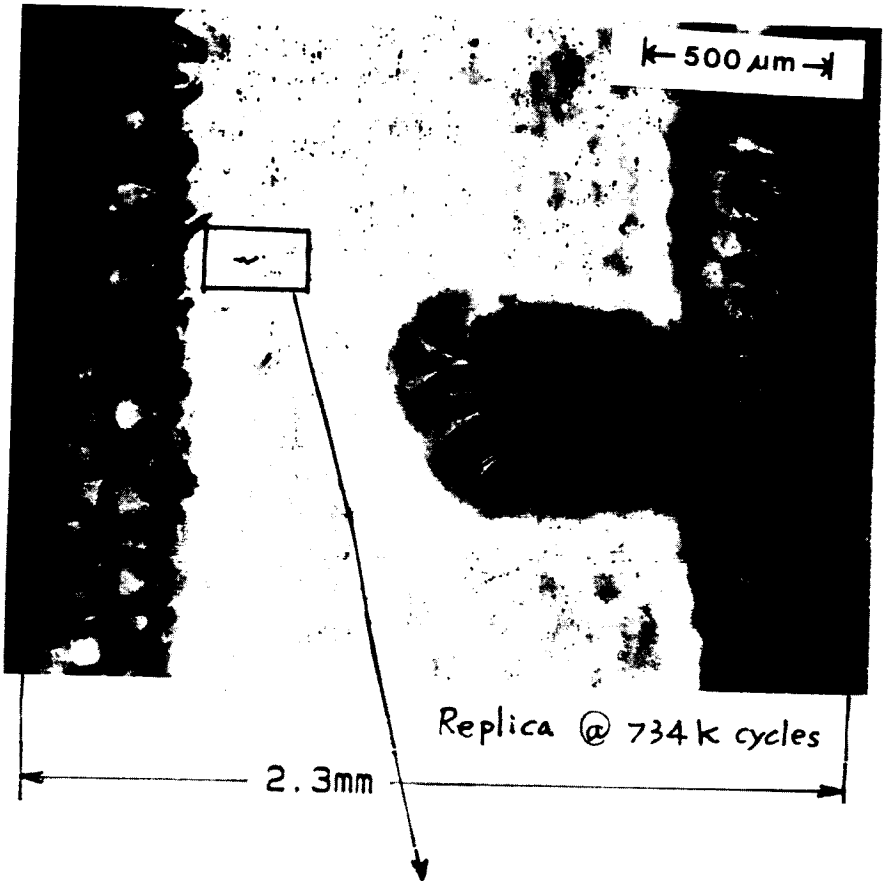

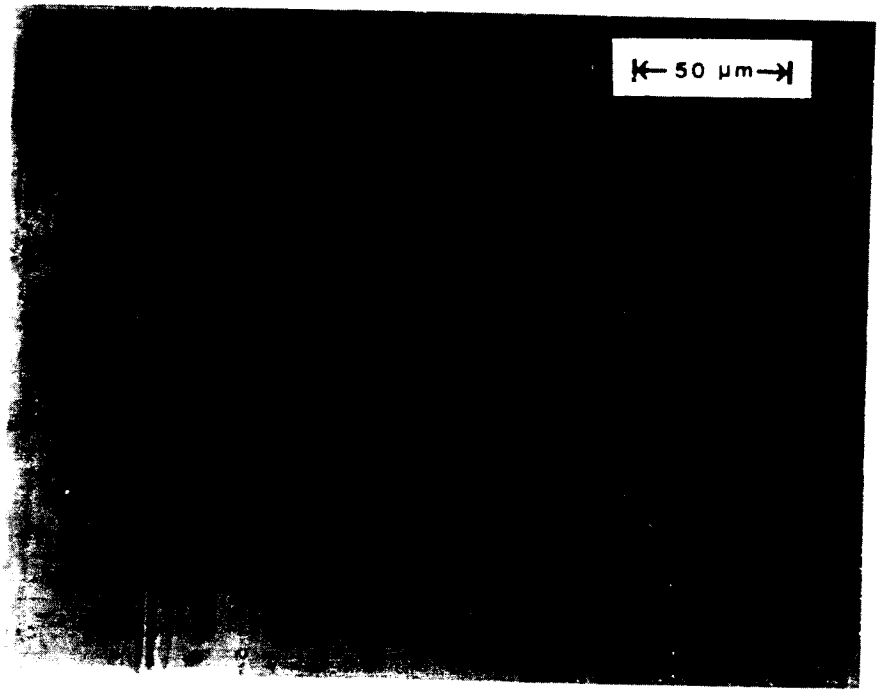

A-80-11

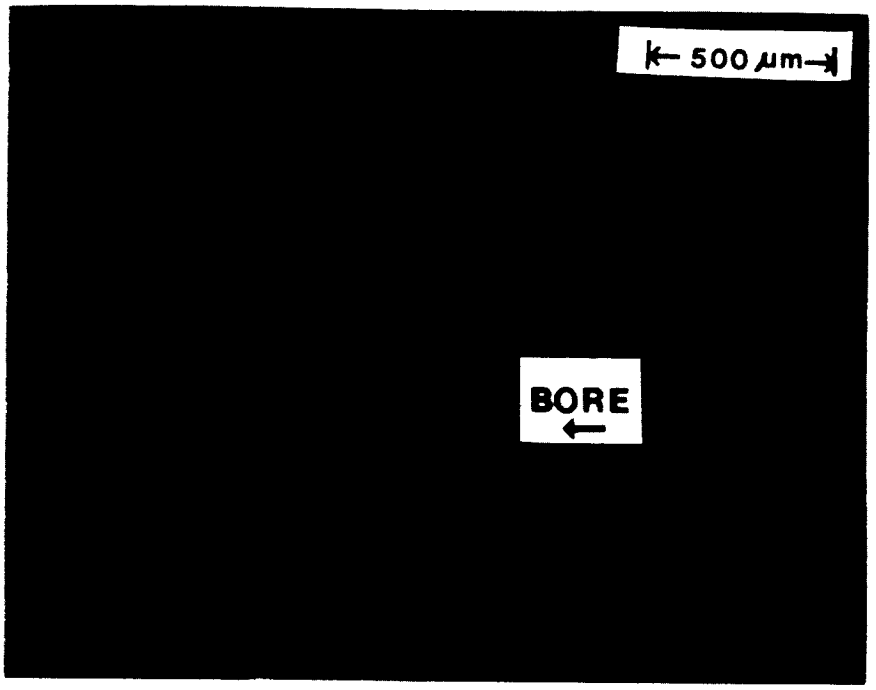

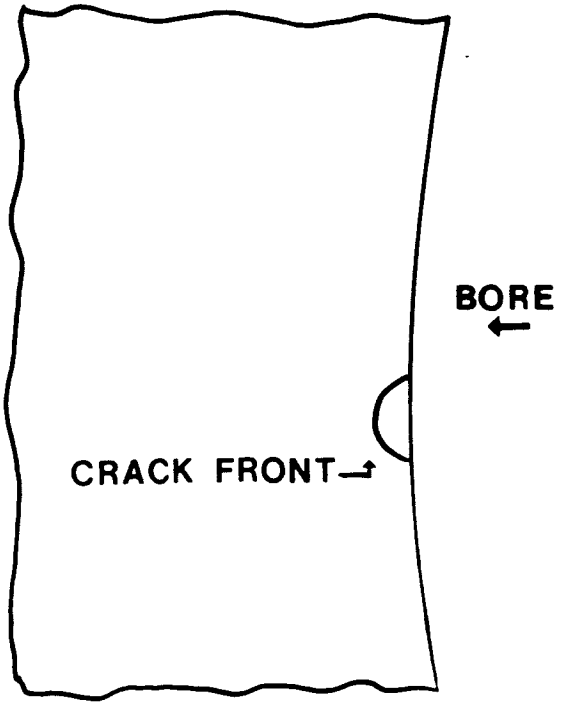

Tracing of Crack Front for A-80-11

TEST DATA

SPECIMEN NUMBER: A-68-05

DATE: 7/16/85

PARTICIPANT'S NAME: Joo-Jin Lee

John Cieslowski

TEST TEMPERATURE: 26° C

RELATIVE HUMIDITY: 67%

WAVEFORM TYPE: Sinusoidal wave, 20 Hz

LOADING SEQUENCE TYPE: Constant amplitude

R-RATIO = -2.0

S max = 50 MPa

S min = -100 MPa

FINAL LENGTH OF CRACK: 2.3 mm (Thru thickness) - L3

COMMENTS:

- Cracks were found at 0.8 mm above and 0.6 mm down the center line.

AGARD Short Crack DATA CHART

Record of crack lengths and map

Page 1 of 6 — Loading Type Const. Amplitude R = -2

Specimen no A-68-05 — Peak Stress 50 MPa

0.1mm grid

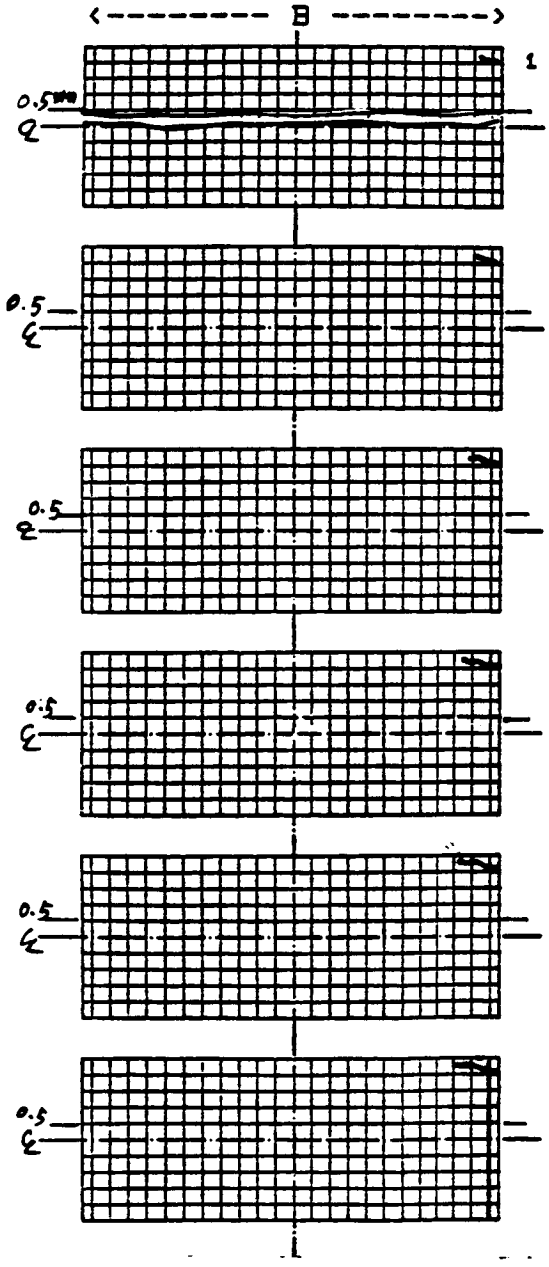

30K Cycles
L1 .093 mm
L2 ____ mm
L3 ____ mm
L4 ____ mm
L5 ____ mm

50K Cycles
L1 .114 mm
L2 ____ mm
L3 ____ mm
L4 ____ mm
L5 ____ mm

60K Cycles
L1 .169 mm
L2 ____ mm
L3 ____ mm
L4 ____ mm
L5 ____ mm

70K Cycles
L1 .213 mm
L2 ____ mm
L3 ____ mm
L4 ____ mm
L5 ____ mm

80K Cycles
L1 .223 mm
L2 ____ mm
L3 ____ mm
L4 ____ mm
L5 ____ mm

90K Cycles
L1 .239 mm
L2 ____ mm
L3 ____ mm
L4 ____ mm
L5 ____ mm

AGARD Short Crack DATA CHART

Record of crack lengths and map

Page 2 of 6- Loading Type R=-2

Specimen no A-68-05 Peak Stress 50 MPa

0.1mm grid

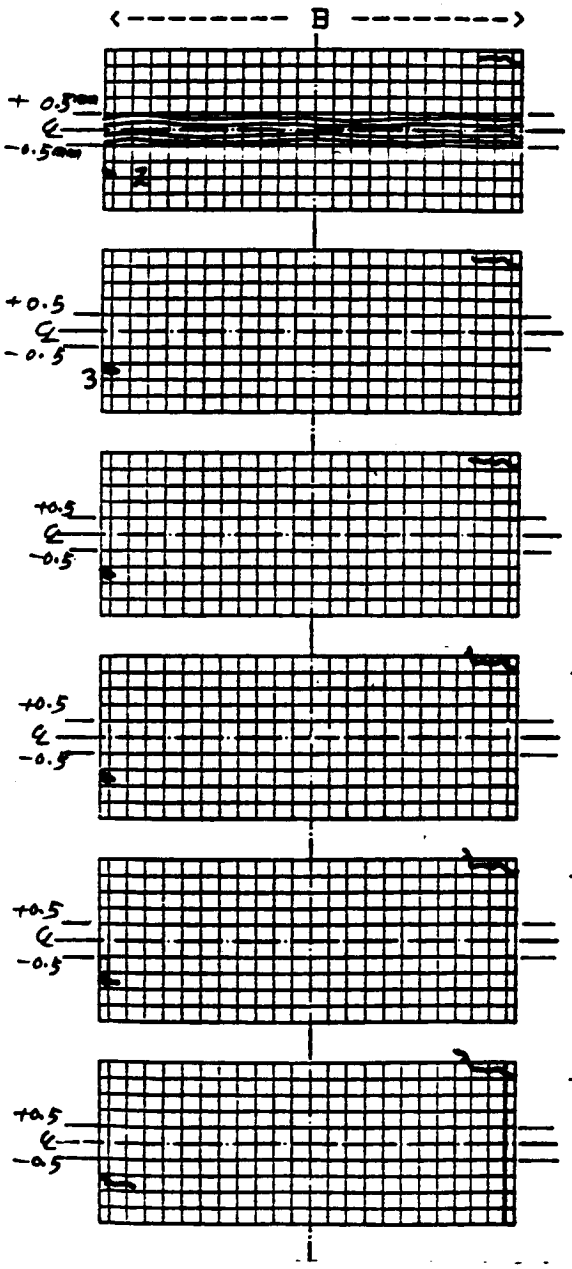

100K Cycles
L1 .245 mm
L2 .060 mm
L3 mm
L4 mm
L5 mm

110K Cycles
L1 .273 mm
L2 .065 mm
L3 .076 mm
L4 mm
L5 mm

120K Cycles
L1 .273 mm
L2 .065 mm
L3 .082 mm
L4 mm
L5 mm

130K Cycles
L1 .278 mm
L2 .065 mm
L3 .082 mm
L4 mm
L5 mm

140K Cycles
L1 .316 mm
L2 .065 mm
L3 .120 mm
L4 mm
L5 mm

150K Cycles
L1 .349 mm
L2 * mm
L3 .120 mm
L4 mm
L5 mm

* Crack was not clear

AGARD Short Crack DATA CHART

Record of crack lengths and map

Page 3 of 6 Loading Type R=-2

Specimen no A-68-05 Peak Stress 50 MPa

0.1mm grid

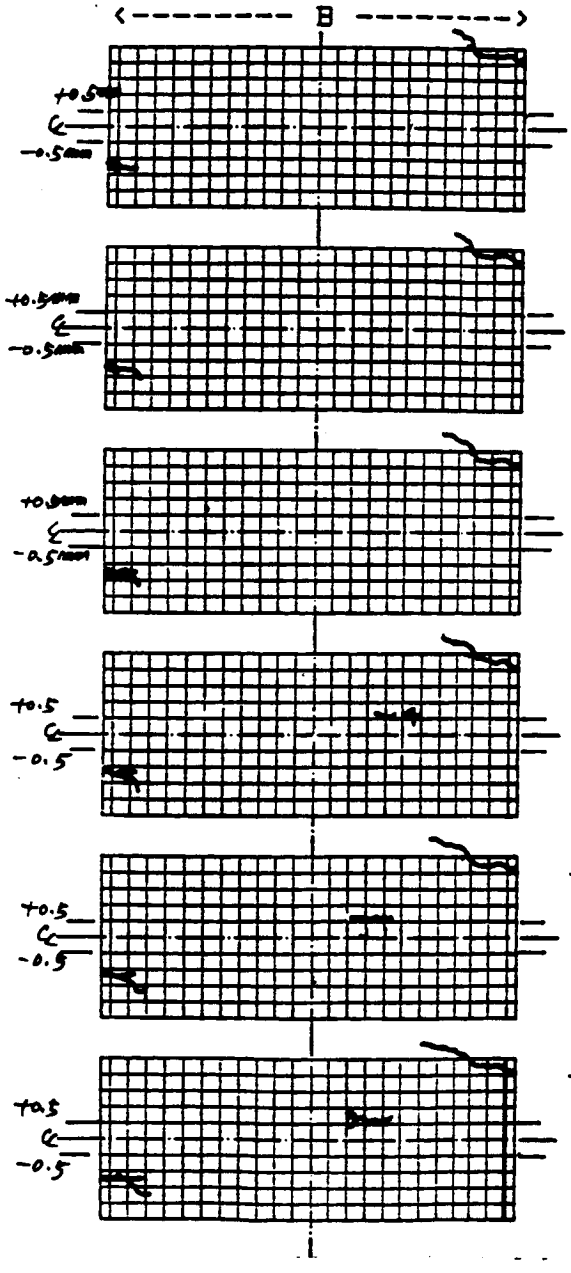

160K Cycles
L1 .414 mm
L2 .065 mm
L3 .153 mm
L4 ____ mm
L5 ____ mm

170K Cycles
L1 * mm
L2 .065 mm
L3 .196 mm
L4 ____ mm
L5 ____ mm

180K Cycles
L1 .441 mm
L2 L3 mm
L3 .196 mm
L4 ____ mm
L5 ____ mm

190K Cycles
L1 .452 mm
L2 ____ mm
L3 .174 mm
L4 .131 mm
L5 ____ mm

200K Cycles
L1 .512 mm
L2 ____ mm
L3 .240 mm
L4 .213 mm
L5 ____ mm

210K Cycles
L1 .540 mm
L2 ____ mm
L3 .262 mm
L4 .245 mm
L5 ____ mm

* Crack was not clear

AGARD Short Crack DATA CHART

Record of crack lengths and map

Page 4 of 6 Loading Type R=-2

Specimen no A-68-05 Peak Stress 50 MPa

0.1mm grid

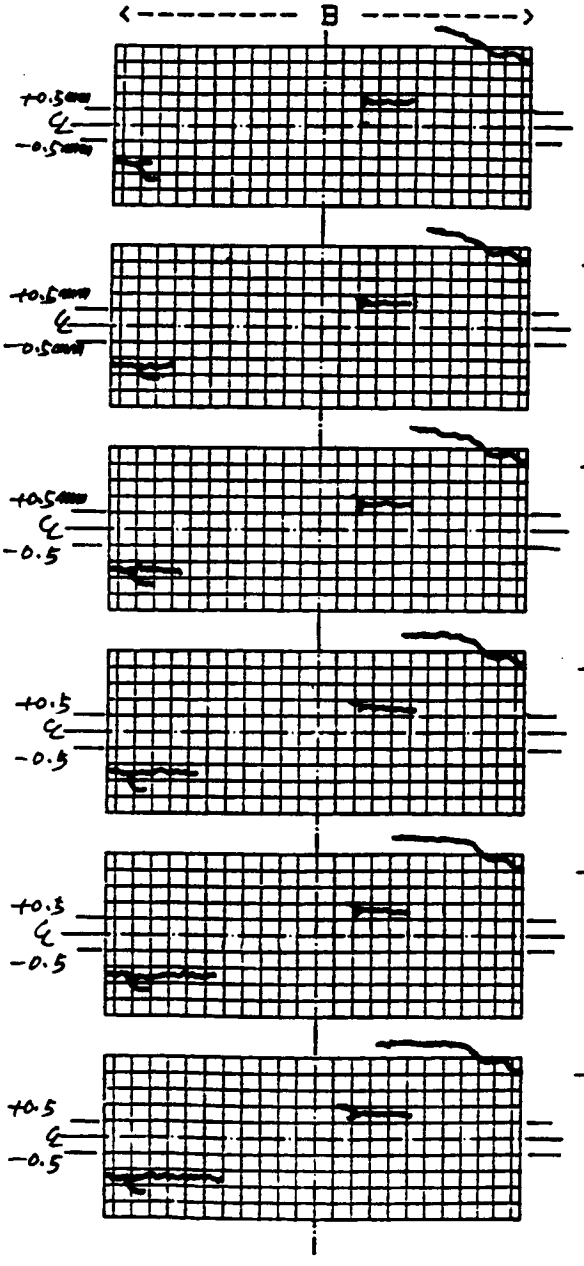

220K Cycles
L1 * mm
L2 mm
L3 * mm
L4 * mm
L5 mm

230K Cycles
L1 .561 mm
L2 mm
L3 .343 mm
L4 .256 mm
L5 mm

240K Cycles
L1 .665 mm
L2 mm
L3 .392 mm
L4 .321 mm
L5 mm

250K Cycles
L1 .681 mm
L2 mm
L3 .512 mm
L4 .337 mm
L5 mm

260K Cycles
L1 .736 mm
L2 mm
L3 .600 mm
L4 .343 mm
L5 mm

270K Cycles
L1 .928 mm
L2 mm
L3 .659 mm
L4 .403 mm
L5 mm

* Replica was not clear

AGARD Short Crack DATA CHART

Record of crack lengths and map

Page 5 of 6 Loading Type R=-2

Specimen no A-68-05 Peak Stress 50 MPa

0.1mm grid

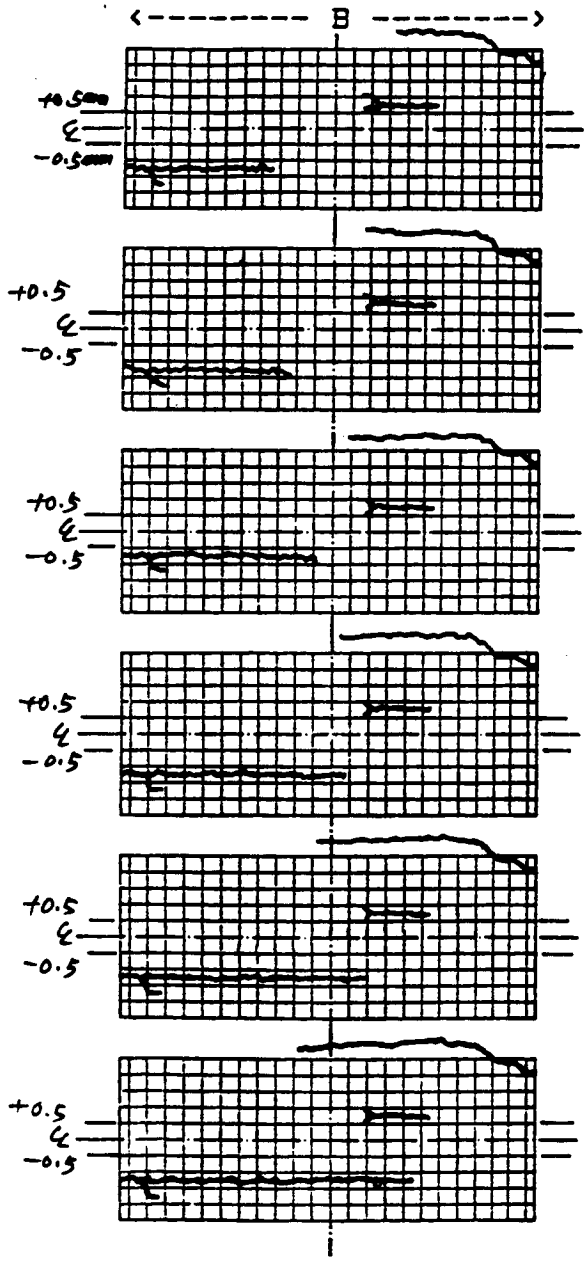

280K Cycles
L1 .872 mm
L2 mm
L3 .806 mm
L4 .397 mm
L5 mm

290K Cycles
L1 .991 mm
L2 mm
L3 .916 mm
L4 .403 mm
L5 mm

300K Cycles
L1 1.079 mm
L2 mm
L3 1.079 mm
L4 .403 mm
L5 mm

310K Cycles
L1 1.166 mm
L2 mm
L3 1.237 mm
L4 .403 mm
L5 mm

320K Cycles
L1 1.221 mm
L2 mm
L3 1.352 mm
L4 .403 mm
L5 mm

330K Cycles
L1 1.335 mm
L2 mm
L3 1.602 mm
L4 .403 mm
L5 mm

AGARD Short Crack DATA CHART

Record of crack lengths and map

Page 6 of 6 Loading Type R=-2

Specimen no A-69-05 Peak Stress 50 MPa

0.1mm grid

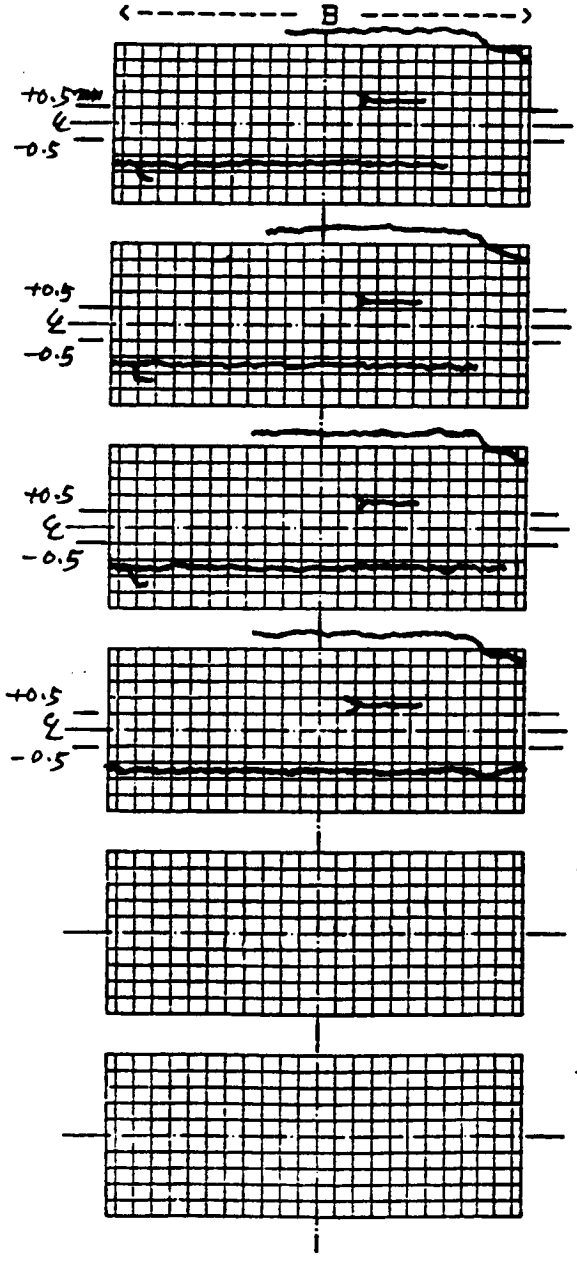

340K Cycles
L1 1.384 mm
L2 _____ mm
L3 1.814 mm
L4 * mm
L5 _____ mm

350K Cycles
L1 1.450 mm
L2 _____ mm
L3 2.006 mm
L4 .371 mm
L5 _____ mm

360K Cycles
L1 1.509 mm
L2 _____ mm
L3 2.150 mm
L4 .371 mm
L5 _____ mm

362K Cycles
L1 1.515 mm
L2 _____ mm
L3 Thru mm
L4 .436 mm
L5 _____ mm

_____ Cycles
L1 _____ mm
L2 _____ mm
L3 _____ mm
L4 _____ mm
L5 _____ mm

_____ Cycles
L1 _____ mm
L2 _____ mm
L3 _____ mm
L4 _____ mm
L5 _____ mm

* Crack was not clear

** DA/DN DATA **

SPECIMEN NO. = A-68-05.L1
NO. OF DATA = 31
R=-2.00
SMAX= 50.0 MPa
Corner Crack

	CYCLE(X1000)	CRK L. 2a(mm)	AVG. a(mm)	DELK(MPa-M)	DADN(mm/CYCLE)
0	30	0.093	0.000	0.00	0.000 X1.E-6
1	50	0.114	0.103	5.69	1.050 X1.E-6
2	60	0.169	0.141	6.57	5.500 X1.E-6
3	70	0.213	0.191	7.53	4.400 X1.E-6
4	80	0.223	0.218	7.99	1.000 X1.E-6
5	90	0.239	0.231	8.20	1.600 X1.E-6
6	100	0.245	0.242	8.38	0.600 X1.E-6
7	110	0.273	0.259	8.63	2.800 X1.E-6
8	130	0.278	0.275	8.87	0.250 X1.E-6
9	140	0.316	0.297	9.17	3.800 X1.E-6
10	150	0.349	0.332	9.65	3.300 X1.E-6
11	160	0.414	0.381	10.25	6.500 X1.E-6
12	180	0.441	0.427	10.78	1.350 X1.E-6
13	190	0.452	0.447	10.99	1.100 X1.E-6
14	200	0.512	0.482	11.36	6.000 X1.E-6
15	210	0.540	0.526	11.81	2.800 X1.E-6
16	230	0.561	0.550	12.05	1.050 X1.E-6
17	240	0.665	0.613	12.63	10.400 X1.E-6
18	250	0.681	0.673	13.16	1.600 X1.E-6
19	260	0.736	0.708	13.46	5.500 X1.E-6
20	270	0.828	0.782	14.06	9.200 X1.E-6
21	280	0.872	0.850	14.58	4.400 X1.E-6
22	290	0.981	0.926	15.14	10.900 X1.E-6
23	300	1.079	1.030	15.85	9.800 X1.E-6
24	310	1.166	1.122	16.45	8.700 X1.E-6
25	320	1.221	1.193	16.90	5.500 X1.E-6
26	330	1.335	1.278	17.41	11.400 X1.E-6
27	340	1.384	1.359	17.89	4.900 X1.E-6
28	350	1.450	1.417	18.22	6.600 X1.E-6
29	360	1.509	1.479	18.58	5.900 X1.E-6
30	362	1.515	1.512	18.76	3.000 X1.E-6

** DA/DN DATA **

SPECIMEN NO. = A-68-05.L3
NO. OF DATA = 22
R=-2.00
SMAX= 50.0 MPa
corner crack

	CYCLE(X1000)	CRK L. 2a(mm)	AVG. a(mm)	DELK(MPa-M)	DADN(mm/CYCLE)
0	110	0.076	0.000	0.00	0.000 X1.E-6
1	120	0.082	0.079	5.01	0.600 X1.E-6
2	140	0.120	0.101	5.62	1.900 X1.E-6
3	160	0.153	0.137	6.46	1.650 X1.E-6
4	170	0.196	0.175	7.23	4.300 X1.E-6
5	200	0.240	0.218	7.99	1.467 X1.E-6
6	210	0.262	0.251	8.51	2.200 X1.E-6
7	230	0.343	0.303	9.25	4.050 X1.E-6
8	240	0.392	0.368	10.08	4.900 X1.E-6
9	250	0.512	0.452	11.05	12.000 X1.E-6
10	260	0.600	0.556	12.10	8.800 X1.E-6
11	270	0.659	0.629	12.78	5.900 X1.E-6
12	280	0.806	0.733	13.66	14.700 X1.E-6
13	290	0.916	0.861	14.66	11.000 X1.E-6
14	300	1.079	0.998	15.63	16.300 X1.E-6
15	310	1.237	1.158	16.68	15.800 X1.E-6
16	320	1.352	1.294	17.51	11.500 X1.E-6
17	330	1.602	1.477	18.57	25.000 X1.E-6
18	340	1.814	1.708	19.85	21.200 X1.E-6
19	350	2.006	1.910	20.94	19.200 X1.E-6

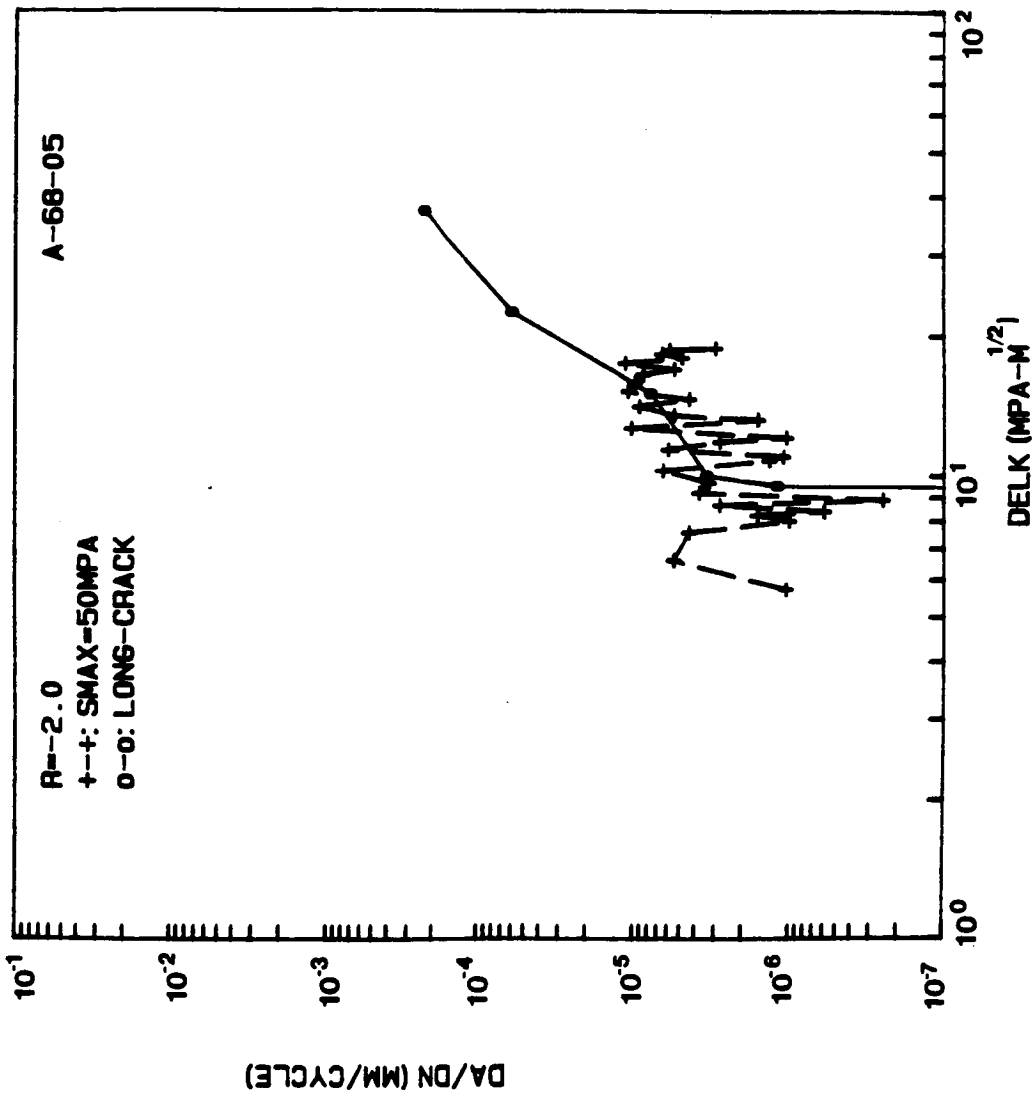
A-68-05
R=-2.0
+-+: SMAX=50MPA
o-o: LONG-CRACK
DA/DN (MM/CYCLE)
DELK (MPA-M^1/2)
10^-1
10^-2
10^-3
10^-4
10^-5
10^-6
10^-7
10^0
10^1
10^2

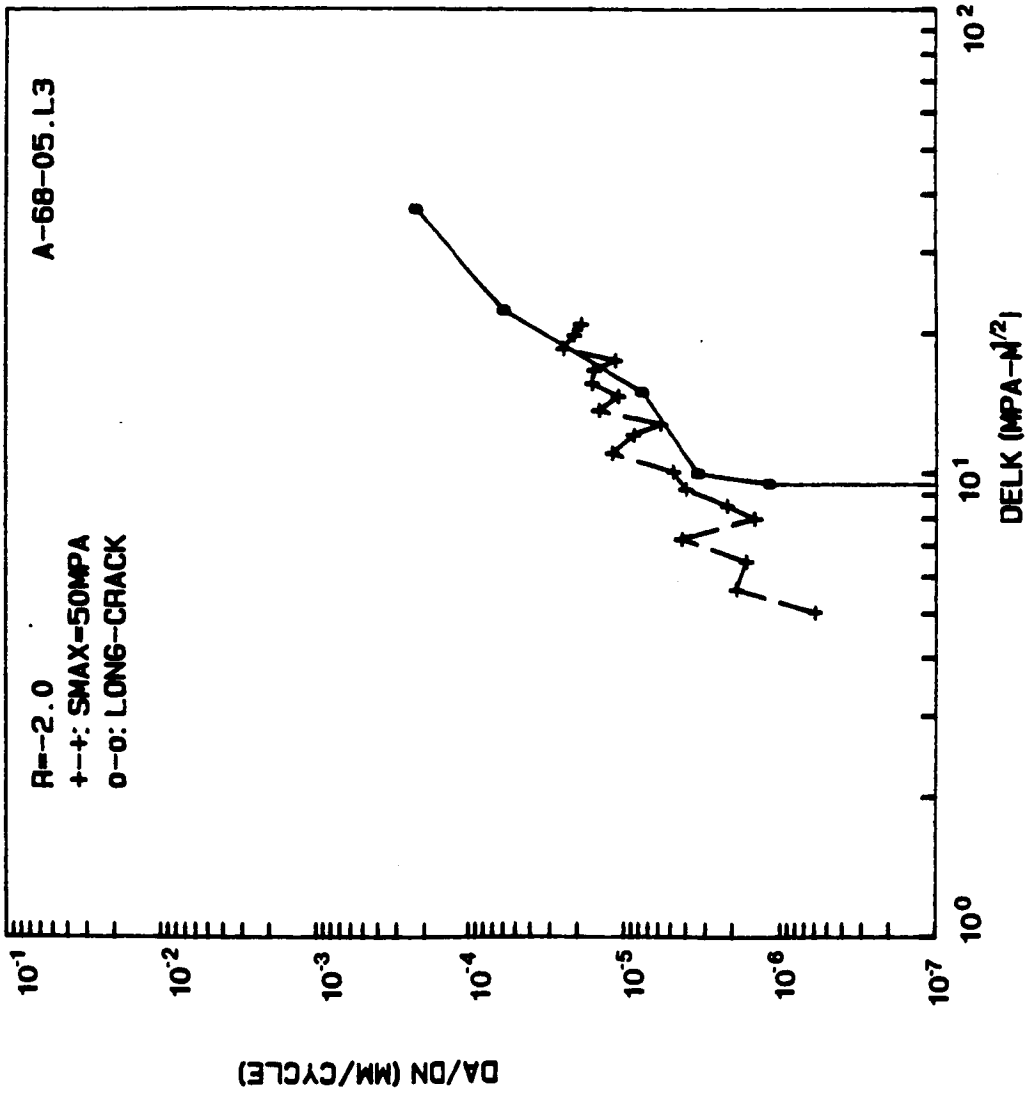
A-68-05.L3
R=-2.0
+-+: SMAX=50MPA
o-o: LONG-CRACK
DA/DN (MM/CYCLE)
DELK (MPA-M^1/2)
10^-1
10^-2
10^-3
10^-4
10^-5
10^-6
10^-7
10^0
10^1
10^2

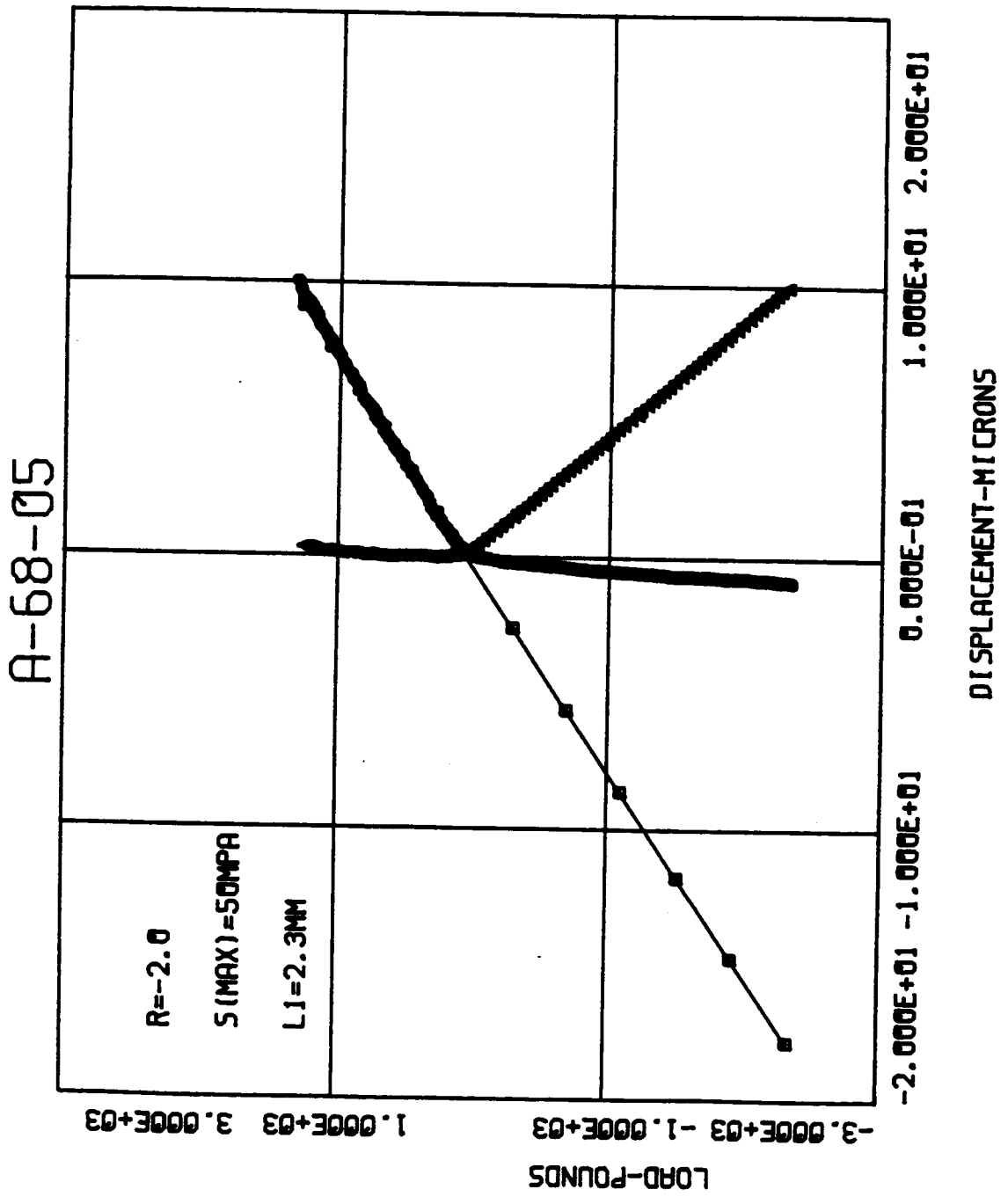
A-68-05
R=-2.0
S(MAX)=50MPA
L1=2.3MM
LOAD-POUNDS
-3.000E+03
-1.000E+03
1.000E+03
3.000E+03
-2.000E+01
-1.000E+01
0.000E-01
1.000E+01
2.000E+01
DISPLACEMENT-MICRONS

A-68-05

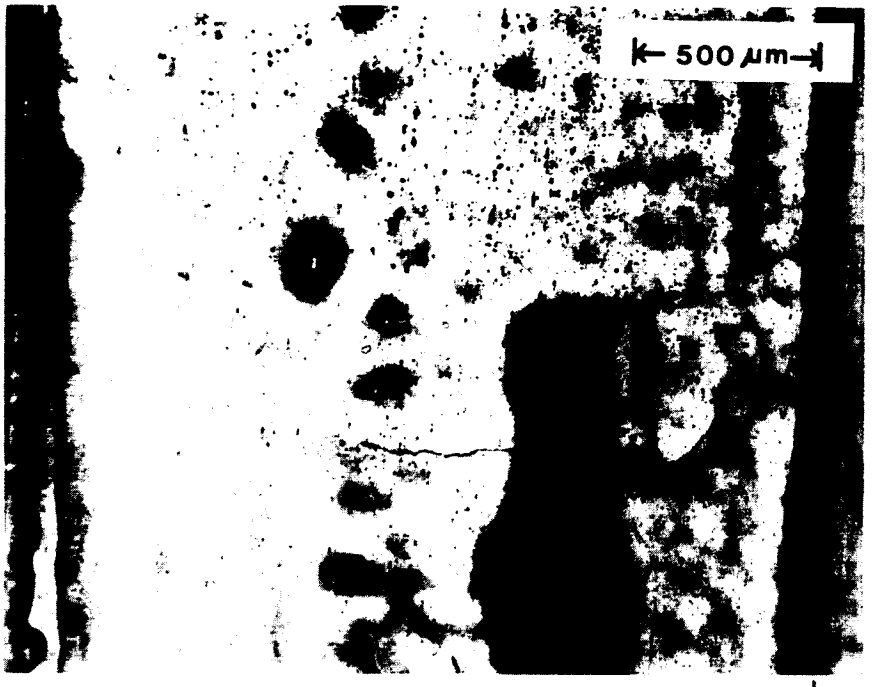

A-68-05

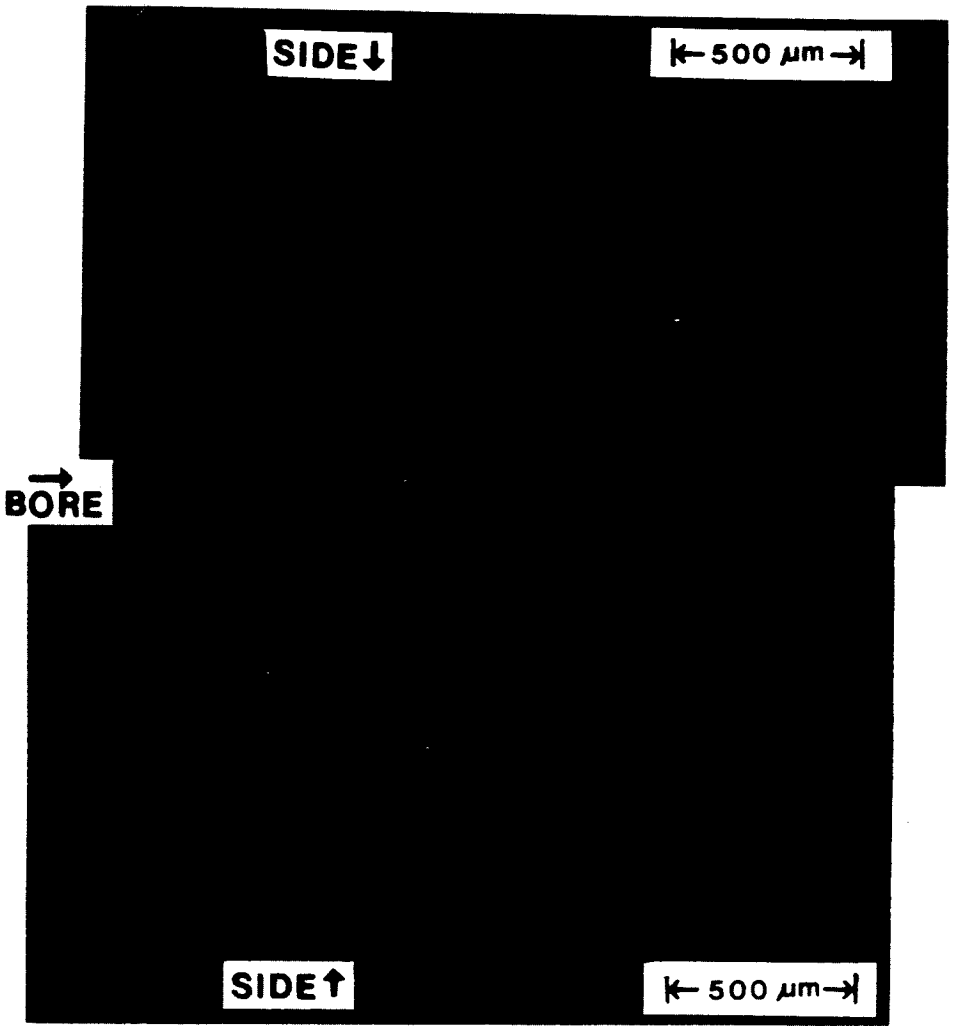

NAG 1-526 IN-39
DOA/LANGLEY 63708
346 P.

1. Report No.	2. Government Accession No.	3. Recipient's Catalog No.

4. Title and Subtitle
Short Fatigue Crack Behavior in Notched 2024-T3 Aluminum Specimens

5. Report Date
July, 1986

6. Performing Organization Code

7. Author(s)
J. J. Lee and W. N. Sharpe, Jr.

8. Performing Organization Report No.

9. Performing Organization Name and Address
Johns Hopkins University
Department of Mechanical Engineering
Baltimore, Maryland 21218

10. Work Unit No.

11. Contract or Grant No.
NAG-1526

12. Sponsoring Agency Name and Address
National Aeronautics and Space Administration
Langley Research Center
Hampton, VA 23665

13. Type of Report and Period Covered
Final

14. Sponsoring Agency Code

15. Supplementary Notes

16. Abstract

Single-edge, semi-circular notched specimens of Al 2024-T3, 2.3 mm thick, were cyclicly loaded at R-ratios of 0.5, 0.0, -1.0, and -2.0, as part of an AGARD-sponsored, round-robin test program. The notch roots were periodically inspected using a replica technique which duplicates the bore surface. The replicas were examined under an optical microscope to determine the initiation of very short cracks and to monitor the growth of short cracks ranging in length from a few tens of microns to the specimen thickness.

In addition to short crack growth measurements, the crack opening displacement (COD) was measured for surface cracks as short as 0.035 mm and for through-thickness cracks using the Interferometric Strain/Displacement Gage (ISDG), a laser-based optical technique.

The growth rates of short cracks were faster than the long crack growth rates for R-ratios of -1.0 and -2.0. No significant difference between short and long crack growth rates was observed for R = 0.0. Short cracks had slower growth rates than long cracks for R = 0.5.

The crack opening stresses measured for short cracks were smaller than those predicted for large cracks, with little difference appearing for positive R-ratios and large differences noted for negative R-ratios.

17. Key Words (Suggested by Author(s))
Aluminum Alloy
COD measurement
Short Crack
Notched Specimen
Fatigue Crack Growth Test
Crack Closure Measurement
Interferometric Strain/Displ. Gage

18. Distribution Statement

19. Security Classif. (of this report)	20. Security Classif. (of this page)	21. No. of Pages	22. Price*
Unclassified		346	

* For sale by the National Technical Information Service, Springfield, Virginia 22161